©Copyright 2017
Jared A. Grummer

Evolutionary History of the Patagonian *Liolaemus fitzingerii* Species Group of Lizards

Jared A. Grummer

A dissertation
submitted in partial fulfillment of the
requirements for the degree of

Doctor of Philosophy

University of Washington

2017

Reading Committee:

Adam D. Leaché, Chair

Raymond B. Huey

Richard G. Olmstead

Program Authorized to Offer Degree:
Biology

University of Washington

Abstract

Evolutionary History of the Patagonian *Liolaemus fitzingerii* Species Group of Lizards

Jared A. Grummer

Chair of the Supervisory Committee:
Dr. Adam D. Leaché
Department of Biology

The majority of the world's land mass and biota reside in the Northern Hemisphere. However, even when land area is accounted for, we know disproportionately less about Southern Hemisphere flora and fauna than their Northern Hemisphere counterparts. The South American biota is extremely unique with high levels of endemism due to a long history of geologic and evolutionary isolation. A prime example of South American endemism is the Squamate family Liolaemidae. In this family, the sole genus *Liolaemus* has one of the widest elevational, latitudinal, and climatic distributions of any lizard genus anywhere. The 258 described species (at the time of this dissertation) in this genus are distributed across 40°of latitude, from southern Peru to Tierra del Fuego, and from sea level to more than 16,000' in elevation. The genus *Liolaemus* is composed of two subclades, *Liolaemus* (*sensu stricto*) and *Eulaemus*, and it is in the second clade that we find the *Liolaemus fitzingerii* species group.

The *L. fitzingerii* group is ∼5 million years old and is distributed in the Patagonian shrub-steppe of central Argentina from approximately 37-50°S latitude. Due to its abundance in the field, high morphological diversity, and broad distribution, this species group has been the subject of many taxonomic, ecological and evolutionary studies. Taxonomic studies of the group began in the mid-19^{th} century when Charles Darwin collected the *L. fitzingerii* holotype; nine species are currently recognized in the group. Approximately a decade ago in 2006, Avila and colleagues performed an in-depth phylogeographic analysis of this species group where they inferred hybridization and

post-Pleistocene glacial range expansion in some of the species in this group.

In light of previous studies, I addressed three specific goals that I partitioned into the three chapters of my dissertation: 1) infer evolutionary relationships between described and candidate species in the *Liolaemus fitzingerii* group, 2) determine the number and geographic extent of genetically distinct populations in the group as a function of geologic features and historic climatic events, and 3) compare evolutionary patterns and processes across independently formed hybrid zones in this group. Each chapter had a distinct molecular dataset. For the first chapter, I collected DNA sequence data for 580 nuclear loci and full mitochondrial genomes of 27 individuals. The dataset for chapter 2 was 178 individuals that were sequenced for $\sim$1,500 genome-wide SNPs (single nucleotide polymorphisms). And for chapter 3, I sampled 267 individuals that were sequenced for $\sim$2,000 SNPs and the mitochondrial *cytochrome B* gene.

I performed a variety of phylogenetic reconstruction techniques in chapter 1, including multi-species coalescent and concatenation approaches. Because hybridization was inferred from previous research on this species group, I also conducted network analyses that consider reticulate evolutionary relationships. Although these methodologies are quite distinct, they all revealed low support for relationships between species. Furthermore, the network analyses supported at least two instances of interspecific hybridization. My conclusion is that the poor phylogenetic support reported across analyses indicates a rapid radiation from a common ancestor, but this signal may also be exacerbated by poor taxonomy and an over-description of species.

In chapter 2, I sought to determine the effects of landscape features and Pleistocene glacial cycling (e.g., over the last $\sim$2.6 million years) on the distribution of populations in the *Liolaemus fitzingerii* group. With 178 individuals covering the known distribution of this group, analyses revealed six distinct populations that are arranged predominantly in east-west bands. In the north, the Somuncura Plateau marks the interface between two populations, as does the Canquel Plateau in the south. Similarly, the Chubut River forms a nearly complete barrier between two populations in the center of the group's distribution. Migration analyses bolstered these results, with low lev-

els of migration inferred around these landscape features. An expected effect of late-Pleistocene glaciations is that genetic diversity should be highest in the east and north where refugial populations were predicted to inhabit. The estimates of genetic diversity support this, with higher genetic diversity in the east and north, and conversely lower genetic diversity in the west and south. My analyses of demographic models also support glacial refugia, in that all populations went through a population bottleneck and only very recently have population sizes begun to recover. These results show the importance of geographic features and climatic events in shaping the evolutionary history of the *L. fitzingerii* species group, and add much needed data to our relatively poor understanding of taxa in this region of the world.

My aims for chapter 3 were to characterize suspected hybrid zones in the *Liolaemus fitzingerii* species group and assess selection on both nuclear and mitochondrial genomes in a comparative manner. Initial analyses revealed a completely unexpected result where four species are connected through three hybrid zones, and two species, *L. melanops* and *L. xanthoviridis* each hybridize with two other species. I calculated linkage disequilibrium coefficients for the SNP data and estimated clines for both nuclear and mitochondrial DNA, which allowed me to calculate selection and compare the strength of selection acting on the same species in the different hybrid zones. In all three hybrid zones, the mitochondrial cline was to the south of the nuclear cline, indicating that either the hybrid zones are moving to the north, or that a northward male-biased dispersal occurs in each of these hybrid zones. When comparing levels of selection acting on the same species in each of the three hybrid zones, *L. melanops* was under stronger selection when hybridizing with *L. xanthoviridis* as compared to *L. shehuen*. This is potentially due to limited dispersal abilities of northern *L. melanops* individuals as compared to individuals in the southern part of the range, or stronger exogenous selection in the south due to differing ecologies of *L. xanthoviridis* and *L. melanops*. In the second comparison, the strength of selection against *L. xanthoviridis* is higher when hybridizing to the south with *L. fitzingerii* than *L. melanops* to its north. The higher selection in the south could be due to differing habitats that these two species occupy, or that the low genetic

diversity of *L. fitzingerii* mathematically inflates the selection estimate.

In summary, my research supports the notion that species in the *Liolaemus fitzingerii* group are the result of a rapid evolutionary radiation, and that this signal is likely strengthened by taxonomic inflation. Prominent geologic features such as plateaus and rivers seem to have strongly influenced the spatial distribution of populations in this group, in tandem with glacial cycling over the past $\sim$2.5 million years. Hybridization is commonplace where distinct populations meet, which has provided a unique opportunity to study independent replicates of the evolutionary process. My research on the Patagonian *Liolaemus fitzingerii* species group has helped reduce the knowledge gap of phylogeographic and evolutionary studies between Northern and Southern Hemisphere taxa.

Lack of phylogenetic support matters: phylogenomic evidence for a recent and rapid radiation in lizards of the Patagonian *Liolaemus fitzingerii* species group

Jared A. Grummer[1], Luciano J. Avila[2], Mariana M. Morando[2], Jack W. Sites, Jr.[3], and Adam D. Leaché[1]

[1]*Department of Biology and Burke Museum of Natural History and Culture, University of Washington, Box 351800, Seattle, WA 98195-1800, USA;*

[2]*Centro Nacional Patagónico – Consejo Nacional de Investigaciones Científicas y Técnicas (CENPAT-CONICET), Boulevard Almirante Brown 2915, ZC: U9120ACD, Puerto Madryn, Argentina*

[3]*Department of Biology and M.L. Bean Life Science Museum, Brigham Young University, Provo, Utah 84602, USA*

Abstract.— Rapid evolutionary radiations are difficult to resolve because divergence events are nearly synchronous and gene flow between nascent species can be high, resulting in a phylogenetic "bush". Large datasets composed of sequence loci from across the genome potentially help resolve some of these difficult phylogenetic problems. A suitable test case is the *Liolaemus fitzingerii* species group of lizards, which is broadly distributed in Argentinean Patagonia and has a complex taxonomic and evolutionary history. Previous research has detected interspecific hybridization within the group as well as population-level effects of Pleistocene glaciations. To infer phylogenetic relationships between species in this species group, we generated a sequence capture dataset for 28 ingroup individuals of 580 nuclear loci, alongside a mitogenomic dataset. Relationships between individuals were generally weakly supported with the nuclear data, with little support for relationships between currently described species. We recovered a signal of mito-nuclear discordance, indicating potential hybridization between some species in this group. Phylogenetic network analyses provided support for 4-5 reticulation events between species. Phasing our nuclear loci did not provide additional insight into relationships or suspected patterns of hybridization. Biogeographically, our analyses indicate a north-to-south colonization pattern. Our results also indicate that this group of morphologically diverse species evolved in rapid succession. Pleistocene post-glacial range expansion can explain the north-south colonization pattern and low genetic diversity within the most southern species, *Liolaemus fitzingerii*. Genomic datasets provide molecular systematists with the best opportunity to resolve rapid radiations. The inability, in the case of this system, of phylogenomic datasets to provide a fully-resolved phylogeny is biologically meaningful and indicative of a recent and rapid evolutionary radiation.
(Keywords: sequence capture, ultraconserved elements, coalescent, population, hybridization, rapid radiation)

Evolutionary radiations occur when one ancestral population diversifies into a variety of forms, typically over relatively short timescales due to ecological opportunity or to evolutionary innovations (Schluter 2000; Glor 2010). However, rapid radiations are difficult to resolve because they are often characterized by incomplete lineage sorting (ILS), introgression, and few fixed differences between species (e.g., short internodes; Rokas and Carroll 2006, Patel et al. 2013). Resolving interspecific relationships in such rapid radiations is important, because the order of branching and relationships among species is a prerequisite for biogeographic inferences and understanding the processes and/or traits that promoted diversification.

Genomic scale datasets are becoming increasingly common for phylogenetic studies because of the reduction of sequencing costs and recent development of reduced genome sequencing techniques (e.g. Faircloth et al. 2012; Lemmon et al. 2012). Analyzing large amounts of the genome not only provide more information for reconstructing phylogenies, but also give independent estimates of the coalescent history across the genome, and therefore a better understanding of a group's evolutionary history. A common first instinct when trying to resolve rapid radiations is to collect and analyze more data (Rokas and Carroll 2006). However, more data will not help resolve "hard" polytomies, which result from near simultaneous divergence of many populations; by definition, these cannot be resolved. In contrast, "soft" polytomies are the result of analytical artifacts; these can be solved with the addition of more data (Maddison 1989). Soft polytomies may be resolved by the addition of more sequence data or taxa, though this isn't always successful.

Hard polytomies characterize rapidly diversifying groups and can give the appearance of a bush rather than a tree. In a rapid radiation, stochastic coalescent processes can cause a high degree of gene tree heterogeneity, which makes it difficult to reconstruct the true species tree. Simulation work has shown that analyzing more data under concatenation can actually increase the support for the incorrect tree (Kubatko and Degnan 2007). Indeed, depending on demographic parameters (e.g., population sizes and divergence times), the evolutionary history of some species is expected to be

in the "anomaly zone", areas of tree space where the majority of gene tree topologies do not match the true species tree topology (e.g., Linkem et al. 2016). In such cases, genomic datasets will not be able to resolve species-level relationships.

Sequence capture datasets hold particular promise in the context of molecular-based phylogenetics and phylogeography (McCormack et al. 2013). Although some methods exist for phylogenetic reconstruction with SNP (single nucleotide polymorphism) datasets (e.g., SNAPP; Bryant et al. 2012), the majority of phylogenetic approaches now utilize sequence data (e.g., BP&P, Yang and Rannala 2010,Yang 2015; *BEAST, Heled and Drummond 2010). Because the ability to sequence has proceeded faster than the ability to analyze large datasets, researchers are often faced with the challenge of finding an appropriate method for estimating a phylogeny from phylogenomic data. Summary methods for inferring the species tree have become popular because of the reduced computational burden; however, they drastically reduce valuable information content in the data (e.g., STAR, STEAC; Liu et al. 2009). Utilizing summary statistic methods that reduce data content is of particular concern when estimating phylogenies and delimiting species in young clades that have recently radiated, where gene flow and a short timescale result in relatively few fixed differences between species.

Determining the phase, or allelic contribution from each parent, of nuclear loci is particularly useful in population- and species-level analyses. Two popular approaches for sequencing a reduced portion of the genome both target genomic regions that are conserved across deeply diverged taxa (e.g., Tetrapoda); such regions are also likely to be relatively conserved at lower phylogenetic levels. When studying lower-level relationships between populations and species, phased data provide rich information for coalescent-based inferences of population-level demography, phylogeography, and gene genealogical relationships. Some authors have argued for the use of sequence capture datasets in lower-level phylogenetic studies (e.g., Harvey et al. 2016), however, relatively few lower-level studies have used this approach (but see Alexander et al. 2016). Sequence capture datasets with phased alleles hold particular promise for

assessing hybridization because they offer many instances to determine hybrids via distinct placement of parental alleles in a gene genealogy.

Hybridization is common in nature. Indeed, approximately 10% and 25% of animal and plant species known to hybridize, respectively (Mallet 2005). Whereas hybridization is often found to occur in limited geographic areas termed "contact" or "hybrid" zones (e.g. Barton and Hewitt 1985), hybridization is sometimes detected across broad areas of sympatry (e.g Martin et al. 2013). Hybridization resulting in fertile offspring represents a porous boundary between closely related species and has the potential to provide insight into the speciation process (Harrison 1993). However, it is difficult to document hybridization in remote geographic regions where species-level natural history is poorly understood.

Liolaemus lizards inhabit remote regions of southern South America, where there are currently ~250 described species (www.reptile-database.org). Although its species-level taxonomy is poorly understood (e.g., ~10 new species are described each year), hybridization has been documented across several *Liolaemus* species (Morando et al. 2004; Olave et al. 2011). Avila et al. (2006) performed an in-depth study on the phylogeography and species limits of species in the *L. boulengeri* group with three mitochondrial and two nuclear genes, with particular attention to the more exclusive *L. fitzingerii* group. In their analyses, they recovered support for multiple range expansions, long-distance colonization events, secondary contact between described species in this group (*L. xanthoviridis* and *L. fitzingerii*), and species-level paraphyly within the larger *L. melanops* clade. Individuals in secondary contact zones have extremely varied phenotypes, indicating local hybridization. The results of Avila et al. (2006) pointed to a complex evolutionary history of range expansions and secondary contact, highlighting a dubious taxonomy and over-description of species in this group.

Nine species are currently recognized in the *L. fitzingerii* group (Avila et al. 2006, 2008, 2010). The *L. fitzingerii* group is broadly distributed in coastal and Patagonian shrub-steppe habitats in central-southern Argentina (Fig. 1). This group is highly morphologically diverse, which has been the basis for many of the described

species. Species range in maximum size (snout-vent length [SVL]) from 74.2 (*L. goetschi*) to 110mm (*L. fitzingerii*) (Abdala et al. 2012b,a), with sexual dichromatism absent in some species and evident in others. Many species have been described based on variation in color and dorsal patterns, where base colors span brown, orange or green and dorsal patterns are either non-existent, reticulated, or barred. Levels of melanism on the head, dorsal, and ventral surfaces are highly variable in this group and were used in species diagnoses. However, Escudero et al. (2012) showed that melanism is highly variable across populations and not conserved at the species level, thus an unreliable character for taxonomy in this group.

Taxonomy of the *L. fitzingerii* group has been muddled since the 19th century when Charles Darwin incorrectly labeled the *L. fitzingerii* holotype as collected in "Chile", when in fact he collected this specimen in Puerto Deseado, Santa Cruz Province, Argentina (Cei 1980a; Abdala 2007). This species group was first proposed by Cei in 1986, but Laurent (1992) later transferred it to the larger clade (subgenus) *Eulaemus*. Many currently recognized species were initially described as subspecies (e.g., *L. fitzingerii canqueli* [Cei 1975], *L. fitzingerii melanops*, and *L. fitzingerii xanthoviridis* [Cei and Scolaro 1980]). Based on morphological data, Etheridge (1993, 1995) later elevated many of these (including *L. canqueli*, *L. fitzingerii*, and *L. melanops* to species. In a phylogeographic study, Morando et al. (2004) proposed the *L. fitzingerii* group was composed of two clades, the *fitzingerii* complex (including *L. fitzingerii* and *L. xanthoviridis*), and the *melanops* complex (including *L. melanops*, *L. canqueli*, *L. martorii*, and *L. morenoi*). Since that study, four new species have been described in the *L. fitzingerii* species group based on morphological data: two in the *fitzingerii* complex (*L. camarones* and *L. shehuen*), and two in the *melanops* complex (*L. dumerili* and *L. purul*) (Abdala et al. 2012a,b). To date, no molecular-based study has elucidated relationships between taxa in the *L. fitzingerii* group (but Olave et al. 2014 included representatives of all species in the *L. fitzingerii* group in a sub-genus wide study).

In this study, we generate a dataset targeting 585 nuclear loci across the genome in addition to mitogenomic DNA and then infer the evolutionary relationships between

species in the *L. fitzingerii* species group. Given the poorly understood evolutionary relationships and previous evidence of hybridization, we sought to infer phylogenetic relationships between described species and candidate taxa in this group. Furthermore, we aimed to gain insight into biogeographic colonization patterns of taxa within this group. We used phased alleles in an attempt to maximize the information content for coalescent-based analyses. We analyzed our data via concatenation, species tree approaches, and network (e.g., reticulate phylogeny) inferences. Our results indicate that this morphologically diverse group evolved recently and then radiated rapidly.

Materials and Methods

Sampling

We performed sequence capture on all nine species and five candidate species in the *L. fitzingerii* group, totaling 28 ingroup individuals (1-4 individuals per described species). All specimens have been deposited into the herpetology collection in the Centro Patagónico Nacional (CENPAT-CONICET), Puerto Madryn, Chubut, Argentina. Most individuals were selected because of their proximity to type localities (Fig. 1). However, five individuals were included because a study by Olave et al. (2014) provided evidence for their potential status as a species. Three geographically widespread species were represented by multiple individuals (*L. fitzingerii*, *L. melanops*, and *L. xanthoviridis*), whereas all other lineages were represented by a single individual (Fig. 1; Supplemental Table S1). Four other *Liolaemus* species (*L. bibronii*, *L. boulengeri*, *L. kingii*, and *L. rothi*) were chosen as outgroups for phylogenetic analyses that were sequenced for a separate *Liolaemus*-wide phylogenetic study (Leaché et al., in prep.; Supplemental Table S1). A single individual of *Liolaemus purul* was also included to test whether this recently described species which had ben assigned to the *L. fitzingerii* species group based on morphological data is genetically a member of this group as well.

Sequence Capture Laboratory Protocol.— We performed a targeted sequence capture

approach and used a set of RNA probes specifically designed for Iguanian lizards (Leaché et al. 2015). We targeted 585 nuclear loci with a probe set that consisted of 1,170 RNA probes. Of the 585 targeted loci, 541 were from the Tetrapods-UCE-5Kv1 set (www.ultraconserved.org) and the remaining 44 were developed to capture loci from the Squamate Assembling the Tree of Life project (Wiens et al. 2012).

Genomic DNA was extracted from tissue (tail tips, liver) with either a Qiagen DNeasy blood and tissue extraction kit (Qiagen Inc., CA, USA) or NaCl extraction method (MacManes 2013). We used a Qubit fluoremeter (Life Technologies, Carlsbad, CA) to measure DNA concentration of extracted samples and standardized to 400ng (nanograms) per sample. Genomic DNA was sheared to a target peak size of 400bp with a Bioruptor Pico (Diagenode Inc., Danville, NJ, USA). Library sequence preparation was done with an Illumina TruSeq Nano kit (Illumina, San Diego, CA), and all cleanups in between steps were done with Ampure XP beads (Beckman Coulter Life Sciences, Indianapolis, IN). We first hybridized genomic DNA to the RNA probes, with a mixture of blocking probes consisting of TruSeq Nano forward and reverse complements, and then used chicken (Chicken Hybloc, Applied Genetics Lab Inc., Melbourne, FL) and salmon blockers to reduce the binding of repetitive DNA sequences; hybridization of RNA probes to genomic DNA lasted for 24 hours at 65°C. Following hybridization, libraries were enriched through 20 PCR cycles with TruSeq adapter primers and Phusion High-Fidelity DNA Taq polymerase (New England Biolabs Inc., Ipswich, MA). We quantified final libraries through quantitative PCR (qPCR) on an Applied Biosystems Step One Plus thermocycler (Applied Biosystems Inc., Foster City, CA) with probes that targeted five loci that are located on different chromosomes in the *Anolis* genome. Final libraries were also quantified with an Agilent Tapestation 2200 (Agilent Technologies, Santa Clara, CA). All samples were pooled in equimolar ratios (based on qPCR results) and combined with 24 samples from other projects (a total of 48 individuals). Sequencing was performed on a single Illumina HiSeq 2500 lane (250bp paired-end, "Rapid run" mode) at the Vincent J. Coates QB3 Sequencing facility at UC Berkeley.

Bioinformatics and Dataset Assembly

We assembled a nuclear dataset consisting of phased alleles where each individual was represented by two alleles/haplotypes per locus. This dataset was assembled with a custom python pipeline (developed by Sonal Singhal, available at https://github.com/singhal/SqCL). We used Illumiprocessor and Trimmomatic (v0.36; Bolger et al. 2014) to remove adaptors and barcodes, de-multiplex individuals, and remove low quality raw sequence reads (raw data stats can be found in Supplemental Table S1); clean reads were merged with PEAR (v0.9.10; Zhang et al. 2014). Reads were then assembled into contigs, per individual, in Trinity (v2.2.0; Grabherr et al. 2011). We then retained the assembled contigs that matched the 1170 probes (585 loci) with BLAT (v36; Kent 2002). Next, we assembled pseudo-reference genomes (PRGs) for each species to be used in variant calling. If an individual's assignment to a species was ambiguous, we assigned that individual to its own "species". We then aligned our raw reads (for each individual) back to these PRGs to determine allelic variants with BWA (v0.7.12; Li and Durbin 2009), samtools (v1.3.1; Li et al. 2009), and Picard (v2.4.1; http://broadinstitute.github.io/picard/). GATK (v3.6; McKenna et al. 2010) was used to remove duplicates, identify SNPs and indels via standard hard filtering parameters and variant quality score recalibration according to best practices recommendations (Auwera et al. 2013). All bases, variant and invariant, were retained in the data matrix if they had $\geq$10x sequencing depth and a Phred quality score $\geq$20. SNPs were phased in relation to each other when paired reads spanned multiple variants, resulting in "blocks" of phased sequence that were hundreds of BPs long. With no good way to orient these phased blocks with respect to each other (e.g., long-range phasing), we oriented blocks randomly in relation to each other. Haplotypes were then combined by locus and then aligned in MAFFT (Katoh and Standley 2013). Resulting alignments were manually inspected for ambiguous regions and hand-edited as needed.

Mitochondrial ("mt") sequence data are often obtained as "by-catch" during sequence capture dataset sequencing, given that mitochondrial genomes are not targeted during library preparation. We used a pipeline developed by Alana Alexander

and freely available on github (https://github.com/laninsky/Pulling-out-mitogenomes-from-UCE-data/) to assemble a whole mitochondrial genome dataset for the individuals sequenced in this study. Briefly, we installed a local version of NCBI BLAST (Altschul et al. 1990) and used the mitochondrial genome of *Liolaemus chehuchekenk* (assembled into a single contig during *de novo* assembly and verified in NCBI BLAST) to serve as a reference library. We then performed a BLAST search of our Trinity contigs from each individual against the reference *L. chehuachekenk* genome at 75% similarity. The program seqtk (https://github.com/lh3/seqtk) was then used to extract the FASTA sequences of the contigs that matched the reference mt genome. A "sample-specific" mt genome was then generated for each individual, and contigs from each individual were then searched against its own reference mt genome at 95% similarity to find any contigs we may have missed during the first search. We ran these last two steps iteratively (creating a sample-specific reference and BLASTing contigs to it) until no new contigs were found matching the reference genome. At that point, we used Geneious v10 (Biomatters; Auckland, New Zealand) to align these contigs to the reference *L. chehuachekenk* mt genome.

Testing for Hybrids

We tested if particular individuals were hybrids because of a signal of mito-nuclear discordance (see Results) and high morphological variation in restricted geographic areas. First, we used a technique developed by Joly et al. (2015) that calculates genetic distances between individuals using SNPs. Using simulations, Joly et al. (2015) showed that these distances identify hybrids that are genetically intermediate between two parental species. The expectation is that a perfectly intermediate hybrid will have a genetic distance ("I") of 0.5, where $I = \frac{D_{AX}}{(D_{AX}+D_{BX})}$; A and B are the parent species, X is the suspected hybrid, and D_{AX} is the genetic distance between parent A and the hybrid. To generate a random distribution of I values with which to compare our suspected hybrids, we assigned random trios of

individuals as parents and hybrid. This distribution will generate an expectation of the average distance between any three individuals, thus providing a background set of I values with which to compare our suspected hybrids. We then compared I values of our suspected hybrids (3 *L. melanops* and 1 *L. martorii* individual) to this background "null" distribution. Joly et al. (2015) showed Nei's distance to be the most accurate at inferring hybrids, so we therefore calculated Nei's distance to infer hybrid individuals.

Also, we tested for putative hybrids through a discriminant analysis of principal components of genetic data in the R package Adegenet (Jombart et al. 2010; Jombart and Ahmed 2011). For this, we used all variable sites (12,651) and not just unlinked single nucleotide polymorphisms (SNPs). Hybrid individuals should fall outside the cluster (in PCA-space) of their parental species (when multiple individuals per species are available), and more specifically, in between (in PCA-space) parental species.

Phylogenetic Analyses

Gene Trees.— Gene trees were inferred to visualize gene genealogical relationships for determining hybrid individuals, and to serve as input for our network analyses (see below). We used jModelTest v2.1.7 (Guindon and Gascuel 2003; Darriba et al. 2012) on each alignment (including outgroup data) to infer the appropriate DNA substitution model based on the Bayesian Information Criterion. We inferred gene trees in RAxML v8.2 (Stamatakis 2014) with the top-ranking DNA substitution model and 100 bootstrap (BS) iterations for each locus, with sequence data for *Liolaemus rothi* rooting all gene trees. To mitigate alignment errors, we examined each gene tree for long branches and hand-checked dubious alignments.

Multi-Species Coalescent Tree.— We inferred the species tree under the multi-species coalescent model (Rannala and Yang 2003; Yang and Rannala 2010) in the program BP&P v3.3 (Yang 2015). This Bayesian method accounts for ILS when estimating the species tree from sequence data. Individuals (and alleles) must be assigned to species before analysis, and we did so based on expert identification and the current taxonomy.

Putative hybrids were conservatively identified (e.g., any suspected as hybrids based on previous morphological and mtDNA data), and assigned to their own lineage. Gene flow is a clear violation of the assumptions of many phylogenetic inference programs, so we ran two sets of analyses: one set including putative hybrids assigned to their own lineage, and the second set with putative hybrid individuals removed.

Two parameters must be specified by the user with priors in BP&P, θ and τ, which correspond to population sizes and divergence times, respectively. Note that in order to estimate θ, a minimum of two sequences per "species" is needed, and many species (terminal nodes) in the genotypes dataset are represented by a single individual/sequence. We specified two different combinations of θ and τ priors to ensure our results were stable, and conducted four replicates of each analysis. One set of analyses used a gamma prior G(5, 1000) on θ, giving a mean value of $5/1000 = 0.005$, with a gamma prior G(5, 2000) on τ, or a mean of 0.0025. These priors were based on the average pairwise sequence distances that we calculated across a subset of our loci. The second set used G(2, 200) for θ and G(2, 400) for τ, representing larger population sizes and longer time between population divergences, which was again based on loci with higher variation in our dataset (e.g., $\sim$1% sequence divergence within a locus). Species tree analyses were run on two datasets, both with and without suspected hybrids, with a burn-in of 25000 generations and post burn-in of 80,000 generations. Convergence was assessed by examining posterior estimates of θ, τ, and topological consistency across independent runs.

SVDquartets.— A new class of multi-species coalescent-based species tree estimation was recently designed, which does not utilize summary statistics nor gene trees, but rather infers a topology based on 4-taxon relationships inferred through site patterns (e.g., SNPs; Chifman and Kubatko 2014, Chifman and Kubatko 2015). The uncertainty in species-level relationships can then be inferred through non-parametric bootstrapping. This method is implemented in the program SVDquartets (through PAUP; Swofford 2003) and can be performed in seconds (inferring just the tree) or minutes (bootstrapping) on a standard desktop computer. Individuals/alleles were

assigned to species as in the BP&P analyses. We inferred the species tree in SVDquartets on these two datasets, evaluating all possible quartets with 100 bootstrap replicates to assess uncertainty in species-level relationships.

Network Analyses.— We also inferred the evolutionary history of this group with Phylonet (Than et al. 2008) to account for possible hybridization between species. As in many "species tree" analysis programs, Phylonet requires that individuals must be assigned to species. We based our assignments on current taxonomy, and inferred the network with the two datasets, one including individuals sampled in putative hybrid zones and the other dataset excluding hybrids. Phylonet analyzes gene tree topologies (e.g., does not take sequence data), so we used the maximum likelihood gene tree topologies inferred in RAxML. Furthermore, the user specifies the number of reticulation events in the phylogeny, which we explored between 0-8 reticulation events. Due to computational costs, we inferred each network under maximum pseudo-likelihood (MPL), with five replicates per analysis. We determined the best-fitting network through AIC model selection (Akaike 1998; Sullivan and Joyce 2005), where the number of free parameters (k) was the sum of internal branches, including the number of reticulations (Y. Yu, pers. comm.).

Concatenation.— We concatenated all nuclear loci and inferred a tree for this "super matrix" in RAxML v8.2 (Stamatakis 2014) with the GTR + Γ DNA substitution model with 100 bootstrap iterations. All "1" and "2" alleles were concatenated together across loci, resulting in two "alleles" per individual in the concatenated tree. We do not know the phase of each allele with respect to the two alleles at each locus, so the concatenation of alleles across loci is arbitrary.

Mitogenomic Trees.— We inferred the mitochondrial ("mt") phylogeny from whole mt genomic alignments in RAxML v8.2 (Stamatakis 2014). The analysis was conducted on a concatenated alignment, which was given a single partition. The best-fit model of sequence evolution was determined in jModelTest v2.1.7 (Guindon and Gascuel 2003; Darriba et al. 2012). Support for phylogenetic relationships was determined through

100 bootstrap iterations.

Results

Alignments

Alignment summaries (created by scripts from Portik et al. 2016), including the number of taxa, alignment lengths, number and percent of informative sites, and percent of gaps and missing data, were generated for datasets both with and without outgroup data and can be found in Supplemental Figures S1-2. Sequence data were poor for the outgroups *Liolaemus bibronii* and *L. kingii*, in addition to the ingroup sample for *L. canqueli*, and therefore were not included in phylogenetic analyses (Supplemental Table S1). Our final dataset therefore consisted of 27 ingroup individuals (including *L. purul*) and two outgroup individuals. We recovered 580 loci with $> 75\%$ taxon coverage per locus (Supplemental Table 1). On average, alignments are 510bp with 11.2 parsimony-informative sites per locus for just ingroup data (Fig. 2; Supplemental Figs. S2).

Hybrid Detection

Our background distribution of I calculations showed a somewhat bimodal distribution, with a large spike at $\sim$0.5 (Supplemental Fig. S3). Three suspected *L. melanops* hybrids (based on unpublished morphological and mtDNA data) had I values of 0.54 – 0.57, whereas the suspected *L. martorii* hybrid had an I value of 0.38. Given that these values fall into the middle of our background distribution, we cannot state with confidence whether or not these individuals are or are not hybrids.

In our Adegenet analyses, the suspected *L. martorii* hybrid ("*L. martorii* N") is inferred to be intermediate (in PCA-space) between its two suspected parental species (*L. martorii* and *L. melanops*; Supplemental Fig. S4). The three individuals sampled from a suspected hybrid zone between *L. melanops* and *L. shehuen* fall outside the space that encompasses the genetic diversity of *L. melanops* (Supplemental Fig. S4).

However, these individuals do not lie between suspected parental species, as did the *L. martorii* sample. Because unpublished morphological evidence suggests these are hybrids, we took a conservative approach and treated these individuals as hybrids and performed all analyses both with and without them to ensure the stability of our phylogenetic results.

Gene Trees

The two most frequent models of DNA substitution were F81 and HKY85 (with or without I and/or Γ; Supplemental Tables S2). With resolved and supported gene trees, putative hybrids can be identified based on distinct placement of their two alleles into divergent parental clades. In general, resolution was low with very few well-supported clades within each gene tree, so we could not identify hybrids with this approach.

Multi-Species Coalescent Tree

The monophyly of the *L. fitzingerii* species group is strongly supported with a posterior probability (pp) value of 1.0, with *L. purul* sister to this clade (pp=0.94). Nevertheless, relationships between species within this group are poorly supported (Fig. 3; Supplemental Fig. S5). The τ prior had a noticeable impact, where shorter branches were estimated under the larger prior means. However, θ estimates were similar under the different priors. Overall, relationships show a north-to-south colonization pattern since divergence from a common ancestor, with northern species appearing at the base of the tree. One clade ((*xanthoviridis*,(*fitzingerii*,*camarones*))) is consistently and strongly (posterior probability [pp] $\geq$0.95) recovered in all analyses. Also, *L. goetschi* and *L. martorii* are recovered as early diverging species with both datasets.

SVDquartets

In general, the trees inferred with SVDquartets are similar to those from BP&P, in terms of both support and topologies (Fig. 4). Relationships between most species were poorly supported, with the northern species *L. goetschi*, *L. sp 17*, and *L. martorii* at the base of the tree, and the southern (*xanthoviridis*,(*fitzingerii*,*camarones*)) clade strongly supported with both datasets.

Phylogenetic Network

AIC model selection determined the best-fitting model included five reticulation events (Table 1; Fig. 5). As with our other analyses, internodes were generally short. However, many internodes between species were very short. Although the (*L. xanthoviridis*, (*L. fitzingerii*, *L. camarones*)) clade was not recovered in this network, affinities existed between these taxa in the network, and two of the inferred reticulation events were between *L. fitzingerii* and *L. camarones*. Two other reticulation events were inferred between *L. melanops* and suspected hybrids of *L. melanops* and *L. shehuen*. The final reticulation was inferred between *L. sp* 17 and the common ancestor of a large clade of many *L. fitzingerii* group species.

Concatenation

The length of all loci combined was 297,000bp. *Liolaemus purul* was inferred to be sister to outgroup species (Supplemental Fig. S6). Both "1" and "2" alleles within each individual were strongly supported as sister to each other, with the exception of *L. fitzingerii* N and *L. fitzingerii* Isla Leones. Alleles from these individuals formed weakly supported relationships (BS <70) inter-digitated with each other (Supplemental Fig. S6). Individuals from the widespread species *L. melanops* appear in distinct parts of the tree, however, these exact placements had little support. The recently described *Liolaemus camarones* (Abdala et al. 2012a) was inferred to form a strongly supported clade (BS = 100) with *L. fitzingerii*. The inclusion of putative hybrid individuals did

not change overall support values, maintaining generally low BS values across the tree, but generally formed clades with geographically proximate individuals (except *L. martorii S* sister to *L. morenoi*).

mtDNA Phylogeny

The percent of the entire mt genome sequenced ranged from 38 to 89, or 6616 to 15379bp, with an average of 78% complete or 13,480bp (Supplemental Table S3). The best model of sequence evolution selected was GTR+I+Γ. Monophyly of the group is supported. Within the *L. fitzingerii* species group, many relationships were supported with BS = 100, and all but one had BS support >70 (Fig. 6; Supplemental Fig. S7). In general, clades were composed of geographically cohesive groups. Similar to the concatenated nDNA trees, we recovered a clade of ((*L. fitzingerii*, *L. camarones*), *L. xanthoviridis*), and this is also part of the most "derived" clade as in the concatenated nDNA tree. However, many notable differences are evident between the mt- and nDNA concatenated phylogenies. First, *L. camarones* is sister to *L. fitzingerii*, vs. within *L. fitzingerii* as in the concatenated nDNA tree. Secondly, the general pattern of a north-to-south colonization pattern is not seen in the mitochondrial tree. Rather, the early diverging species are those from the central part of the *L. fitzingerii* group range (e.g., *L. canqueli*, *L. sp 16*, *L. sp 17*, and *L. sp Cona Niyeu*). Third, individuals from the species *L. melanops* are strongly supported as occurring in different parts of the tree. Interestingly, these individuals that have highly different placement between the mt- and nDNA trees map to phylogeographic clade boundaries of the mtDNA tree (Fig. 6). Similarly, the southern *L. martorii* sample is placed with *L. melanops* individuals, distant in the tree from the northern *L. martorii* individual.

Discussion

Our results indicated that despite of the high level of morphological diversity seen in the *Liolaemus fitzingerii* group, many of the relationships between species were poorly

supported in several genomic analyses. This suggests that this species group underwent a rapid and somewhat simultaneous radiation from a common ancestor, or, not enough information/variation in the genetic data. Most analyses also revealed a topology supporting a north-to-south colonization pattern of species in this group; the only clade consistently recovered was that of the southern-most species, *L. xanthoviridis*, *L. fitzingerii*, and *L. camarones*. A comparison of n- and mtDNA phylogenies revealed strong discordance in terms of phylogenetic placement of certain individuals, and these individuals occur at phylogeographic clade boundaries (Fig. 6), suggesting introgression as the cause of this discordance (Funk and Omland 2003; Leaché 2009). However, two methods that we used specifically to detect hybrids were not able to support this hypothesis.

Resolving Rapid Evolutionary Radiations

Evolutionary radiations generally follow the evolution of morphological novelties or the availability of novel ecological niches in a particular environment, and are therefore inferred to be adaptive (Schluter 2000). Many radiations from an ancestral form are rapid. When this happens, the resulting phylogenetic pattern will approximate a star phylogeny, where internal nodes are either short or non-existent. For such radiations, estimating relationships between lineages is difficult at best. Many simulation studies have shown that dozens or even thousands of loci are needed to obtain correct/accurate phylogenetic estimates (e.g. Liu et al. 2009). But as we have shown in this study, even a genomic scale dataset cannot provide significant support for interspecific relationships in some rapid radiations.

One impediment to estimating a resolved phylogeny is homoplasy, which makes it difficult to resolve ancient divergences, where even model-based approaches can fail (e.g. Dopazo and Dopazo 2005). Rare genomic changes (RGCs), such as insertion-deletion events (particularly in coding regions), can be particularly informative for resolving ancient rapid radiations (e.g. Venkatesh et al. 2001), but are more difficult to employ with younger radiations where these characters have not sorted

by species. A second factor that could lead to an unresolved and poorly supported phylogeny is the lack of phylogenetic information in a dataset. Internal nodes exist because of shared nucleotide changes across descendent taxa, and in the case of a rapid radiation, little time exists for phylogenetic information in the form of shared nucleotide changes to evolve. Given the paucity of these changes, obtaining sequence data from as much of the genome as possible will increase the odds of observing these few characters to provide phylogenetic resolution.

It might be argued that using sequence capture datasets composed of "ultra-conserved elements" at shallow levels (e.g., population and inter-species studies) is ill-advised, as these loci were developed to match genomic regions that have been conserved across deep evolutionary time (tens and hundreds of millions of years). However, some authors (e.g. Harvey et al. 2016) have shown that UCEs are useful in population-level studies. Given their higher levels of variation, 44 of the loci we targeted were originally developed for the Squamate Assembling the Tree of Life project (Wiens et al. 2012) with Sanger sequencing approaches. For ingroup only, our dataset had an average of ~11 informative sites per locus, corresponding to 2.24% of sites being informative. This level of genetic variation and informativeness puts this species group in the realm of other study systems that did produce resolved phylogenies (Smith et al. 2014). Therefore, the incompletely resolved phylogeny of this group probably does not reflect limited genetic variation in our data.

An unresolved phylogeny, at least when analyzed with a substantial amount of data, still provides an important signal of biological history because it provides information about the evolutionary process (Hoelzer and Meinick 1994; Rokas and Carroll 2006). An often underlying assumption of cladogenesis is that this process creates a bifuraction of evolutionary lineages. But as we have noted, polytomous branching can be the result of a rapid radiation. Another biological reason for an unresolved/poorly supported phylogeny is hybridization between nascent species following divergence from a common ancestor (Davis and Nixon 1992). In tandem, a rapid radiation followed by hybridization of incipient species could lead to weakly

supported relationships between "species", which is indeed biologically meaningful.

Detecting Hybridization with Sequence Data

Sequence data can effectively detect hybrids, particularly when viewed in a phylogenetic perspective. Based on intermediate morphology and mito-nuclear discordance, we hypothesized some of the individuals in this study were of hybrid origin. Because rapid radiations show short internodes, distinguishing between ILS and hybridization is difficult (Holder et al. 2001). Alternatively, when parent species are well-differentiated and form independent clades, the alleles of hybrid individuals are readily recovered in the two different clades (e.g. Alexander et al. 2016). Furthermore, when an entire species/population is of hybrid origin, or when hybrid individuals are represented by a single consensus genotype (e.g., not phased alleles), phylogenetic support values will be reduced (due to the ambiguous placement of the admixed genotypes/individuals); this fact has been formalized into software that detects hybrids (Schneider et al. 2016). We did not witness a systematic change in bootstrap values when removing putative hybrid individuals from our dataset. In a related context, network approaches such as Phylonet seem promising for detecting hybridization events, because the majority of inferred reticulation events in our dataset seemed to make sense and corroborated independent hypotheses based on unpublished morphological and mtDNA analyses of hybridization in those individuals.

Another popular method for measuring gene flow with sequence data is via an isolation-migration model such as that implemented in IMa2 (Hey 2010). This method requires an input topology of species-level relationships, rendering it difficult to implement when interspecific relationships are poorly supported, as is the case in the *L. fitzingerii* group. We were therefore unable to test for gene flow with this method, so we sought to identify hybrids via variable sites alone – SNPs. The first approach we took calculates genetic distances between individuals based on phased SNPs; simulations showed that this approach can detect hybrids even with as few as tens of SNPs (Joly et al. 2015). However, these simulations were based on an allopolyploidization event

between parental species that diverged 30,000 generations in the past (τ=0.003). Our BP&P results indicate much shallower divergences for *L. fitzingerii* group species (τ<<0.001), providing little time for genetic drift or other evolutionary processes to generate differences between putative parental species. Putative *L. fitzingerii* group hybrids had I values in the 0.4 – 0.5 range (results not shown), which fell in the middle of the range of our randomized I distribution. This signifies that the genomes of many individuals/species in the *L. fitzingerii* group are equally/distantly divergent from one another, rendering hybrid detection difficult.

Evolutionary History and Taxonomy of the Liolaemus fitzingerii Species Group

All of our analyses recovered poorly supported relationships between many of the species in this group. This lack of support could be due to three causes, the first two of which are biological and the third is human-mediated. The first reason is because of a rapid radiation, which is well justified in this study given that the short internodes between species is likely not due to insufficient data. A second reason could be hybridization, which would effectively reduce the distinctiveness of each species across the genome (except for genomic regions putatively involved in species identity). The final potential cause of poor resolution between species is poor taxonomy. Individuals in this study were "assigned" to species based on current taxonomy, but if what are currently described as species are actually not distinct evolutionary lineages and thus don't warrant status as species (as evidenced by molecular data), we simply inferred population-level relationships within a single species. In fact, this last point may well be justified, since the taxonomy of *Liolaemus* lizards has been criticized (Lobo et al. 2010) due to the description of taxa with little data or supporting information.

The taxonomy of the *L. fitzingerii* group is particularly complex. Whereas some species have been described based on both molecular (generally mtDNA) and morphological characters (e.g., *L. chehuachekenk*, Avila et al. 2008; *L. casamiquelai*, Avila et al. 2010), other species have been described solely based on morphological

characters (e.g., *L. dumerili* and *L. purul*, Abdala et al. 2012a; *L. camarones* and *L. shehuen*, Abdala et al. 2012b). Relationships inferred from mtDNA and morphological characters are in stark contrast to one another (e.g., this study and Avila et al. 2006; Abdala et al. 2012a and Abdala et al. 2012b). External morphological characters such as color and patterning are highly variable within species. And melanism, a character used in the diagnosis of many *L. fitzingerii* group species, varies ontogenetically, and between males and females (Escudero et al. 2012). Although we did not formally test species limits here, the candidate species from the Olave et al. (2014) study strengthened our conclusions regarding the biogeographic history of this group. An in-depth species delimitation analysis with finer-scale sampling would be necessary to fully test the species-level status of both described and undescribed taxa in the *Liolaemus fitzingerii* group and is in fact underway (Grummer et al. 2017).

We recovered the *L. fitzingerii* species group as monophyletic, which is corroborated by previous studies (e.g. Avila et al. 2006; Olave et al. 2014). Based on a fossil calibration applied to a combined n- and mtDNA dataset, Fontanella et al. (2012) inferred the date of the *L. fitzingerii* species crown group at 4.67 million years ago (mya). We estimated an age of 2.55 million years (1.9 – 3.17my 95% HPD; results not shown) for the *L. fitzingerii* group based on a molecular clock rate of 1.9355% sequence divergence per million years (calculated from Olave et al. 2014) applied to the *cyt. B* locus. Despite the discrepancy in these estimates, both results confirm the young age of the *L. fitzingerii* group. Our phylogenetic analyses showed *Liolaemus purul* as sister to the *L. fitzingerii* group (Figs. 3,4). Whether or not this species is a part of the *L. fitzingerii* group is ambiguous, as it could either be the earliest diverging member of the clade, or sister to the *L. fitzingerii* species group. Sampling other outgroup species that are close relatives of this group may have provided more conclusive results for this question. Nonetheless, our results show a close relationship between *Liolaemus purul* and the *L. fitzingerii* species group *sensu strictu*.

Across 580 nuclear loci, the mean number of parsimony-informative sites (PIS) was 11.2 (range 0-47). The loci derived from ultraconserved elements showed a wider

range of PIS (0-47) as compared to the loci from the Squamate Tree of Life project (5-34). However, on average, the Squamate loci were more informative with 16.8 vs. 10.9 PIS (Supplemental Table S4). A comparable amount of genetic variation seen in the *L. fitzingerii* species group has been found in other Squamate systems both where there are multiple species with clear-cut boundaries, and also within systems where only a single species is recognized. For instance, the *Uma scoparia* and *Uma notata* complexes had an average 11.2 segregating sites across 14 nuclear loci (Gottscho et al. 2014). Jackson and Austin (2010) reported a similar diversity with an average of 14.1 PIS across seven nuclear loci (after removing the outlier locus "SELT") in the widespread and morphologically conserved eastern North American species *Scincella lateralis*. The high phenotypic diversity seen in the *L. fitzingerii* group led to many species being described solely on external characteristics with little regard to molecular-based estimates of diversity and relationships. The amount of molecular diversity we see in the *L. fitzingerii* species group is not in agreement with the number of species that have been described.

Our nDNA data suggest a north-to-south colonization pattern of the *L. fitzingerii* group over time. Whereas relationships between many of the species in the central part of the range (southern Rio Negro and northern Chubut provinces) are poorly resolved, a strongly supported (*L. xanthoviridis*,(*L. fitzingerii*,*L. camarones*)) clade (also recovered in Avila et al. 2006) in the southern portion of the group's range was consistently recovered (Fig. 1). The southern part of the *L. fitzingerii* group's distribution, which in its entirety spans ~39-50°S, is well within the latitudes expected to have been affected by Pleistocene glaciations (Rabassa et al. 2005). In fact, studies of other *Liolaemus* species have shown that late middle- and late-Pleistocene glaciations affected various populations in this same latitudinal region (Victoriano et al. 2008; Vera-Escalona et al. 2012; Vidal et al. 2012). Though we did not formally test the effects of Pleistocene glaciations here, it is certainly plausible that the southern (*L. xanthoviridis*,(*L. fitzingerii*,*L. camarones*)) clade was the result of an ancestral population that colonized southern regions of this group's range following glacial

retreat; the presumably bottlenecked/small nature of this colonizing population would in-part explain this clade's distinctiveness due to genetic drift.

Conclusions

Through a rigorous investigation of genomic DNA, we have inferred a rapid evolutionary radiation that gave rise to the nine described species seen in the *L. fitzingerii* species group today. The conflicting set of relationships inferred between mt- and nDNA datasets, in particular with individuals at clade boundaries, strongly suggests hybridization. However, we were not able to quantitatively verify hybrids in our sample. In regards to phylogenetic relationships, few were well-supported. Nonetheless, this information is still important in understanding the biogeographic and evolutionary history of the *Liolaemus fitzingerii* species group. Our results provide a phylogenetic hypothesis and historic context with which to better understand the evolutionary processes that gave rise to the patterns we inferred in this study.

Acknowledgments

This work used the Vincent J. Coates Genomics Sequencing Laboratory at UC Berkeley, supported by NIH S10 OD018174 Instrumentation Grant. This research was funded in part by a National Science Foundation Doctoral Dissertation Improvement Grant (DEB-1500933) to JAG, and was facilitated though the use of advanced computational, storage, and networking infrastructure provided by the Hyak supercomputer system at the University of Washington.

*

References

Abdala, C. S. 2007. Phylogeny of the boulengeri group (iguania: Liolaemidae, liolaemus) based on morphological and molecular characters. Zootaxa Pages 1–84.

Abdala, C. S., J. Díaz Gómez, and V. Juarez Heredia. 2012a. From the far reaches of patagonia: new phylogenetic analyses and description of two new species of the *Liolaemus fitzingerii* clade (iguania: Liolaemidae). Zootaxa 3301:34–60.

Abdala, C. S., R. Semhan, D. M. Azocar, M. Bonino, M. Paz, and F. Cruz. 2012b. Taxonomic study and morphology based phylogeny of the patagonic clade *Liolaemus melanops* group (iguania: Liolaemidae), with the description of three new taxa. Zootaxa 3163:1–32.

Akaike, H. 1998. Information theory and an extension of the maximum likelihood principle. Pages 199–213 *in* Selected Papers of Hirotugu Akaike. Springer.

Alexander, A. M., Y.-C. Su, C. H. Oliveros, K. V. Olson, S. L. Travers, and R. M. Brown. 2016. Genomic data reveals potential for hybridization, introgression, and incomplete lineage sorting to confound phylogenetic relationships in an adaptive radiation of narrow-mouth frogs. Evolution .

Altschul, S. F., W. Gish, W. Miller, E. W. Myers, and D. J. Lipman. 1990. Basic local alignment search tool. Journal of molecular biology 215:403–410.

Auwera, G. A., M. O. Carneiro, C. Hartl, R. Poplin, G. del Angel, A. Levy-Moonshine, T. Jordan, K. Shakir, D. Roazen, J. Thibault, et al. 2013. From fastq data to high-confidence variant calls: the genome analysis toolkit best practices pipeline. Current protocols in bioinformatics Pages 11–10.

Avila, L., M. Morando, and J. Sites. 2006. Congeneric phylogeography: hypothesizing species limits and evolutionary processes in patagonian lizards of the liolaemus

boulengeri group (squamata: Liolaemini). Biological Journal of the Linnean Society 89:241–275.

Avila, L. J., M. Morando, and J. W. Sites Jr. 2008. New species of the iguanian lizard genus liolaemus (squamata, iguania, liolaemini) from central patagonia, argentina. Journal of Herpetology 42:186–196.

Avila, L. J., C. H. F. Pérez, M. Morando, and J. Sites Jr. 2010. A new species of liolaemus (reptilia: Squamata) from southwestern rio negro province, northern patagonia, argentina. Zootaxa 2434:47–59.

Barton, N. H. and G. M. Hewitt. 1985. Analysis of hybrid zones. Annual review of Ecology and Systematics 16:113–148.

Bolger, A. M., M. Lohse, and B. Usadel. 2014. Trimmomatic: a flexible trimmer for illumina sequence data. Bioinformatics Page btu170.

Bryant, D., R. Bouckaert, J. Felsenstein, N. A. Rosenberg, and A. RoyChoudhury. 2012. Inferring species trees directly from biallelic genetic markers: bypassing gene trees in a full coalescent analysis. Molecular biology and evolution 29:1917–1932.

Cei, J. M. 1975. *Liolaemus melanops* (burmeister) and the subspecific status of the *fitzingeri* group (sauria, iguanidae). Journal of Herpetology 9:217–222.

Cei, J. M. 1980a. L'identité des syntypes de proctotretus fitzingeri duméril et bibron. Bulletin Museum National d'Historie Naturelle (Paris) 4:317–320.

Cei, J. M. 1980b. Reptiles del centro, centro-oeste y sur de la Argentina. Herpetofauna de las zonas áridas y semiáridas. Museo Regionale di Scienze Naturali.

Cei, J. M. and J. A. Scolaro. 1980. Two new subspecies of the *Liolaemus fitzingeri* complex from argentina. Journal of Herpetology 14:37–43.

Chifman, J. and L. Kubatko. 2014. Quartet inference from snp data under the coalescent model. Bioinformatics 30:3317–3324.

Chifman, J. and L. Kubatko. 2015. Identifiability of the unrooted species tree topology under the coalescent model with time-reversible substitution processes, site-specific rate variation, and invariable sites. Journal of theoretical biology 374:35–47.

Darriba, D., G. L. Taboada, R. Doallo, and D. Posada. 2012. jmodeltest 2: more models, new heuristics and parallel computing. Nature methods 9:772–772.

Davis, J. I. and K. C. Nixon. 1992. Populations, genetic variation, and the delimitation of phylogenetic species. Systematic biology 41:421–435.

Dopazo, H. and J. Dopazo. 2005. Genome-scale evidence of the nematode-arthropod clade. Genome biology 6:R41.

Escudero, P. C., I. Minoli, N. Frutos, L. J. Avila, and M. Morando. 2012. Estudio comparativo del melanismo en lagartijas del grupo liolaemus fitzingerii (liolaemini: Liolaemus). Cuadernos de herpetología 26:79–89.

Etheridge, R. E. 1993. Lizards of the *Liolaemus darwinii* complex (squamata: Iguania: Tropiduridae) in northern argentina. Bollettino del Museo Regionale di Scienze Naturali, Torino 11:137–199.

Etheridge, R. E. 1995. Redescription of *Ctenoblepharys adspersa* tschudi, 1845, and the taxonomy of liolaeminae (reptilia: Squamata: Tropiduridae). American Museum of Natural History Novitates 3142:1–34.

Faircloth, B. C., J. E. McCormack, N. G. Crawford, M. G. Harvey, R. T. Brumfield, and T. C. Glenn. 2012. Ultraconserved elements anchor thousands of genetic markers spanning multiple evolutionary timescales. Systematic biology Page sys004.

Fontanella, F. M., M. Olave, L. J. Avila, M. MORANDO, et al. 2012. Molecular dating and diversification of the south american lizard genus liolaemus (subgenus eulaemus) based on nuclear and mitochondrial dna sequences. Zoological Journal of the Linnean Society 164:825–835.

Funk, D. J. and K. E. Omland. 2003. Species-level paraphyly and polyphyly: frequency, causes, and consequences, with insights from animal mitochondrial dna. Annual Review of Ecology, Evolution, and Systematics 34:397–423.

Glor, R. E. 2010. Phylogenetic insights on adaptive radiation. Annual Review of Ecology, Evolution, and Systematics 41:251–270.

Gottscho, A. D., S. B. Marks, and W. B. Jennings. 2014. Speciation, population structure, and demographic history of the mojave fringe-toed lizard (uma scoparia), a species of conservation concern. Ecology and evolution 4:2546–2562.

Grabherr, M. G., B. J. Haas, M. Yassour, J. Z. Levin, D. A. Thompson, I. Amit, X. Adiconis, L. Fan, R. Raychowdhury, Q. Zeng, et al. 2011. Trinity: reconstructing a full-length transcriptome without a genome from rna-seq data. Nature biotechnology 29:644.

Grummer, J. A., M. M. Morando, L. J. Avila, and A. D. Leaché. 2017. Rocks and ice: the effects of geographic features and pleistocene glaciations on the gondwanan *Liolaemus fitzingerii* species group. In Preparation .

Guindon, S. and O. Gascuel. 2003. A simple, fast, and accurate algorithm to estimate large phylogenies by maximum likelihood. Systematic biology 52:696–704.

Harrison, R. G. 1993. Hybrid zones and the evolutionary process. Oxford University Press on Demand.

Harvey, M. G., B. T. Smith, T. C. Glenn, B. C. Faircloth, and R. T. Brumfield. 2016. Sequence capture versus restriction site associated dna sequencing for shallow systematics. Systematic biology 65:910–924.

Heled, J. and A. J. Drummond. 2010. Bayesian inference of species trees from multilocus data. Molecular biology and evolution 27:570–580.

Hey, J. 2010. Isolation with migration models for more than two populations. Molecular biology and evolution 27:905–920.

Hoelzer, G. A. and D. J. Meinick. 1994. Patterns of speciation and limits to phylogenetic resolution. Trends in ecology & evolution 9:104–107.

Holder, M. T., J. A. Anderson, and A. K. Holloway. 2001. Difficulties in detecting hybridization. Systematic Biology 50:978–982.

Jackson, N. D. and C. C. Austin. 2010. The combined effects of rivers and refugia generate extreme cryptic fragmentation within the common ground skink (*Scincella lateralis*). Evolution 64:409–428.

Joly, S., D. Bryant, and P. J. Lockhart. 2015. Flexible methods for estimating genetic distances from single nucleotide polymorphisms. Methods in Ecology and Evolution 6:938–948.

Jombart, T. and I. Ahmed. 2011. adegenet 1.3-1: new tools for the analysis of genome-wide snp data. Bioinformatics 27:3070–3071.

Jombart, T., S. Devillard, and F. Balloux. 2010. Discriminant analysis of principal components: a new method for the analysis of genetically structured populations. BMC genetics 11:94.

Katoh, K. and D. M. Standley. 2013. Mafft multiple sequence alignment software version 7: improvements in performance and usability. Molecular biology and evolution 30:772–780.

Kent, W. J. 2002. Blat—the blast-like alignment tool. Genome research 12:656–664.

Kubatko, L. S. and J. H. Degnan. 2007. Inconsistency of phylogenetic estimates from concatenated data under coalescence. Systematic Biology 56:17–24.

Laurent, R. F. 1992. On some overlooked species of the genus *Liolaemus* wiegmann (reptilia tropiduridae) from peru. Breviora 494:1–33.

Leaché, A. D. 2009. Species tree discordance traces to phylogeographic clade boundaries in north american fence lizards (sceloporus). Systematic Biology 58:547–559.

Leaché, A. D., A. S. Chavez, L. N. Jones, J. A. Grummer, A. D. Gottscho, and C. W. Linkem. 2015. Phylogenomics of phrynosomatid lizards: conflicting signals from sequence capture versus restriction site associated dna sequencing. Genome biology and evolution 7:706–719.

Lemmon, A. R., S. A. Emme, and E. M. Lemmon. 2012. Anchored hybrid enrichment for massively high-throughput phylogenomics. Systematic biology Page sys049.

Li, H. and R. Durbin. 2009. Fast and accurate short read alignment with burrows–wheeler transform. Bioinformatics 25:1754–1760.

Li, H., B. Handsaker, A. Wysoker, T. Fennell, J. Ruan, N. Homer, G. Marth, G. Abecasis, R. Durbin, et al. 2009. The sequence alignment/map format and samtools. Bioinformatics 25:2078–2079.

Linkem, C. W., V. N. Minin, and A. D. Leaché. 2016. Detecting the anomaly zone in species trees and evidence for a misleading signal in higher-level skink phylogeny (squamata: Scincidae). Systematic biology 65:465–477.

Liu, L., L. Yu, D. K. Pearl, and S. V. Edwards. 2009. Estimating species phylogenies using coalescence times among sequences. Systematic Biology 58:468–477.

Lobo, F., R. E. Espinoza, and S. Quinteros. 2010. A critical review and systematic discussion of recent classification proposals for liolaemid lizards. Zootaxa 2549:1–30.

MacManes, M. 2013. Available from: http://dx.doi.org/10.6084/m9.figshare.658946. Figshare 5.

Maddison, W. 1989. Reconstructing character evolution on polytomous cladograms. Cladistics 5:365–377.

Mallet, J. 2005. Hybridization as an invasion of the genome. Trends in ecology & evolution 20:229–237.

Martin, S. H., K. K. Dasmahapatra, N. J. Nadeau, C. Salazar, J. R. Walters, F. Simpson, M. Blaxter, A. Manica, J. Mallet, and C. D. Jiggins. 2013. Genome-wide

evidence for speciation with gene flow in heliconius butterflies. Genome Research 23:1817–1828.

McCormack, J. E., S. M. Hird, A. J. Zellmer, B. C. Carstens, and R. T. Brumfield. 2013. Applications of next-generation sequencing to phylogeography and phylogenetics. Molecular Phylogenetics and Evolution 66:526–538.

McKenna, A., M. Hanna, E. Banks, A. Sivachenko, K. Cibulskis, A. Kernytsky, K. Garimella, D. Altshuler, S. Gabriel, M. Daly, et al. 2010. The genome analysis toolkit: a mapreduce framework for analyzing next-generation dna sequencing data. Genome research 20:1297–1303.

Morando, M., L. J. Avila, J. Baker, J. W. Sites Jr, and M. Ashley. 2004. Phylogeny and phylogeography of the liolaemus darwinii complex (squamata: Liolaemidae): evidence for introgression and incomplete lineage sorting. Evolution 58:842–861.

Olave, M., L. J. Avila, J. W. Sites, and M. Morando. 2014. Multilocus phylogeny of the widely distributed south american lizard clade eulaemus (liolaemini, liolaemus). Zoologica Scripta 43:323–337.

Olave, M., L. E. Martinez, L. J. Avila, J. W. Sites, and M. Morando. 2011. Evidence of hybridization in the argentinean lizards liolaemus gracilis and liolaemus bibronii (iguania: Liolaemini): An integrative approach based on genes and morphology. Molecular Phylogenetics and Evolution 61:381–391.

Patel, S., R. T. Kimball, and E. L. Braun. 2013. Error in phylogenetic estimation for bushes in the tree of life. Journal of Phylogenetics & Evolutionary Biology .

Portik, D. M., L. L. Smith, and K. Bi. 2016. An evaluation of transcriptome-based exon capture for frog phylogenomics across multiple scales of divergence (class: Amphibia, order: Anura). Molecular ecology resources 16:1069–1083.

Rabassa, J., A. M. Coronato, and M. Salemme. 2005. Chronology of the late cenozoic

patagonian glaciations and their correlation with biostratigraphic units of the pampean region (argentina). Journal of South American Earth Sciences 20:81–103.

Rannala, B. and Z. Yang. 2003. Bayes estimation of species divergence times and ancestral population sizes using dna sequences from multiple loci. Genetics 164:1645–1656.

Rokas, A. and S. B. Carroll. 2006. Bushes in the tree of life. PLoS Biol 4:e352.

Schluter, D. 2000. The ecology of adaptive radiation. OUP Oxford.

Schneider, K., S. Koblmüller, and K. M. Sefc. 2016. hext, a software supporting tree-based screens for hybrid taxa in multilocus data sets, and an evaluation of the homoplasy excess test. Methods in Ecology and Evolution 2016:358–368.

Smith, B. T., M. G. Harvey, B. C. Faircloth, T. C. Glenn, and R. T. Brumfield. 2014. Target capture and massively parallel sequencing of ultraconserved elements (uces) for comparative studies at shallow evolutionary time scales. Systematic biology 63:83–95.

Stamatakis, A. 2014. Raxml version 8: a tool for phylogenetic analysis and post-analysis of large phylogenies. Bioinformatics 30:1312–1313.

Sullivan, J. and P. Joyce. 2005. Model selection in phylogenetics. Annu. Rev. Ecol. Evol. Syst. 36:445–466.

Swofford, D. L. 2003. Paup*. phylogenetic analysis using parsimony (* and other methods). version 4. .

Than, C., D. Ruths, and L. Nakhleh. 2008. Phylonet: a software package for analyzing and reconstructing reticulate evolutionary relationships. BMC bioinformatics 9:322.

Venkatesh, B., M. V. Erdmann, and S. Brenner. 2001. Molecular synapomorphies resolve evolutionary relationships of extant jawed vertebrates. Proceedings of the National Academy of Sciences 98:11382–11387.

Vera-Escalona, I., G. D'Elía, N. Gouin, F. M. Fontanella, C. Muñoz-Mendoza, J. W. Sites Jr, and P. F. Victoriano. 2012. Lizards on ice: evidence for multiple refugia in liolaemus pictus (liolaemidae) during the last glacial maximum in the southern andean beech forests. PloS one 7:e48358.

Victoriano, P. F., J. C. Ortiz, E. Benavides, B. J. Adams, et al. 2008. Comparative phylogeography of codistributed species of chilean liolaemus (squamata: Tropiduridae) from the central-southern andean range. Molecular Ecology 17:2397–2416.

Vidal, M. A., P. I. Moreno, and E. Poulin. 2012. Genetic diversity and insular colonization of liolaemus pictus (squamata, liolaeminae) in north-western patagonia. Austral Ecology 37:67–77.

Wiens, J. J., C. R. Hutter, D. G. Mulcahy, B. P. Noonan, T. M. Townsend, J. W. Sites, and T. W. Reeder. 2012. Resolving the phylogeny of lizards and snakes (squamata) with extensive sampling of genes and species. Biology letters 8:1043–1046.

Yang, Z. 2015. The bpp program for species tree estimation and species delimitation. Current Zoology 61:854–865.

Yang, Z. and B. Rannala. 2010. Bayesian species delimitation using multilocus sequence data. Proceedings of the National Academy of Sciences 107:9264–9269.

Zhang, J., K. Kobert, T. Flouri, and A. Stamatakis. 2014. Pear: a fast and accurate illumina paired-end read merger. Bioinformatics 30:614–620.

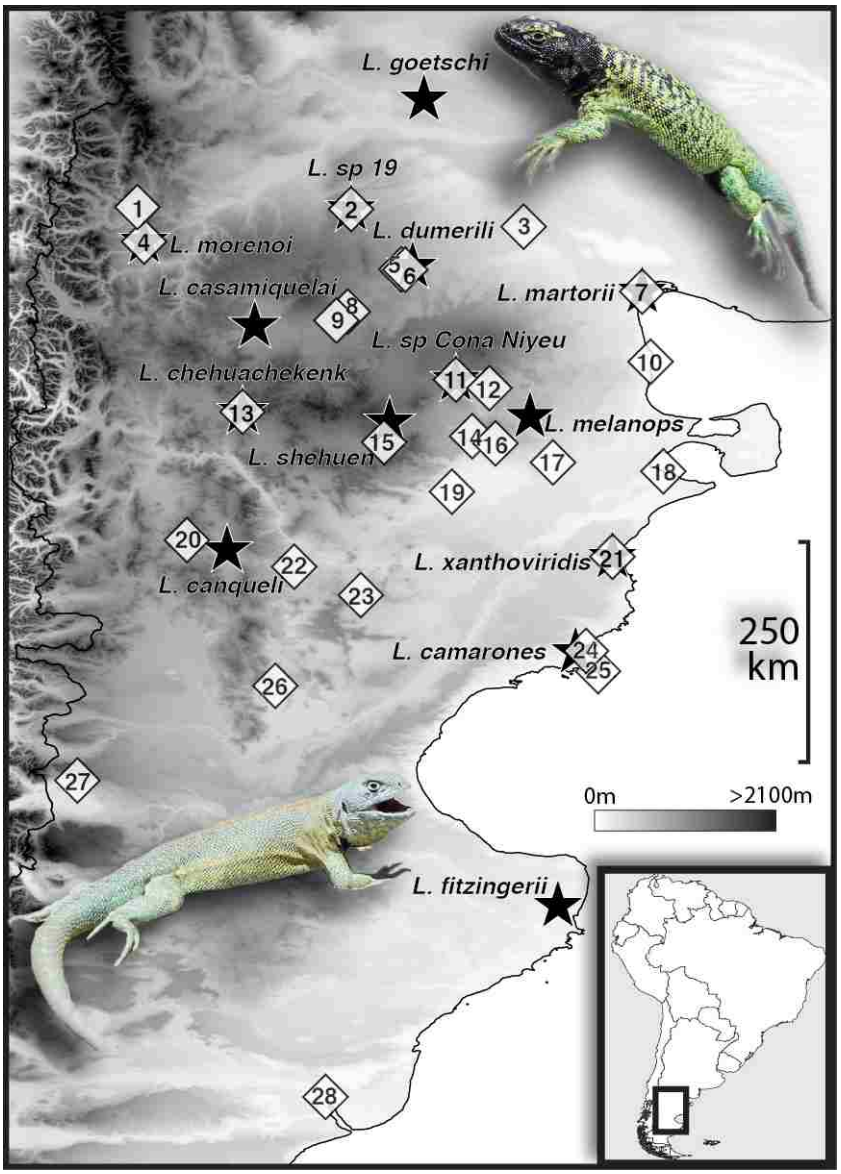

Figure 1: Sampling map of southern-central Argentina showing type localities for described and undescribed potential species in the *L. fitzingerii* species group (stars) and locations where individuals were sampled for this study (diamonds). Sampling numbers on the map correspond to the following individuals and their names used throughout this study: 1 - *Liolaemus purul*, 2 - *Liolaemus sp. 19*, 3 - *Liolaemus goetschi*, 4 - *Liolaemus morenoi*, 5 - *Liolaemus melanops* N1, 6 - *Liolaemus dumerili*, 7 - *Liolaemus martorii* N, 8 - *Liolaemus melanops* N2, 9 - *Liolaemus casamiquelai*, 10 - *Liolaemus martorii* S, 11 - *Liolaemus sp.* Cona Niyeu, 12 - *Liolaemus melanops* C, 13 - *Liolaemus chehuachekenk*, 14 - *Liolaemus sp. 18*, 15 - *Liolaemus shehuen*, 16 - *Liolaemus melanops* S1 (pictured, TR), 17 - *Liolaemus melanops* S3, 18 - *Liolaemus sp. 17*, 19 - *Liolaemus melanops* S2, 20 - *Liolaemus sp. 16*, 21 - *Liolaemus xanthoviridis* E, 22 - *Liolaemus canqueli*, 23 - *Liolaemus xanthoviridis* W, 24 - *Liolaemus camarones*, 25 - *Liolaemus fitzingerii* Isla Leones, 26 - *Liolaemus fitzingerii* N (pictured, BL), 27 - *Liolaemus fitzingerii* W, 28 - *Liolaemus fitzingerii* S.

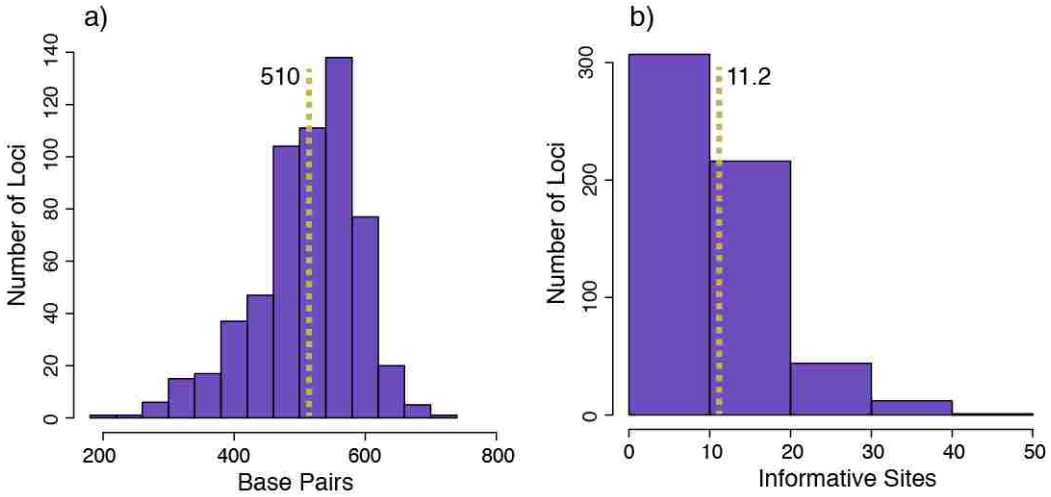

Figure 2: Sequence length (a) and number of informative sites (b) per nuclear locus for only ingroup individuals with means depicted with gold dashed lines. See Supplemental Figures S1-2 for further sequence statistics.

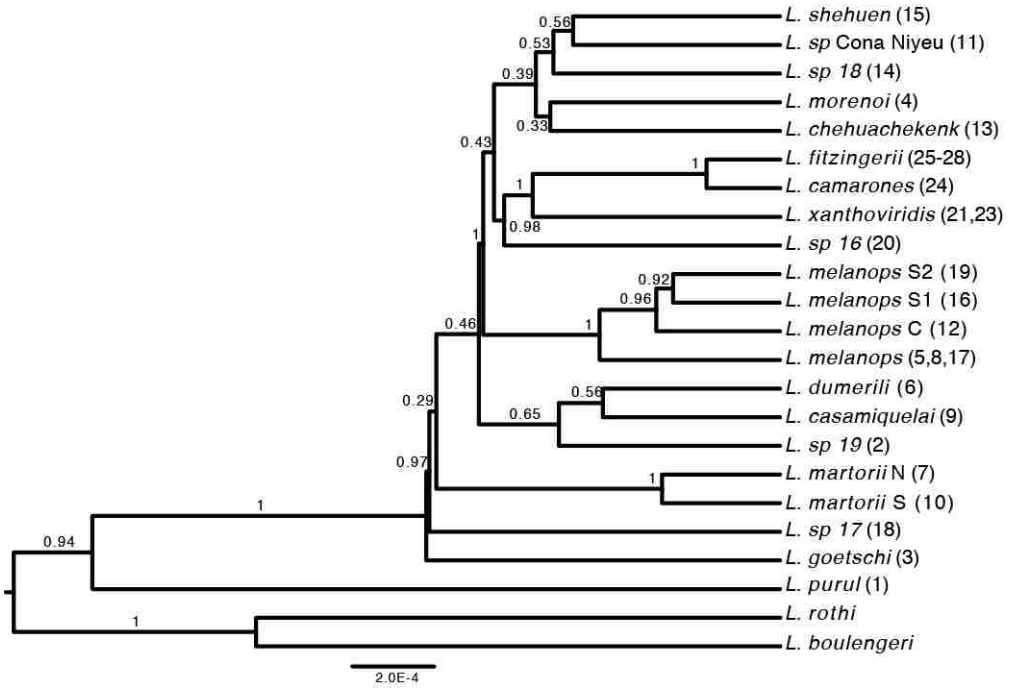

Figure 3: Multi-species coalescent phylogeny inferred with G(2, 200) for the θ prior and G(2, 400) for the τ prior, with posterior probability values shown. Numbers following taxon names correspond to sample numbers in Figure 1. Note the change in branch lengths when using priors with smaller mean values in Supplemental Figure S5. There are fewer tips than individuals because multiple individuals/alleles are assigned to each species in this tree.

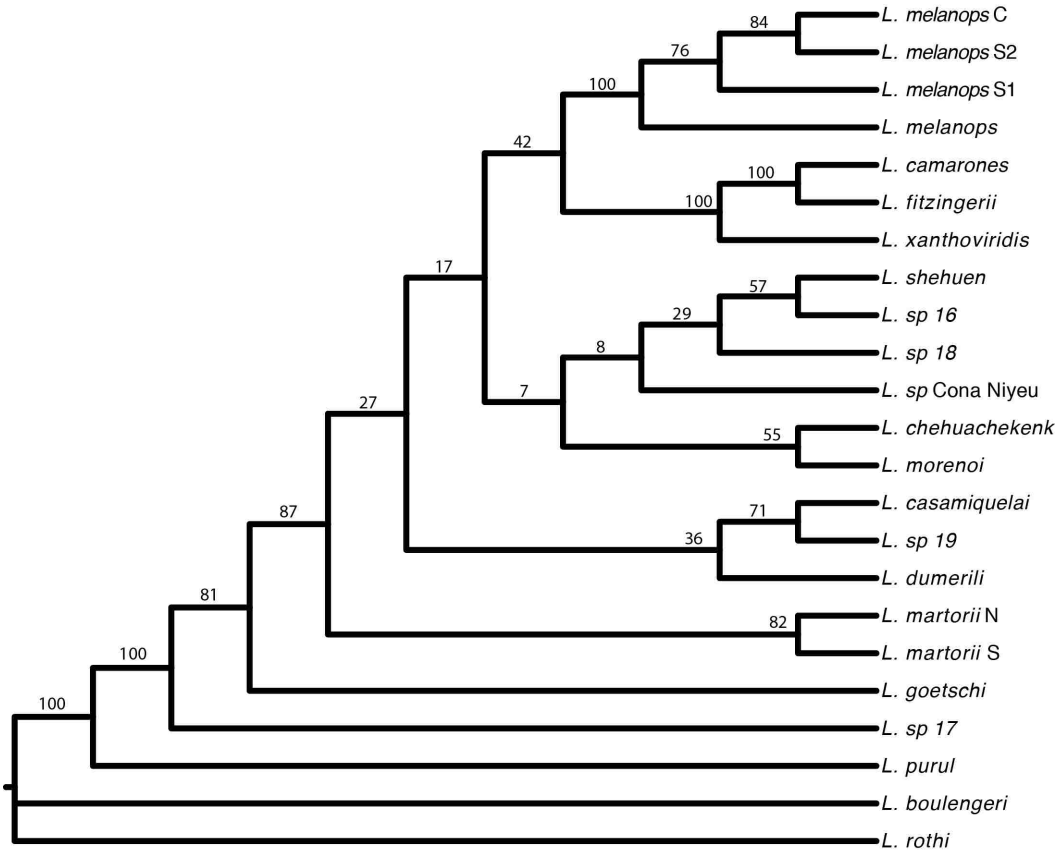

Figure 4: Phylogeny inferred in SVDquartets, with relationship support values calculated from 100 bootstrap replicates. Assignments of individuals to species is the same as in Figure 3.

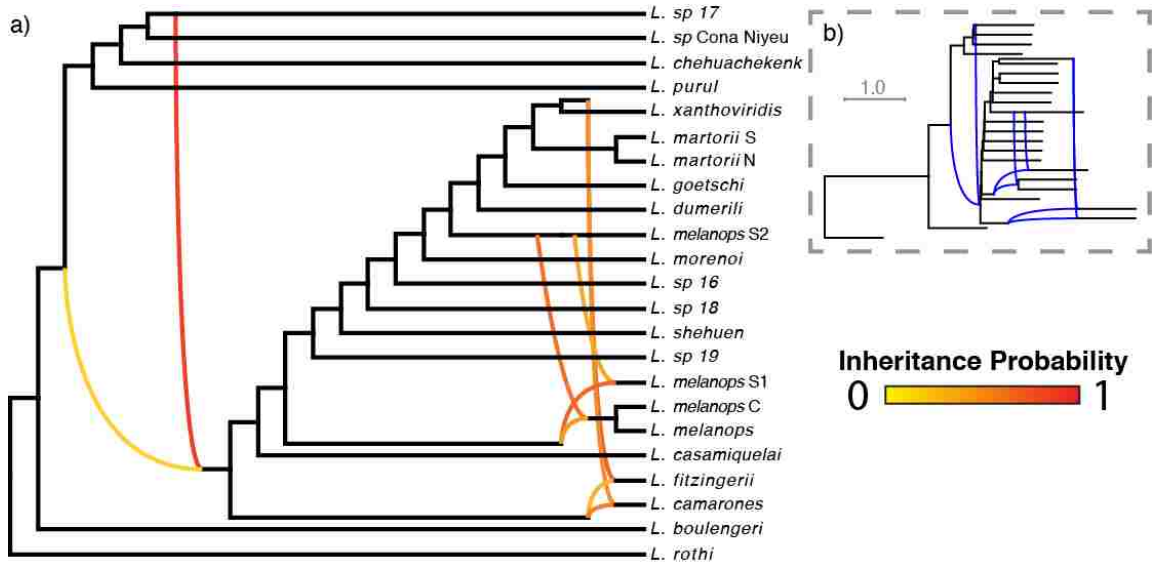

Figure 5: Phylonet network inferred with the AIC-preferred five reticulations. Reticulation events and relationships are shown in the larger network (a) and inferred branch lengths are shown in the (b) inset.

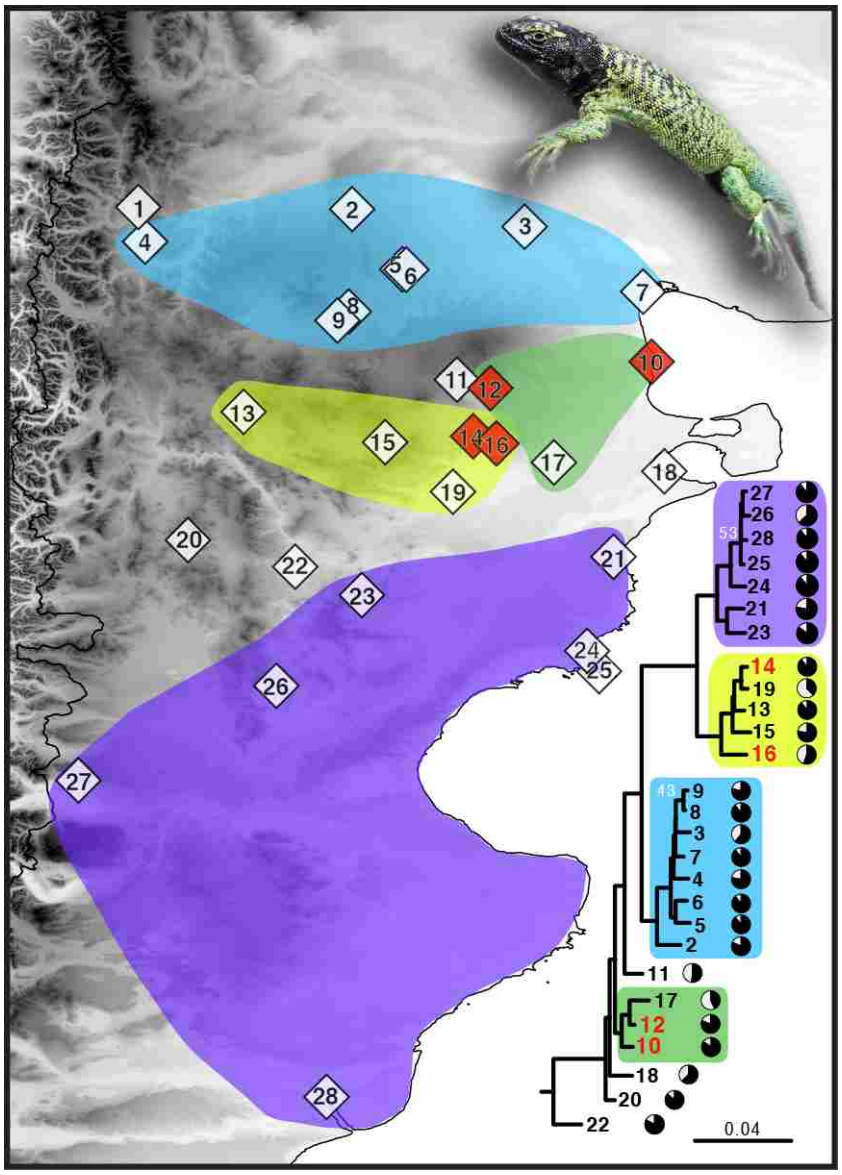

Figure 6: Maximum likelihood phylogeny inferred from the mitogenomic dataset along with geographic distributions of clades. Fraction of the mitogenome sequenced for each individual is shown in pie charts to the right (black = data present), and nodes without labels received a bootstrap support >70. Sample numbering corresponds to the names given in Figure 1. Individuals labeled in red are suspected hybrids based on morphology and discordant placement in the nDNA tree. See Supplemental Figure S7 for the full mitochondrial genealogy including outgroup data.

Table 1: Phylonet results and AIC phylogenetic network model selection, with the optimal network in bold. "BL" stands for number of branch lengths estimated, and k is the number of parameters used in the AIC calculation.

# Retics.	lnL	ΔlnL	# BLs	# Inferred Retics.	k	AIC	ΔAIC
0	-12015285		21	0	21	24030612	18821
1	-12011478	3807	22	1	23	24023002	11211
2	-12008493	2985	22	2	24	24017033	5242
3	-12007447	1046	23	3	26	24014945	3154
4	-12006527	920	22	4	26	24013105	1313
5	**-12005865**	**662**	**26**	**5**	**31**	**24011791**	**0**

Supplemental figures and tables for "Lack of phylogenetic support matters: phylogenomic evidence for a recent and rapid radiation in lizards of the Patagonian *Liolaemus fitzingerii* species group"

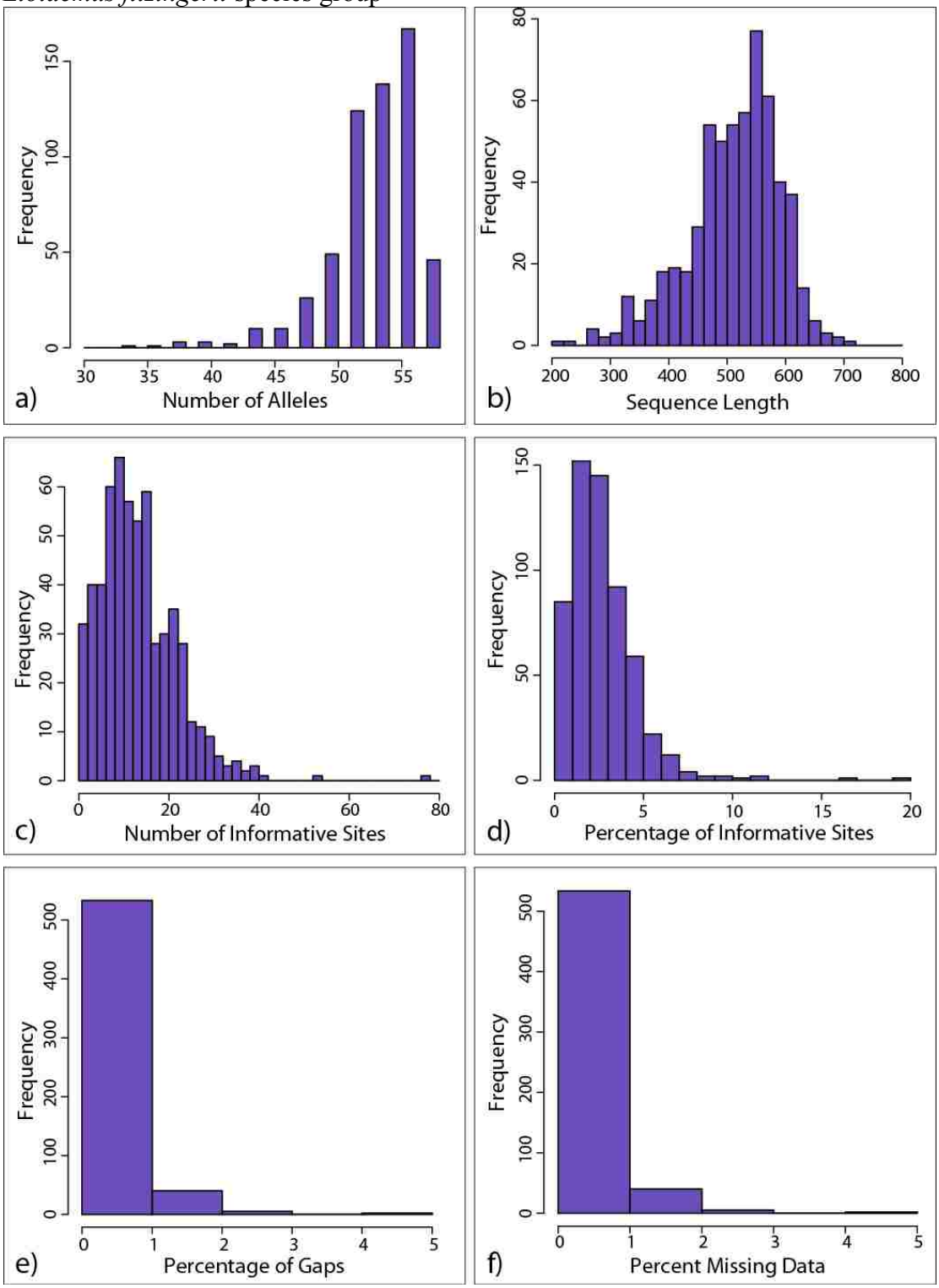

Supplemental Figure S1. Sequence data statistics when including outgroups in the alignments, including (a) number of alleles per alignment, (b) alignment length distribution, (c) number of informative sites, (d) percentage of informative sites, (e) percentage of gaps (-) per alignment, and (f) percentage of total missing data (- and ?) per alignment.

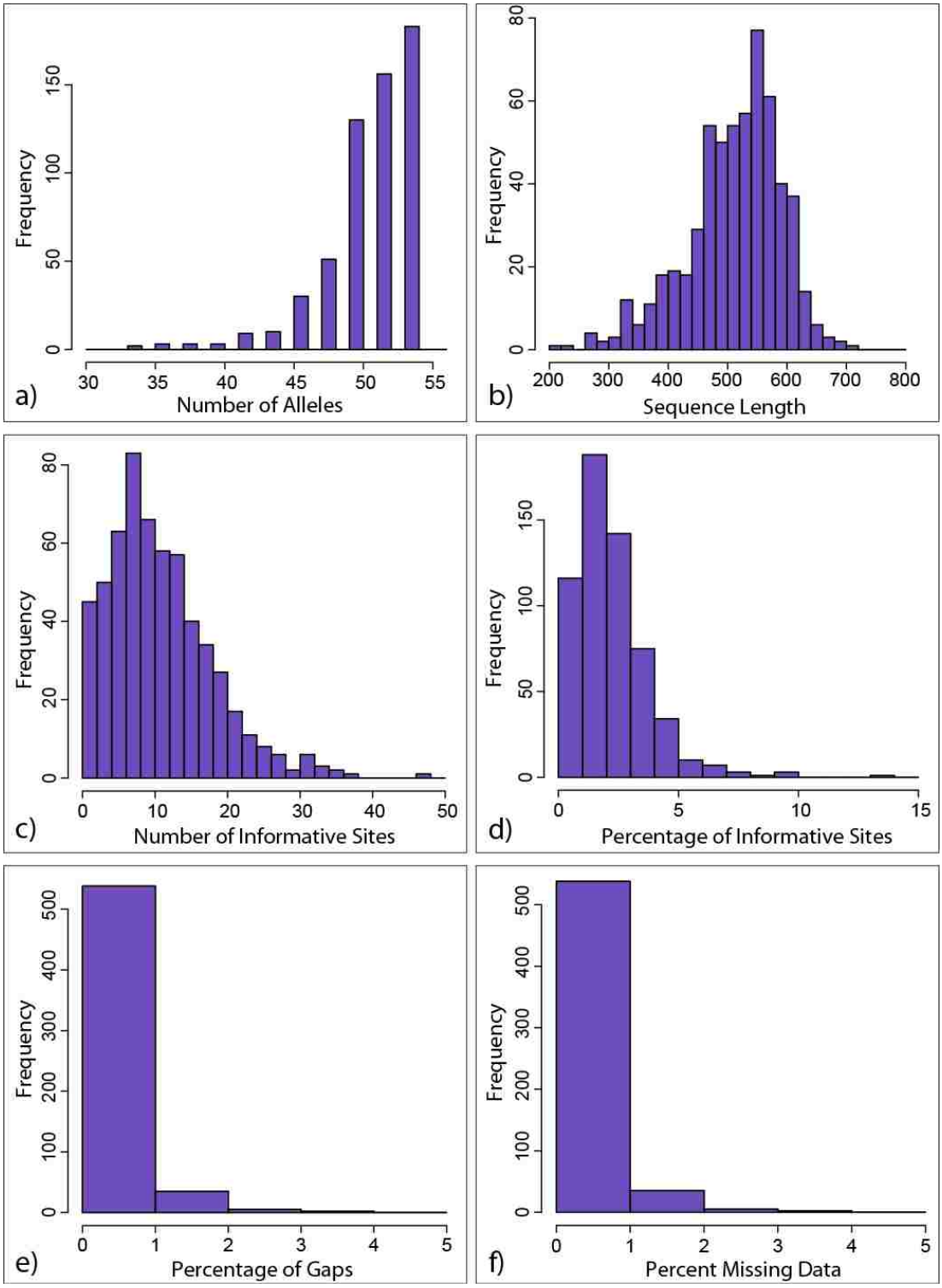

Supplemental Figure S2. Sequence data statistics when including only ingroup data in the alignments, including (a) number of alleles per alignment, (b) alignment length distribution, (c) number of informative sites, (d) percentage of informative sites, (e) percentage of gaps (-) per alignment, and (f) percentage of total missing data (- and ?) per alignment.

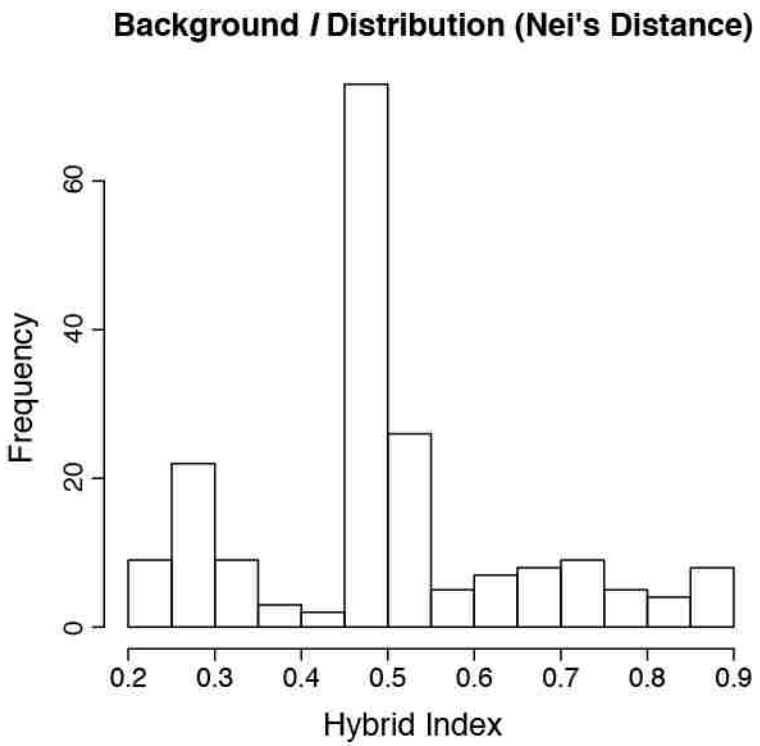

Supplemental Figure S3. Distribution of randomized *I* (hybrid index) calculations of all ingroup individuals with Nei's distance in POFAD. See the main text for a description of the *I* calculation. A hybrid F1 is expected to have an *I* value of 0.5.

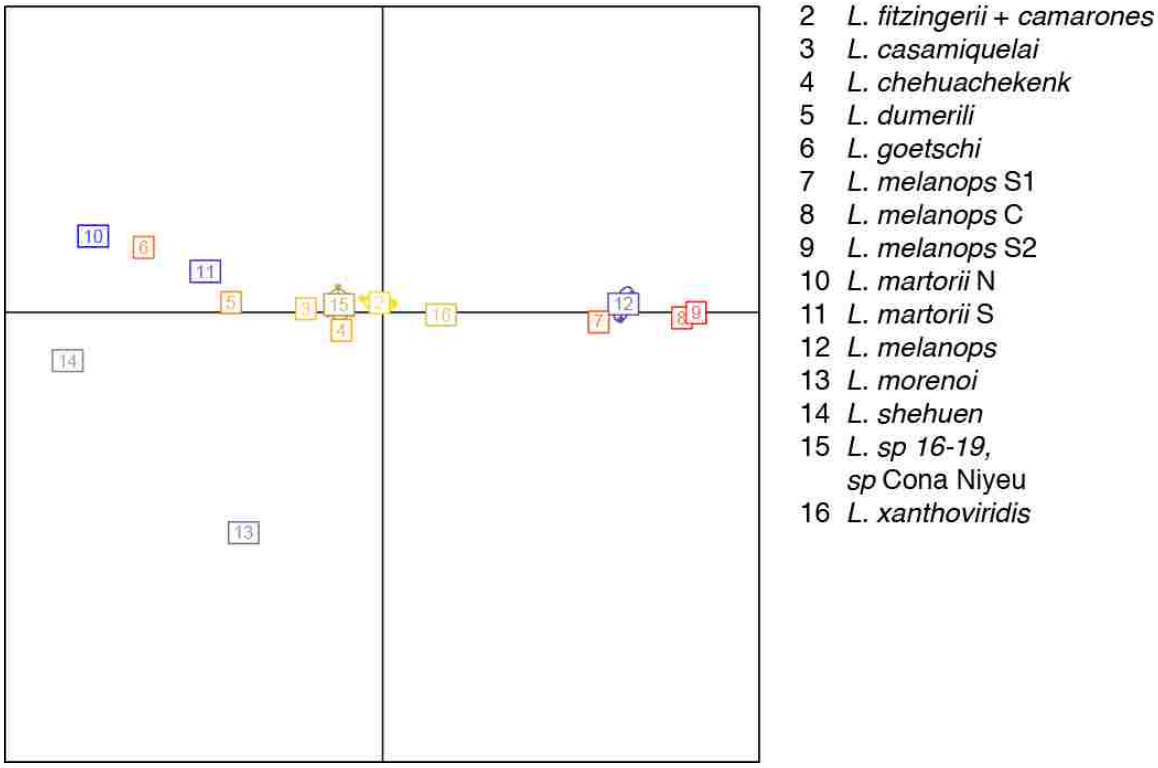

2 *L. fitzingerii* + *camarones*
3 *L. casamiquelai*
4 *L. chehuachekenk*
5 *L. dumerili*
6 *L. goetschi*
7 *L. melanops* S1
8 *L. melanops* C
9 *L. melanops* S2
10 *L. martorii* N
11 *L. martorii* S
12 *L. melanops*
13 *L. morenoi*
14 *L. shehuen*
15 *L. sp 16-19, sp* Cona Niyeu
16 *L. xanthoviridis*

Supplemental Figure S4. Discriminant analysis of principal components performed in Adegenet. Numbered individuals in the plots correspond to the legend on the right. The suspected hybrids are *L. martorii* N and *L. melanops* C, S1, and S2.

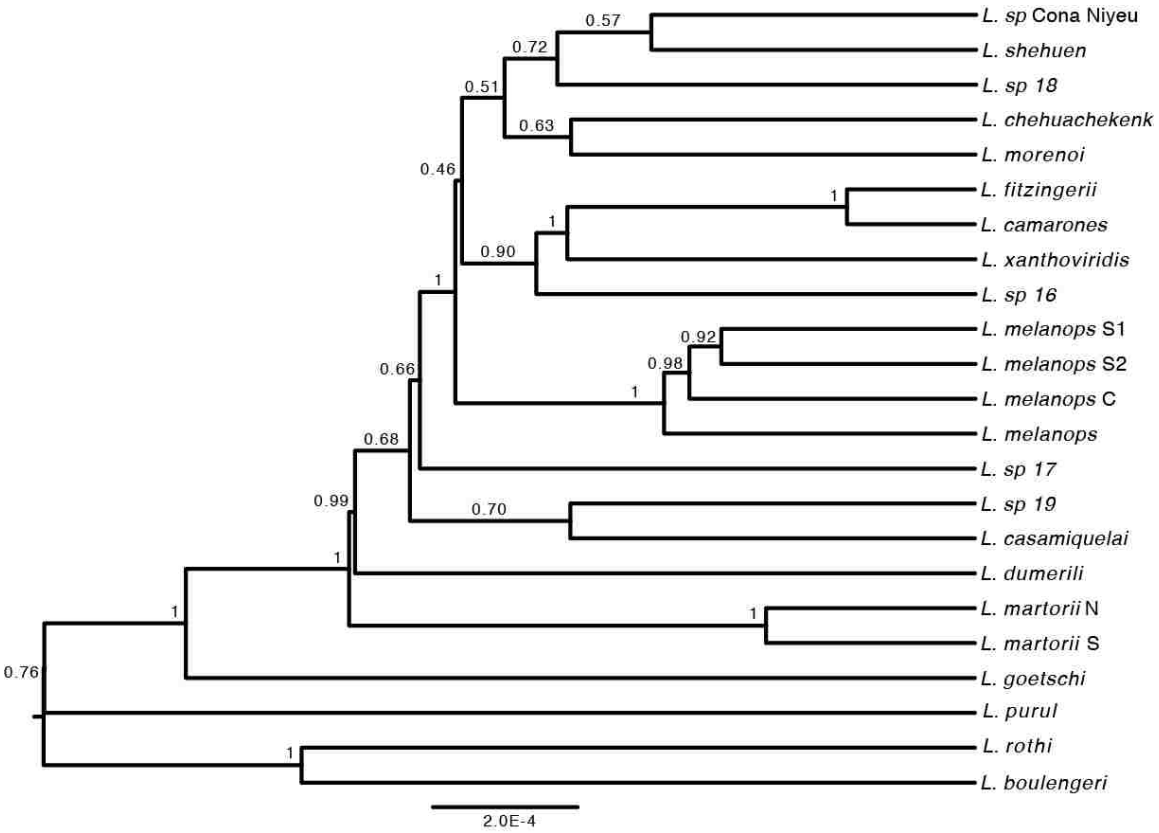

Supplemental Figure S5. Multi-species coalescent phylogeny inferred using G(5, 1000) for the θ theta prior and G(5, 2000) for the τ prior, with posterior probability values shown. Individuals were assigned to "species" as described in the main text and Figure 3. Note the change in branch lengths when using priors with smaller mean values in Figure 3.

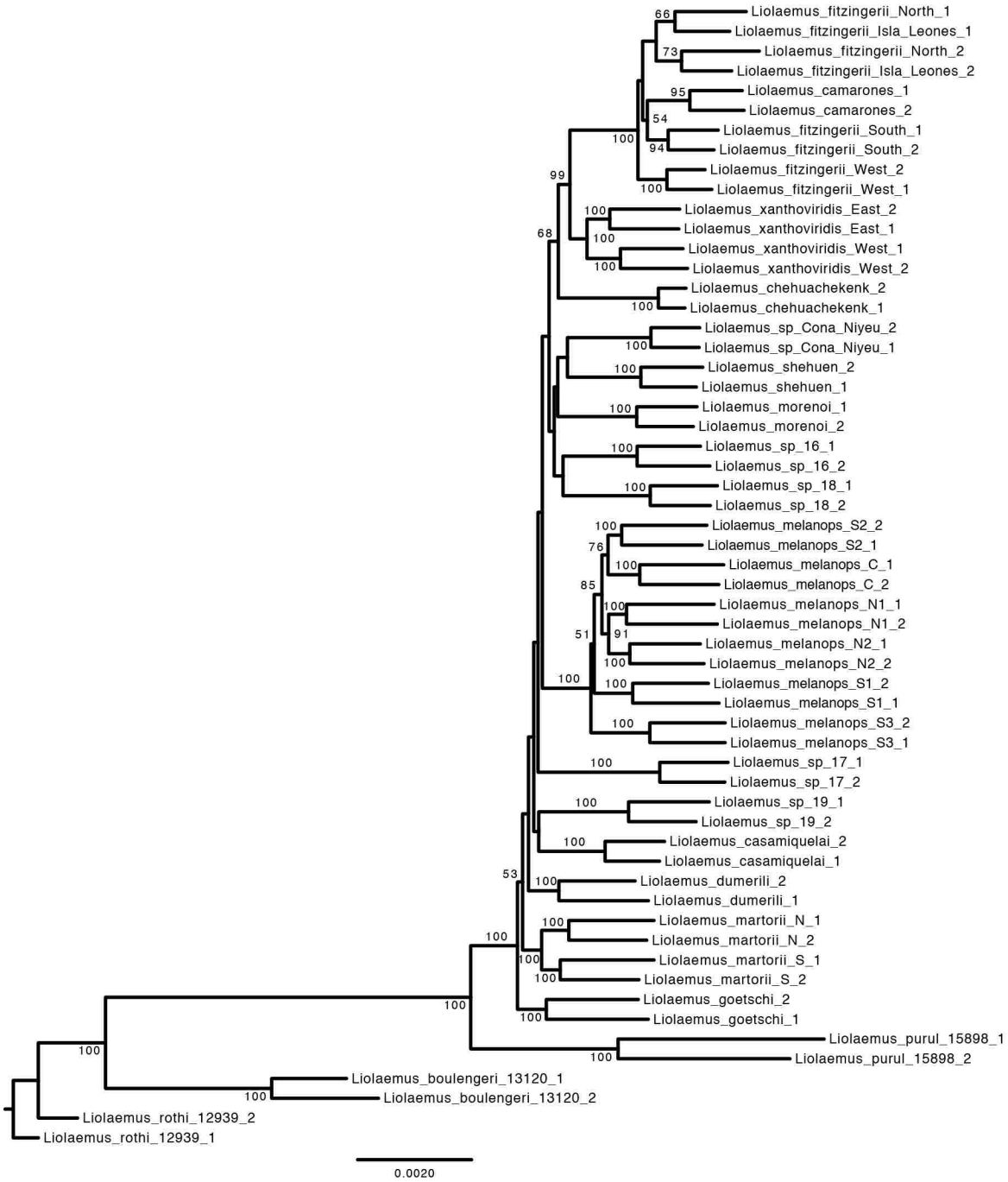

Supplemental Figure S6. RAxML maximum likelihood phylogeny inferred from the concatenated dataset. Support values assessed through 100 bootstrap iterations, and nodes without support values indicate a bootstrap < 50. Concatenation of "1" and "2" alleles across loci was done randomly with respect to phase.

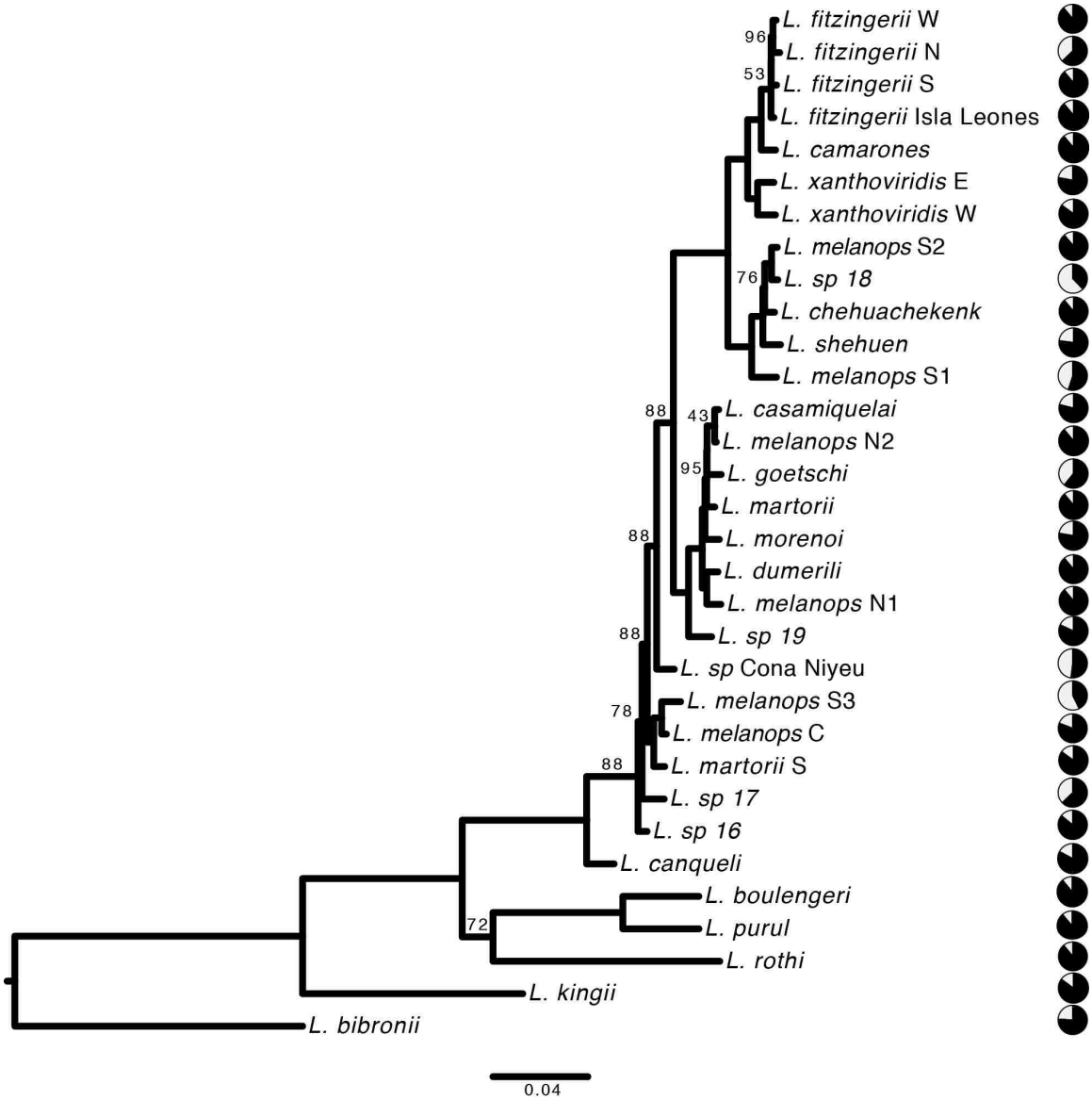

Supplemental Figure S7. Maximum likelihood phylogeny inferred from the mitogenomic dataset. Numbers at nodes represent bootstrap values (out of 100 replicates), and if not listed, are 100. Pies on the right represent percent of the mitogenome recovered (black = data present).

Supplemental Table S1. Sample information including localities and raw sequence data statistics. All specimens have been deposited into the herpetology collection in the Centro Patagónico Nacional (CENPAT-CONICET), Puerto Madryn, Chubut, Argentina, where they have been assigned accession numbers. *Liolaemus bibronii*, *L. boulengeri*, *L. kingii*, and *L. rothi* were used as outgroups in this study.

Accession Number	Number on Map	Species	Latitude	Longitude	Province	Clusters (Passed Filter)	Yield (Megabases)	Number of Reads	Final Number of Loci
LJAMM9890	N/A	Liolaemus bibronii	-47.715	-65.839	Santa Cruz	Not Available	Not Available	Not Available	0
LJAMM13120	N/A	Liolaemus boulengeri	-42.954	-69.929	Chubut	Not Available	Not Available	1303207	99
LJAMM2462	24	Liolaemus camarones	-44.839	-65.723	Chubut	4958047	1273	4293074	580
LJAMM12357	22	Liolaemus canqueli	-43.892	-68.975	Chubut	Not Available	Not Available	2829586	0
LJAMM8676	9	Liolaemus casamiquelai	-41.062	-68.382	Rio Negro	2683356	660	2223469	559
LJAMM5628	13	Liolaemus chehuachekenk	-42.174	-69.548	Chubut	Not Available	Not Available	2016296	509
LJAMM11231	6	Liolaemus dumerili	-40.597	-67.744	Rio Negro	2668122	663	2509055	580
LJAMM9141	26	Liolaemus fitzingerii N	-45.213	-69.184	Chubut	1867134	444	1466390	302
LJAMM9265	27	Liolaemus fitzingerii W	-46.263	-71.378	Santa Cruz	1591534	408	1700904	580
LJAMM11458	28	Liolaemus fitzingerii S	-49.773	-68.627	Santa Cruz	2044820	524	1553986	580
LJAMM15267	25	Liolaemus fitzingerii Isla Leones	-45.050	-65.607	Chubut	3070350	770	1485927	580
LJAMM7034	3	Liolaemus goetschi	-40.119	-66.432	Rio Negro	2784420	710	2767502	575
LJAMM16328	16	Liolaemus melanops S1	-42.524	-66.743	Chubut	1622123	415	946385	577
LJAMM16317	12	Liolaemus melanops C	-41.911	-66.811	Rio Negro	3638182	938	1027153	580
LJAMM16396	19	Liolaemus melanops S2	-43.060	-67.227	Chubut	3546656	921	1581106	580
LJAMM7457	N/A	Liolaemus kingii	-47.717	-65.841	Santa Cruz	Not Available	Not Available	2427141	0
LJAMM2561	7	Liolaemus martorii N	-40.841	-65.118	Rio Negro	10184324	2612	9635974	580
LJAMM6126	10	Liolaemus martorii S	-41.625	-65.025	Rio Negro	2109039	534	2200642	580
LJAMM14545	5	Liolaemus melanops N1	-40.592	-67.787	Rio Negro	Not Available	Not Available	2201202	580
LJAMM11101	8	Liolaemus melanops N2	-41.304	-69.286	Rio Negro	15902049	4144	6478364	580
LJAMM5442	17	Liolaemus melanops S3	-42.734	-66.106	Chubut	1071362	277	1360446	545
LJAMM11392	4	Liolaemus morenoi	-40.285	-70.638	Neuquen	4773014	1230	1160379	571
LJAMM15898	1	Liolaemus purul	-39.902	-70.714	Neuquen	Not Available	Not Available	3010058	469
LJAMM12939	N/A	Liolaemus rothi	-41.264	-71.029	Rio Negro	Not Available	Not Available	1288628	579

LJAMM6097	15	Liolaemus shehuen	-42.511	-67.978	Chubut	2710910	667	2641782	571
LJAMM9049	20	Liolaemus sp. 16	-43.596	-70.165	Chubut	5004018	1265	4819355	573
LJAMM13149	18	Liolaemus sp. 17	-42.833	-64.883	Chubut	817491	201	865464	442
LJAMM5580	14	Liolaemus sp. 18	-42.445	-67.002	Chubut	3465888	906	1405433	549
LJAMM2431	2	Liolaemus sp. 19	-39.926	-68.344	Rio Negro	4410980	1132	4272486	561
LJAMM5995	11	Liolaemus sp. Cona Niyeu	-41.817	-67.183	Rio Negro	3808869	974	3488373	435
LJAMM2418	21	Liolaemus xanthoviridis E	-43.782	-65.447	Chubut	1338142	350	767611	580
LJAMM3738	23	Liolaemus xanthoviridis W	-44.206	-68.237	Chubut	1303933	338	941074	577

Supplemental Table S2. Models of DNA sequence evolution selected by jModelTest for each locus.

Locus	Top Model	Other models in the 95% Credibility Interval			
ADNP	K80	JC	K80+G	JC+G	K80+I
AKAP9	HKY	HKY+I			
ANR	HKY	HKY+G	HKY+I		
BDNF	K80+I	K80+G	K80		
BHLHB2	K80+G				
BMP2	K80+G	K80+I			
CAND1	K80+I	HKY+I	K80+I+G	K80+G	JC+G
CARD4	HKY+G	HKY+I	K80+I	K80+G	HKY
chr12_1169	F81	HKY	F81+G		
chr12_1475	HKY	HKY+I	HKY+G		
chr12_2213	HKY+G	HKY+I+G	HKY+I		
chr12_2426	F81	F81+G	F81+I	HKY	
chr12_3124	K80+I	K80+G	K80		
chr12_3154	HKY+I	K80+I			
chr12_3865	HKY+I	HKY+G	F81+G	HKY+I+G	HKY
chr12_5665	K80+I	HKY+I			
chr12_5671	HKY	F81	HKY+I		
chr12_5730	F81	HKY	F81+G		
chr12_5739	F81	HKY	F81+G		
chr12_5828	F81	HKY	F81+G		
chr12_5837	HKY	HKY+I	HKY+G		
chr12_5840	HKY+I	F81+I	HKY+G	HKY+I+G	F81+G
chr12_5851	HKY+I	HKY+G	HKY		
chr12_5895	F81	HKY	HKY+I	F81+G	
chr12_5903	F81	F81+G	F81+I	F81+I+G	HKY
chr12_5908	F81	HKY	F81+G	F81+I	HKY+G

chr12_5912	HKY+I									
chr12_5949	HKY	K80	HKY+I	HKY+G	K80+G	K80+I				
chr12_5969	HKY+I+G	HKY+I								
chr13_1225	F81	F81+I	HKY							
chr13_4268	HKY+G	HKY+I+G								
chr13_5059	F81	HKY	F81+G							
chr13_5324	F81	HKY	F81+G							
chr13_710	F81	HKY	HKY+I	F81+G						
chr13_720	F81	HKY	F81+I							
chr13_726	F81	HKY	F81+G							
chr18_1422	HKY+I	HKY+G								
chr18_4493	F81	HKY	F81+G							
chr1_10949	K80	K80+G								
chr1_13198	K80+I	K80+G								
chr1_13698	K80+I									
chr1_1378	HKY+I	HKY+G	HKY+I+G							
chr1_1418	F81	F81+G	F81+I							
chr1_14389	HKY+I	HKY+I+G								
chr1_14672	K80	F81	JC	HKY	K80+G	JC+G	F81+G	HKY+G	K80+I	HKY+I
chr1_15412	F81	F81+G	F81+I							
chr1_15480	HKY+I	HKY+G	HKY+I+G							
chr1_15632	F81	F81+G	F81+I							
chr1_16199	F81+I	HKY+I	F81+I+G							
chr1_18915	HKY+I	HKY+G	K80+I							
chr1_19202	F81	HKY	F81+G							
chr1_19246	HKY	F81	HKY+I							
chr1_19292	F81	HKY								
chr1_19426	HKY+I	K80+I								

chr1_19885	F81+G	F81	HKY+G	HKY	F81+I	
chr1_21570	HKY+I					
chr1_22432	K80+I	K80+I+G				
chr1_23573	HKY+I	GTR+I	K80+I	SYM+I		
chr1_24625	F81	HKY	F81+G			
chr1_24640	F81	JC	HKY	K80	F81+G	
chr1_24817	F81	F81+G	F81+I			
chr1_25630	F81	HKY	HKY+I	F81+G	HKY+G	
chr1_25670	HKY	HKY+G	HKY+I			
chr1_25675	F81	HKY				
chr1_25680	F81	HKY	F81+G			
chr1_25692	F81	HKY	F81+I			
chr1_25699	F81	HKY	F81+G			
chr1_25705	HKY+G	F81+G	HKY+I	HKY	F81	HKY+I+G
chr1_26035	F81	F81+G	F81+I	HKY		
chr1_27509	HKY+I	K80+I				
chr1_27552	F81	HKY	F81+G			
chr1_2930	HKY	HKY+I	HKY+G			
chr1_29790	F81	F81+G	F81+I			
chr1_29835	F81	JC	HKY	F81+I	F81+G	K80
chr1_29841	HKY	F81	HKY+I	HKY+G		
chr1_29912	K80+I	K80+I+G				
chr1_30195	HKY+I	HKY+I+G				
chr1_31673	HKY+I	HKY+G	HKY	F81+G	F81	
chr1_31677	HKY+I	HKY+I+G				
chr1_31709	HKY+I	HKY+G				
chr1_31743	HKY+I					
chr1_31749	HKY	HKY+I	HKY+G			

chr1_31783	K80+I	K80+I+G	JC+I				
chr1_32194	K80+G	K80+I					
chr1_32208	HKY+I	HKY+G	HKY+I+G				
chr1_32232	HKY+I	HKY+G	HKY	HKY+I+G			
chr1_32234	F81	F81+G	HKY+I	F81+I	HKY		
chr1_32266	HKY+I	HKY+G					
chr1_32286	HKY+I+G						
chr1_32322	F81	HKY					
chr1_32333	F81	F81+G	F81+I				
chr1_32337	HKY	HKY+G					
chr1_32356	HKY+I	HKY	HKY+G	F81			
chr1_32365	HKY	F81	HKY+I				
chr1_32370	HKY	F81	HKY+I	HKY+G			
chr1_32429	HKY	F81	HKY+I				
chr1_32443	F81	HKY	F81+G				
chr1_32461	HKY+I	HKY+I+G					
chr1_33834	HKY+I	HKY+G	HKY				
chr1_34776	HKY+I	HKY+G	HKY				
chr1_3857	HKY+I	HKY+G	GTR+I	GTR+G			
chr1_4680	HKY+I	HKY+G					
chr1_5277	K80	HKY	JC	K80+I	K80+G	F81	HKY+I
chr1_5279	HKY+I	HKY+G					
chr1_5288	HKY	HKY+G					
chr1_5301	HKY+I	HKY+I+G					
chr1_5319	JC	K80	JC+G	JC+I			
chr1_5334	HKY	F81	HKY+I				
chr1_5365	HKY	F81	HKY+I	HKY+G			
chr1_5379	HKY	F81	HKY+I				

chr1_5409	F81	HKY	F81+G				
chr1_5426	F81	HKY	F81+G				
chr1_5466	F81	HKY	F81+G				
chr1_5470	HKY	F81	HKY+I	HKY+G			
chr1_5474	F81	HKY	F81+G				
chr1_5479	F81+I	HKY+I					
chr1_5492	F81	HKY	F81+G	F81+I			
chr1_8658	HKY+I	HKY+I+G					
chr1_8991	HKY	HKY+I	F81				
chr20_1391	HKY	HKY+I	HKY+G				
chr20_253	F81	HKY	F81+G				
chr20_3629	JC+I	K80+I	JC+I+G	K80+I+G			
chr26_2189	HKY	F81	HKY+I	HKY+G			
chr26_2766	F81	HKY	F81+G				
chr26_2850	F81	F81+G	HKY	F81+I			
chr2_11494	HKY	HKY+I	HKY+G				
chr2_11510	HKY+I	HKY+G					
chr2_11732	F81	HKY	F81+G	F81+I	HKY+G		
chr2_11785	F81	JC	HKY	F81+G	F81+I	JC+G	K80
chr2_11789	HKY+I	HKY+G	HKY				
chr2_11804	F81	HKY	F81+G	F81+I			
chr2_12928	F81	HKY	F81+G				
chr2_12992	HKY	F81	HKY+G	HKY+I			
chr2_12994	HKY	F81	HKY+G				
chr2_13030	F81+G	F81+I	F81+I+G	F81	HKY+G		
chr2_13032	F81	HKY	F81+G				
chr2_13034	F81+G	F81	F81+I				
chr2_13064	F81	HKY	F81+G				

chr2_13460	K80	HKY	K80+G				
chr2_13502	HKY+G	HKY+I	HKY+I+G				
chr2_1647	F81	HKY	F81+I	F81+G			
chr2_17005	HKY	F81	F81+G	HKY+G	HKY+I		
chr2_17019	F81	HKY					
chr2_17532	HKY	F81	HKY+I	HKY+G			
chr2_18468	HKY+I						
chr2_18477	HKY+I	HKY+G	HKY+I+G				
chr2_18557	HKY+I	HKY+G	HKY				
chr2_18578	HKY	F81	HKY+G				
chr2_18589	F81	HKY	F81+G				
chr2_18608	HKY+I	HKY+G	HKY				
chr2_18614	HKY+I	HKY+G	HKY+I+G				
chr2_18619	HKY	HKY+G	HKY+I				
chr2_18662	HKY+I	HKY+G	HKY				
chr2_18677	F81+I	F81+G	F81+I+G	HKY+I	HKY+G	HKY+I+G	JC+I
chr2_18686	K80+I	K80+I+G	K80+G				
chr2_18743	F81	HKY	F81+G				
chr2_20477	HKY	HKY+I					
chr2_21229	HKY	HKY+G					
chr2_21265	HKY	F81	HKY+I				
chr2_21284	F81	HKY	F81+G	F81+I			
chr2_21308	JC	K80	JC+G	JC+I			
chr2_21320	F81	F81+G	F81+I				
chr2_21344	F81	HKY	F81+G				
chr2_21358	HKY+I+G	HKY+I					
chr2_21401	F81+I	HKY+I	F81+I+G				
chr2_21445	HKY+G	HKY+I	HKY	F81+G	F81	HKY+I+G	

chr2_2239	K80+I	K80+G	HKY+I	K80	HKY+G					
chr2_23113	F81	HKY	F81+G							
chr2_23221	F81+I	F81+I+G	F81+G							
chr2_23621	HKY	F81	HKY+I	F81+G	HKY+G					
chr2_23635	HKY	F81	JC	K80	HKY+I	HKY+G	K80+I	F81+G	JC+G	K80+G
chr2_23648	K80+I	HKY+I	K80+I+G							
chr2_23668	HKY	HKY+I	HKY+G							
chr2_24173	F81	HKY	F81+G							
chr2_24655	HKY+I	HKY+G	HKY+I+G							
chr2_24672	HKY+I	HKY+G	HKY							
chr2_24684	HKY	F81	HKY+I							
chr2_24697	HKY	HKY+I								
chr2_24704	HKY+I	HKY+G								
chr2_24800	F81	HKY	F81+G							
chr2_24815	JC	F81	K80	JC+G	JC+I					
chr2_24827	F81+G	F81+I+G	F81+I	HKY+G	HKY+I+G					
chr2_24841	HKY+I	F81	F81+G	HKY	HKY+G	F81+I				
chr2_24859	K80+I									
chr2_24876	HKY+I	HKY+G	F81+G	HKY+I+G	HKY					
chr2_24879	F81	HKY	F81+G							
chr2_24910	K80	JC	HKY	F81	K80+G	K80+I				
chr2_25833	HKY+I									
chr2_27241	HKY	F81	HKY+G							
chr2_27258	F81	HKY	F81+G	HKY+I	F81+I					
chr2_27261	HKY	HKY+I								
chr2_27280	F81	HKY	F81+I	F81+G						
chr2_27294	F81	HKY	F81+G							
chr2_27313	F81+G	F81	HKY+G	HKY	HKY+I	F81+I				

chr2_27968	HKY+I	HKY+G	HKY	F81+G			
chr2_29406	F81	HKY	F81+G				
chr2_4395	HKY	HKY+I					
chr2_5491	JC	JC+G	JC+I	K80			
chr2_5499	HKY+I	HKY+G	HKY				
chr2_5526	HKY+I						
chr2_5991	HKY	HKY+G	HKY+I				
chr2_6341	HKY+I						
chr2_6444	F81	HKY	JC	K80	F81+G	F81+I	HKY+G
chr2_6685	F81	HKY	F81+G	F81+I			
chr2_6737	HKY+I+G	HKY+I					
chr2_6787	HKY	HKY+I					
chr2_7409	HKY+I	HKY+G					
chr2_7420	HKY+I	HKY+I+G					
chr2_7927	F81	HKY	F81+G				
chr2_7945	HKY	F81	HKY+I	HKY+G			
chr2_7954	HKY	HKY+I	HKY+G	K80	F81		
chr2_8583	HKY	F81	HKY+G	HKY+I			
chr2_8590	HKY+I	HKY+G	F81+G	HKY	F81		
chr2_8600	HKY+I	HKY+G					
chr2_8609	HKY	F81	HKY+G	HKY+I			
chr2_8620	HKY	HKY+I	HKY+G				
chr2_8629	HKY+I	HKY+G					
chr2_8651	K80	JC	HKY	K80+I	K80+G	F81	
chr2_8655	HKY+I	HKY+G					
chr2_8677	F81	HKY	F81+G				
chr2_8688	HKY+I	HKY+G					
chr2_8698	HKY+I	HKY+G	HKY				

chr2_8747	HKY+I							
chr2_8754	HKY	HKY+G	HKY+I					
chr3_11795	F81	HKY	F81+G					
chr3_11879	JC+I+G	JC+G	JC+I					
chr3_1282	F81	HKY	F81+G					
chr3_1300	HKY	F81	HKY+I					
chr3_13359	HKY+I	HKY+G	F81+G	HKY	F81	F81+I	HKY+I+G	GTR+I
chr3_13404	HKY+I	HKY+I+G						
chr3_16820	HKY+G	HKY+I	K80+G	HKY	K80+I	F81+G	HKY+I+G	
chr3_16833	HKY+I	HKY+G						
chr3_17607	K80	K80+I	JC	K80+G				
chr3_17623	HKY+I	HKY+G	HKY					
chr3_17699	HKY+I	HKY+G						
chr3_17721	HKY+I	K80+I						
chr3_17747	HKY+I	HKY+G	HKY	K80+I	K80+G			
chr3_17769	JC	K80	F81	HKY	JC+G			
chr3_17781	F81	HKY	F81+G	F81+I				
chr3_17860	K80	JC	K80+I	K80+G				
chr3_17890	HKY+I	HKY+G						
chr3_17991	HKY	HKY+I	HKY+G	F81				
chr3_18203	HKY	F81	HKY+G					
chr3_18256	HKY	F81	HKY+I	HKY+G				
chr3_18306	HKY+I	HKY+G	HKY					
chr3_19568	HKY+G	HKY+I						
chr3_19997	HKY+I	HKY+G	HKY					
chr3_20013	F81+I	F81+I+G	GTR+I	HKY+I				
chr3_21510	HKY+G	HKY+I						
chr3_22024	K80	HKY	K80+G	K80+I	JC			

chr3_23724	F81	HKY+I	F81+G	F81+I	F81+I+G	HKY	
chr3_24903	JC	K80	JC+G				
chr3_24963	K80	K80+G					
chr3_25095	HKY	F81	HKY+G	HKY+I			
chr3_2698	F81	HKY	F81+G				
chr3_2735	F81	HKY	F81+G				
chr3_2742	F81	HKY	F81+G				
chr3_2999	F81	F81+G	HKY	F81+I			
chr3_300	F81+G	F81	HKY+G	F81+I			
chr3_3073	JC	JC+G	K80	JC+I			
chr3_3180	HKY	HKY+G					
chr3_3247	HKY	HKY+G	HKY+I				
chr3_362	HKY+I	HKY+G	F81+I	K80+I	F81+G	F81+I+G	HKY+I+G
chr3_3805	K80+I	JC+I	HKY+I	K80+I+G	JC+I+G		
chr3_3876	HKY+G	HKY+I	HKY	F81+G	F81		
chr3_457	HKY+G	HKY+I	HKY+I+G	HKY			
chr3_509	HKY+I	HKY+G					
chr3_5445	F81	HKY	F81+G				
chr3_5455	K80+I	K80+G	K80				
chr3_5476	K80+I	HKY+I	HKY+G	K80+G	HKY		
chr3_5520	HKY	F81	HKY+I				
chr3_5552	HKY	F81	HKY+I	HKY+G	F81+G		
chr3_5573	HKY	K80	HKY+G	HKY+I	F81		
chr3_5605	F81+G	F81	HKY	HKY+G	HKY+I	F81+I	
chr3_5687	F81	F81+G	F81+I				
chr3_5691	HKY+I	HKY+G	HKY				
chr3_5766	F81	HKY	F81+G	HKY+G	HKY+I		
chr3_5767	HKY	F81	HKY+G				

chr3_576	F81	HKY	F81+G					
chr3_5781	HKY	HKY+I						
chr3_5815	HKY+I	HKY+I+G						
chr3_5848	HKY+I	HKY+I+G	HKY+G					
chr3_5854	HKY	HKY+I	HKY+G					
chr3_5857	HKY+I							
chr3_5873	HKY+I	HKY+I+G						
chr3_5877	HKY	F81	HKY+I	HKY+G				
chr3_5894	F81	HKY	F81+G	F81+I				
chr3_5918	HKY	HKY+I	HKY+G					
chr3_5934	HKY	HKY+I	HKY+G					
chr3_6118	HKY+G	HKY+I	HKY					
chr3_6129	F81	HKY	HKY+I	JC	K80	F81+G	HKY+G	F81+I
chr4_10540	K80	K80+I	K80+G					
chr4_10550	K80+I	HKY+I	HKY+I+G					
chr4_10564	HKY+I+G	HKY+I						
chr4_11155	HKY+I	HKY+G						
chr4_11159	HKY+I	K80+I	GTR+I					
chr4_13410	HKY	HKY+I	HKY+G					
chr4_13431	JC	K80	JC+G	JC+I	K80+I			
chr4_13654	HKY	HKY+G	HKY+I	F81				
chr4_15363	F81	HKY	F81+G					
chr4_15987	F81+I	HKY+I	F81+G	HKY+G	F81+I+G			
chr4_17221	F81	HKY	JC	K80	F81+G	F81+I	HKY+G	JC+G
chr4_17640	HKY	F81	HKY+I	HKY+G	K80			
chr4_6701	HKY	F81	HKY+I	HKY+G				
chr4_6739	HKY+G	HKY+I	K80+I					
chr4_7199	HKY+I	HKY+I+G						

chr4_7243	K80+I	K80+I+G					
chr4_7258	HKY	HKY+I					
chr4_7282	HKY+I						
chr4_7513	HKY	K80	HKY+G	HKY+I			
chr4_7559	K80+I	K80+G	K80	HKY+I			
chr4_7570	K80+I	K80+G	HKY+I	HKY+G	K80		
chr4_9665	F81	HKY	F81+G				
chr4_9725	HKY	HKY+I	HKY+G				
chr4_9746	K80	K80+I	K80+G	SYM	HKY		
chr5_10115	F81	F81+G					
chr5_10176	F81	F81+G	F81+I	F81+I+G	HKY	JC	HKY+G
chr5_10180	F81	F81+G	HKY				
chr5_10184	HKY+I						
chr5_10207	HKY+I	HKY+G	K80+I	K80+G			
chr5_10239	K80	HKY	K80+I	K80+G	JC	HKY+I	
chr5_10251	HKY	HKY+G					
chr5_10254	HKY	HKY+I	HKY+G				
chr5_10266	HKY	F81					
chr5_10353	F81	HKY	F81+G	F81+I			
chr5_10416	HKY	HKY+I	HKY+G	F81			
chr5_10787	HKY	K80	HKY+I	HKY+G			
chr5_10841	F81+G	F81+I+G	F81+I	HKY+G			
chr5_10846	F81	JC	HKY	F81+G			
chr5_10859	HKY	HKY+I	HKY+G	F81			
chr5_10906	HKY	K80	F81	HKY+I			
chr5_11139	F81	HKY	F81+G				
chr5_11146	HKY	HKY+I	HKY+G	F81			
chr5_11148	HKY	HKY+I	HKY+G				

chr5_11165	HKY	F81	K80	JC	HKY+G					
chr5_11198	F81+I+G	F81+G	F81+I	HKY+I+G						
chr5_11202	HKY	HKY+G	HKY+I							
chr5_11206	HKY+I									
chr5_11226	HKY+I	HKY+I+G								
chr5_11240	HKY+I+G	HKY+I								
chr5_11245	HKY	HKY+I								
chr5_11286	HKY	HKY+I	HKY+G	F81						
chr5_11302	HKY	F81	HKY+I	HKY+G						
chr5_11304	K80	K80+I	K80+G	HKY	HKY+I					
chr5_11321	HKY+I	HKY+G	HKY+I+G	GTR+I						
chr5_11325	F81+G	F81+I	F81+I+G	HKY+I						
chr5_11342	HKY+I	HKY+G	GTR+I	HKY						
chr5_11359	HKY	HKY+G	HKY+I							
chr5_11571	F81+G	F81	HKY+G	F81+I+G	HKY	F81+I				
chr5_11637	JC	JC+G	K80	K80+G	JC+I					
chr5_11657	F81	F81+G	HKY							
chr5_11783	HKY+G	F81+G	F81+I+G	HKY+I+G	HKY					
chr5_11955	F81	HKY								
chr5_12397	F81	F81+G	HKY	F81+I						
chr5_12400	HKY+I	HKY+G	K80+I	HKY						
chr5_12422	K80	K80+I	K80+G							
chr5_12835	HKY+I	HKY+G	HKY	F81+G	F81					
chr5_13040	F81	HKY	F81+G	F81+I						
chr5_13042	JC	JC+G	F81	K80	K80+I	F81+G	K80+G	JC+I	HKY+I	HKY
chr5_14403	HKY	F81	K80	HKY+I						
chr5_14621	HKY	HKY+G								
chr5_14632	HKY	HKY+I	HKY+G							

chr5_14720	HKY+I	HKY	HKY+G									
chr5_14766	K80	K80+G	K80+I									
chr5_14864	HKY+I	HKY+G	HKY+I+G									
chr5_14870	K80+I	K80+G	HKY+I	HKY+G	HKY							
chr5_14876	HKY	F81	HKY+I	HKY+G								
chr5_14914	K80+I	HKY+I										
chr5_15022	HKY	K80	HKY+I	HKY+G								
chr5_15078	HKY+I	HKY+G										
chr5_1597	K80+I	HKY+I	K80+I+G									
chr5_1675	F81+G	HKY+G	F81+I	F81+I+G	HKY+I							
chr5_1689	HKY+I	F81	F81+G	JC	K80+I	HKY	JC+G	F81+I+G	HKY+G	K80	F81+I	JC+I+G
chr5_1701	HKY	F81	F81+G	HKY+G	HKY+I							
chr5_1746	F81	HKY	F81+G									
chr5_1757	F81	HKY	JC	K80	F81+G							
chr5_1800	F81	F81+G	HKY	F81+I								
chr5_1813	F81	HKY	F81+I									
chr5_1834	F81	HKY	F81+G	HKY+I								
chr5_1989	HKY	HKY+I	HKY+G									
chr5_3191	HKY	F81	HKY+I	HKY+G								
chr5_3204	HKY	F81	HKY+G									
chr5_3273	HKY+I											
chr5_3353	F81	HKY	F81+G	HKY+G								
chr5_3377	HKY+I+G	HKY+I	HKY+G									
chr5_3407	HKY+I	HKY+I+G										
chr5_3418	F81	HKY	F81+G									
chr5_4018	K80+I	K80	K80+G	HKY	HKY+I							
chr5_5657	F81+G	F81	F81+I	HKY+G								
chr5_8793	F81	F81+G	F81+I									

chr6_6814	HKY+I	HKY+G	HKY						
chr6_8253	F81	HKY							
chr6_8786	F81	HKY	F81+G						
chr6_8806	F81	HKY	F81+G	HKY+G	HKY+I				
chr6_8829	HKY	F81	HKY+I	HKY+G					
chr6_9069	HKY	HKY+G							
chr6_9474	JC	JC+G	K80	F81	JC+I	K80+G			
chr6_9529	F81+G	F81	HKY+G	HKY	F81+I				
chr6_9532	JC	K80	JC+G	JC+I					
chr6_9559	HKY	HKY+I	HKY+G	F81					
chr6_9640	F81	HKY	F81+G						
chr6_9737	F81	HKY	F81+G	HKY+I					
chr6_9746	F81	HKY	F81+G						
chr6_9762	F81	HKY	F81+G						
chr6_9783	HKY	F81	HKY+I						
chr6_9787	HKY	F81	HKY+I	HKY+G					
chr6_9797	HKY+I	HKY	HKY+G						
chr6_9804	K80	K80+I	K80+G						
chr6_9806	F81+I	F81+I+G							
chr6_9809	HKY	F81	K80	JC	HKY+G	HKY+I	F81+G	K80+G	K80+I
chr6_9838	HKY+G	F81+G	HKY+I	HKY	HKY+I+G	F81+I+G	F81		
chr7_10269	HKY+G	F81+G	HKY+I+G	F81+I+G	HKY+I				
chr7_10305	F81	HKY	F81+G						
chr7_10322	F81	HKY	F81+G	F81+I					
chr7_10380	HKY+I	HKY+I+G							
chr7_10394	HKY+G	HKY	HKY+I						
chr7_10440	F81	HKY	F81+I						
chr7_10443	HKY+I	HKY+G							

chr7_10480	HKY+I								
chr7_10497	HKY+I								
chr7_10502	F81	HKY	F81+G	HKY+I	F81+I				
chr7_10532	F81+I+G	F81+G	F81+I	HKY+I+G	HKY+G				
chr7_10675	F81	HKY							
chr7_10681	HKY+I	HKY+G	K80+I	K80+G	HKY	F81+G	JC+G	F81	K80
chr7_10694	HKY	HKY+I	HKY+G						
chr7_1370	HKY	F81	HKY+I	HKY+G	F81+G				
chr7_1380	F81	JC	HKY	F81+G					
chr7_6327	JC	K80	JC+G						
chr7_6333	F81	HKY	F81+G						
chr7_6366	K80	JC	HKY	K80+G	K80+I	F81			
chr7_9094	HKY	HKY+I							
chr7_9104	HKY+I	HKY+G	HKY+I+G	F81+G					
chr8_3308	HKY	HKY+G	HKY+I						
chr8_4014	K80	JC	K80+G						
chr8_4067	HKY	F81	HKY+I	HKY+G					
chr8_4091	HKY	HKY+G							
chr8_4241	HKY+I+G	HKY+I							
chr8_4243	HKY	F81	HKY+G	HKY+I					
chr8_4319	HKY+I	HKY+G							
chr8_4333	HKY+I	K80+I	K80+I+G						
chr8_4340	K80	HKY	K80+I	K80+G					
chr8_4410	HKY	HKY+I							
chr8_6218	HKY	F81	HKY+G						
chr8_6224	K80	JC	K80+G						
chr8_6230	HKY	F81	JC	K80	HKY+I	HKY+G	F81+G		
chr8_6277	K80	JC	K80+I	K80+G	HKY				

chr8_6872	HKY+I	HKY+G	F81+G	HKY	F81	F81+I			
chr8_7441	F81	F81+G	F81+I						
chr8_7449	HKY	K80	F81	JC	HKY+I				
chr8_7513	HKY	F81	HKY+G	HKY+I					
chr8_7534	HKY	HKY+G	HKY+I						
chr8_8877	HKY	HKY+I	HKY+G	F81					
chr8_8942	F81	HKY	F81+G	HKY+G					
chr8_9173	HKY	F81	HKY+I	HKY+G					
chr9_1152	HKY+I								
chr9_1164	F81	HKY	HKY+I	F81+G	HKY+G				
chr9_1169	HKY+I	HKY	HKY+G						
chr9_1191	F81	F81+G	F81+I						
chr9_2499	HKY+I	HKY+I+G							
chr9_3289	F81	HKY	F81+G						
chr9_5181	HKY+I	HKY+I+G	HKY+G						
chr9_5205	F81	HKY	F81+G	F81+I	JC				
chr9_5246	HKY	F81	HKY+G						
chr9_6320	HKY+I	F81+I	HKY+I+G	HKY+G					
chr9_6322	F81+I	HKY+I							
chr9_6325	F81+I	F81+I+G							
chr9_6414	JC	JC+G	JC+I	K80					
chr9_7171	F81	HKY	JC	K80	F81+G				
chr9_7188	HKY+I	HKY	HKY+G	F81	F81+G				
chr9_7189	F81	HKY	F81+G	HKY+I					
chr9_7434	HKY+I	HKY+G	HKY+I+G						
chrun_random_11933	HKY	HKY+I	HKY+G						
chrun_random_3551	F81	F81+G	F81+I						
chrun_random_7197	JC	F81	JC+G	F81+G	HKY	K80	JC+I	F81+I	HKY+G

chrz_11272	F81+G	F81	F81+I	HKY+G	F81+I+G	HKY
chrz_11397	HKY+I	HKY+G	HKY			
chrz_11457	HKY	HKY+I				
chrz_11465	F81	F81+G	HKY			
chrz_11477	HKY+I	HKY+I+G				
chrz_11491	HKY+G	HKY	F81+G	HKY+I	F81	
chrz_11540	HKY+I	HKY+I+G	HKY+G			
chrz_11557	HKY+I	HKY	HKY+G	F81		
chrz_11584	F81	HKY	F81+G	F81+I		
chrz_11684	F81	HKY	F81+G			
chrz_4313	F81	HKY	F81+G			
chrz_467	HKY	K80	K80+I	HKY+I	HKY+G	
chrz_4740	HKY	F81	HKY+G	HKY+I		
chrz_4747	HKY	HKY+I	HKY+G			
chrz_4759	F81	HKY	F81+G			
chrz_4772	K80+I	HKY+I	K80+G	HKY+G		
chrz_4782	HKY+I	HKY+G				
chrz_4787	HKY+I	HKY+G	HKY			
chrz_4794	K80+I	K80+I+G				
chrz_4816	GTR+I+G					
chrz_4832	HKY	F81	HKY+I	HKY+G		
chrz_4838	F81	HKY	F81+G			
chrz_4841	F81	HKY	F81+G			
chrz_5495	K80+I	HKY+I	K80+G			
chrz_5501	F81	HKY				
chrz_5971	HKY+I	HKY+G				
chrz_6357	HKY	HKY+I	HKY+G	F81		
chrz_6396	HKY+I	HKY+G	K80+I	HKY+I+G		

chrz_646	HKY	HKY+I	HKY+G					
chrz_6575	HKY+I	HKY+G						
chrz_6612	HKY+I	HKY+G	HKY					
chrz_6686	HKY+I+G	HKY+I						
chrz_6690	K80+I	K80+G	K80					
chrz_6703	HKY+I	K80+I	HKY+I+G	SYM+I				
chrz_6778	HKY	F81	HKY+I					
chrz_6799	F81	F81+G	JC	HKY	F81+I	JC+G	HKY+G	F81+I+G
chrz_7406	HKY+I	HKY+G						
chrz_7416	HKY	F81	HKY+G					
chrz_7824	HKY+I	HKY+G	HKY	F81+G	F81			
chrz_7889	JC+I	K80+I						
chrz_7923	HKY+I+G	F81+I+G						
chrz_7943	HKY+I	HKY	HKY+G					
chrz_7982	HKY	F81	HKY+I					
chrz_7997	F81	HKY	F81+G	F81+I				
chrz_8024	HKY	F81	HKY+I	HKY+G				
CILP	K80+I+G	K80+I	K80+G					
CXCR4	JC	JC+G	K80	K80+G	JC+I			
DLL1	K80+I	K80+G	K80+I+G					
ECEL	HKY+I+G	K80+I+G						
ENC6	K80+G	K80+I	K80					
FSHR	K80+G	K80+I	HKY+G					
FSTL5	HKY+G	HKY+I	F81+G	HKY	HKY+I+G	F81		
GALR1	HKY+I	HKY+G						
GHSR	K80+I							
GPR37	K80+I	K80+I+G						
HLCS	HKY+I	HKY+G	HKY					

INHIBA	HKY+G	HKY+I					
LRRN1	HKY+I	HKY+G					
LZTSS1	HKY+I	HKY+G	HKY+I+G				
MKL1	K80	K80+G	K80+I	HKY			
MLL3	HKY	HKY+G	HKY+I				
MSH6	K80+I	K80+G	HKY+I	HKY+G			
NGFB	K80+G	K80+I	K80				
NKTR	HKY+I	HKY+G					
NTF3	F81	HKY	F81+G				
PNN	K80+G	JC+G	K80+I	JC+I	K80+I+G	JC+I+G	K80
PRLR	HKY+G	HKY+I					
PTGER4	HKY+G	HKY+I					
PTPN	HKY+I	HKY+G					
RAG1	K80+I	HKY+I	K80+G				
SINAIP	K80+G	K80+I	K80				
SLC30A1	K80+I	K80	K80+G	HKY+I			
SLC8A1	K80+I	K80+I+G					
SLC8A3	K80+I	K80+G	K80+I+G				
TRAF6	K80	K80+I	K80+G				
ZEB2	K80	HKY	K80+I	K80+G			
ZFP36L1	HKY+G	HKY+I+G					
BACH1	HKY+G	HKY+I	HKY+I+G				
chr1_13047	K80+I	K80+I+G	JC+I	HKY+I	JC+I+G	HKY+I+G	
chr1_24644	F81	F81+G	F81+I	HKY			
chr1_29894	HKY	HKY+I	HKY+G				
chr1_30635	HKY+I	HKY+I+G					
chr1_32378	HKY+I	HKY+G	F81+I	GTR+I			
chr2_11187	HKY+I	HKY+G					

chr2_11743	K80+I	K80+I+G						
chr2_1916	F81	HKY	JC	K80	F81+G	F81+I		
chr2_23160	HKY+I	HKY+G						
chr2_23596	HKY+I	HKY+G						
chr2_25851	K80+G	JC+G	K80+I	HKY+G	SYM+G	K80+I+G	F81+G	JC+I+G
chr2_8589	F81	HKY	F81+G	HKY+G	HKY+I			
chr3_17448	HKY+I	HKY+G	HKY+I+G					
chr3_21949	HKY	K80	HKY+I	HKY+G	K80+I	K80+G		
chr3_2723	F81	HKY	F81+G					
chr3_5536	HKY	F81	HKY+G	HKY+I	F81+G			
chr5_11214	HKY+I	HKY+G	HKY+I+G					
chr5_1749	HKY+I							
chr6_9046	F81	HKY	F81+G	HKY+I	HKY+G			
chr6_9631	F81+I	HKY+I						
chr8_4342	F81	HKY	F81+G	F81+I				
chr8_6299	K80+I	K80	K80+G	HKY+I	HKY			
chr8_9143	HKY	F81	HKY+I	HKY+G				
chr9_1949	HKY+I	HKY	HKY+G	F81+G	F81	F81+I		
chr9_3633	HKY	HKY+I						
chr9_5220	F81+I	HKY+I						
chrz_4763	JC	K80	JC+G					
chr12_5878	HKY+I	HKY+G	GTR+I	HKY+I+G				

Supplemental Table S3. Sequence information for the mitogenomic dataset.

Individual	Sequence Length	% Complete
Liolaemus bibronii	13115	76.2
Liolaemus boulengeri	15379	89.3
Liolaemus camarones	15309	88.9
Liolaemus canqueli	14299	83.0
Liolaemus casamiquelai	13560	78.7
Liolaemus chehuachekenk	15370	89.3
Liolaemus dumerili	15330	89.0
Liolaemus fitzingerii Isla Leones	15365	89.2
Liolaemus fitzingerii N	10792	62.7
Liolaemus fitzingerii S	15365	89.2
Liolaemus fitzingerii W	15302	88.9
Liolaemus goetschi	10449	60.7
Liolaemus kingii	14561	84.6
Liolaemus martorii N	15367	89.2
Liolaemus martorii S	14721	85.5
Liolaemus melanops C	13981	81.2
Liolaemus melanops N1	15264	88.6
Liolaemus melanops N2	15368	89.2
Liolaemus melanops S1	9398	54.6
Liolaemus melanops S2	15249	88.6
Liolaemus melanops S3	7414	43.1
Liolaemus morenoi	13400	77.8
Liolaemus purul	15250	88.6
Liolaemus rothi	15273	88.7
Liolaemus shehuen	13319	77.3
Liolaemus sp 16	14758	85.7
Liolaemus sp 17	10778	62.6
Liolaemus sp 18	6616	38.4
Liolaemus sp 19	14200	82.5
Liolaemus sp Cona Niyeu	8913	51.8
Liolaemus xanthoviridis E	13351	77.5
Liolaemus xanthoviridis W	14554	84.5

Supplemental Table S4. Alignment statistics for all nuclear loci without outgroup sequences. The Squamate Assembling the Tree of Life genes are shown first, followed by the ultra-conserved elements loci.

Locus	Taxa No	Seq Length	Percent Gaps Aln	Number Inform Sites	Percent Inform sites Aln	Percent Ns Aln	Percent Missing Data	Seqs with no missing data
ADNP	48	368	2.4	5	1.4	0	2.4	0
AKAP9	48	396	0.2	12	3	0	0.2	22
ANR	50	332	0.6	9	2.7	0	0.6	20
BACH1	52	460	0.4	19	4.1	0	0.4	20
BDNF	54	572	0.1	14	2.4	0	0.1	24
BHLHB2	54	498	0.6	14	2.8	0	0.6	4
BMP2	54	466	0.8	18	3.9	0	0.8	14
CAND1	50	508	0.3	7	1.4	0	0.3	20
CARD4	52	488	0.4	21	4.3	0	0.4	18
CILP	54	347	1.6	33	9.5	0	1.6	6
CXCR4	54	399	0.3	10	2.5	0	0.3	36
DLL1	54	444	0.6	18	4.1	0	0.6	10
ECEL	46	388	1	30	7.7	0	1	2
ENC6	50	556	0.6	13	2.3	0	0.6	14
FSHR	54	526	0.5	17	3.2	0	0.5	10
FSTL5	54	567	0.5	17	3	0	0.5	22
GALR1	50	235	1.2	32	13.6	0	1.2	10
GHSR	54	394	0.5	25	6.3	0	0.5	18
GPR37	50	608	0.5	18	3	0	0.5	26
HLCS	52	451	0.6	18	4	0	0.6	22
INHIBA	52	513	0.3	15	2.9	0	0.3	32
LRRN1	54	510	0.1	17	3.3	0	0.1	40
LZTSS1	50	391	0.6	21	5.4	0	0.6	12
MKL1	52	476	0.1	9	1.9	0	0.1	38
MLL3	48	327	0.6	8	2.4	0	0.6	18
MSH6	52	483	0.9	13	2.7	0	0.9	14

NGFB	52	344	1	24	7	0	1	12
NKTR	46	376	0.1	18	4.8	0	0.1	32
NTF3	50	471	0.3	7	1.5	0	0.3	34
PNN	38	211	0.6	13	6.2	0	0.6	8
PRLR	42	332	0.6	19	5.7	0	0.6	14
PTGER4	48	374	1.1	34	9.1	0	1.1	16
PTPN	48	433	1.1	20	4.6	0	1.1	10
RAG1	52	445	0.3	13	2.9	0	0.3	18
SINAIP	50	347	0.6	12	3.5	0	0.6	12
SLC30A1	50	520	0.6	14	2.7	0	0.6	20
SLC8A1	52	477	0.4	21	4.4	0	0.4	18
SLC8A3	54	535	0.3	14	2.6	0	0.3	26
TRAF6	44	350	0	6	1.7	0	0	44
ZEB2	48	301	0.5	8	2.7	0	0.5	24
ZFP36L1	50	329	1.5	32	9.7	0	1.5	6
Squamate TOL Means	**50.39**	**428.00**	**0.62**	**16.78**	**4.22**	**0.00**	**0.62**	**18.68**
chr12_1169	48	596	0.4	4	0.7	0	0.4	18
chr12_1475	54	469	0.5	16	3.4	0	0.5	12
chr12_2213	54	601	0.4	31	5.2	0	0.4	30
chr12_2426	44	573	1	13	2.3	0	1	0
chr12_3124	52	537	0.5	12	2.2	0	0.5	2
chr12_3154	42	553	0	27	4.9	0	0	42
chr12_3865	50	651	0.5	22	3.4	0	0.5	2
chr12_5665	54	623	3.7	17	2.7	0	3.7	28
chr12_5671	52	565	0.2	3	0.5	0	0.2	24
chr12_5730	52	472	0.2	8	1.7	0	0.2	30
chr12_5739	48	462	0.1	7	1.5	0	0.1	34
chr12_5828	52	425	0.2	10	2.4	0	0.2	32
chr12_5837	54	608	0.2	17	2.8	0	0.2	8

chr12_5840	52	534	0.5	20	3.7	0	0.5	24
chr12_5851	50	553	0.4	16	2.9	0	0.4	16
chr12_5878	54	477	0.2	14	2.9	0	0.2	32
chr12_5895	54	547	0.2	5	0.9	0	0.2	36
chr12_5903	52	439	0.8	9	2.1	0	0.8	12
chr12_5908	52	445	0.3	12	2.7	0	0.3	2
chr12_5912	52	575	0.3	8	1.4	0	0.3	14
chr12_5949	52	352	0.3	6	1.7	0	0.3	14
chr12_5969	50	501	0.3	14	2.8	0	0.3	18
chr13_1225	52	456	0.1	0	0	0	0.1	42
chr13_4268	54	396	1	31	7.8	0	1	0
chr13_5059	54	380	0.9	12	3.2	0	0.9	20
chr13_5324	42	547	0	4	0.7	0	0	42
chr13_710	48	567	0.6	1	0.2	0	0.6	26
chr13_720	54	462	0.1	2	0.4	0	0.1	38
chr13_726	46	479	0.7	5	1	0	0.7	22
chr18_1422	54	620	0.4	14	2.3	0	0.4	0
chr18_4493	54	591	0.3	4	0.7	0	0.3	42
chr1_10949	54	588	0.2	7	1.2	0	0.2	22
chr1_13047	54	535	0.5	20	3.7	0	0.5	2
chr1_13198	54	460	0.4	10	2.2	0	0.4	26
chr1_13698	54	520	0.3	20	3.8	0	0.3	28
chr1_1378	54	538	0.3	16	3	0	0.3	30
chr1_1418	52	596	0.8	12	2	0	0.8	0
chr1_14389	52	574	1.2	19	3.3	0	1.2	4
chr1_14672	54	495	2	18	3.6	0	2	0
chr1_15412	52	571	0.3	8	1.4	0	0.3	16
chr1_15480	54	505	0.2	9	1.8	0	0.2	28
chr1_15632	52	477	0.3	6	1.3	0	0.3	22

chr1_16199	44	551	0	23	4.2	0	0	44
chr1_18915	52	572	0.4	15	2.6	0	0.4	16
chr1_19202	52	434	0.3	2	0.5	0	0.3	22
chr1_19246	52	513	0.5	9	1.8	0	0.5	36
chr1_19292	50	548	1.2	11	2	0	1.2	8
chr1_19426	52	531	0.2	10	1.9	0	0.2	16
chr1_19885	46	665	0.6	11	1.7	0	0.6	2
chr1_21570	52	567	0.2	15	2.6	0	0.2	28
chr1_22432	52	594	0.3	19	3.2	0	0.3	32
chr1_23573	50	586	1	25	4.3	0	1	20
chr1_24625	40	409	0.6	5	1.2	0	0.6	16
chr1_24640	54	567	0.2	14	2.5	0	0.2	22
chr1_24644	50	450	0.6	13	2.9	0	0.6	26
chr1_24817	54	494	0.5	8	1.6	0	0.5	26
chr1_25630	50	489	0.3	8	1.6	0	0.3	2
chr1_25670	38	560	0	4	0.7	0	0	36
chr1_25675	50	589	0.3	4	0.7	0	0.3	10
chr1_25680	54	534	0.4	3	0.6	0	0.4	22
chr1_25692	54	467	1	16	3.4	0	1	2
chr1_25699	50	525	0.7	2	0.4	0	0.7	4
chr1_25705	52	602	1	17	2.8	0	1	24
chr1_26035	36	284	1.1	9	3.2	0	1.1	12
chr1_27509	52	417	0.6	17	4.1	0	0.6	18
chr1_27552	52	571	0.7	13	2.3	0	0.7	14
chr1_2930	50	469	0.5	8	1.7	0	0.5	10
chr1_29790	50	550	0.5	9	1.6	0	0.5	34
chr1_29835	50	261	0	0	0	0	0	50
chr1_29841	54	409	0.3	5	1.2	0	0.3	38
chr1_29894	50	578	0.4	8	1.4	0	0.4	32

chr1_29912	52	410	0.4	10	2.4	0	0.4	22
chr1_30195	48	571	0.9	20	3.5	0	0.9	0
chr1_30635	46	584	0.5	22	3.8	0	0.5	12
chr1_31673	52	515	0.6	12	2.3	0	0.6	24
chr1_31677	46	601	0.6	14	2.3	0	0.6	14
chr1_31709	52	529	0.5	18	3.4	0	0.5	0
chr1_31743	46	527	0.7	13	2.5	0	0.7	22
chr1_31749	50	488	0.2	8	1.6	0	0.2	30
chr1_31783	54	330	1.3	12	3.6	0	1.3	4
chr1_32194	50	314	0.4	19	6.1	0	0.4	24
chr1_32208	54	520	0.3	16	3.1	0	0.3	22
chr1_32232	48	483	0.5	12	2.5	0	0.5	32
chr1_32234	50	476	0.6	5	1.1	0	0.6	20
chr1_32266	52	533	1	23	4.3	0	1	16
chr1_32286	54	614	1	27	4.4	0	1	2
chr1_32322	54	581	0.1	2	0.3	0	0.1	42
chr1_32333	50	526	0.9	15	2.9	0	0.9	18
chr1_32337	54	518	0	4	0.8	0	0	46
chr1_32356	48	610	0.2	7	1.1	0	0.2	22
chr1_32365	48	572	0.4	5	0.9	0	0.4	4
chr1_32370	46	398	0	1	0.3	0	0	46
chr1_32378	52	480	0.1	7	1.5	0	0.1	40
chr1_32429	52	495	0.1	2	0.4	0	0.1	38
chr1_32443	50	520	0.3	11	2.1	0	0.3	24
chr1_32461	54	606	0.8	24	4	0	0.8	11
chr1_33834	50	581	0.8	17	2.9	0	0.8	2
chr1_34776	48	479	1.1	15	3.1	0	1.1	8
chr1_3857	48	515	0.1	11	2.1	0	0.1	32
chr1_4680	50	486	0.2	16	3.3	0	0.2	34

chr1_5277	54	553	0.3	8	1.4	0	0.3	44
chr1_5279	46	587	1.6	15	2.6	0	1.6	0
chr1_5288	52	564	0	11	2	0	0	48
chr1_5301	50	500	0.4	19	3.8	0	0.4	32
chr1_5319	54	363	0.3	5	1.4	0	0.3	20
chr1_5334	54	551	0.1	5	0.9	0	0.1	42
chr1_5365	52	525	0.5	2	0.4	0	0.5	28
chr1_5379	52	505	0.2	6	1.2	0	0.2	36
chr1_5409	48	385	0.4	6	1.6	0	0.4	14
chr1_5426	52	500	0.3	1	0.2	0	0.3	36
chr1_5466	48	464	1	13	2.8	0	1	10
chr1_5470	48	546	0.5	7	1.3	0	0.5	38
chr1_5474	50	489	0.7	6	1.2	0	0.7	26
chr1_5479	54	583	0.6	14	2.4	0	0.6	36
chr1_5492	52	504	0.5	4	0.8	0	0.5	6
chr1_8658	52	505	0.4	9	1.8	0	0.4	2
chr1_8991	54	459	0.4	8	1.7	0	0.4	26
chr20_1391	48	398	0.1	6	1.5	0	0.1	36
chr20_253	54	461	0.5	6	1.3	0	0.5	26
chr20_3629	54	340	0.3	16	4.7	0	0.3	24
chr26_2189	48	560	0	6	1.1	0	0	48
chr26_2766	46	477	0.2	8	1.7	0	0.2	22
chr26_2850	52	481	0.2	13	2.7	0	0.2	26
chr2_11187	54	529	0.4	11	2.1	0	0.4	6
chr2_11494	52	487	0.6	11	2.3	0	0.6	8
chr2_11510	52	593	0.3	29	4.9	0	0.3	22
chr2_11732	48	389	0.3	2	0.5	0	0.3	22
chr2_11743	52	554	1.2	21	3.8	0	1.2	0
chr2_11785	52	507	0.3	15	3	0	0.3	26

chr2_11789	54	554	0.5	9	1.6	0	0.5	10
chr2_11804	48	519	0.5	3	0.6	0	0.5	28
chr2_12928	50	497	0.9	7	1.4	0	0.9	10
chr2_12992	54	548	0.2	18	3.3	0	0.2	32
chr2_12994	52	570	0.1	10	1.8	0	0.1	32
chr2_13030	50	544	0.1	6	1.1	0	0.1	38
chr2_13032	50	439	0.2	4	0.9	0	0.2	30
chr2_13034	38	700	0	6	0.9	0	0	38
chr2_13064	46	554	0.4	0	0	0	0.4	18
chr2_13460	48	274	0.5	5	1.8	0	0.5	26
chr2_13502	54	573	0.9	47	8.2	0	0.9	0
chr2_1647	42	393	1.2	6	1.5	0	1.2	0
chr2_17005	54	480	0.8	6	1.2	0	0.8	32
chr2_17019	50	553	0.8	7	1.3	0	0.8	24
chr2_17532	50	507	0.3	3	0.6	0	0.3	12
chr2_18468	52	575	0.5	10	1.7	0	0.5	8
chr2_18477	52	571	0.5	9	1.6	0	0.5	18
chr2_18557	54	548	0.3	11	2	0	0.3	16
chr2_18578	48	577	0.9	6	1	0	0.9	2
chr2_18589	52	541	1	4	0.7	0	1	0
chr2_18608	52	535	0.2	12	2.2	0	0.2	26
chr2_18614	54	392	0.3	12	3.1	0	0.3	24
chr2_18619	50	583	0.8	9	1.5	0	0.8	14
chr2_18662	54	605	0.1	13	2.1	0	0.1	40
chr2_18677	50	618	0.5	17	2.8	0	0.5	14
chr2_18686	52	535	0.4	14	2.6	0	0.4	26
chr2_18743	52	528	0.1	11	2.1	0	0.1	36
chr2_1916	52	550	0.2	4	0.7	0	0.2	32
chr2_20477	52	511	0.2	11	2.2	0	0.2	28

chr2_21229	50	504	0.3	15	3	0	0.3	14
chr2_21265	54	556	0.1	10	1.8	0	0.1	28
chr2_21284	50	419	0.6	8	1.9	0	0.6	32
chr2_21308	52	331	0.2	6	1.8	0	0.2	44
chr2_21320	50	460	0	22	4.8	0	0	44
chr2_21344	52	395	0.2	6	1.5	0	0.2	32
chr2_21358	54	584	0.6	26	4.5	0	0.6	0
chr2_21401	48	574	0.7	17	3	0	0.7	2
chr2_21445	54	441	0.6	27	6.1	0	0.6	26
chr2_2239	52	480	0.6	10	2.1	0	0.6	8
chr2_23113	50	536	0.2	4	0.7	0	0.2	34
chr2_23160	54	486	0.6	13	2.7	0	0.6	24
chr2_23221	52	433	0.1	19	4.4	0	0.1	39
chr2_23596	54	554	1.4	15	2.7	0	1.4	2
chr2_23621	52	514	0.1	8	1.6	0	0.1	36
chr2_23635	54	557	0.8	11	2	0	0.8	34
chr2_23648	50	507	0.9	14	2.8	0	0.9	12
chr2_23668	54	545	0.4	2	0.4	0	0.4	30
chr2_24173	50	455	0.1	2	0.4	0	0.1	32
chr2_24655	54	615	0.8	31	5	0	0.8	20
chr2_24672	50	561	0.6	12	2.1	0	0.6	14
chr2_24684	52	480	0.3	15	3.1	0	0.3	34
chr2_24697	52	531	0.3	9	1.7	0	0.3	28
chr2_24704	50	619	1.2	22	3.6	0	1.2	2
chr2_24800	46	502	0.4	2	0.4	0	0.4	0
chr2_24815	50	510	0.1	11	2.2	0	0.1	44
chr2_24827	50	519	1.1	15	2.9	0	1.1	6
chr2_24841	54	508	0.2	8	1.6	0	0.2	36
chr2_24859	52	406	0.5	12	3	0	0.5	12

chr2_24876	50	481	0.4	7	1.5	0	0.4	18
chr2_24879	52	525	0.2	17	3.2	0	0.2	30
chr2_24910	52	443	0.3	3	0.7	0	0.3	6
chr2_25833	52	666	1.3	21	3.2	0	1.3	2
chr2_25851	52	449	0.7	16	3.6	0	0.7	0
chr2_27241	48	404	0.2	6	1.5	0	0.2	30
chr2_27258	54	484	0.5	6	1.2	0	0.5	0
chr2_27261	50	566	0.1	8	1.4	0	0.1	44
chr2_27280	54	440	0	0	0	0	0	46
chr2_27294	52	494	0.4	4	0.8	0	0.4	14
chr2_27313	54	461	0.3	7	1.5	0	0.3	34
chr2_27968	54	590	0.7	10	1.7	0	0.7	12
chr2_29406	44	518	0.6	10	1.9	0	0.6	2
chr2_4395	52	496	0.5	8	1.6	0	0.5	24
chr2_5491	54	448	0.1	8	1.8	0	0.1	38
chr2_5499	52	596	0.8	20	3.4	0	0.8	22
chr2_5526	46	465	0.6	10	2.2	0	0.6	0
chr2_5991	50	543	0.5	11	2	0	0.5	0
chr2_6341	50	548	0.6	12	2.2	0	0.6	0
chr2_6444	54	448	0.8	18	4	0	0.8	4
chr2_6685	36	414	0	17	4.1	0	0	36
chr2_6737	50	478	0.6	15	3.1	0	0.6	12
chr2_6787	50	575	0.6	4	0.7	0	0.6	20
chr2_7409	50	513	0.5	11	2.1	0	0.5	12
chr2_7420	52	561	0.4	19	3.4	0	0.4	27
chr2_7927	54	498	0.1	2	0.4	0	0.1	42
chr2_7945	52	597	0.2	6	1	0	0.2	40
chr2_7954	50	480	1	10	2.1	0	1	6
chr2_8583	42	506	1	10	2	0	1	22

chr2_8589	50	537	0	7	1.3	0	0	50
chr2_8590	54	572	0.3	9	1.6	0	0.3	22
chr2_8600	52	476	1.1	14	2.9	0	1.1	24
chr2_8609	50	445	0.4	14	3.1	0	0.4	20
chr2_8620	52	459	0.2	7	1.5	0	0.2	38
chr2_8629	52	539	0.2	21	3.9	0	0.2	20
chr2_8651	48	464	0.3	15	3.2	0	0.3	18
chr2_8655	54	613	0.5	38	6.2	0	0.5	38
chr2_8677	54	511	0.3	10	2	0	0.3	22
chr2_8688	54	624	0.4	13	2.1	0	0.4	4
chr2_8698	44	476	0	7	1.5	0	0	42
chr2_8747	54	627	2.6	24	3.8	0	2.6	2
chr2_8754	48	418	0.3	13	3.1	0	0.3	26
chr3_11795	52	424	0.2	4	0.9	0	0.2	26
chr3_11879	54	519	0.8	8	1.5	0	0.8	14
chr3_1282	52	565	0.3	8	1.4	0	0.3	22
chr3_1300	54	455	0.1	8	1.8	0	0.1	42
chr3_13359	52	559	0.4	10	1.8	0	0.4	2
chr3_13404	54	603	0.8	16	2.7	0	0.8	0
chr3_16820	52	602	0.7	16	2.7	0	0.7	0
chr3_16833	52	535	0.8	8	1.5	0	0.8	20
chr3_17448	54	543	0.1	11	2	0	0.1	36
chr3_17607	50	543	0.6	10	1.8	0	0.6	22
chr3_17623	54	551	0.2	12	2.2	0	0.2	20
chr3_17699	54	545	0.2	8	1.5	0	0.2	24
chr3_17721	54	645	0.2	17	2.6	0	0.2	28
chr3_17747	54	582	0.6	13	2.2	0	0.6	24
chr3_17769	54	567	0.1	9	1.6	0	0.1	38
chr3_17781	48	370	0.2	4	1.1	0	0.2	36

chr3_17860	54	389	0.2	20	5.1	0	0.2	46
chr3_17890	48	614	0.1	7	1.1	0	0.1	32
chr3_17991	52	515	0.4	12	2.3	0	0.4	14
chr3_18203	54	562	0	2	0.4	0	0	46
chr3_18256	52	469	0.3	5	1.1	0	0.3	40
chr3_18306	54	578	0.2	12	2.1	0	0.2	25
chr3_19568	42	630	0.4	36	5.7	0	0.4	8
chr3_19997	54	531	1.4	13	2.4	0	1.4	0
chr3_20013	50	549	1.4	27	4.9	0	1.4	0
chr3_21510	50	416	0.4	22	5.3	0	0.4	22
chr3_21949	54	424	0.1	4	0.9	0	0.1	28
chr3_22024	48	377	0.4	5	1.3	0	0.4	22
chr3_23724	50	534	0.7	4	0.7	0	0.7	0
chr3_24903	54	398	0.1	0	0	0	0.1	40
chr3_24963	52	495	0.2	6	1.2	0	0.2	24
chr3_25095	54	493	0.5	0	0	0	0.5	2
chr3_2698	50	523	0.8	13	2.5	0	0.8	30
chr3_2723	54	615	0.3	7	1.1	0	0.3	14
chr3_2735	48	581	0.1	2	0.3	0	0.1	36
chr3_2742	52	498	0.2	4	0.8	0	0.2	34
chr3_2999	54	463	0.3	7	1.5	0	0.3	38
chr3_300	50	542	0.5	15	2.8	0	0.5	2
chr3_3073	50	471	0.2	2	0.4	0	0.2	24
chr3_3180	54	514	0.6	7	1.4	0	0.6	20
chr3_3247	52	544	0.3	20	3.7	0	0.3	32
chr3_362	48	660	0.5	15	2.3	0	0.5	4
chr3_3805	54	500	2.1	21	4.2	0	2.1	0
chr3_3876	50	530	0.6	15	2.8	0	0.6	2
chr3_457	48	624	0.3	12	1.9	0	0.3	4

chr3_509	50	636	0.5	21	3.3	0	0.5	12
chr3_5445	54	525	0.2	6	1.1	0	0.2	36
chr3_5455	50	536	0.2	13	2.4	0	0.2	24
chr3_5476	52	616	0.1	13	2.1	0	0.1	28
chr3_5520	50	553	0.3	1	0.2	0	0.3	30
chr3_5536	46	580	0.6	16	2.8	0	0.6	2
chr3_5552	48	510	0.3	6	1.2	0	0.3	26
chr3_5573	54	538	0.1	10	1.9	0	0.1	36
chr3_5605	44	410	0.6	8	2	0	0.6	20
chr3_5687	54	461	0.4	3	0.7	0	0.4	30
chr3_5691	46	373	0	9	2.4	0	0	46
chr3_576	52	500	0.6	5	1	0	0.6	14
chr3_5766	54	560	0.2	12	2.1	0	0.2	26
chr3_5767	52	464	0.1	7	1.5	0	0.1	26
chr3_5781	52	683	0.2	2	0.3	0	0.2	22
chr3_5815	46	610	0.4	11	1.8	0	0.4	2
chr3_5848	52	429	0.1	7	1.6	0	0.1	36
chr3_5854	54	573	1.1	12	2.1	0	1.1	4
chr3_5857	46	588	0.5	27	4.6	0	0.5	0
chr3_5873	54	539	0.5	19	3.5	0	0.5	12
chr3_5877	54	618	0.1	10	1.6	0	0.1	36
chr3_5894	52	553	0.4	16	2.9	0	0.4	16
chr3_5918	54	555	0.3	13	2.3	0	0.3	12
chr3_5934	52	487	1	8	1.6	0	1	28
chr3_6118	52	438	3.7	17	3.9	0	3.7	6
chr3_6129	52	480	0.2	4	0.8	0	0.2	26
chr4_10540	50	441	0.3	8	1.8	0	0.3	22
chr4_10550	48	558	0.6	23	4.1	0	0.6	14
chr4_10564	50	566	0.4	14	2.5	0	0.4	6

chr4_11155	50	629	0.3	9	1.4	0	0.3	15
chr4_11159	54	478	0.2	10	2.1	0	0.2	18
chr4_13410	50	523	0.4	19	3.6	0	0.4	6
chr4_13431	48	330	0.1	12	3.6	0	0.1	34
chr4_13654	54	416	0.2	13	3.1	0	0.2	32
chr4_15363	52	543	0.1	3	0.6	0	0.1	32
chr4_15987	40	487	0	36	7.4	0	0	40
chr4_17221	54	616	0.4	17	2.8	0	0.4	2
chr4_17640	52	479	0.3	7	1.5	0	0.3	28
chr4_6701	52	559	0.6	6	1.1	0	0.6	2
chr4_6739	50	552	0.7	26	4.7	0	0.7	2
chr4_7199	54	546	0.4	11	2	0	0.4	0
chr4_7243	46	409	0	8	2	0	0	46
chr4_7258	50	617	1.6	13	2.1	0	1.6	4
chr4_7282	52	620	0.5	19	3.1	0	0.5	4
chr4_7513	54	527	0.1	5	0.9	0	0.1	40
chr4_7559	52	468	0.6	14	3	0	0.6	10
chr4_7570	54	553	0.5	19	3.4	0	0.5	8
chr4_9665	50	471	0.2	0	0	0	0.2	28
chr4_9725	52	587	0.2	11	1.9	0	0.2	28
chr4_9746	54	483	0.5	6	1.2	0	0.5	4
chr5_10115	50	512	0.1	5	1	0	0.1	34
chr5_10176	54	530	0.1	3	0.6	0	0.1	36
chr5_10180	52	533	0.4	5	0.9	0	0.4	2
chr5_10184	54	516	1.3	15	2.9	0	1.3	2
chr5_10207	48	431	0.9	9	2.1	0	0.9	0
chr5_10239	50	410	0.5	8	2	0	0.5	36
chr5_10251	52	501	0.2	6	1.2	0	0.2	26
chr5_10254	44	374	0.8	17	4.5	0	0.8	2

chr5_10266	52	578	0.1	4	0.7	0	0.1	36
chr5_10353	52	384	0.2	5	1.3	0	0.2	38
chr5_10416	52	627	2.6	9	1.4	0	2.6	10
chr5_10787	54	585	0.1	2	0.3	0	0.1	34
chr5_10841	50	581	0.7	10	1.7	0	0.7	0
chr5_10846	48	432	0.1	5	1.2	0	0.1	26
chr5_10859	52	559	0.2	10	1.8	0	0.2	30
chr5_10906	54	520	0.2	3	0.6	0	0.2	6
chr5_11139	50	550	0.3	4	0.7	0	0.3	8
chr5_11146	54	564	0.1	7	1.2	0	0.1	42
chr5_11148	48	585	0.3	4	0.7	0	0.3	0
chr5_11165	54	578	0	12	2.1	0	0	46
chr5_11198	44	539	0.4	8	1.5	0	0.4	0
chr5_11202	50	490	0.2	6	1.2	0	0.2	27
chr5_11206	50	537	0.3	8	1.5	0	0.3	6
chr5_11214	54	561	0.5	19	3.4	0	0.5	4
chr5_11226	50	603	0.2	14	2.3	0	0.2	16
chr5_11240	52	557	0.1	15	2.7	0	0.1	38
chr5_11245	46	570	0.2	8	1.4	0	0.2	40
chr5_11286	50	328	0.4	6	1.8	0	0.4	22
chr5_11302	54	507	0.2	16	3.2	0	0.2	30
chr5_11304	52	534	0.5	7	1.3	0	0.5	2
chr5_11321	50	575	0.2	18	3.1	0	0.2	24
chr5_11325	52	570	0.5	21	3.7	0	0.5	32
chr5_11342	50	586	0.1	9	1.5	0	0.1	28
chr5_11359	54	570	0.5	17	3	0	0.5	4
chr5_11571	54	615	0.5	8	1.3	0	0.5	28
chr5_11637	50	518	0.2	5	1	0	0.2	29
chr5_11657	46	562	0.1	8	1.4	0	0.1	30

chr5_11783	50	610	0.5	19	3.1	0	0.5	4
chr5_11955	50	527	0	5	0.9	0	0	48
chr5_12397	54	493	0.7	2	0.4	0	0.7	32
chr5_12400	52	535	0.6	16	3	0	0.6	12
chr5_12422	50	382	0.4	23	6	0	0.4	18
chr5_12835	52	543	0.4	13	2.4	0	0.4	8
chr5_13040	52	378	0.8	10	2.6	0	0.8	14
chr5_13042	54	552	0.4	8	1.4	0	0.4	14
chr5_14403	52	643	0.5	8	1.2	0	0.5	20
chr5_14621	42	489	0	2	0.4	0	0	42
chr5_14632	50	523	0.7	9	1.7	0	0.7	20
chr5_14720	50	425	0.8	9	2.1	0	0.8	34
chr5_14766	44	701	0.9	11	1.6	0	0.9	4
chr5_14864	52	554	1.1	18	3.2	0	1.1	0
chr5_14870	50	505	0.2	12	2.4	0	0.2	28
chr5_14876	46	323	0.8	13	4	0	0.8	24
chr5_14914	54	560	0.7	25	4.5	0	0.7	12
chr5_15022	46	315	0.4	2	0.6	0	0.4	14
chr5_15078	50	591	0.5	34	5.8	0	0.5	8
chr5_1597	54	557	0.4	14	2.5	0	0.4	26
chr5_1675	54	606	0.6	20	3.3	0	0.6	2
chr5_1689	52	550	1.5	9	1.6	0	1.5	8
chr5_1701	50	584	0.7	6	1	0	0.7	26
chr5_1746	54	523	0.2	6	1.1	0	0.2	28
chr5_1749	54	657	0.8	14	2.1	0	0.8	4
chr5_1757	52	417	0.2	0	0	0	0.2	38
chr5_1800	54	624	1.4	4	0.6	0	1.4	4
chr5_1813	50	511	0.3	5	1	0	0.3	2
chr5_1834	48	556	0	3	0.5	0	0	38

chr5_1989	50	472	0.4	9	1.9	0	0.4	24
chr5_3191	50	375	0.3	3	0.8	0	0.3	22
chr5_3204	50	526	0.2	6	1.1	0	0.2	30
chr5_3273	50	470	1.3	17	3.6	0	1.3	2
chr5_3353	52	537	0.1	6	1.1	0	0.1	36
chr5_3377	54	493	1.5	19	3.9	0	1.5	10
chr5_3407	54	430	0.2	14	3.3	0	0.2	18
chr5_3418	52	609	0.2	4	0.7	0	0.2	8
chr5_4018	54	563	1.3	7	1.2	0	1.3	0
chr5_5657	52	523	0.2	11	2.1	0	0.2	28
chr5_8793	48	571	0.5	5	0.9	0	0.5	0
chr6_6814	54	541	0.8	10	1.8	0	0.8	44
chr6_8253	50	466	0.4	0	0	0	0.4	8
chr6_8786	52	554	0.7	2	0.4	0	0.7	0
chr6_8806	48	497	0.2	13	2.6	0	0.2	16
chr6_8829	54	577	0.3	6	1	0	0.3	40
chr6_9046	54	495	0.5	10	2	0	0.5	4
chr6_9069	54	544	0.2	12	2.2	0	0.2	26
chr6_9474	54	574	0.4	9	1.6	0	0.4	2
chr6_9529	50	499	0.6	10	2	0	0.6	6
chr6_9532	50	545	0.8	7	1.3	0	0.8	2
chr6_9559	50	565	0.5	10	1.8	0	0.5	18
chr6_9631	54	498	0.5	12	2.4	0	0.5	12
chr6_9640	54	466	0.1	2	0.4	0	0.1	38
chr6_9737	54	620	0.3	16	2.6	0	0.3	28
chr6_9746	50	517	0.5	2	0.4	0	0.5	36
chr6_9762	42	456	0.6	2	0.4	0	0.6	2
chr6_9783	52	593	0.1	12	2	0	0.1	36
chr6_9787	50	507	0.7	9	1.8	0	0.7	4

chr6_9797	54	529	0.3	9	1.7	0	0.3	18
chr6_9804	54	498	0.1	3	0.6	0	0.1	24
chr6_9806	50	554	0.3	9	1.6	0	0.3	2
chr6_9809	52	553	0.3	19	3.4	0	0.3	28
chr6_9838	50	531	0.1	12	2.3	0	0.1	32
chr7_10269	54	559	0.3	15	2.7	0	0.3	23
chr7_10305	54	505	0.6	2	0.4	0	0.6	10
chr7_10322	54	487	0.2	14	2.9	0	0.2	32
chr7_10380	46	562	0.2	12	2.1	0	0.2	38
chr7_10394	52	442	1.9	8	1.8	0	1.9	2
chr7_10440	48	449	1.9	8	1.8	0	1.9	18
chr7_10443	54	604	0.3	15	2.5	0	0.3	8
chr7_10480	46	522	0.5	9	1.7	0	0.5	16
chr7_10497	54	508	0.8	24	4.7	0	0.8	8
chr7_10502	50	481	0.6	7	1.5	0	0.6	28
chr7_10532	52	568	0.6	10	1.8	0	0.6	2
chr7_10675	46	537	0.5	12	2.2	0	0.5	32
chr7_10681	52	464	0.3	10	2.2	0	0.3	24
chr7_10694	52	544	0.7	16	2.9	0	0.7	16
chr7_1370	50	574	0.2	8	1.4	0	0.2	28
chr7_1380	54	581	0.6	8	1.4	0	0.6	18
chr7_6327	36	333	0	1	0.3	0	0	36
chr7_6333	46	514	0.4	2	0.4	0	0.4	30
chr7_6366	54	475	0.2	3	0.6	0	0.2	42
chr7_9094	54	470	0.1	7	1.5	0	0.1	38
chr7_9104	54	615	1.8	25	4.1	0	1.8	10
chr8_3308	54	495	2.2	12	2.4	0	2.2	2
chr8_4014	52	458	0.1	7	1.5	0	0.1	32
chr8_4067	52	463	0.3	9	1.9	0	0.3	40

chr8_4091	54	499	0.3	13	2.6	0	0.3	18
chr8_4241	54	574	0.3	25	4.4	0	0.3	2
chr8_4243	48	427	0.4	11	2.6	0	0.4	20
chr8_4319	52	492	0.4	14	2.8	0	0.4	6
chr8_4333	54	529	0.3	17	3.2	0	0.3	24
chr8_4340	52	475	0.2	7	1.5	0	0.2	30
chr8_4342	52	585	0.5	8	1.4	0	0.5	4
chr8_4410	50	538	0.5	11	2	0	0.5	40
chr8_6218	52	548	0.6	12	2.2	0	0.6	6
chr8_6224	50	417	0.4	3	0.7	0	0.4	12
chr8_6230	54	547	0.3	4	0.7	0	0.3	34
chr8_6277	54	449	0.3	8	1.8	0	0.3	32
chr8_6299	52	512	0.7	16	3.1	0	0.7	2
chr8_6872	50	477	0.5	9	1.9	0	0.5	2
chr8_7441	46	545	1.7	13	2.4	0	1.7	2
chr8_7449	54	565	0.1	7	1.2	0	0.1	40
chr8_7513	34	490	0	2	0.4	0	0	34
chr8_7534	54	446	0.3	6	1.3	0	0.3	22
chr8_8877	54	594	0.2	12	2	0	0.2	34
chr8_8942	46	558	1.3	13	2.3	0	1.3	0
chr8_9143	54	615	0.5	14	2.3	0	0.5	8
chr8_9173	46	433	0	2	0.5	0	0	44
chr9_1152	48	593	0.4	24	4	0	0.4	20
chr9_1164	50	553	0.3	4	0.7	0	0.3	6
chr9_1169	44	618	0	7	1.1	0	0	40
chr9_1191	50	494	0.5	5	1	0	0.5	0
chr9_1949	50	509	0.2	7	1.4	0	0.2	35
chr9_2499	52	586	0.2	14	2.4	0	0.2	16
chr9_3289	48	669	0.3	5	0.7	0	0.3	0

chr9_3633	54	492	0.3	3	0.6	0	0.3	36
chr9_5181	52	473	0.4	12	2.5	0	0.4	20
chr9_5205	52	492	0.3	4	0.8	0	0.3	16
chr9_5220	52	569	0.1	8	1.4	0	0.1	36
chr9_5246	42	597	0	2	0.3	0	0	42
chr9_6320	54	600	0.5	27	4.5	0	0.5	0
chr9_6322	54	480	0.1	13	2.7	0	0.1	38
chr9_6325	52	548	0.8	23	4.2	0	0.8	2
chr9_6414	52	517	0.3	4	0.8	0	0.3	24
chr9_7171	54	584	0.2	1	0.2	0	0.2	40
chr9_7188	34	416	0	4	1	0	0	34
chr9_7189	52	597	0.4	10	1.7	0	0.4	16
chr9_7434	50	502	0.5	17	3.4	0	0.5	4
chrun_random_11933	54	571	0.5	8	1.4	0	0.5	4
chrun_random_3551	50	296	0	12	4.1	0	0	50
chrun_random_7197	54	554	0.4	17	3.1	0	0.4	20
chrz_11272	52	522	0.2	17	3.3	0	0.2	22
chrz_11397	50	628	0.6	10	1.6	0	0.6	14
chrz_11457	52	523	1	7	1.3	0	1	6
chrz_11465	54	450	0.7	1	0.2	0	0.7	16
chrz_11477	54	500	0.7	19	3.8	0	0.7	46
chrz_11491	52	569	0.6	15	2.6	0	0.6	0
chrz_11540	54	606	0.7	24	4	0	0.7	2
chrz_11557	54	517	0.1	9	1.7	0	0.1	36
chrz_11584	54	406	0.4	7	1.7	0	0.4	18
chrz_11684	52	553	0.4	5	0.9	0	0.4	26
chrz_4313	52	623	0.7	4	0.6	0	0.7	0
chrz_467	52	274	0.3	15	5.5	0	0.3	36

chrz_4740	48	441	0.1	4	0.9	0	0.1	40
chrz_4747	54	528	0.5	14	2.7	0	0.5	8
chrz_4759	50	569	0.8	4	0.7	0	0.8	2
chrz_4763	54	273	0.4	6	2.2	0	0.4	28
chrz_4772	52	586	0.5	13	2.2	0	0.5	6
chrz_4782	54	557	0.1	16	2.9	0	0.1	34
chrz_4787	50	621	0.2	5	0.8	0	0.2	8
chrz_4794	52	480	0.4	26	5.4	0	0.4	16
chrz_4816	52	469	0.4	32	6.8	0	0.4	16
chrz_4832	50	577	0.5	4	0.7	0	0.5	0
chrz_4838	48	430	1	7	1.6	0	1	20
chrz_4841	40	359	0.2	7	1.9	0	0.2	26
chrz_5495	54	573	0.1	10	1.7	0	0.1	38
chrz_5501	52	629	0.3	4	0.6	0	0.3	0
chrz_5971	54	552	0.6	20	3.6	0	0.6	22
chrz_6357	50	460	0.3	6	1.3	0	0.3	14
chrz_6396	52	549	0.3	13	2.4	0	0.3	26
chrz_646	50	322	0.6	10	3.1	0	0.6	0
chrz_6575	52	609	0.2	11	1.8	0	0.2	20
chrz_6612	50	605	0.8	12	2	0	0.8	12
chrz_6686	54	559	0.3	22	3.9	0	0.3	22
chrz_6690	54	540	0.1	6	1.1	0	0.1	30
chrz_6703	50	403	0.7	18	4.5	0	0.7	24
chrz_6778	48	647	0.2	8	1.2	0	0.2	32
chrz_6799	48	562	0.3	8	1.4	0	0.3	2
chrz_7406	54	573	0.6	22	3.8	0	0.6	22
chrz_7416	54	590	0.2	8	1.4	0	0.2	26
chrz_7824	52	490	0.2	10	2	0	0.2	44
chrz_7889	54	640	0.1	3	0.5	0	0.1	30

chrz_7923	46	471	1	21	4.5	0	1	4
chrz_7943	50	554	0.6	14	2.5	0	0.6	0
chrz_7982	50	527	0.3	5	0.9	0	0.3	34
chrz_7997	54	510	0.7	1	0.2	0	0.7	4
chrz_8024	50	391	0.3	9	2.3	0	0.3	24
UCE Means	**50.99**	**518.46**	**0.47**	**10.82**	**2.09**	**0.00**	**0.47**	**20.54**

Rocks and ice: effects of geographic features and Pleistocene glaciations on the Gondwanan *Liolaemus fitzingerii* Species Group

Jared A. Grummer[1], Luciano J. Avila[2], Mariana M. Morando[2], Jack W. Sites, Jr.[3], and Adam D. Leaché[1]

[1]*Department of Biology and Burke Museum of Natural History and Culture, University of Washington, Box 351800, Seattle, WA 98195-1800, USA;*

[2]*Centro Nacional Patagónico – Consejo Nacional de Investigaciones Científicas y Técnicas (CENPAT-CONICET), Boulevard Almirante Brown 2915, ZC: U9120ACD, Puerto Madryn, Argentina*

[3]*Department of Biology and M.L. Bean Life Science Museum, Brigham Young University, Provo, Utah 84602, USA*

Abstract.— Our understanding of phylogeographic patterns has flourished in the past ten years largely due to molecular lab advances. However, this knowledge base is heavily geographically skewed towards northern hemisphere taxa. A real knowledge gap exists in phylogeographic patterns of Gondwanan taxa, particularly in relation to Pleistocene glacial cycles. We collected SNP data for 178 individuals in the *Liolaemus fitzingerii* group of southern-central Argentina to infer phylogeographic patterns with particular focus on geologic and climatic impacts by identifying population-level boundaries via population clustering analyses, inferring patterns of migration and genetic diversity across the landscape, and through demographic model testing. Although current taxonomy recognizes nine species, our analyses identified six distinct genetic clusters in this group. Phylogenetic relationships between these populations are weakly supported – only a single clade composed of the southern two populations received strong support. Our spatially-aware migration analyses identified many large geographic features such as plateaus and rivers as barriers to gene flow, where genetic diversity estimates generally lower in individuals inhabiting western (higher elevation) and southern (higher latitude) regions. Demographic model testing supported a process of population expansion, followed by bottlenecks and recent population re-expansion accommodated by gene flow for all populations in this group. These results are in agreement with expectations that populations retreated and expansed during recent glacial cycles. Our results add to the collective understanding of phylogeographic patterns of temperate Gondwanan taxa.
(Keywords: SNP, ddRADseq, Allele frequency spectrum, Model testing, Pleistocene glaciation, Population, Hybridization)

Phylogeography lies at the intersection of population genetics and phylogenetics, and similarly links the understanding of microevolutionary processes and macroevolutionary patterns (Avise et al. 1987). Over the past 15 years, this field has evolved from qualitative correlations based on single-locus (typicallly mitochondrial DNA [mtDNA] in vertebrates) analyses to statistical, hypothesis-based studies utilizing multi-locus data (Hickerson et al. 2010). In spite of these advances, our understanding of the evolutionary processes governing relationships and geographic distributions of remotely distributed taxa remains poor, particularly for Gondwanan taxa (Beheregaray 2008). In South America, we know relatively little about how geologic and climatic forces shaped the phylogeographic and evolutionary histories of temperate taxa.

The advancement of the field of statistical phylogeography (Knowles 2009) is largely due to increased phylogeographic model testing (e.g. Pelletier and Carstens 2014; Thomé and Carstens 2016). Geology, climatology, or paleontology/palynology are used to construct hypotheses for phylogeographic models. These models include (but are not limited to) parameters for population divergence times, effective population sizes, and migration (gene flow) rates. Knowledge of historic climatic or geologic events provides the information for constructing models that include population contractions into refugia or expansions from refugia into suitable habitat depending on environmental suitability and geologic barriers. Parameter estimates are then generated, given the hypothetical population-level demographic processes that would occur under each scenario. The parameter estimates from empirical data are then compared to the model to select the most likely historic scenario that gave rise to the data.

Although substantial work has been done to understand the biotic effects of Pleistocene glaciations in temperate northern hemisphere taxa (e.g. Klicka and Zink 1999; Mila et al. 2000), relatively few studies have been conducted on temperate fauna and flora in Gondwana (Beheregaray 2008). Southern South America is of particular importance in understanding the biotic effects of Pleistocene climatic fluctuations, because this region represents a substantial portion of land in the temperate latitudes of the southern hemisphere (apart from Antarctica). Terrestrial organisms in this part of

the world were affected by Pliocene and Pleistocene glaciations during the past ~5 million years because glaciers extended on top of the Andes as far north as 36°S at various points. Furthermore, sea levels dropped within the past 120,000 years more than 100m below current levels, extending the southeastern coastline of South America some 200 kilometers further to the east than its present location (Lambeck and Chappell 2001; Rabassa et al. 2005). Although few empirical studies have tested glacial effects on southern South American taxa, a study on fish (genus *Galaxias*) from this region identified refugial populations and secondary contact following Pleistocene glacial retreat (Zemlak et al. 2008). Quaternary glacial cycles likely played a vital role in shaping geographic patterns of *Liolaemus* lizards as well(Victoriano et al. 2008; Vera-Escalona et al. 2012; Vidal et al. 2012).

Liolaemus is a broadly temperate-distributed diverse clade of lizards that contains the furthest south distributed lizard species in the world (*L. magellanicus* in Tierra del Fuego, Chile). This genus is composed of two large clades corresponding to the subgenera *Liolaemus sensu stricto* ("Chileno group") and *Eulaemus* ("Argentino group"), which are distributed respectively to the west and east of the crest of the Andean Mountain range. Previous studies have provided a wide range of ages for the *Eulaemus* clade, the subgenus to which the focal group of this study, the *L. fitzingerii* group, belongs, ranging from 12.6 million years ago (ma) based on mtDNA (Schulte et al. 2000) to 18.1 ma with combined nuclear and mtDNA (Fontanella et al. 2012). Schulte et al. (2000) concluded that the divergence between many *Liolaemus* species preceded Plio-Pleistocene climatic fluctuations, and that Andean vicariance was therefore likely the cause for the majority of species-level divergences in this group. With regards to the *L. fitzingerii* species group, only a single member (*L. melanops*) was included in the Schulte et al. (2000) study. These studies suggest a deep evolutionary history of *Liolaemus* in South America that has been affected, in part, by historic geologic events.

The *Liolaemus fitzingerii* species group is currently composed of nine recognized species (Avila et al. 2006, 2008, 2010), which inhabit Patagonian shrub-steppe and

coastal dune ecosystems from ∼37 – 50°S in Argentina. A fossil-calibrated molecular phylogeny provided a date of 4.67 million years (3.62–8.59 HPD) for the common ancestor of this group (Fontanella et al. 2012). Previous research by Minoli et al. (2014) showed incongruence between predicted and realized distributions based on ecological niche modeling and highlighted morphological-based taxonomic discrepancies in this group. Avila et al. (2006) used a combined dataset of mtDNA (*cyt. B*, ND4, 12S) and two nuclear DNA (nDNA) markers (c-mos and gapdh) to infer phylogeographic patterns in the *L. fitzingerii* species group through nested clade phylogeographic analysis (NCPA). They found a high level of geographic structure in this species group, with the Somuncura Plateau seeming to be a geographical boundary for some clades. Overall, their analyses revealed a complex mixture of evolutionary processes for this group including gene flow, long distance dispersal/population expansion, habitat fragmentation, and post-glacial range expansion. Most recently, Grummer et al. (2017b) conducted a phylogenomic analysis to infer evolutionary relationships of both described and candidate species within this group with 580 nuclear loci alongside a mitogenomic dataset. Their analyses revealed poor support for relationships between many of the described species, with a strong sister-species relationship inferred between *L. xanthoviridis* and *L. fitzingerii*. Furthermore, network analyses and contrasting relationships inferred from nuclear and mitochondrial genomes indicated hybridization and gene flow between *L. melanops* and *L. martorii*.

We have formalized the results of Avila et al. (2006) into hypotheses to be tested with a genomic dataset. In populations to the west of the Valdes Peninsula (*Liolaemus melanops* "north" and "south" in the Avila et al. 2006 study), they inferred range expansions from a northeast to southwest direction that led to isolation-by-distance and gene flow. In the south, fragmentation of ancestral ranges was inferred, where *L. fitzingerii* was hypothesized to be derived from a peripheral population of *L. xanthoviridis*. Furthermore, secondary contact was inferred between *L. fitzingerii* and *L. xanthoviridis* following post-glacial range expansion. If late Pleistocene glaciations affected the *L. fitzingerii* group as hypothesized by Avila et al. (2006), we would expect

higher genetic diversity in populations to the east (lower elevations) and north (lower latitudes). Furthermore, glacially-affected populations should show signs of genetic reduction and bottlenecks owing to reduced population sizes in glacial refugia. Although the model testing that we performed is not spatially explicit, the demographic model testing framework is highly flexible and allowed us to test these hypotheses, in addition to a variety of conceptually similar models that we discuss below.

In this study of the *Liolaemus fitzingerii* species group, we test phylogeographic/demographic models based on hypotheses proposed by Avila et al. (2006) in addition to novel hypotheses guided heuristically by our own results. We used a dataset composed of densely sampled individuals covering the known geographic range of this species group that were sequenced for genome-wide single nucleotide polymorphisms (SNPs). In doing so, we identify the population-level geographic boundaries and test the aforementioned hypotheses through a combination of demographic modeling and estimates of migration and genetic diversity.

Materials and Methods

Sampling

We sampled 205 individuals that cover the known geographical extent of taxa in the *Liolaemus fitzingerii* group. We also chose two *Liolaemus mapuche* individuals and two *L. josei* individuals to serve as outgroups. We subsequently removed 27 ingroup individuals due to poor data quality, which made our final SNP dataset composed of 178 individuals (Fig. 1; Supplemental Table S1). Of these 178 individuals, 20 were also included in the Grummer et al. (2017b) study that generated a phylogeny for the *L. fitzingerii* species group based on 580 sequence capture loci (Supplemental Table S1).

DNA Data Collection

DNA was extracted from tissue (tails tips, liver) with either a Qiagen DNeasy blood and tissue extraction kit (Qiagen Inc., CA, USA) or NaCl extraction method (MacManes 2013). We discarded samples that had degraded genomic DNA with little high molecular weight DNA.

Laboratory SNP Acquisition.— We generated a SNP dataset through the double digestion restriction site-associated DNA sequencing approach (Peterson et al. 2012). The double digestion of genomic DNA was performed with the enzymes SbfI (8bp recognition sequence [5' CCTGCAGG 3'], "rare cutter"; New England Biolabs, Ipswich, MA) and MspI (4bp recognition sequence [5' CCGG 3'], "common cutter"; New England Biolabs, Ipswich, MA). After ligation of unique barcoded primers for demultiplexing, we selected for genomic fragments between 365-465bp (415-515bp after ligating barcoded oligonucleotides) with the Blue Pippin DNA fragment size selector (Sage Science, MA, USA). Polymerase chain reaction (PCR) was performed on pooled samples consisting of eight individuals each, with NEB Phusion Taq polymerase (New England Biolabs Inc., MA, USA) and the following thermocycler conditions: 98°for 0:30, (98°for 0:10, 58°for 0:30, 72°for 0:30) x 12 cycles, and a final 10:00 extension at 72°C. Individuals were then multiplexed (either 96 or 144 samples) and sequenced on an Illumina HiSeq 2500 (Illumina Inc., CA, USA) with 50bp single-end reads at the Vincent J. Coates QB3 Sequencing Facility at the University of California, Berkeley.

Bioinformatics and Dataset Assembly

Raw Illumina reads were processed to generate "clusters" (e.g., loci) and SNPs through the program pyRAD v3.0.66 (Eaton 2014). PyRAD is well suited for this dataset because unlike its main competitor STACKS (Catchen et al. 2013), pyRAD allows for indels (insertion-deletion events) when creating alignments (and ultimately loci) that are likely to be present in interspecific datasets. After demultiplexing individuals with a unique combination of a 5bp barcode and 6bp index, each read contained 39bp of sequenced genomic DNA. pyRAD uses the programs VSEARCH (Rognes et al. 2016) and MUSCLE (Edgar 2004) to assemble reads into loci. Reads were discarded if they

had ≥4bp with a Phred quality score <20. Reads were first clustered within individuals, and then across individuals, with a 90% clustering threshold. We used a minimum depth of sequencing coverage of 10 for all loci. When generating a dataset of unlinked SNPs, pyRAD's paralog filter allows the user to modulate the number of heterozygous base calls (e.g., "ambiguities") at a given locus. This value will scale with the amount of evolutionary divergence between samples because heterozygous positions can also arise through true polymorphism and not just fixed allelic differences. With a final dataset of 178 ingroup taxa (see Results section below), we set this value to 134, allowing approximately 75% of individuals to share a heterozygosity at a given SNP. We set our missing data threshold to a maximum of 25% per locus.

Population Identification

We used the program Structure (Pritchard et al. 2000; Falush et al. 2003) to identify distinct populations in the *L. fitzingerii* group. We implemented a hierarchical approach to identify populations (similar to Gowen et al. 2014); we successively ran $k = 2$ until all individuals in each analysis were assigned to a single population. We ran ten replicates of each analysis with a burn-in of 100,000 generations and post-burn-in also of 100,000 generations, with the admixture model with correlated allele frequencies. Structure Harvester (Earl and vonHoldt 2012) was used to generate input files for CLUMPP (Jakobsson and Rosenberg 2007), which combined results across replicate analyses. DISTRUCT (Rosenberg 2004) was used to visualize our Structure results as bar plots.

Species Tree Estimation

We inferred a coalescent-based species tree in SNAPP (Bryant et al. 2012) to estimate relationships between populations in this group. Because gene flow has been shown to lead to incorrect inference of the true species-level history in species tree analyses (Leaché et al. 2014), we attempted to reduce its impact by selecting a subset of non-admixed individuals for phylogenetic analysis. We selected individuals that had an

admixture proportion >0.80 based on our Structure analyses and were not located near the edge of population boundaries. Individuals were assigned to "species" based on our Structure results. Our sampling and assignment scheme resulted in four individuals per ingroup species, with two individuals each of *Liolaemus mapuche* and *L. josei* outgroup species. We set the mutation rates of the 0 → 1 allele (U) and 1 → 0 allele (V) to 1.0, with the birth rate for the Yule model prior on the species tree given a gamma prior. Analyses were run for 10^6 generations, logging the state every 10^2 generations with a burnin of $2x10^5$ generations. Convergence of the MCMC chain was assessed via Tracer v1.5 (Rambaut and Drummond 2007).

Demographic Model Testing

We tested historical demographic scenarios through the multi-population allele frequency spectrum (AFS), implemented in ∂a∂i (Gutenkunst et al. 2009). ∂a∂i uses diffusion approximation to generate a simulated AFS distribution under demographic models specified by the user. The AFS generated under the specified model is then compared against the empirical AFS to determine model fit. Allele frequency spectra are either 1-, 2-, or 3-dimensions, corresponding to the number of populations modeled. We tested 1- and 2-D demographic models that were generated by 1) formalizing phylogeographic hypotheses proposed by Avila et al. (2006), or 2) heuristically based on inferred population distributions from our own results. The five 1-D models we tested were 1) standard neutral model, 2) instantaneous size change some time in the past, 3) exponential growth starting some time in the past, 4) an instantaneous size change some time ago followed by exponential growth, and 5) an instantaneous population size change that continues for some duration, followed by a second size change ("recovery"); the 12 2-D models we tested are summarized graphically in Figure 2.

The populations we analyzed in each 1- and 2-D model were informed by our Structure results (see Results). As our populations were predominantly arranged in latitudinal bands, our 2-D models were composed of neighboring (parapatric) pairs: populations 2 and 3, populations 3 and 4, populations 4 and 5, and populations 5 and 6

(see Fig. 3 for population numbering). We did not consider population 1 in our 2-D demographic analyses because along with previous results from Grummer et al. (2017b), our Structure and species tree results here show that this population is divergent from the remaining five populations. We performed model testing on these four population pairs.

For each demographic model, we re-compiled a new dataset consisting of just the population (or two) for which we were modeling the demographic history, with a 25% missing data threshold. When calculating the AFS for each model, we "projected" down the number of alleles (=2 x N individuals) so as to find a balance between missing data and maximizing the number of segregating sites (with the *allele frequency spectrum*.S() command in ∂a∂i). Our projections typically reduced the size of our original dataset by $\sim$ 25-35% (Table 1). Analyses that used outgroup data from *Liolaemus josei* to polarize the AFS presented problems with ancestral state misidentification, so we therefore excluded outgroup reference sequence data and therefore present results of "folded" spectra.

We began parameter optimization by first randomly perturbing parameters (parameter perturbation at 3x) and optimizing each parameter set with the *dadi.Inference.optimize_log* command; each optimization was run for 100 iterations. The multinomial approach (*dadi.Inference.ll_multinom*) was used to calculate the log-likelihood for each parameter set, and the best parameter set was then used in the second round of parameter optimizations. In the second round of optimization, the best parameter values from the first round were used as starting parameter estimates, which were perturbed as in round one, only to a lesser extent (2x), also for 100 iterations. We finally performed a third round of optimizations, this time only perturbing starting parameters 1x. The estimated log-likelihood and AIC model selection was used to select the best 1-D or 2-D demographic model for each one- or two-population model, and the optimal parameter set was then used to simulate the 1-D or 2-D allele frequency spectrum. The top model was inferred to be significantly better than the other models if it was >2 AIC points lower.

∂a∂i parameter estimates of timed events (e.g., population divergences) and migration rates are in relation to population size (N_{ref}), which must be calculated based on a θ estimate from ∂a∂i and mutation rate (μ). We used a mutation rate of 1.358 x 10^{-9} substitutions per site per generation, based on a generation time of two years and the rate 6.79 x 10^{-4} substitutions per site per million years calculated by Fontanella et al. (2012) for the nuclear gene *CMOS*.

Genetic Diversity and Migration Estimation

Given our hypotheses that these populations were affected by Pleistocene glaciations, we wanted to visualize genetic diversity on the landscape. Our hypothesis is that genetic diversity will be highest in the east and north, where refugial populations presumably existed during the last glacial maximum. Following global temperature rise, populations expanded to the west (higher elevations) and south (higher latitudes); if so, genetic diversity will be relatively low in western and southern populations.

We used the Bayesian EEMS ("estimating effective migration surfaces") method developed by Petkova et al. (2015) to estimate both genetic diversity and migration. A virtual grid is created on the landscape whereby migration can occur only between neighboring grid points. The program then uses estimates of genetic diversity and their decay across the landscape to infer migration rates. When genetic similarity decays quickly, effective migration rates are inferred to be low. Because migration is only allowed to occur between adjacent grid points, the model is similar to that of many landscape genetics circuit theory approaches (Hanks and Hooten 2013). Additionally, this program also estimates isolation by distance.

Structure identified one individual in population 2 and three individuals in population 3 (two with the exact same locality) that were far to the west of the remaining individuals in their respective populations (Fig. 3), so we removed those individuals prior to our EEMS analyses. We varied the grid density ("ndemes" parameter) to ensure this parameter was not affecting our analyses, with ndemes = 250 and 500. Each analysis was run for 5x10^7 generations, with a burn-in of 3x10^7

generations and sampling every $2x10^4$ generations. We ran four replicates of each analysis and assessed convergence via parameter trace plots and consistency of results across independent replicates.

Results

Population Identification

Our hierarchical Structure analyses revealed six populations that are predominantly latitudinally distributed with areas of parapatric contact on the north and south distribution margins of central populations (e.g., populations 2-5; Fig. 3). The furthest north population (which includes the type localities of *L. goetschi*, *L. martorii* and *L. dumerili*) was identified during the first iteration, whereas the northern-central populations (populations "2" and "3") were identified during the last (fifth) round of analysis. Five individuals were recovered as distinct in population 4 that were near the margins of populations 3 and 5, and so we re-analyzed these along with each population, 3 and 5, but they still formed a unique cluster in Structure. Because these individuals do not form a geographically cohesive group, we removed them from subsequent analyses.

Coalescent SNP Species Tree

After removing individuals that were near population boundaries and had an admixture proportion <0.80, we were able to use four individuals per population, for a total of 24 ingroup individuals. At the deepest divergence, two clades with strong support were recovered, with the northern-most population (population 1) forming a clade with the two outgroup species (Fig. 4). This is similar to the results of our hierarchical population structure analyses, which identified this population during the first round of analysis.The remaining five *L. fitzingerii* species group populations (populations 2-5) formed a strongly supported clade, but with relationships between populations

generally poorly supported. However, the two southern-most populations, populations 5 and 6, formed a strongly supported clade (posterior probability = 0.99).

Demographic Models

1-D Models.— The most complex model, an instantaneous population size change that continues for some duration, followed by a second size change, was favored for all 1-D demographic models (Supplemental Table S2). Generally, the data for each population fit the model well, but the model tended to under-predict the number of low-frequency alleles (Supplemental Figure S1). The top model is shown graphically in Figure 5, and the parameter estimates are shown by population in Table 1. In general, ancestral populations expanded ∼10x in the past (with a range of 3-35x), followed by a population bottleneck (current population size of 0.005 - 0.82x the size of the ancestral population), which happened very recently (∼25-300 generations; Table 2).

2-D Models.— For the northern-most population pair (2 + 3), three top models were within two AIC points of each other (Supplemental Table S3), and the allele frequency spectrum for the top model is shown in Figure 6. All top models share some form of migration (historic/continuous or secondary contact) and current population sizes that are larger than historic population sizes. Specifically, the top model showed that these populations diverged ∼280,000 years ago and then came into secondary contact 100,000 years ago, with a symmetric migration rate of 1.7-8.36 individuals per generation (Fig. 2ix; Tables 3,4). The range in migration rates is due to a symmetric migration rate with different population sizes in each population. Following divergence from their common ancestor, population 2 has continued to expand to a population size 8x that of the ancestral population. In contrast, population 3 expanded to a size 5x that of the ancestral population, but has since reduced to a size only ∼60% bigger than the ancestral population (Table 3).

In contrast to populations 2 and 3, only a single model was within the 2-point AIC confidence interval for populations 3 and 4 (Supplemental Table S3). This was a

simple model of population divergence, in which the populations diverged ∼285,000 years ago, followed by symmetric migration at a rate of 2.3-6 individuals per generation (Fig. 2iii; Tables 3,4). As in the other northern populations, these current populations are larger than their ancestral counterparts, where populations 3 and 4 were inferred to be ∼6.5x and ∼2.5x larger than the ancestral population, respectively. Although only 2.26 AIC points worse than this top model, the second-best model indicated secondary contact between these two populations ∼130,000 years ago at a similar migration rate (Supplemental Table S3).

For the two southern-most populations pairs, populations 4 + 5 and 5 + 6, the same demographic model was selected, in which the populations diverged, followed by a size change and then an exponential expansion in both populations, with migration since the time of the population split; this model is shown in Figure 2xii. The optimized parameter estimates for the optimal model are shown by population pair in Table 3, and the allele frequency spectra are shown in Figure 6, where the data are a good fit to the model (residuals can be seen in Supplemental Figs. S2,S3). Populations 4 and 5 diverged from one another ∼520,000 years ago, and following population divergence, the size of population 4 doubled. In contrast, population 5 went through a bottleneck to a population size $\frac{1}{100}$th its original size, but subsequently expanded to a size 40% larger than the size before the bottleneck. The inferred migration rate between populations 4 and 5 was 1.45-2.38 individuals per generation (Table 4). The demographic model of populations 5 + 6 inferred a deeper divergence time than that of populations 4 and 5, which was ∼635,000 years ago. As in the population 4 + 5 model, population 5 was inferred to have gone through a bottleneck followed by an expansion. However, both post-bottleneck and contemporary population sizes were inferred to be larger in the population 5 + 6 model (Table 3). Population 6 similarly went through a bottleneck, followed by an expansion that doubled the post-bottleneck population size. The inferred migration rate between populations 5 and 6 was 1.92-2.22 individuals per generation (Table 4).

Genetic Diversity and Migration Estimates

In the northern populations (2-4), the areas of highest diversity are generally in the east (Fig. 7a,b). In the central and southern populations (4-6), which are found between approximately 41 and 49°S latitude, genetic diversity is generally higher in the northern populations, irrespective of their location in relation to the coast (Fig. 7c,d). Migration rates are higher in the lower elevation habitats in the east for populations 2 and 3 (Fig. 7a). Notably, a low migration rate is inferred to the north and east of the Somuncura Plateau, with high migration rates on the plateau itself. Similarly in populations 3 and 4, a low rate of migration is inferred to the east and south of the Somuncura Plateau, with higher migration to the south and west of those areas (Fig. 7b). In populations 4 and 5, high migration rates are inferred between individuals in the southern and eastern coastal regions, with central populations acting as a genetic barrier to more interior populations to the north. And lastly, many of the southern individuals from population 6 are connected through migration, whereas low migration exists between individuals from population 5 (Fig. 7d).

Discussion

In this study, we identified six genetically distinct populations in the *Liolaemus fitzingerii* species group based on dense geographic sampling and genome-wide SNP data. Although these populations are geographically distinct and their boundaries largely coincide with prominent landscape features, relationships between them are generally poorly supported. This could be due to gene flow between parapatrically distributed populations, which migration and demographic analyses support. The analyses of Grummer et al. (2017b) also recovered poor support for relationships between species in this group, which they conclude was due to a rapid radiation from a common ancestor along with interspecific gene flow. Estimates of genetic diversity inferred in this study are generally higher in eastern and northern populations, which agrees with the hypothesis of these areas serving as glacial refugia during Pleistocene glaciations. This hypothesis was also supported in our demographic modeling of single populations, but is not supported by the two-population demographic models, which

generally indicate population expansion following historic population divergences. Together, our results suggest a complex history of population contractions and expansions that have provided ample opportunities for gene flow during population divergence.

Genetic and Geographic Population Boundaries

Our analysis of ~900 putatively unlinked SNPs identified six genetically distinct populations (Fig. 3). These populations were largely geographically cohesive, except for four individuals of populations two and three that were well to the north and west of the remaining individuals of these populations. Apart from cross-contamination or sample mix-up, this result is difficult to interpret. The habitat in which these individuals were collected is superficially similar to the environments that characterize the core of these population ranges to the east, and some authors have even posited that a seaway existed here in the past. It is therefore possible that these individuals are part of a refugial/relictual population. Although less likely, these individuals could be the result of a long-distance dispersal event, or even human-mediated dispersal. However, these hypotheses would need to be tested with more sampled individuals.

Our data supported six populations, which is in contrast with current taxonomy that recognizes nine species in the *Liolaemus fitzingerii* group that have primarily been diagnosed by morphological analyses (Avila et al. 2006, 2008, 2010). Our northern-most population, population "1", is composed of the species *L. casamiquelai*, *L. dumerili*, *L. goetschi*, *L. martorii*, and *L. morenoi*. In unpublished morphological analyses, Minoli et al. (*in prep.*) concluded that *L. dumerili* could not be distinguished from *L. goetschi*, supporting a similar result from the genetic data here (the remaining three species were not included in their analysis). Based on our sampling, it is not entirely clear if a geographic boundary separates population 1 from the remaining five populations, particularly in the eastern, coastal areas. However, the northern edge of the Somuncura Plateau lies on the southwestern border of population 1 (Figs. 1,3). The Somuncura Plateau quickly rises up out of the surrounding areas to a maximum elevation of

∼1600m. This area is biologically distinct from its surroundings with a number of endemic species only found there (Muzón et al. 2005).

Population 2 is made up of *L. martorii* and *L. melanops* individuals. Abdala (2003) described *Liolaemus martorii*, and diagnosed this species as different from *L. melanops* on the basis of its smaller size (67mm snout-vent length [SVL] vs. 89+mm) and lack of a black head. However, some of the populations that were originally described as *L. melanops* are now described as *L. martorii* (Abdala 2003; Avila et al. 2006). Unpublished morphological analyses by Avila et al. (*in prep.*) show a possible zone of hybridization between these two taxa to the west of the San Matias Gulf, indicating the close evolutionary history of these taxa. Our migration analyses showed high connectivity between individuals in this area and individuals to the west. Similar to population 1, the Somuncura Plateau appears to be a migration barrier for individuals in this population. In fact, a contact zone of hybridization between populations 2 and 3 has been identified that corresponds to eastern edge of this plateau, and can be seen in Figure 7a at the interface of high and low migration rates, and is under investigation (Grummer et al. 2017a).

Population 3 is composed of individuals from *L. shehuen* and *L. canqueli*. Abdala et al. (2012) described *L. shehuen* as distinct from *L. canqueli* in that *L. shehuen* lacks transverse black and yellow-orange bands and a black head that are present in *L. canqueli*. The species-level status of these taxa has not been addressed through rigorous morphological or genetic analysis, but our data indicate that they are genetically indistinguishable. Whereas the Somuncura Plateau seems to be a barrier to populations 1 and 2, individuals from population 3 are found both below (to the east) and on the Somuncura Plateau (Figs. 3,7). The southern edge of population 3 corresponds very well to the Chubut River, where estimated migration rates are inferred to be low (Figs. 1,3,7b). This river's headwaters are in the eastern Andean mountains and its mouth is at the provincial capitol city of Chubut, Rawson. We are not aware of other studies that show this river as a phylogeographic barrier.

Population 4 is composed of individuals from three described species, *L. canqueli*,

L. chehuachekenk, and *L. melanops*. *Liolaemus canqueli* and *L. melanops* share a black head and alternating yellowish and black dorsal bands, which morphologically distinguish these species from *L. chehuachekenk*. *Liolaemus chehuachekenk* is also larger than *L. melanops* with a maximum SVL of 90 vs. 82mm (Avila et al. 2008). Similar to population 3, the Chubut River seems to be a barrier to migration for these individuals, particularly for individuals in the central and eastern parts of this population's range (Fig. 7b). However, this river seems to be a more porous barrier in the west, where individuals from population 4 are found on the north side of the river. Just as the Somuncura Plateau acts as a barrier in the north, the Canquel Plateau appears to partition population 4 from population 5 (Fig. 7c). Similar in age to the Somuncura Plateau, the Canquel Plateau is ∼25 million years old (Kay et al. 2007) and is ∼1000m high at its highest point, ∼500m higher than most of its surroundings.

Population 5 is composed of *Liolaemus xanthoviridis* individuals. The habitat is more or less continuous to the south of this population, with a gradual transition into coastal dunes. Overall, individuals from population 5 appear to be genetically isolated from one another (Fig. 7d), indicating low levels of gene flow within this population. Along with population 6, these two are the most southerly distributed populations in the group. They are two of the three largest taxa in the group (along with *L. canqueli*; Etheridge 2000), and form the only strongly supported sister relationship in the species group (Fig. 4). Population 6 is composed of *L. camarones* and *L. fitzingerii* individuals. In a rigorous analysis of morphological and climatic data, Minoli et al. (2014) determined that *L. camarones* is not distinct from *L. fitzingerii*, a result that was mainly driven by morphological analyses because *L. camarones* is only known from its type locality. Our genetic analyses here did not reveal any distinction between *L. fitzingerii* and *L. camarones* sampled from its type locality.

In spite of population-level genetic structure revealed by our Structure analyses (Fig. 3), the relationships between populations in the *L. fitzingerii* group are poorly supported (Fig. 4). Unexpectedly, population 1 was strongly recovered as sister to our outgroup taxa (*L. josei*, *L. mapuche*) to the exclusion of the remainder of the *L.*

fitzingerii group populations. This relationship is similar to that inferred by Grummer et al. (2017b), where the northern populations were early-diverging in the group's evolutionary history. The first possibility for population 1 forming a clade with outgroup taxa is due to a phylogenetic rooting issue. But secondly, whereas *L. josei* is found much further to the north and is hypothesized to be distantly related to taxa in the *L. fitzingerii* group (Abdala 2005), *Liolaemus mapuche* occurs within the range of the *L. fitzingerii* group. *Liolaemus mapuche* was described based on morphological analyses and hypothesized to be related to the *L. boulengeri* group which includes the *L. fitzingerii* species group (Abdala 2002). Abdala (2003) hypothesized its morphology-based placement within the *L. fitzingerii* group, and our analyses support its close relation to taxa in this group.

The remaining five populations (2-6) form a strongly supported clade (Fig. 4). However, the only strongly supported relationship (pp $\geq$0.95) is between the two southern-most populations, 5 and 6. The relationships between all other populations are poorly supported, which may be due to gene flow between populations. The favored demographic models for all population pairs included migration between populations, and significant migration will over time homogenize previously distinct gene pools in the absence of strong selection. This creates the expectation that gene flow will obscure the true evolutionary relationships between taxa. In support of this idea, a simulation study on the effect of gene flow on species tree estimation showed that migration across lineages does indeed increase the uncertainly in inferred relationships (Leaché et al. 2014). Although we sought to minimize the impacts of gene flow on our estimate of relationships between populations by only selecting individuals that had low admixture proportions and were in the core of each population's range, it is possible that the low level of support we see between populations is due to historic and/or contemporary gene flow. An alternative hypothesis is that these populations evolved from an ancestral population in rapid succession and that populations retain ancestral polymorphisms. This hypothesis is further supported by Grummer et al. (2017b) who concluded that these populations rapidly evolved from a common ancestor. These hypotheses are not

mutually exclusive.

Demographic and Climatologic Histories

The *Liolaemus fitzingerii* species group originated in the early Pliocene ~4.7 million years ago (Fontanella et al. 2012). During this time, temperatures in the south Atlantic region were warmer than current conditions (Fig. 8a; Shackleton 1995). Since ~6.8 million years ago, >50 cold-warm climatic cycles were recorded in the global δ^{18}O record (Shackleton 1995). Approximately 2.6 million years ago, global temperatures reached colder-than-present environmental conditions. In the late Pliocene, environmental conditions allowed for the development of a continuous ice sheet along the eastern Andes to latitudes as far north as 36°S, which would have grown during subsequent cooling events. These fluctuating climatic cycles ended at the end of the Pleistocene approximately 15,000 years ago with the terminus of the last glacial maximum (LGM) (Kaplan et al. 2004). During the LGM, the surface of the Atlantic Ocean was ~120m lower than its current position, exposing a broad coastline of eastern Argentina approximately 200km to the east of the current shoreline (Lambeck and Chappell 2001).

With genome-wide SNP data, we modeled the demographic history of populations in the *Liolaemus fitzingerii* species group. We first estimated demographic models for each population independently before inferring joint demographic models with species pairs that we determined to be parapatric. When analyzing each population separately, the same model was favored that showed an instantaneous population growth followed by a bottleneck (Fig. 5; Table 1). After populations expanded, they remained that size for ~50,000 – 500,000 years, after which point they shrank to <5% of their ancestral size in the past couple hundred generations. The bottleneck that population 2 went through was much less severe than the remaining populations (Table 1). However, even though this was the optimal model, the fit of this model to the data was not good with a high number of residuals (Supplemental Figure S1), drawing doubt on the accuracy of the parameter estimates for this population.

The qualitatively coincident parameter estimates for all populations suggests

that they were similarly affected by environmental/climatic factors. For the northern populations (2-4), our results suggest that these populations diverged in rapid succession from their ancestor (Table 4); presumably in the north, where the closest relatives of the *L. fitzingerii* species group are currently found), at which point populations, and likely ranges, expanded. Rapid and nearly simultaneous divergences of these populations is supported by our demographic analyses, which showed divergence times of these populations within 5,000 years of each other (Table 4). Starting at ~130,000 years ago when the last glacial cooling event began, individuals and therefore distributional ranges had to retreat to lower elevation habitats that are in the eastern coastal areas of central-southern Argentina. Although our demographic modeling analyses don't support this model, our estimates of genetic diversity do. During contraction of populations 2 and 3 into glacial refugia along the coast, it is possible that refugia were also established in the north where some isolated individuals of these populations were identified. However, we need further sampling to test this hypothesis.

In their confined geographic glacial refugia, population sizes would have been reduced, leading to the reduction of genetic diversity through increased genetic drift (e.g., population bottleneck effects). Following the end of the LGM, warming temperatures during the Holocene would have allowed populations to once again expand to the west. Under this hypothesis, genetic diversity would be lowest in the west because these individuals would be the result of a series of founder events. In fact, this is what we see with our data, where estimates of genetic diversity are highest in the east and lowest in the west (Fig. 7a,b). The same logic holds for the southern populations, 5 and 6, but their increased latitude led us to hypothesize that cooler temperatures would not only force them to lower elevations (eastward), but also lower latitudes (northward). Again, our results support this hypothesis, where genetic diversity is lowest in the south, suggesting these individuals might have reached their current locations via recent population expansion (Fig. 7c,d). But we note, however, that these results need to be interpreted cautiously where sampling is low and the program has to interpolate genetic diversity estimates between distant samples.

Whereas the same best-fitting model was selected for each population in the 1-D demographic analyses, three separate models were selected for the two-population models (Supplemental Table S3). Furthermore, two of the four population pairs had 2-3 models within the 2 AIC-point confidence intervals. Nonetheless, population size changes were included in the optimal model for three of the four population-pairs, and migration in all four population-pairs (Table 3). In the populations 2 + 3 model, both populations were not inferred to go through a bottleneck (e.g., were always larger than ancestral populations), and in the populations 3 + 4 model, a size change was not inferred. Another incongruent result we recovered was between divergence times inferred in our demographic modeling analyses and relative divergence times in our species tree analysis. Although relationships between many of the populations were poorly supported (Fig. 4), the support for the sister relationship between populations 5 and 6 was strong, and also the most recent. In contrast, our demographic model estimates placed this as the most ancient divergence of all species-pairs. Because the demographic modeling of ∂a∂i is within a maximum likelihood framework, the only way to ensure stability of results to run multiple independent analyses and verify similarity of results across replicate runs. We were not able to perform replicate runs and therefore assume that the incongruence in inferred divergence times is due to incorrect estimates from our ∂a∂i demographic analyses.

In a similar fashion, we noticed incongruent results between our 1- and 2-D demographic analyses. The first reason why these results may differ is because migration is not accounted for in the 1-D models. When the genetic variation sampled from a population is the product of a gene pool supplemented by emigrant alleles through migration from a second distinct population, the extant population size will be inferred to be larger than the "true" population size. Essentially, this situation is mimicking the genetic effects of not sampling a "ghost population" in migration analyses (Beerli 2004). How this ghost population effect affects the inference of 1-D models is not known, but nonetheless is a plausible explanation for the 1-D vs. 2-D differences. Secondly, the difference could come from a low/reduced ancestral genetic

diversity that would lead to incorrect parameter estimations. Specifically, a population bottleneck that happened in the recent past would eliminate much of the genetic diversity that existed before the population contraction, leaving little information for inferring historic population genetic parameters and false inferences of the true evolutionary history. And finally, the discordant results could simply be due to inaccurate inference as noted above. The 1-D model for population 2 and 2-D models for two population pairs (2 + 3 and 3 + 4) showed a somewhat poor fit to the data with high residuals (Fig. 7; Supplemental Fig. S1), which appeared systematic because they were not randomly distributed in the AFS. Running further analyses to confirm our parameter estimates could address this final point.

Conclusions

We inferred the phylogeographic history of the populations within the *Liolaemus fitzingerii* species group. Many boundaries separating these populations correspond to large geographic features, such as the Chubut River, and Somuncura and Canquel Plateaus. Although our 1- and 2-population demographic modeling results were not completely in agreement, commonalities between the models show that populations in this group expanded during the Pleistocene, but have recently gone through population bottlenecks. Our results also showed high levels of migration between all pairwise population comparisons, with genetic diversity highest in the eastern and northern populations. These results support the notion that populations in the *L. fitzingerii* species group were affected by Pleistocene glaciations and large geographic features in southern-central Argentina. Our study has thus provided further insight into the phylogeographic history of biota in southern Gondwana over the past five million years.

Acknowledgments

This work used the Vincent J. Coates Genomics Sequencing Laboratory at UC Berkeley, supported by NIH S10 OD018174 Instrumentation Grant. This research was funded in part by a National Science Foundation Doctoral Dissertation Improvement Grant (DEB-1500933) to JAG, and was facilitated though the use of advanced computational, storage, and networking infrastructure provided by the Hyak supercomputer system at the University of Washington.

*

References

Abdala, C. S. 2002. Nuevo liolaemus (iguania: Liolaemidae) perteneciente al grupo boulengeri de la provincia de neuquén, argentina. Cuadernos de Herpetología 16:3–13.

Abdala, C. S. 2003. Cuatro nuevas especies del género liolaemus (iguania: Liolaemidae), pertenecientes al grupo boulengeri, de la patagonia, argentina. Cuadernos de Herpetología 17:3–32.

Abdala, C. S. 2005. Dos nuevas especies del género liolaemus (iguania: Liolaemidae) y redescripción de liolaemus boulengeri (koslowsky, 1898). Cuadernos de Herpetología 19:3–33.

Abdala, C. S., J. Díaz Gómez, and V. Juarez Heredia. 2012. From the far reaches of patagonia: new phylogenetic analyses and description of two new species of the *Liolaemus fitzingerii* clade (iguania: Liolaemidae). Zootaxa 3301:34–60.

Avila, L., M. Morando, and J. Sites. 2006. Congeneric phylogeography: hypothesizing species limits and evolutionary processes in patagonian lizards of the liolaemus boulengeri group (squamata: Liolaemini). Biological Journal of the Linnean Society 89:241–275.

Avila, L. J., M. Morando, and J. W. Sites Jr. 2008. New species of the iguanian lizard genus liolaemus (squamata, iguania, liolaemini) from central patagonia, argentina. Journal of Herpetology 42:186–196.

Avila, L. J., C. H. F. Pérez, M. Morando, and J. Sites Jr. 2010. A new species of liolaemus (reptilia: Squamata) from southwestern rio negro province, northern patagonia, argentina. Zootaxa 2434:47–59.

Avise, J. C., J. Arnold, R. M. Ball, E. Bermingham, T. Lamb, J. E. Neigel, C. A. Reeb, and N. C. Saunders. 1987. Intraspecific phylogeography: the mitochondrial dna

bridge between population genetics and systematics. Annual review of ecology and systematics 18:489–522.

Beerli, P. 2004. Effect of unsampled populations on the estimation of population sizes and migration rates between sampled populations. Molecular Ecology 13:827–836.

Beheregaray, L. B. 2008. Twenty years of phylogeography: the state of the field and the challenges for the southern hemisphere. Molecular Ecology 17:3754–3774.

Bryant, D., R. Bouckaert, J. Felsenstein, N. A. Rosenberg, and A. RoyChoudhury. 2012. Inferring species trees directly from biallelic genetic markers: bypassing gene trees in a full coalescent analysis. Molecular biology and evolution 29:1917–1932.

Catchen, J., P. A. Hohenlohe, S. Bassham, A. Amores, and W. A. Cresko. 2013. Stacks: an analysis tool set for population genomics. Molecular ecology 22:3124–3140.

Earl, D. A. and B. M. vonHoldt. 2012. Structure harvester: a website and program for visualizing structure output and implementing the evanno method. Conservation genetics resources 4:359–361.

Eaton, D. A. 2014. Pyrad: assembly of de novo radseq loci for phylogenetic analyses. Bioinformatics Page btu121.

Edgar, R. C. 2004. Muscle: multiple sequence alignment with high accuracy and high throughput. Nucleic acids research 32:1792–1797.

Etheridge, R. 2000. A review of lizards of the liolaemus wiegmannii group (squamata, iguania, tropiduridae), and a history of morphological change in the sand-dwelling species. Herpetological Monographs Pages 293–352.

Falush, D., M. Stephens, and J. K. Pritchard. 2003. Inference of population structure using multilocus genotype data: linked loci and correlated allele frequencies. Genetics 164:1567–1587.

Fontanella, F. M., M. Olave, L. J. Avila, M. MORANDO, et al. 2012. Molecular dating and diversification of the south american lizard genus liolaemus (subgenus *Eulaemus*)

based on nuclear and mitochondrial dna sequences. Zoological Journal of the Linnean Society 164:825–835.

Gowen, F. C., J. M. Maley, C. Cicero, A. T. Peterson, B. C. Faircloth, T. C. Warr, and J. E. McCormack. 2014. Speciation in western scrub-jays, haldane's rule, and genetic clines in secondary contact. BMC evolutionary biology 14:135.

Grummer, J. A., L. J. Avila, M. M. Morando, and A. D. Leaché. 2017a. Four species linked by three hybrid zones: two instances of repeated hybridization in one species group (genus *Liolaemus*). In Preparation .

Grummer, J. A., L. J. Avila, M. M. Morando, J. W. Sites, and A. D. Leaché. 2017b. Lack of phylogenetic support matters: phylogenomic evidence for a recent and rapid radiation in lizards of the patagonian *Liolaemus fitzingerii* species group. In Preparation .

Gutenkunst, R. N., R. D. Hernandez, S. H. Williamson, and C. D. Bustamante. 2009. Inferring the joint demographic history of multiple populations from multidimensional snp frequency data. PLoS Genet 5:e1000695.

Hanks, E. M. and M. B. Hooten. 2013. Circuit theory and model-based inference for landscape connectivity. Journal of the American Statistical Association 108:22–33.

Hickerson, M., B. Carstens, J. Cavender-Bares, K. Crandall, C. Graham, J. Johnson, L. Rissler, P. Victoriano, and A. Yoder. 2010. Phylogeography's past, present, and future: 10 years after. Molecular Phylogenetics and Evolution 54:291–301.

Jakobsson, M. and N. A. Rosenberg. 2007. Clumpp: a cluster matching and permutation program for dealing with label switching and multimodality in analysis of population structure. Bioinformatics 23:1801–1806.

Kaplan, M. R., R. P. Ackert, B. S. Singer, D. C. Douglass, and M. D. Kurz. 2004. Cosmogenic nuclide chronology of millennial-scale glacial advances during o-isotope stage 2 in patagonia. Geological Society of America Bulletin 116:308–321.

Kay, S. M., A. Ardolino, M. Gorring, and V. Ramos. 2007. The somuncura large igneous province in patagonia: interaction of a transient mantle thermal anomaly with a subducting slab. Journal of Petrology 48:43–77.

Klicka, J. and R. M. Zink. 1999. Pleistocene effects on north american songbird evolution. Proceedings of the Royal Society of London B: Biological Sciences 266:695–700.

Knowles, L. L. 2009. Statistical phylogeography. Annual Review of Ecology, Evolution, and Systematics 40:593–612.

Lambeck, K. and J. Chappell. 2001. Sea level change through the last glacial cycle. Science 292:679–686.

Leaché, A. D., R. B. Harris, B. Rannala, and Z. Yang. 2014. The influence of gene flow on species tree estimation: a simulation study. Systematic Biology 63:17–30.

MacManes, M. 2013. Available from: http://dx.doi.org/10.6084/m9.figshare.658946. Figshare 5.

Mila, B., D. J. Girman, M. Kimura, and T. B. Smith. 2000. Genetic evidence for the effect of a postglacial population expansion on the phylogeography of a north american songbird. Proceedings of the Royal Society of London B: Biological Sciences 267:1033–1040.

Minoli, I., M. Morando, and L. J. Avila. 2014. Integrative taxonomy in the liolaemus fitzingerii complex (squamata: Liolaemini) based on morphological analyses and niche modeling. Zootaxa 3856:501–528.

Muzón, J., G. R. Spinelli, P. Pessacq, N. Von Ellenrieder, A. L. Estevez, P. I. Marino, P. J. Pérez Goodwyn, E. B. Angrisano, F. Díaz, L. A. Fernández, et al. 2005. Insectos acuáticos de la meseta del somuncurá, patagonia, argentina. inventario preliminar. Revista de la Sociedad Entomológica Argentina 64:47–67.

Pelletier, T. A. and B. C. Carstens. 2014. Model choice for phylogeographic inference using a large set of models. Molecular ecology 23:3028–3043.

Peterson, B. K., J. N. Weber, E. H. Kay, H. S. Fisher, and H. E. Hoekstra. 2012. Double digest radseq: an inexpensive method for de novo snp discovery and genotyping in model and non-model species. PloS one 7:e37135.

Petkova, D., J. Novembre, and M. Stephens. 2015. Visualizing spatial population structure with estimated effective migration surfaces. Nature genetics .

Pritchard, J. K., M. Stephens, and P. Donnelly. 2000. Inference of population structure using multilocus genotype data. Genetics 155:945–959.

Rabassa, J., A. M. Coronato, and M. Salemme. 2005. Chronology of the late cenozoic patagonian glaciations and their correlation with biostratigraphic units of the pampean region (argentina). Journal of South American Earth Sciences 20:81–103.

Rambaut, A. and A. Drummond. 2007. Tracer v1. 4.

Rognes, T., T. Flouri, B. Nichols, C. Quince, and F. Mahé. 2016. Vsearch: a versatile open source tool for metagenomics. PeerJ 4:e2584.

Rosenberg, N. A. 2004. Distruct: a program for the graphical display of population structure. Molecular Ecology Notes 4:137–138.

Schulte, J. A. I., R. J. Macey, R. E. Espinoza, and A. Larson. 2000. Phylogenetic relationships in the iguanid lizard genus liolaemus: multiple origins of viviparous reproduction and evidence for recurring andean vicariance and dispersal. Biological Journal of the Linnean Society 69:75–102.

Shackleton, N. 1995. New data on the evolution of Pliocene climatic variability. Yale University Press.

Thomé, M. T. C. and B. C. Carstens. 2016. Phylogeographic model selection leads to insight into the evolutionary history of four-eyed frogs. Proceedings of the National Academy of Sciences 113:8010–8017.

Vera-Escalona, I., G. D'Elía, N. Gouin, F. M. Fontanella, C. Muñoz-Mendoza, J. W. Sites Jr, and P. F. Victoriano. 2012. Lizards on ice: evidence for multiple refugia in liolaemus pictus (liolaemidae) during the last glacial maximum in the southern andean beech forests. PloS one 7:e48358.

Victoriano, P. F., J. C. Ortiz, E. Benavides, B. J. Adams, et al. 2008. Comparative phylogeography of codistributed species of chilean liolaemus (squamata: Tropiduridae) from the central-southern andean range. Molecular Ecology 17:2397–2416.

Vidal, M. A., P. I. Moreno, and E. Poulin. 2012. Genetic diversity and insular colonization of liolaemus pictus (squamata, liolaeminae) in north-western patagonia. Austral Ecology 37:67–77.

Zemlak, T. S., E. M. Habit, S. J. Walde, M. A. Battini, E. D. Adams, and D. E. Ruzzante. 2008. Across the southern andes on fin: glacial refugia, drainage reversals and a secondary contact zone revealed by the phylogeographical signal of galaxias platei in patagonia. Molecular Ecology 17:5049–5061.

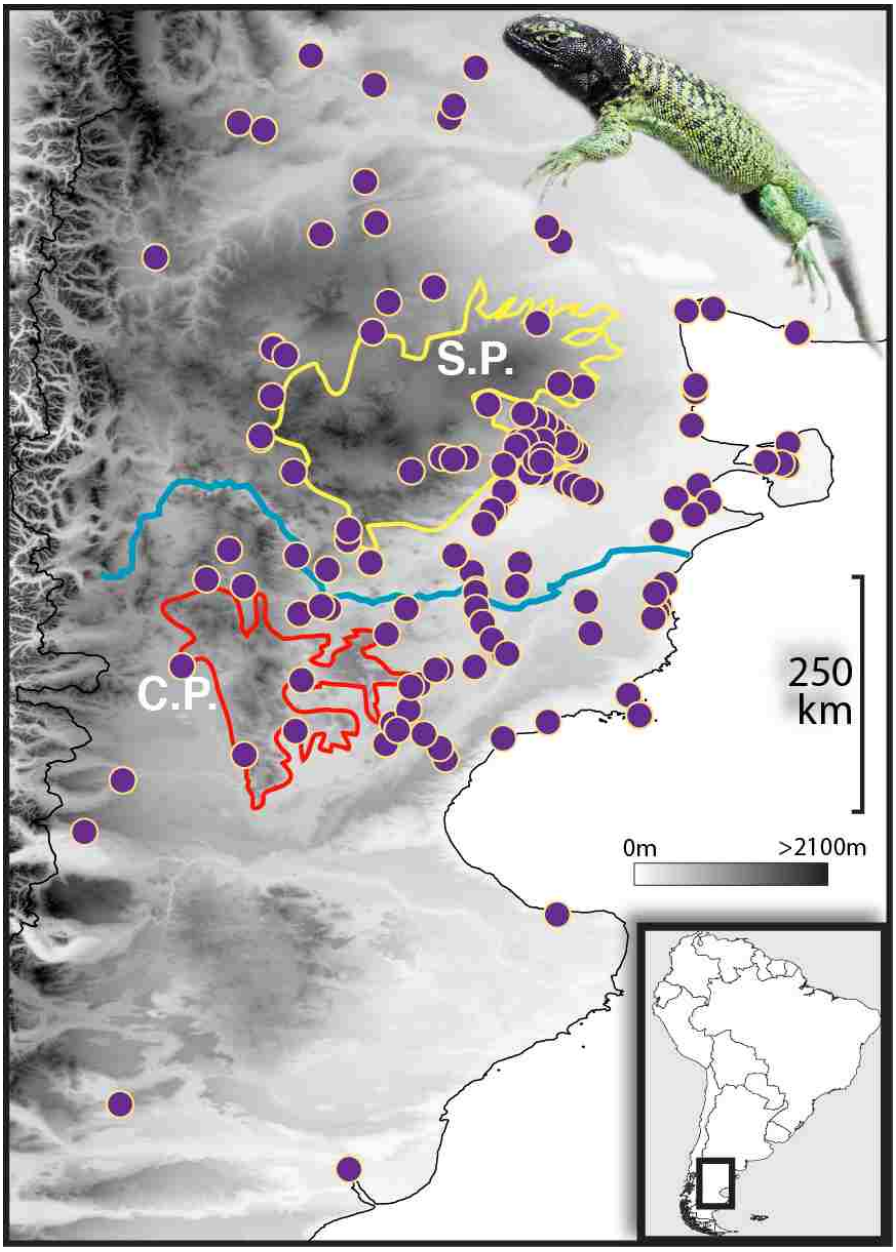

Figure 1: Sampling map of individuals included in this study. The Somuncura Plateau ("S.P.") and Canquel Plateau ("C.P.") are roughly outlined in yellow and red, respectively, with the Chubut River shown in blue. A *Liolaemus melanops* male is shown in the top right.

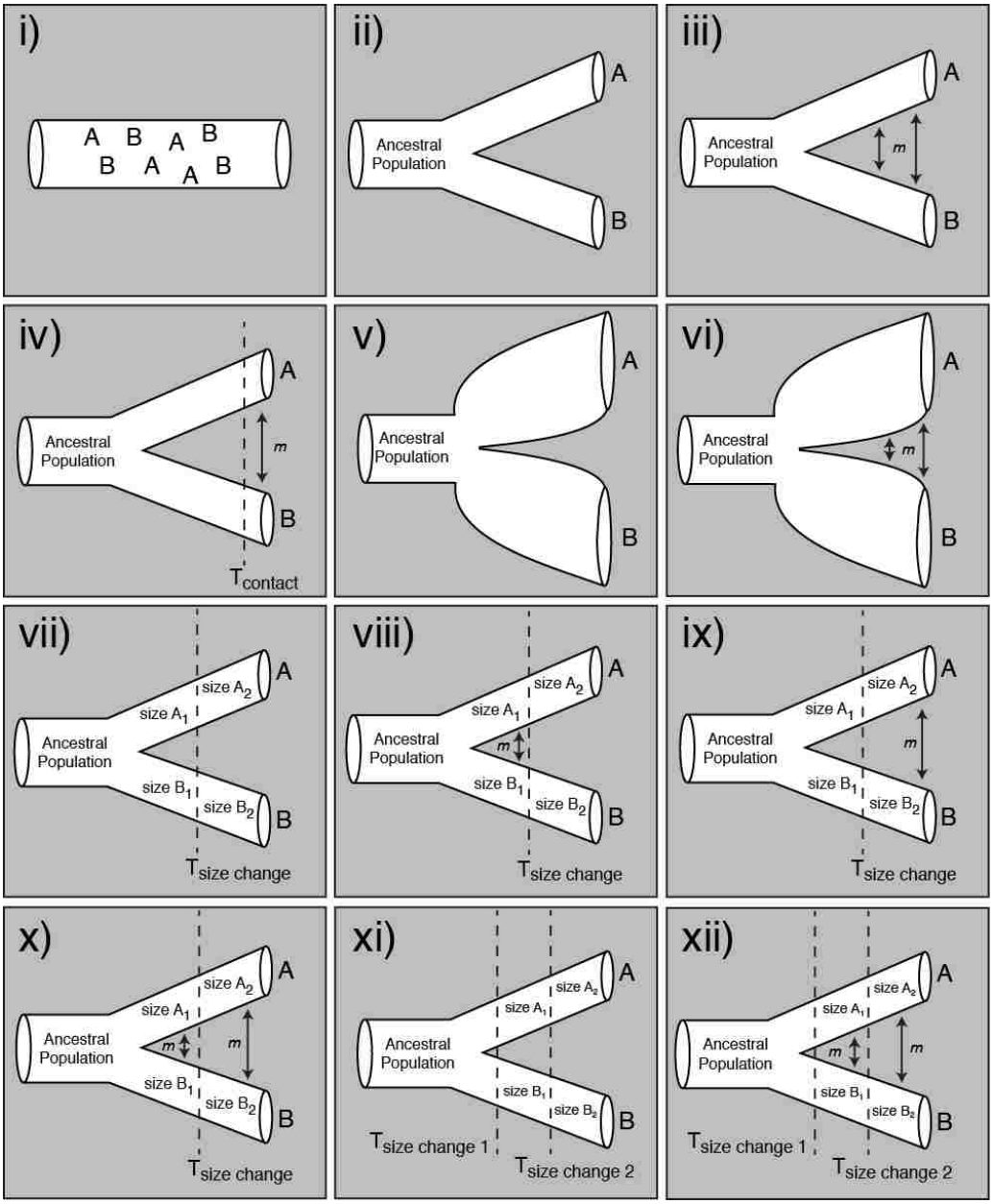

Figure 2: Graphical representation of the 12 2-D demographic models we tested in ∂a∂i. We tested each model set on pairs of populations – populations 2 and 3, populations 3 and 4, populations 4 and 5, and populations 5 and 6. A description of each model follows: (i) standard neutral model, populations never diverge, (ii) population divergence with no migration, (iii) divergence into two populations with symmetric migration, (iv) divergence followed by a period of population isolation and then secondary contact, (v) divergence followed by exponential population size change, (vi) divergence followed by exponential population size change and symmetric migration, (vii) population divergence followed by a population size change, (viii) divergence followed by ancient symmetric migration followed by a population size change, (ix) divergence followed by a period of isolation, then a size change followed by secondary contact and symmetric migration, (x) population divergence followed by a population size change with symmetric migration before and after size change, (xi) divergence followed by a size change, then a second size change ("recovery"), (xii) divergence followed by a size change, then a second size change ("recovery"), with symmetric migration.

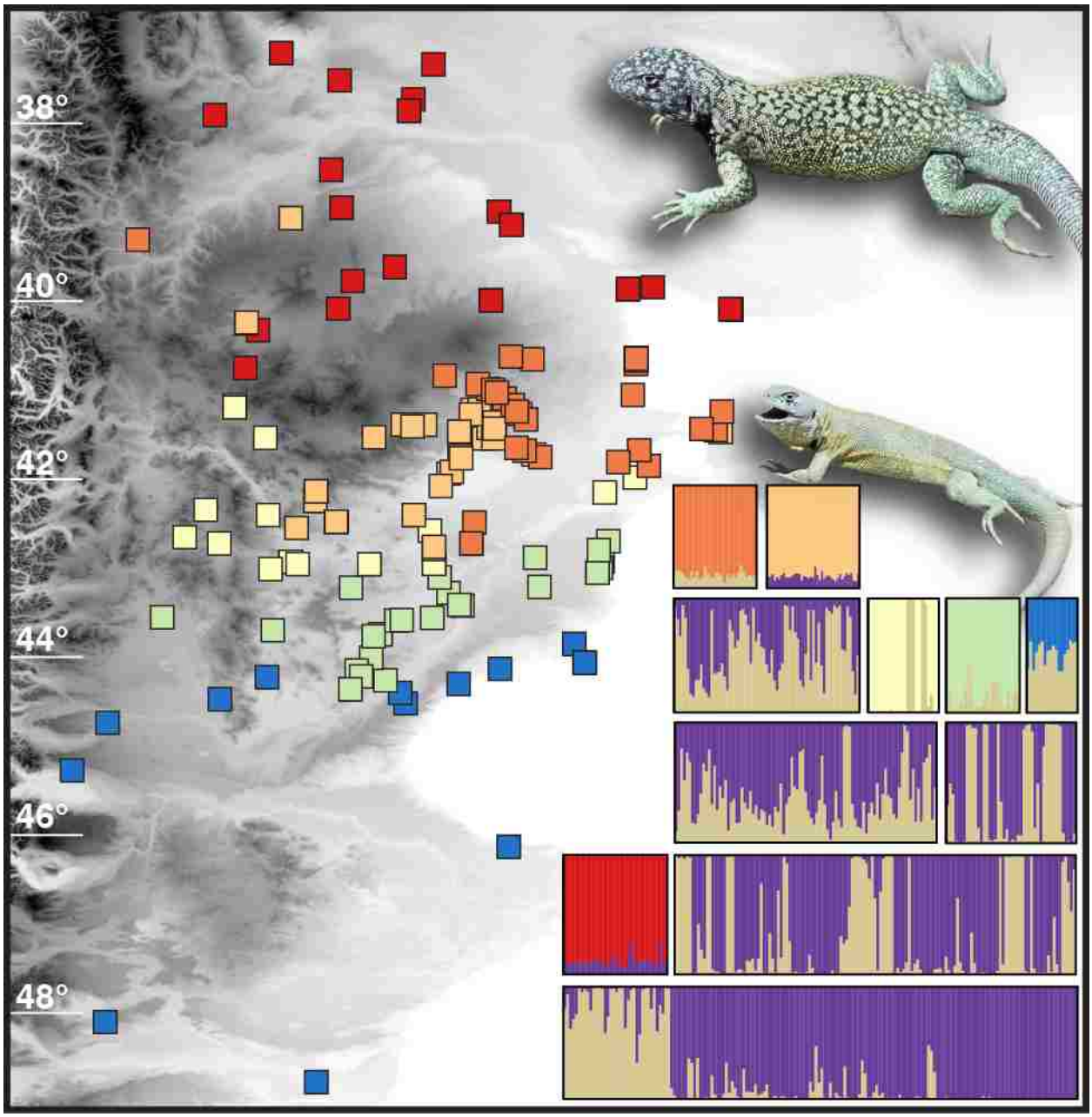

Figure 3: Results of the Structure hierarchical analysis, which identified six populations. Sampling locality colors correspond to the Structure results in the lower-right. The purple and gold bar plots represent groups during intermediate stages of the hierarchical analysis; these individuals have not yet been assigned to a population. Populations are numbered north-to-south, where 1= red, 2 = dark orange, 3 = light orange, 4 = yellow, 5 = green, and 6 = blue.

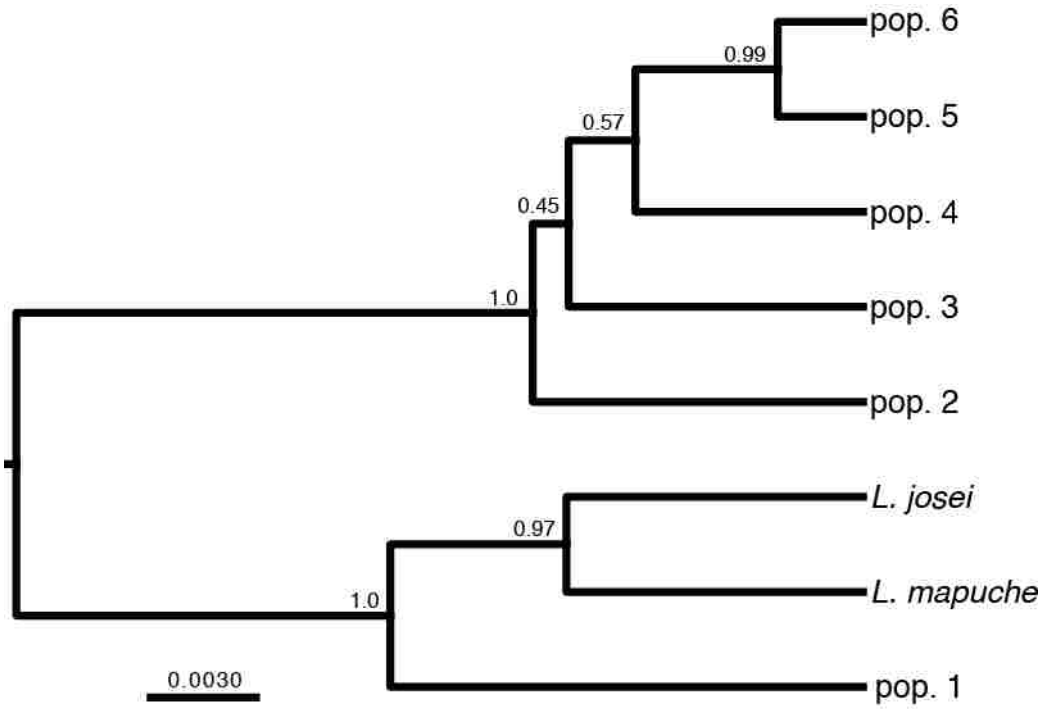

Figure 4: Coalescent-based species tree inferred in SNAPP with posterior probabilities shown. Population numbers (and assignments) correspond to a subset of the individuals seen in Figure 3.

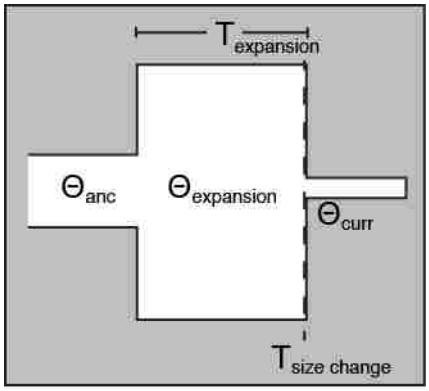

Figure 5: Graphical representation of the optimal 1-D model favored by AIC model selection for all six populations in ∂a∂i. Population sizes and times are relative and not to scale; refer to **Table 1** for exact parameter estimates by population. Θ_{anc}, $\Theta_{expansion}$, and Θ_{curr} represent ancestral, expanded, and current population sizes, respectively. $T_{expansion}$ represents the duration of the population at the expanded size (in 2N generations), and $T_{size\ change}$ is when the population changed to its current size.

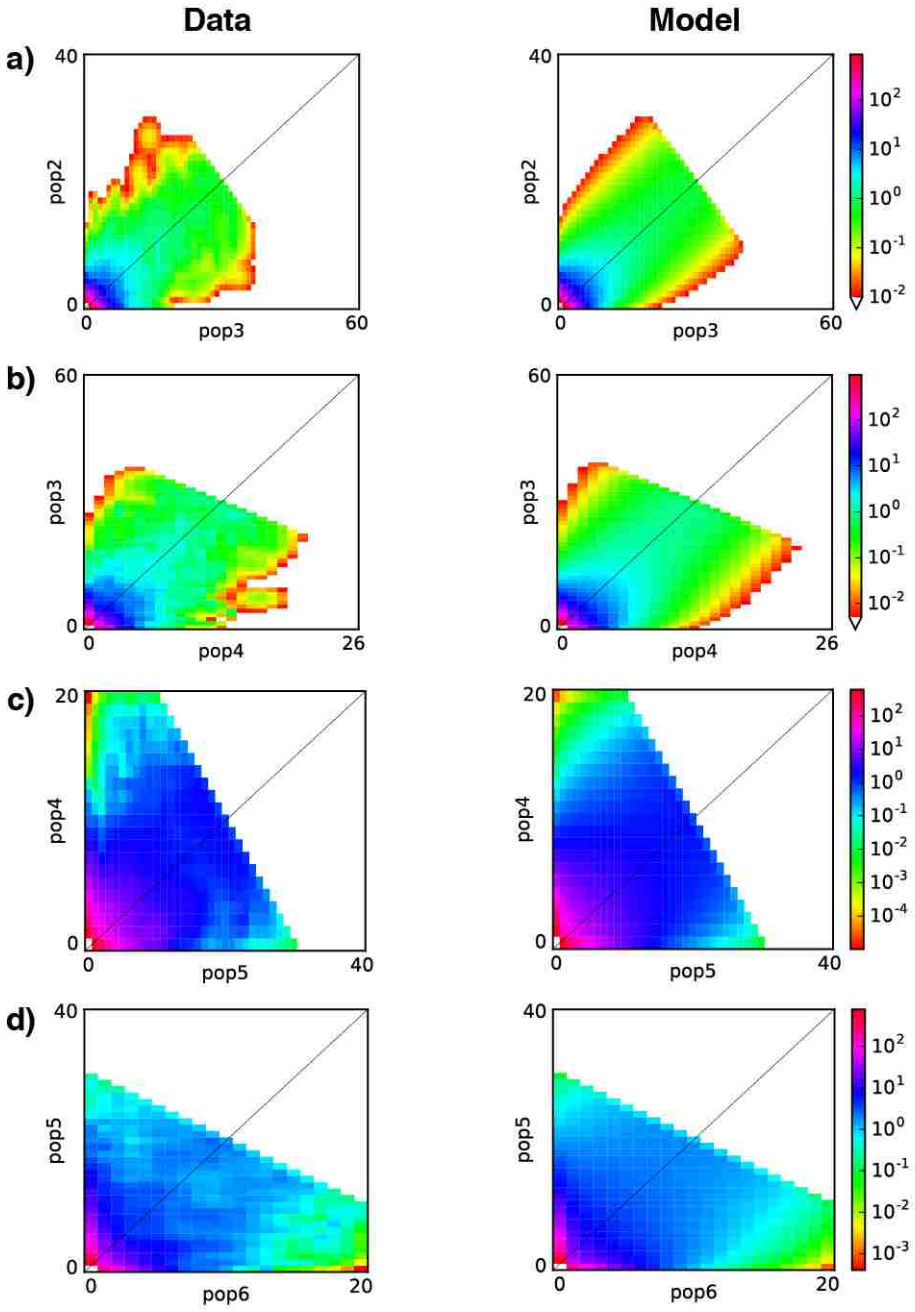

Figure 6: Allele frequency spectra inferred with optimized parameter estimates in ∂a∂i for the best-fit demographic model as determined through AIC model selection for (a) populations 2 + 3, (b) populations 3 + 4, (c) populations 4 + 5, and (d) populations 5 + 6. Parameter estimates for the models in this figure can be seen in Table 3.

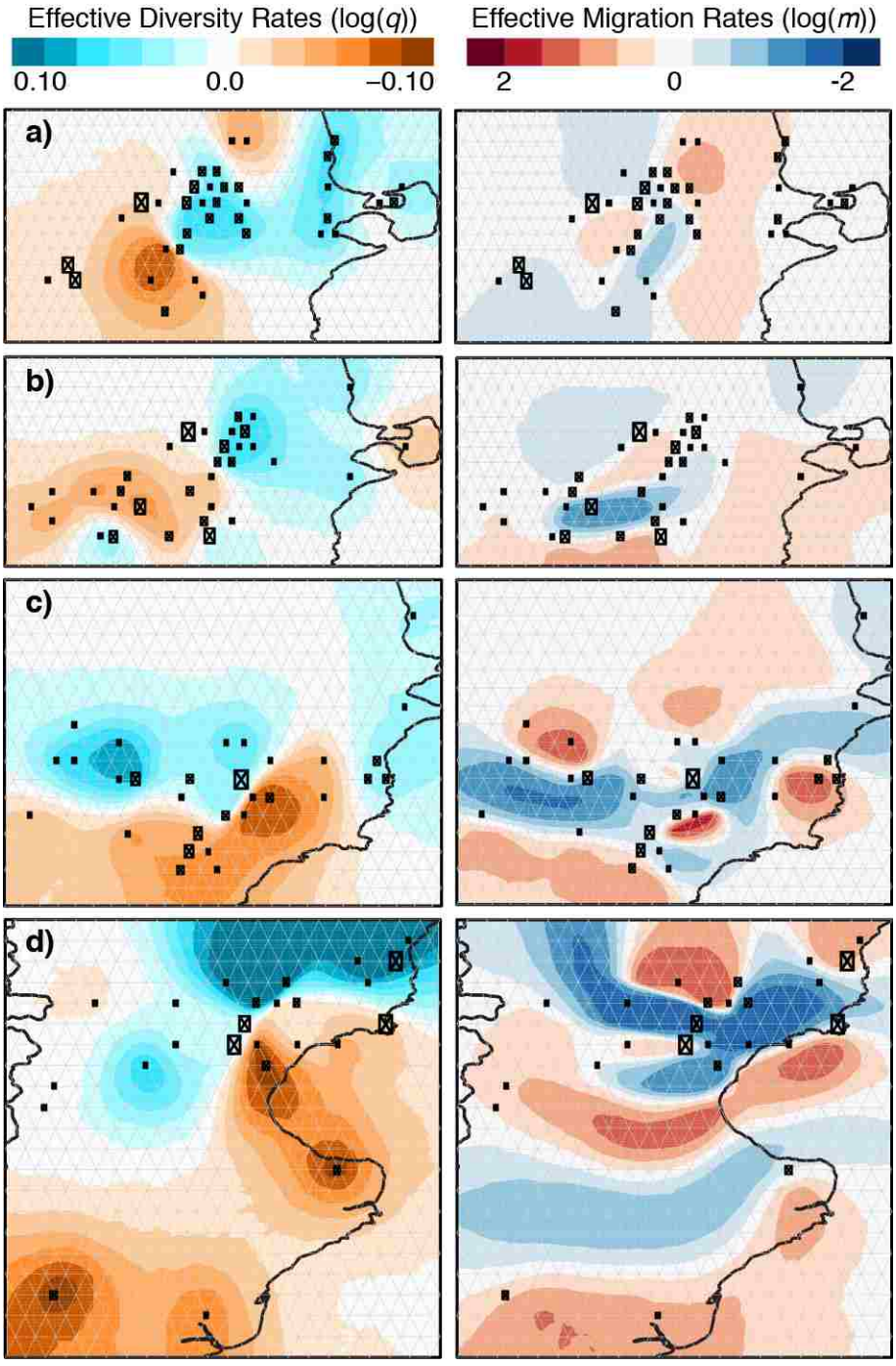

Figure 7: EEMS results of genetic diversity (left column) and migration rates (right column) in (a) populations 2 and 3, (b) populations 3 and 4, (c) populations 4 and 5, and (d) populations 5 and 6. The population grid is shown in thin grey lines, and country borders are shown in dark black lines. Sampling localities are plotted on the population grid apex nearest to their actual sampling location, and relative sample sizes are shown by the size of the bounded black "X".

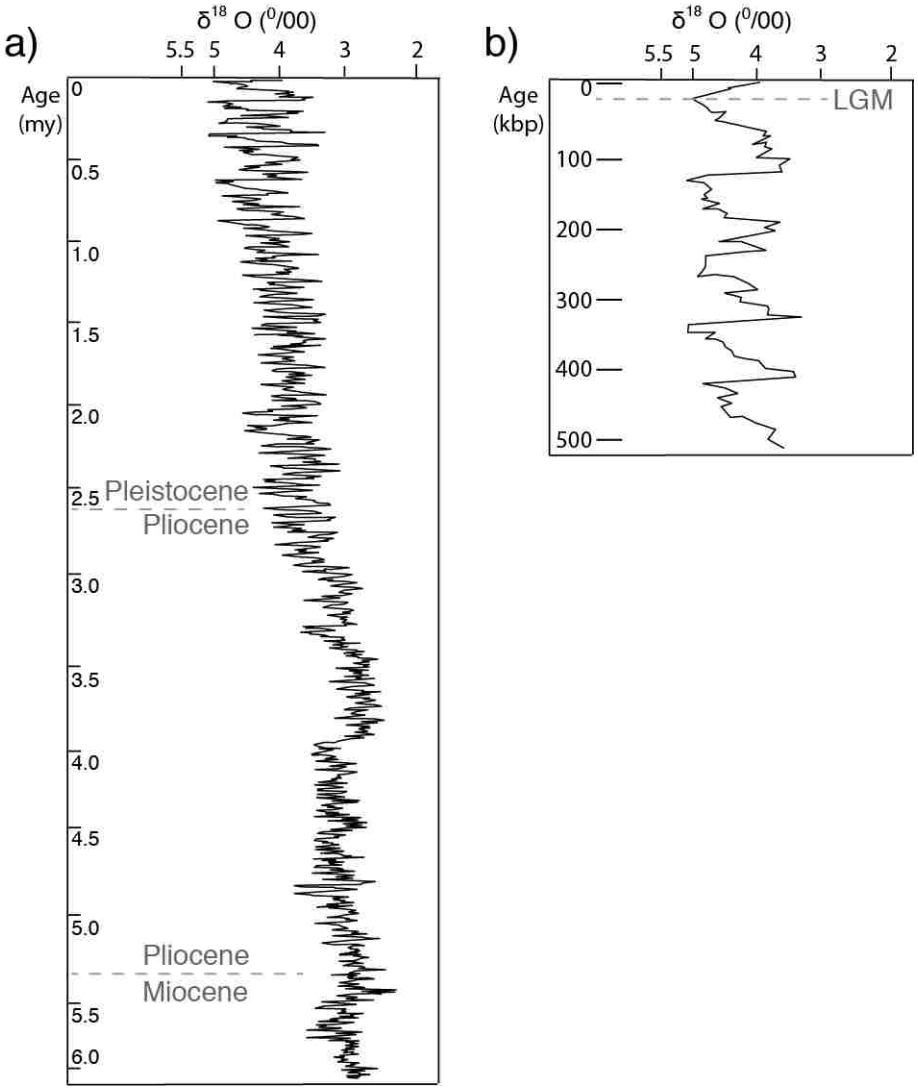

Figure 8: Global temperature for the south Atlantic as inferred from O^{18} (parts per thousand) since a) the late Miocene and b) a higher resolution of the last 500,000 years. Modified from Shackleton (1995) and Rabassa et al. (2005).

Table 1: Optimized demographic parameters from the optimal 1-D model in ∂a∂i; the same model was favored for all populations. Refer to Figure 5 for a graphical representation and interpretation of the following parameters: nuB represents the ratio of the expansion population size to ancestral population size ($\Theta_{expansion}/\Theta_{anc}$), nuF = the ratio of the current to ancestral population ($\Theta_{current}/\Theta_{anc}$), Tb = duration of population expansion (in units of 2N generations; $T_{expansion}$), and Tr = time since the population size change ($T_{size\ change}$) in units of 2N generations.

				Parameter Estimates			
Population	# Individuals	# Loci	Projection	nuB	nuF	Tb	Tr
1	37	1253	52	9.4677	0.0162	1.2757	0.0001
2	30	1484	42	8.4556	0.8205	0.5798	0.0147
3	41	1483	56	7.79	0.0106	1.0614	0.0001
4	19	1267	26	10.9993	0.005	0.6216	0.0002
5	28	1732	40	3.2151	0.0379	0.6331	0.0002
6	18	1926	24	35.2829	0.0133	0.1108	0.0005

Table 2: Demographic model parameter estimates for the 1-D models converted into number of individuals in the reference population (N_{ref}), number of years each population had an expanded population size ("Expansion Duration"), and number of years since the bottleneck recovery.

	Population					
	1	2	3	4	5	6
N_{ref}	5.15E+05	7.55E+05	5.23E+05	8.03E+05	7.24E+05	1.08E+06
Expansion Duration	3.29E+05	2.19E+05	2.77E+05	2.50E+05	2.29E+05	5.96E+04
Time Since Bottleneck	26	5546	26	80	72	269

Table 3: Optimized demographic parameters from the AIC-selected top 2-D models in ∂a∂i. nu1a and nu2a represent the final sizes of populations 1 and 2, nu1b and nu2b represent the sizes of populations 1 and 2 after the size change, Ts is the time when the two populations split (in units of 2*Na generations), T1 is the time between population split and secondary contact (in units of 2*Na generations), T2 = the time between the secondary contact and the present (in units of 2*Na generations), and m represents the migration rate between populations (in 2*Na*m individuals per generation). Dashes indicate that that parameter was not estimated for that model.

			Parameters and Estimates							
Populations	# Individuals	# Loci	nu1a	nu1b	nu2a	nu2b	Ts	T1	T2	m
2 + 3	71	1113	8.081	5.361	1.636	5.160	—	0.941	0.492	2.070
3 + 4	60	1091	6.434	—	2.473	—	1.416	—	—	1.858
4 + 5	47	1182	2.294	2.045	1.397	0.011	1.173	—	—	2.077
5 + 6	46	1509	3.820	0.339	1.100	0.559	2.733	—	—	1.007

Table 4: Demographic model parameter estimates for the 2-D models converted into number of individuals in the reference population (N_{ref}), low and high estimates of migration rate in number of migrants per generation, and divergence time in years.

	Populations			
	2 + 3	3 + 4	4 + 5	5 + 6
N_{ref}	5.29E+05	5.44E+05	1.21E+06	6.31E+05
Migration	1.69	2.3	1.45	1.92
	8.36	5.98	2.38	2.22
Divergence Times	2.79E+05	2.84E+05	5.23E+05	6.35E+05

Supplemental figures and tables for “Rocks and ice: effects of geographic features and Pleistocene glaciations on the Gondwanan *Liolaemus fitzingerii* Species Group”

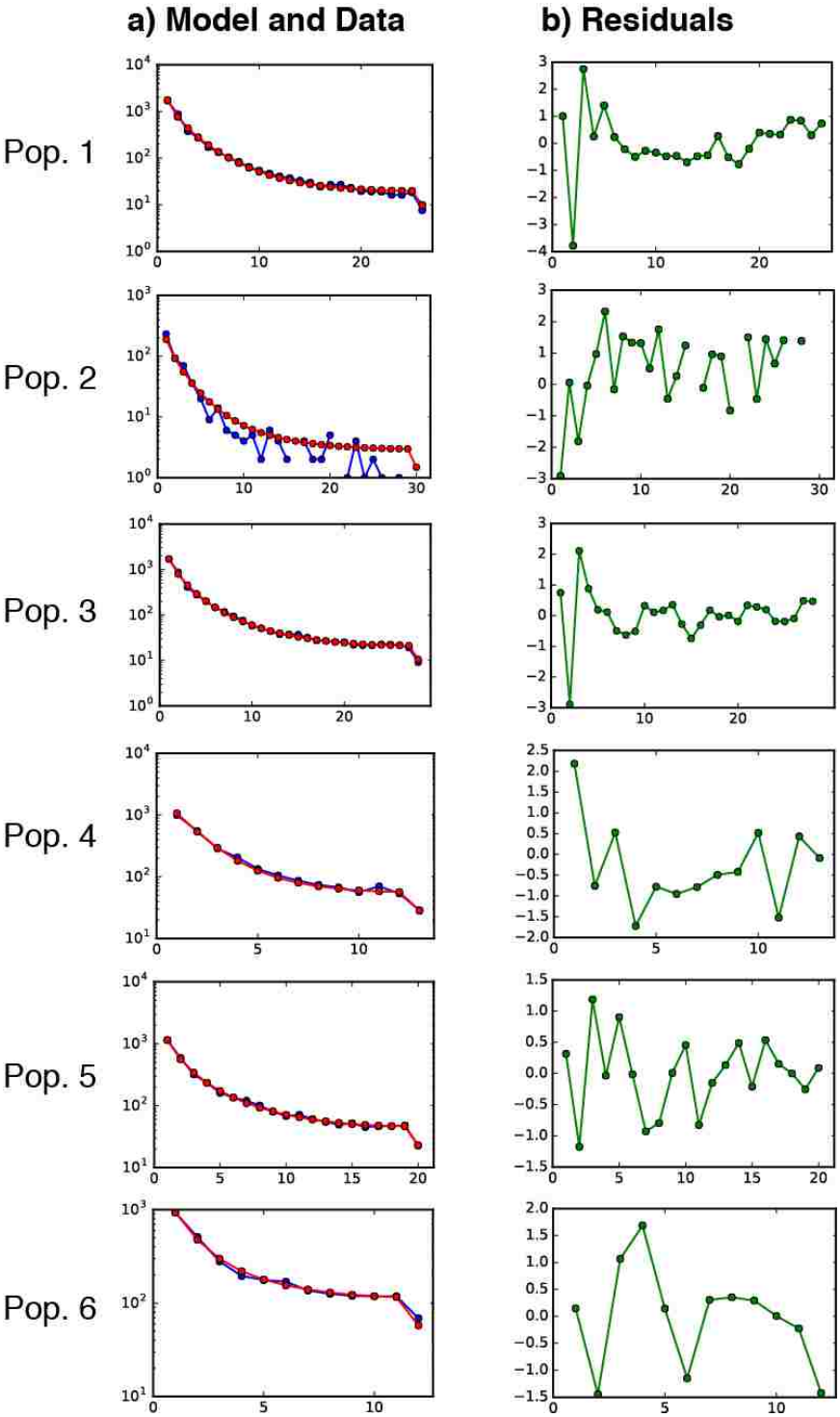

Supplemental Figure S1. δaδi results by population for the 1-D optimized model, an instantaneous population size change that continues for some duration, followed by a second size change. In figure (a), the model is shown in red and the data are shown in blue, whereas (b) shows a plot of the residuals.

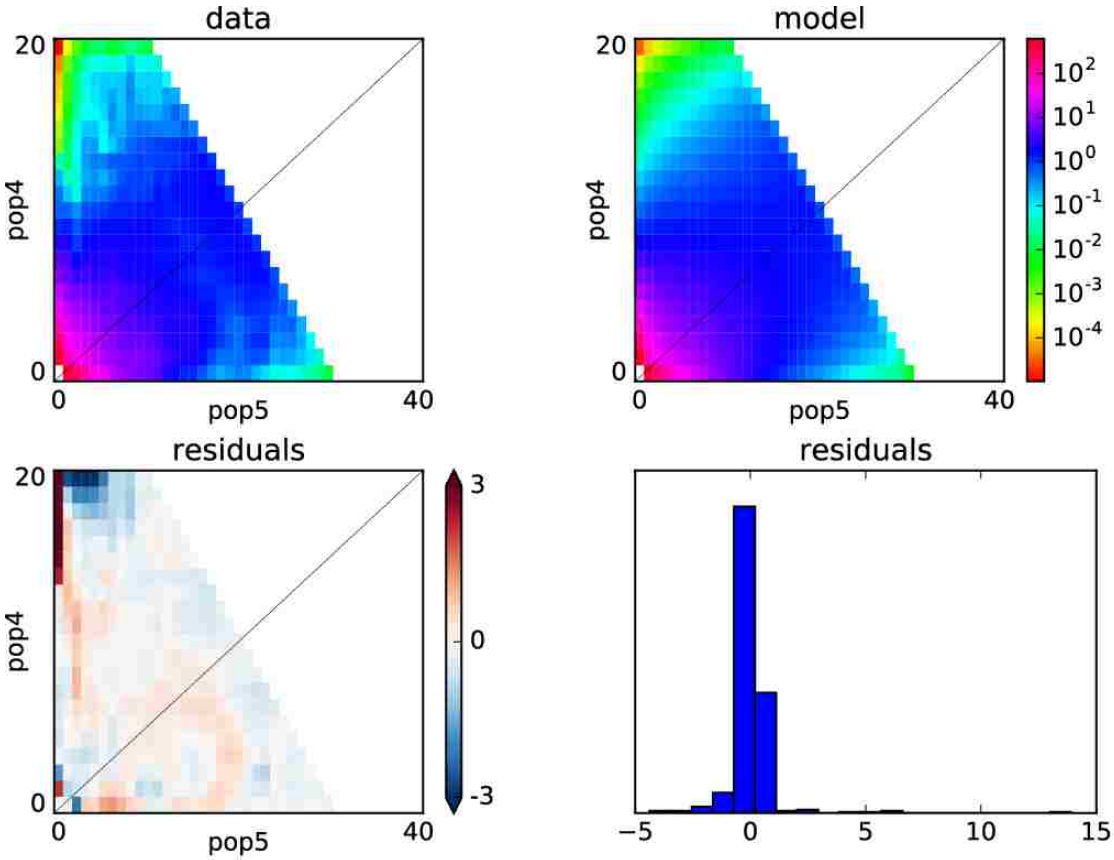

Supplemental Figure S2. δaδi results for the 2-D model of populations 4 and 5, showing both allele frequency spectra of the data and model, as well as the residuals.

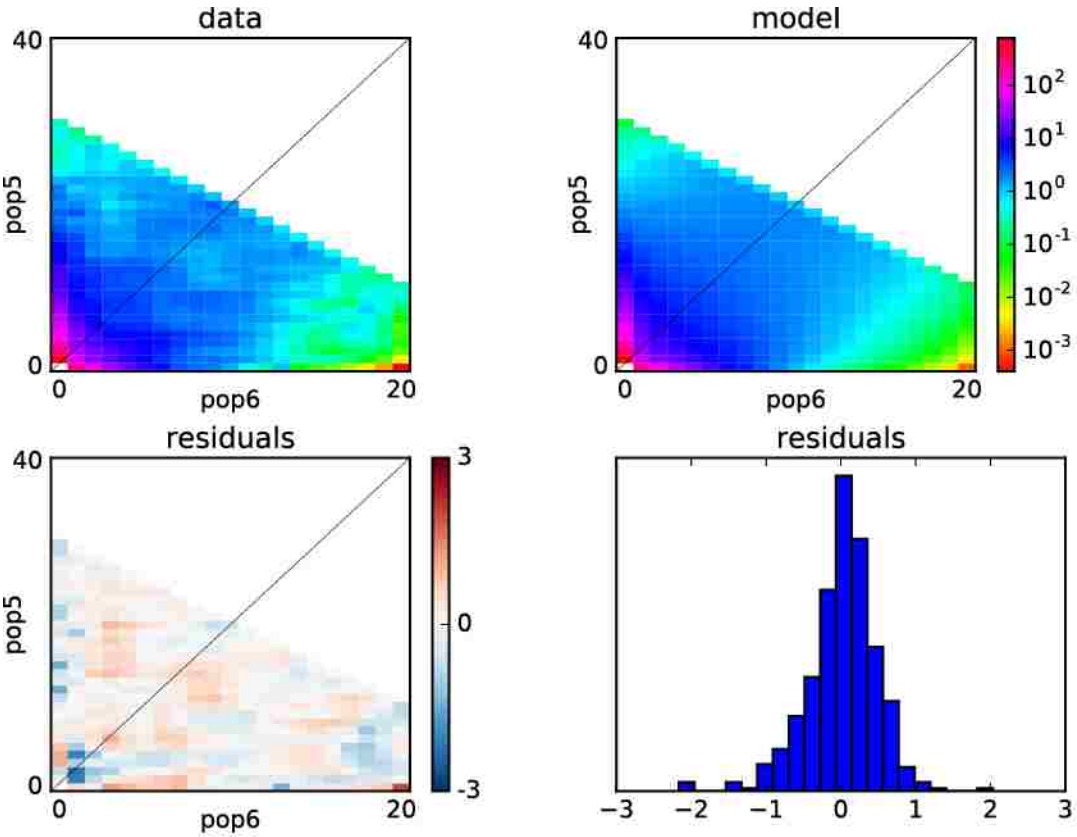

Supplemental Figure S3. δaδi results for the 2-D model of populations 5 and 6 with both allele frequency spectra of the data and model, as well as the residuals, for the optimal model - divergence, population size change followed by exponential expansion in both populations, with migration.

Supplemental Table S1. Locality and sequencing information for the specimens used in this study.

Accession ID	Morphological Designation	Latitude	Longitude	Seq. Capt. Data?
LJAMM-CNP 5762	L. josei	-36.513	-69.665	
LJAMM-CNP 5763	L. josei	-36.513	-69.665	
LJAMM-CNP 8767	L. mapuche	-38.960	-69.515	
LJAMM-CNP 8768	L. mapuche	-38.960	-69.515	
LJAMM-CNP 2201	L. xanthoviridis	-43.682	-65.340	
LJAMM-CNP 2231	L. canqueli	-43.939	-68.837	
LJAMM-CNP 2285	L. casamiquelai	-43.910	-65.403	
LJAMM-CNP 2427	L. fitzingerii	-43.981	-65.424	
LJAMM-CNP 2431	L. goetschi	-39.926	-68.344	Y
LJAMM-CNP 2432	L. goetschi	-39.926	-68.344	
LJAMM-CNP 2461	L. casamiquelai	-41.073	-63.953	
LJAMM-CNP 2462	L. fitzingerii	-45.461	-69.714	Y
LJAMM-CNP 2464	L. fitzingerii	-44.839	-65.723	
LJAMM-CNP 2465	L. fitzingerii	-44.839	-65.723	
LJAMM-CNP 2561	L. casamiquelai	-40.841	-65.118	Y
LJAMM-CNP 2567	L. casamiquelai	-40.841	-65.118	
LJAMM-CNP 2617	L. canqueli	-42.657	-64.992	
LJAMM-CNP 2618	L. melanops S	-42.657	-64.992	
LJAMM-CNP 2659	L. casamiquelai	-41.073	-63.953	
LJAMM-CNP 2670	L. casamiquelai	-40.841	-65.118	
LJAMM-CNP 2947	L. casamiquelai	-41.219	-69.412	
LJAMM-CNP 3275	L. melanops S	-41.633	-66.195	
LJAMM-CNP 3304	L. melanops S	-41.602	-66.438	
LJAMM-CNP 3375	L. casamiquelai	-40.752	-68.218	
LJAMM-CNP 3924	L. fitzingerii	-45.726	-70.979	
LJAMM-CNP 4514	L. melanops S	-42.791	-65.227	
LJAMM-CNP 4670	L. canqueli	-43.707	-69.719	
LJAMM-CNP 4886	L. melanops	-40.970	-66.660	
LJAMM-CNP 4896	L. canqueli	-42.222	-64.062	
LJAMM-CNP 5520	L. chehuachekenk	-42.368	-67.656	
LJAMM-CNP 5521	L. chehuachekenk	-42.368	-67.656	
LJAMM-CNP 5522	L. chehuachekenk	-42.368	-67.656	
LJAMM-CNP 5580	L. chehuachekenk	-42.445	-67.002	Y
LJAMM-CNP 5581	L. chehuachekenk	-42.445	-67.002	
LJAMM-CNP 5596	L. chehuachekenk	-42.369	-67.402	
LJAMM-CNP 5628	L. chehuachekenk	-42.174	-69.548	Y
LJAMM-CNP 5630	L. chehuachekenk	-42.174	-69.548	
LJAMM-CNP 5637	L. melanops	-43.133	-65.380	
LJAMM-CNP 5709	L. melanops	-38.185	-69.023	

LJAMM-CNP 5728	L. melanops	-38.185	-69.023	
LJAMM-CNP 5995	L. melanops N	-41.817	-67.183	Y
LJAMM-CNP 6001	L. melanops S	-41.976	-66.638	
LJAMM-CNP 6035	L. canqueli	-42.451	-64.074	
LJAMM-CNP 6097	L. chehuachekenk	-42.511	-67.978	Y
LJAMM-CNP 6122	L. xanthoviridis	-43.866	-66.165	
LJAMM-CNP 6127	L. melanops S	-41.618	-65.024	
LJAMM-CNP 6129	L. melanops S	-41.618	-65.024	
LJAMM-CNP 6137	L. chehuachekenk	-42.747	-66.999	
LJAMM-CNP 6876	L. casamiquelai	-40.970	-66.665	
LJAMM-CNP 6896	L. canqueli	-42.629	-66.375	
LJAMM-CNP 6931	L. chehuachekenk	-42.524	-66.634	
LJAMM-CNP 7027	L. casamiquelai	-40.119	-66.432	
LJAMM-CNP 7034	L. casamiquelai	-40.119	-66.432	Y
LJAMM-CNP 8110	L. canqueli	-42.150	-66.415	
LJAMM-CNP 8421	L. casamiquelai	-39.970	-66.570	
LJAMM-CNP 8425	L. casamiquelai	-39.970	-66.570	
LJAMM-CNP 8665	L. casamiquelai	-41.062	-68.382	
LJAMM-CNP 8676	L. casamiquelai	-41.062	-68.382	Y
LJAMM-CNP 8677	L. casamiquelai	-41.062	-68.382	
LJAMM-CNP 8708	L. casamiquelai	-38.884	-69.771	
LJAMM-CNP 8781	L. canqueli	-43.470	-66.849	
LJAMM-CNP 8793	L. canqueli	-43.461	-68.403	
LJAMM-CNP 8797	L. canqueli	-43.461	-68.403	
LJAMM-CNP 8816	L. canqueli	-43.387	-69.171	
LJAMM-CNP 8826	L. chehuachekenk	-43.225	-68.639	
LJAMM-CNP 8830	L. chehuachekenk	-43.225	-68.639	
LJAMM-CNP 8832	L. chehuachekenk	-43.120	-68.632	
LJAMM-CNP 8833	L. chehuachekenk	-43.120	-68.632	
LJAMM-CNP 8841	L. canqueli	-43.532	-68.852	
LJAMM-CNP 9020	L. fitzingerii	-44.539	-70.363	
LJAMM-CNP 9105	L. canqueli	-43.995	-69.143	
LJAMM-CNP 9119	L. xanthoviridis	-44.684	-69.120	
LJAMM-CNP 9141	L. fitzingerii	-45.213	-69.184	Y
LJAMM-CNP 9265	L. fitzingerii	-46.263	-71.378	Y
LJAMM-CNP 9292	L. fitzingerii	-49.097	-71.006	
LJAMM-CNP 9295	L. fitzingerii	-49.097	-71.006	
LJAMM-CNP 9681	L. fitzingerii	-47.123	-66.463	
LJAMM-CNP 9688	L. fitzingerii	-47.123	-66.463	
LJAMM-CNP 10226	L. xanthoviridis	-45.347	-68.246	
LJAMM-CNP 10230	L. xanthoviridis	-45.347	-68.246	
LJAMM-CNP 10243	L. xanthoviridis	-45.137	-68.174	
LJAMM-CNP 10298	L. xanthoviridis	-44.729	-67.907	

LJAMM-CNP 10300	L. xanthoviridis	-44.729	-67.907	
LJAMM-CNP 10304	L. xanthoviridis	-44.570	-67.666	
LJAMM-CNP 11023	L. chehuachekenk	-42.389	-67.545	
LJAMM-CNP 11043	L. chehuachekenk	-42.389	-67.545	
LJAMM-CNP 11049	L. canqueli	-43.936	-67.302	
LJAMM-CNP 11050	L. canqueli	-43.936	-67.302	
LJAMM-CNP 11057	L. xanthoviridis	-43.936	-67.302	
LJAMM-CNP 11071	L. xanthoviridis	-44.398	-67.018	
LJAMM-CNP 11074	L. fitzingerii	-45.506	-67.624	
LJAMM-CNP 11085	L. canqueli	-43.328	-69.874	
LJAMM-CNP 11090	L. casamiquelai	-41.231	-69.415	
LJAMM-CNP 11099	L. casamiquelai	-40.044	-68.915	
LJAMM-CNP 11100	L. casamiquelai	-40.044	-68.915	
LJAMM-CNP 11101	L. casamiquelai	-41.304	-69.286	
LJAMM-CNP 11194	L. melanops S	-42.201	-66.869	
LJAMM-CNP 11207	L. casamiquelai	-40.597	-67.744	
LJAMM-CNP 11218	L. casamiquelai	-40.597	-67.744	
LJAMM-CNP 11231	L. casamiquelai	-40.597	-67.744	Y
LJAMM-CNP 11232	L. casamiquelai	-39.497	-68.460	
LJAMM-CNP 11342	L. casamiquelai	-40.597	-67.744	
LJAMM-CNP 11392	L. casamiquelai	-40.285	-70.638	Y
LJAMM-CNP 11458	L. fitzingerii	-49.773	-68.627	Y
LJAMM-CNP 11682	L. casamiquelai	-41.068	-63.967	
LJAMM-CNP 11719	L. martorii	-40.821	-64.841	
LJAMM-CNP 11749	L. fitzingerii	-45.120	-66.559	
LJAMM-CNP 11753	L. fitzingerii	-45.289	-67.026	
LJAMM-CNP 12268	L. casamiquelai	-41.730	-69.428	
LJAMM-CNP 12372	L. canqueli	-43.914	-68.916	
LJAMM-CNP 12373	L. canqueli	-43.914	-68.916	
LJAMM-CNP 12918	L. canqueli	-43.635	-70.109	
LJAMM-CNP 12996	L. canqueli	-43.705	-66.881	
LJAMM-CNP 12999	L. canqueli	-43.705	-66.881	
LJAMM-CNP 13010	L. canqueli	-42.429	-64.131	
LJAMM-CNP 13149	L. canqueli	-42.833	-64.883	Y
LJAMM-CNP 13213	L. melanops S	-42.309	-66.267	
LJAMM-CNP 13271	L. canqueli	-42.964	-65.041	
LJAMM-CNP 13549	L. xanthoviridis	-44.035	-65.462	
LJAMM-CNP 13556	L. melanops	-42.248	-66.334	
LJAMM-CNP 13585	L. melanops S	-41.648	-65.026	
LJAMM-CNP 13607	L. melanops S	-41.686	-65.029	
LJAMM-CNP 13653	L. melanops S	-42.033	-65.064	
LJAMM-CNP 13663	L. chehuachekenk	-42.900	-67.103	
LJAMM-CNP 13714	L. casamiquelai	-38.833	-67.583	

LJAMM-CNP 13767	L. casamiquelai	-38.833	-67.583	
LJAMM-CNP 13802	L. casamiquelai	-38.312	-67.310	
LJAMM-CNP 13803	L. casamiquelai	-38.492	-68.364	
LJAMM-CNP 14341	L. xanthoviridis	-44.035	-65.462	
LJAMM-CNP 14849	L. canqueli	-42.416	-64.291	
LJAMM-CNP 15267	L. fitzingerii	-45.050	-65.607	Y
LJAMM-CNP 15268	L. fitzingerii	-45.050	-65.607	
LJAMM-CNP 16288	Hybrid Zone	-42.074	-66.509	
LJAMM-CNP 16299	Hybrid Zone	-42.008	-66.596	
LJAMM-CNP 16314	Hybrid Zone	-41.966	-66.692	
LJAMM-CNP 16318	Hybrid Zone	-41.911	-66.811	
LJAMM-CNP 16324	Hybrid Zone	-42.220	-66.371	
LJAMM-CNP 16329	Hybrid Zone	-42.524	-66.743	
LJAMM-CNP 16343	Hybrid Zone	-42.719	-67.014	
LJAMM-CNP 16350	Hybrid Zone	-42.193	-66.609	
LJAMM-CNP 16363	Hybrid Zone	-42.195	-66.790	
LJAMM-CNP 16377	Hybrid Zone	-42.252	-66.888	
LJAMM-CNP 16386	Hybrid Zone	-42.920	-67.140	
LJAMM-CNP 16399	Hybrid Zone	-43.060	-67.227	
LJAMM-CNP 16652	Hybrid Zone	-42.447	-67.019	
LJAMM-CNP 16668	Hybrid Zone	-42.662	-66.284	
LJAMM-CNP 16676	Hybrid Zone	-42.405	-66.690	
LJAMM-CNP 16683	Hybrid Zone	-42.344	-66.620	
LJAMM-CNP 16823	Hybrid Zone	-42.414	-66.623	
LJAMM-CNP 16849	Hybrid Zone	-43.561	-67.349	
LJAMM-CNP 16854	Hybrid Zone	-43.744	-67.303	
LJAMM-CNP 16865	Hybrid Zone	-43.769	-67.309	
LJAMM-CNP 16869	Hybrid Zone	-43.931	-67.305	
LJAMM-CNP 16887	Hybrid Zone	-44.088	-67.239	
LJAMM-CNP 16894	Hybrid Zone	-44.264	-67.140	
LJAMM-CNP 16903	Hybrid Zone	-44.408	-66.982	
LJAMM-CNP 16915	Hybrid Zone	-45.390	-67.682	
LJAMM-CNP 16920	Hybrid Zone	-45.246	-67.849	
LJAMM-CNP 16949	Hybrid Zone	-44.993	-68.009	
LJAMM-CNP 16955	Hybrid Zone	-44.752	-67.983	
LJAMM-CNP 16976	Hybrid Zone	-44.576	-67.728	
LJAMM-CNP 16981	Hybrid Zone	-44.545	-67.322	
LJAMM-CNP 5926	L. chehuachekenk	-42.146	-69.544	
LJAMM-CNP 5961	L. chehuachekenk	-42.517	-69.202	
LJAMM-CNP 15269	L. fitzingerii	-45.050	-65.607	
LJAMM-CNP 8786	L. canqueli	-43.386	-67.530	
LJAMM-CNP 8788	L. canqueli	-43.386	-67.530	
LJAMM-CNP 8793	L. canqueli	-43.461	-68.403	

LJAMM-CNP 8796	L. melanops S	-43.461	-68.403	
LJAMM-CNP 5200	L. casamiquelai	-38.707	-67.537	
LJAMM-CNP 2423	L. melanops S	-41.625	-65.025	
LJAMM-CNP 2482	L. melanops S	-41.625	-65.025	
LJAMM-CNP 6126	L. melanops S	-41.618	-65.024	Y
LJAMM-CNP 3453	L. canqueli	-43.941	-68.031	
LJAMM-CNP 3457	L. canqueli	-43.941	-68.031	
LJAMM-CNP 5442	L. melanops S	-42.734	-66.106	Y
LJAMM-CNP 6734	L. melanops S	-42.704	-66.180	
LJAMM-CNP 3875	L. xanthoviridis	-45.203	-68.123	
LJAMM-CNP 3876	L. xanthoviridis	-45.203	-68.123	
LJAMM-CNP 2418	L. xanthoviridis	-43.782	-65.447	Y
LJAMM-CNP 3738	L. xanthoviridis	-44.206	-68.237	Y
LJAMM-CNP 6124	L. xanthoviridis	-44.197	-66.115	

Supplemental Table S2. Optimized results for the 1-D models analyzed in δaδi showing their likelihood (lnL) and AIC scores. The parameters are defined as nuB – the ratio of expanded population size to ancient pop size, nuF – the ratio of contemporary to ancient pop size TB – the length of expansion (in units of 2*Na generations), and TF – the time since population expansion recovery (in units of 2*Na generations).

				Parameter Estimates			
Population	Optimal Model	lnL	AIC	nuB	nuF	TB	TF
1	Instantaneous pop. size change, then recovery	-88.24	182.48	9.4677	0.0162	1.2757	0.0001
2	Instantaneous pop. size change, then recovery	-198.85	403.7	8.4556	0.8205	0.5798	0.0147
3	Instantaneous pop. size change, then recovery	-90.08	186.16	7.79	0.0106	1.0614	0.0001
4	Instantaneous pop. size change, then recovery	-45.94	97.88	10.9993	0.005	0.6216	0.0002
5	Instantaneous pop. size change, then recovery	-67.44	140.88	3.2151	0.0379	0.6331	0.0002
6	Instantaneous pop. size change, then recovery	-47.33	100.66	35.2829	0.0133	0.1108	0.0005

Supplemental Table S3. Top-scoring 2-D models by population-pair in δaδi, with all models in the top 2 AIC-point interval shown.

Population Pair	Model	lnL	AIC
2+3	Divergence and symmetrical secondary contact, size change	-708.36	1430.72
	Divergence, bottleneck in both pops, pop. size recovery, migration	-708.41	1430.82
	Divergence with symmetric migration, size change	-709.04	1432.08
3+4	Divergence with symmetric migration	-588.13	1184.26
	Divergence and symmetrical secondary contact	-588.26	1186.52
4+5	Divergence, bottleneck and exponential recovery in both populations, migration	-499.64	1013.28
5+6	Divergence, bottleneck and exponential recovery in both populations, migration	-588.75	1191.5

Four species linked by three hybrid zones: two instances of repeated hybridization in one species group (genus *Liolaemus*)

Jared A. Grummer[1], Luciano J. Avila[2], Mariana M. Morando[2] and Adam D. Leaché[1]

[1]*Department of Biology and Burke Museum of Natural History and Culture, University of Washington, Box 351800, Seattle, WA 98195-1800, USA;*

[2]*Centro Nacional Patagónico – Consejo Nacional de Investigaciones Científicas y Técnicas (CENPAT-CONICET), Boulevard Almirante Brown 2915, ZC: U9120ACD, Puerto Madryn, Argentina*

Abstract.—Hybrid zones offer unique opportunities to study in a natural setting evolutionary processes that keep species as distinct evolutionary lineages. In particular, systems in which the same species hybridizes with multiple species provide an important perspective on the repeatability of evolutionary processes. Previous studies have shown unique outcomes of the evolutionary process in similar empirical systems with repeated instances of hybridization. We studied three hybrid zones in the *Liolaemus fitzingerii* species group in Central Argentina that have a distinctly unique arrangement. In the northern part of the group's distribution, *L. melanops* forms a sickle-shaped distribution where it hybridizes with *L. shehuen* in the north and *L. xanthoviridis* in the south. In the southern part of the group's range, *L. xanthoviridis* hybridizes with *L. melanops* and *L. fitzingerii* in a sandwich arrangement; the result is that two species each hybridize with two other species. We sampled three transects that were each approximately 120km in length, and collected 267 individuals that we sequenced for both mitochondrial and genome-wide SNP data. We performed population structure analyses to determine population boundaries and to quantify admixture proportions (Q), which were then used to construct geographic clines. Using estimates of cline width and linkage disequilibrium, we estimated selection in three hybrid zones. In relation to the nuclear DNA clines, mitochondrial clines are ∼half as wide and shifted 4-20km southward in all three hybrid zones, indicating either male-biased dispersal northward or that the hybrid zones are moving north. Levels of selection varied from 0.0067 to 0.0304, with the highest selection levels occurring in the southern-most hybrid zone between *L. xanthoviridis* and *L. fitzingerii*. Our results are similar to previous studies – the evolutionary processes of selection and dispersal are unique in each of these replicate hybrid zones, potentially owing to unique exogenous (environmental) and endogenous (genetic) interactions.

(Keywords: SNP, ddRADseq, admixture, selection, population, hybridization, cline, Patagonia)

Hybridization, or interbreeding between distinct populations, has captivated evolutionary biologists for nearly two centuries (Darwin 1862; Harrison 1993). Hybridization is common in nature, and approximately 10% and 25% of animal and plant species hybridize, respectively (Mallet 2005). Hybrid zones provide researchers with the opportunity to understand evolutionary processes that generate and maintain boundaries between species. Whereas many hybridization studies only involve a single species-species comparison in a single contact zone, systems in which multiple contact zones have been independently formed between closely related species offer the power of replication in understanding evolutionary processes such as selection and migration. What is the role of selection in maintaining species boundaries? Does hybridization leave the same signature on nuclear (n) and mitochondrial (mt) genomes? Is the hybrid zone stable or moving?

Hybrid zones form at the interface between two distinct populations and in some cases are best described as "clines", which represent transitions between populations and character states (Barton and Hewitt 1985). Clines inferred from different characters that share the same center are said to be coincident, and those that share the same shape/width are said to be concordant. Clines and contact zones are often formed in ecotones where two distinct habitats fuse (Leaché and Cole 2007). These contact zones typically occur in one area between species and therefore offer a single perspective into the evolutionary process. However, some species complexes have established themselves into loosely formed "rings" (or perhaps more aptly, horseshoes) around uninhabitable habitat, where species grade into each other at contact zones, but the forms are reproductively isolated where the "ring" closes (e.g., *Ensatina* salamanders, Moritz et al. 1992; *Phylloscopus* warblers, Irwin et al. 2001). In other conceptually related instances, "mosaic" hybrid zones can be formed when individuals from distinct species repeatedly come into contact with each other across the landscape (e.g., *Helianthus* sunflowers; Rieseberg et al. 1999). In all of these cases, replicate hybrid zones are formed where one species participates in hybridization in >1

geographic area.

Many hybrid zones act as "tension zones", where clines are maintained by a balance between dispersal and selection against hybrids (Barton and Hewitt 1985). Selection and dispersal in hybrid zones can be measured by quantifying cline shape and width: both steeper and narrower clines indicate either stronger levels of selection or low dispersal rates. Selection can also be quantified by estimating linkage disequilibrium, or the non-random association of haplotypes, in clines (Mallet et al. 1990). Linkage disequilibrium is generated by dispersal of parental allelic combinations into the hybrid zone, and species-specific allelic blocks are broken down via hybridization and meiosis/recombination. If selection against hybrids acts stronger than dispersal, linkage disequilibrium will be high and clines will be steep and narrow.

In hybrid zones, gene flow may homogenize characters that are unimportant in species recognition, or reinforcement can cause characters involved in reproductive isolation to further diverge (Servedio and Noor 2003). Similarly, different molecular markers might respond to hybridization in distinct manners. For instance, n- and mtDNA have distinct modes of inheritance, nDNA being biparentally inherited and mtDNA maternally inherited in vertebrates (Ballard and Whitlock 2004). Consequently, sex-biased dispersal can be seen by comparing n- and mtDNA patterns in hybrid zones. Furthermore, many mitochondrial genes code for proteins involved in the electron transport chain and ATP production, making the whole mt genome subject to selection via linkage. However, assuming that mtDNA is neutrally evolving allows for the estimation of hybrid zone movement, because neutral markers lag behind non-neutral markers (McGuire et al. 2007). Differing selection pressures and inheritance patterns of these two molecular data types mean that cline shape and geographic center for these two characters in a given hybrid zone may in fact be distinct from one another (e.g. Leaché et al. 2017). Depending on the concordance or discordance between n- and mtDNA clines, an inference can be made about hybrid zone

movement or the dispersal behavior of the two sexes in the hybrid zone.

The genus *Liolaemus* represents a speciose clade of ∼250 South American Iguanian lizard species that inhabit elevation ranges from 0 to 5000m and span ∼40˚of latitude (Schulte et al. 2000). Many phylogeographic studies have been performed within this clade that often discover distinct, undescribed lineages (e.g. Breitman et al. 2011; Camargo et al. 2012). These and other studies have detected hybridization within many *Liolaemus* species complexes (Morando et al. 2004; Avila et al. 2006; Olave et al. 2011). However, because these species complexes span large geographic areas and because of difficulties of remote fieldwork, few studies have delineated contact zones or thoroughly investigated hybrid zone dynamics in this genus.

The *Liolaemus fitzingerii* species group is distributed in the Patagonian shrub-steppe of central Argentina and is currently composed of nine described species (Avila et al. 2006, 2008, 2010). Grummer et al. (2017b) performed a phylogeographic analysis on this group with genome-wide single nucleotide polymorphism (SNP) data across a dense geographic sampling of individuals and identified six distinct genetic groups. This study identified two putative contact zones: a "northern" hybrid zone between *L. melanops* and *L. shehuen* (populations "2" and "3" in the Grummer et al. 2017 study), and a "southern" hybrid zone between *L. xanthoviridis* and *L. fitzingerii* (populations "5" and "6"). These contact zones are further supported by unpublished analyses, which show high levels of color polymorphism in these areas in addition to signs of localized hybridization in the *cytochrome B* mitochondrial gene.

Here, we study hybrid zones in the *Liolaemus fitzingerii* species group of central Argentina in a comparative manner to contrast the evolutionary processes occurring in three uniquely positioned hybrid zones – one between *L. melanops* and *L. shehuen*, a second between *L. melanops* and *L. xanthoviridis*, and a third between *L. xanthoviridis* and *L. fitzingerii*. In this setup, two species, *L. melanops* and *L. xanthoviridis*, each hybridize

with two species. This offers a unique opportunity to study the outcomes of hybridization as a function of species-specific interactions, at both the genetic and ecological levels. Such close connections between species moderated by gene flow offers the opportunity for beneficial alleles and/or traits to spread between species, with the speed of the transfer inversely related to levels of selection. We studied these hybrid zones via transects, in which multiple individuals were collected per site along a line set ∼orthogonal to the interface of population contact. We collected both n- and mtDNA data for these individuals to investigate the potentially contrasting evolutionary processes that may be acting on these two distinct genomes.

Materials and Methods

Sampling and DNA Extraction

Northern Hybrid Zone.— During January and December of 2015, we collected 169 individuals from 17 distinct localities in Rio Negro and Chubut provinces (Fig. 1; Supplemental Table S1). Sampling was performed every ∼15-20 kilometers along the transects.

Southern Hybrid Zone.— In December 2015, we collected 120 individuals from 13 distinct localities in Chubut province (Fig. 1; Supplemental Table S2).

All specimens were deposited into the herpetology collection in the Centro Patagónico Nacional (CENPAT-CONICET), Puerto Madryn, Chubut, Argentina. DNA was extracted from tissue (tails tips and liver) through a salt (NaCl) extraction method (MacManes 2013). Prior to library sequencing preparation, we discarded samples that had low DNA concentration or had degraded genomic DNA with little high molecular weight DNA.

nDNA and mtDNA Sequence Preparation

ddRAD Sequencing Library Preparation.— We generated our dataset with the double digestion restriction site-associated DNA sequencing approach (Peterson et al. 2012). Genomic DNA was first digested with two enzymes, SbfI (8bp recognition sequence [5' CCTGCAGG 3'], "rare cutter"; New England Biolabs, Ipswich, MA) and MspI (4bp recognition sequence [5' CCGG 3'], "common cutter"; New England Biolabs, Ipswich, MA). Unique barcoded primers were then ligated to all genomic DNA fragments for demultiplexing, then we size-selected for genomic fragments between ∼365-465bp (415-515bp after ligating barcoded oligonucleotides) with the Blue Pippin DNA fragment size selector (Sage Science, MA, USA). We then performed polymerase chain reaction (PCR) on pooled samples consisting of eight individuals in each pool, with NEB Phusion Taq polymerase (New England Biolabs Inc., MA, USA) and the following thermocycler conditions: 98°for 0:30, (98°for 0:10, 58°for 0:30, 72°for 0:30) x 12 cycles, and a final 10:00 extension at 72°C. Individuals were then multiplexed (up to 160 individuals per sequencing lane, some runs with individuals from other studies) and sequenced on Illumina HiSeq 2500 and 4000 machines (Illumina Inc., CA, USA) with 50bp single-end reads at the University of California Berkeley's QB3 Vincent J. Coates sequencing facility. After de-multiplexing, each read contained 39bp of sequenced genomic DNA.

mtDNA Sequence Generation.— We targeted a fragment of the *cytochrome B* (*cytB*) gene to sequence for all individuals in the two hybrid zones. Two sets of primers were used, an "external" pair that amplified an ∼800bp fragment, and an "internal" pair that amplified a ∼360bp fragment; primer sequences are given in Morando et al. (2003). Twenty-three μL of Tankara EmeraldAmp GT PCR Master Mix (Takara Bio USA, Inc.; Mountain View, CA, USA) were mixed with 2 μL genomic DNA, and amplified with the following thermocycler conditions: 95°for 5:00, (95°for 0:45, 55°for 0:30, 72°for 1:00) x 35 cycles, with

a final 10:00 extension at 72°. If individuals did not amplify for the larger fragment, we attempted to amplify the smaller fragment with the internal primers. PCR products were sent to Genewiz (South Plainfield, NJ, USA), where they were purified and sequenced in both forward and reverse directions.

nDNA and mtDNA Dataset Assemblies

ddRAD Bioinformatics and Dataset Assembly.— Raw sequence reads were processed to generate "clusters" (e.g., loci) and SNPs with the program pyRAD v3.0.66 (Eaton 2014). After demultiplexing individuals, pyRAD uses VSEARCH (https://github.com/torognes/vsearch) and MUSCLE (Edgar 2004) to cluster reads into loci. Raw sequence reads were discarded if they had ≥4bp with a Phred quality score <20. Reads were first clustered within individuals, and then across individuals, with a 92% clustering threshold. We used a minimum depth of coverage of 10 for all loci. We set the paralog filter in pyRAD to 90% (see Grummer et al. 2017a for more details on the paralog filter), as we expect many heterozygous positions to be due to shared ancestry (e.g., homology) and not due to fixed paralogous differences. We set the missing data threshold at 25%, meaning that ≤25% of individuals were allowed to have missing data at a locus during dataset assembly.

Unlinked SNPs vs. Sequence Data.— Unlinked SNPs can generate ≤4 alleles per locus, and more commonly provide two. However, DNA sequence data contain much more allelic information and can generate up to 4^x alleles for a sequence x bp in length. PyRAD generates a ".alleles" file that contains allelic sequence data (e.g., two alleles per individual) for all loci that met all quality and assembly parameters; sequences need not be 39bp, as indels can cause loci to be >39bp. These ≥39bp RAD loci were then coded as alleles, two per individual. We generated a custom Python script to parse the ".alleles" file

into a file formatted for the program Structure (Pritchard et al. 2000), where any non-N difference at a site between alleles constituted a unique and new allele. This dataset (hereon termed "alleles") was then analyzed in parallel to the unlinked SNPs dataset to compare the power of each to identify populations and admixture proportions.

mtDNA Dataset Assembly.— Raw sequence data (".ab1" chromatograms) from both directions were made into contigs and hand-edited in Geneious v10 (Biomatters; Auckland, New Zealand). Consensus sequences were exported as .fasta sequences and aligned with Clustal2 (Larkin et al. 2007) in Mesquite v3.2 (Maddison and Maddison 2017). Outgroup sequence data were included for the taxon *Liolaemus cuyanus* in phylogenetic analyses.

Geographic Cline Analyses

To generate transect distances along a single axis between sampling localities of each hybrid zone, we first calculated pairwise distances between every sampling locality as the great circle distance with latitude-longitude coordinates in the R package "Fossil" with the function "earth.dist". We note that this method does not consider topography when calculating distances. We then used multidimensional scaling through principal coordinates analysis to reduce the pairwise matrix of distances between each locality into a single distance value for each locality that retained the original overall pairwise distance structure (as in Gompert et al. 2010). This ordination represents sampling locations along a single axis where kilometer (km) 0 was converted to represent the northern-most sampling site of each transect.

nDNA Clines.— We used Structure v2.3 (Pritchard et al. 2000; Falush et al. 2007) and the Evanno method (Evanno et al. 2005) to identify the number of populations (k) in each hybrid zone. Analyses on the northern hybrid zone dataset were run for 250,000 generations following a 75,000 generation burn-in period with five replicates of each k value

of 1 to 5. Because of a higher number of loci (see Results below), the southern hybrid zone dataset was run for 300,000 generations with 100,000 burn-in generations, also with five replicate runs of k 1-5.

After identifying the optimal k value, we used Structure to determine the admixture proportions (Q) of all individuals and therefore of each sampling locality. Results from five replicate Structure runs were combined through CLUMPP (Jakobsson and Rosenberg 2007) which served as input for cline analyses. We then used the Q proportions of each sampling locality to generate geographic clines. For the southern hybrid zone, the Evanno et al. (2005) method selected k=3, where a central population intergrades with two distinct populations, one to the north and another to the south. This southern hybrid zone was therefore split into two separate hybrid zones, where the northern hybrid zone was designated as localities A-I and the southern hybrid zone as localities F-M (Fig. 4). The northern half of our bigger southern transect will be referred to as the "southern A" hybrid zone, and the southern portion of the southern transect will be referred to as the "southern B" hybrid zone.

With the use of the Q proportions and geographic locations as described above, and the R package *Hzar* (Derryberry et al. 2014), we estimated geographic maximum likelihood clines, including cline centers and cline widths. Cline models were tested with minimum and maximum values fixed to the observed data, without allowing exponential tails on both sides of the cline. The cline fit request was run for 200,000 generations and a burn-in of 40,000 generations, from which the maximum likelihood parameter estimates of the cline were generated. The best-fit cline model (along with 95% confidence interval) was then plotted as a function of geographic distance along the transect.

mtDNA Clines.— We used two approaches to determine admixture proportions for each sampling locality to estimate mitochondrial clines. The first approach was tree-based,

where we used jModelTest v2.1.7 (Guindon and Gascuel 2003; Darriba et al. 2012) to determine the optimal DNA substitution model (HKY + Γ for all datasets), which was then used to estimate maximum likelihood trees in RAxML v8.2 (Stamatakis 2014) with 100 bootstrap iterations, with outgroup sequence data from *Liolaemus cuyanus* to root the trees. To calculate admixture proportions in each hybrid zone, we calculated the proportion of individuals from each locality that belonged to the "northern" clade (the "complementary" proportion would result if we calculated this value for the other clade), resulting in a frequency ranging from 0 to 1.

Our second approach was analogous to the tree-based approach, but instead was network-based. We inferred minimum-spanning networks (Bandelt et al. 1999) by using the program PopART (http://popart.otago.ac.nz), and divided the network into two groups on the edge (branch) with the highest number of sequence substitutions. As in the tree-based approach, we determined admixture proportions by calculating the proportion of individuals from each locality that were in each of the two major groups. These proportions were then used in Hzar to estimate the mt-based clines with the same methodology as in the nDNA cline estimates.

In addition to inferring clines for the mt- and nDNA datasets, we also quantitatively tested how different the cline estimates were for these two datasets. To do so, we constrained the nuclear data to have either the cline center or cline width that was estimated from the mtDNA, and then estimated the log likelihood of the constrained clines (for both alleles and unlinked SNPs datasets). With the maximum likelihood estimate and number of free parameters in the model, we were able to estimate AIC scores for each cline (with the "hzar.AIC.hzar.cline" function). A difference in AIC score >2 points was interpreted as the cline center or width being statistically different between n- and mtDNA datasets.

Linkage Disequilibrium and Selection

On the ends of a cline, allelic associations are maintained through linkage disequilibrium (LD). When individuals disperse into the contact zone and reproduce with individuals from the other population, LD breaks down through meiosis and recombination of distinct parental haplotypes. Assuming a tension zone of a given width, where the cline is maintained by a balance between dispersal and selection against hybrids, LD is related to dispersal, $D = \frac{\sigma^2(1+r)}{rw^2}$, where D = linkage disequilibrium, σ = the variance of parent-offspring geographic distance (hereafter referred to as "dispersal"), w is the cline width, and r is the recombination rate (Barton 1982). Note that the $(1 + r)$ term has been added to the numerator to account for samples taken after dispersal and before breeding (Barton and Gale 1993). For each hybrid zone, we estimated LD in the R package *Genetics* between all pair-wise combinations of SNPs, with the LD value $D = p(AB) - p(A)*p(B)$, which was then averaged across all SNPs within each hybrid zone. We then used our estimates of LD and w along with a r value of 0.5 (assuming all SNPs are unlinked) to estimate σ.

With the tension zone model as we have assumed here, cline width w at equilibrium $= \frac{4\sigma}{\sqrt{2s}}$, where s is the selection against a heterozygote. By first solving for σ for both alleles and unlinked SNPs datasets, we calculated the strength of selection (s) operating on heterozygotes in each cline.

Results

After we removed individuals with poor genomic DNA or sequence data quality, our nuclear datasets consisted of 157 individuals and 1295 loci in the northern hybrid zone, 73 in the southern A hybrid zone, and 61 in the southern B hybrid zone (2436 loci in both southern hybrid zones). We removed individuals from a single locality in the northern

hybrid zone because our analyses showed it to be geographically outside (to the east) of the hybrid zone. We also removed a single locality from analysis from the southern hybrid zone because this locality was represented by a single individual. Samples per locality ranged from 3-13 in the northern hybrid zone with an average of 7.8, and a range of 3-15 with an average of 8.1 in the southern hybrid zone (Supplemental Tables S1,S2). In the mitochondrial dataset (832 base pairs), the northern transect was represented by 146 individuals, whereas the southern A and B transects had 75 and 59 individuals, respectively (Supplemental Tables S3, S4). The 16 localities in the northern transect had an average sample size of 8.75 and ranged from 2-13 individuals; the average number of mitochondrial samples per locality in the southern A and B transects ranged from 2-15 ($\overline{x}$ = 9.38) and 2-13 ($\overline{x}$ = 8.00), respectively.

Population Identification

Coding the sequence data into alleles resulted in an average of 6.6 and 4.9 alleles per locus and a maximum of 32 and 28 alleles in the northern and southern transects, respectively (Fig. 2).

Northern Hybrid Zone.— The Evanno et al. (2005) method favored two populations (k=2) with the unlinked SNPs and alleles datasets alike (Supplemental Fig. S1). The interface between the two populations is sharp and occurs on the eastern edge of the Somuncura Plateau (Fig. 3).

Southern Hybrid Zone.— Estimates of the optimal k value via the Evanno et al. (2005) were in conflict: the unlinked SNPs dataset favored four populations, whereas the alleles dataset supported three (Supplemental Fig. S2). Visualizing the results of $k = 4$ reveals that the fourth inferred population is almost completely confined to individuals in the northern-most sampling locality ("A"; Fig. 4; Supplemental Fig. S3). The $k = 4$ result

doesn't make biological sense and is in conflict with the results from the alleles dataset, so we therefore focus on the k=3 results for the southern transect. Visualizing the k=3 result reveals a "sandwich" hybrid zone in which individuals from the center of the transect (roughly equivalent to the described species *Liolaemus xanthoviridis*) hybridize with two distinct populations – one to the north (*L. melanops*) and one to the south (*L. fitzingerii*; Fig. 4). Furthermore the northern population in the southern A hybrid zone is the same "species", *L. melanops*, that constitutes the northern populations of the northern transect (Supplemental Fig. S4).

Clines

Northern Hybrid Zone.— Cline center and width estimates for the alleles and unlinked SNPs datasets were ∼0.5 and 5.0km different from one another, respectively, in the northern hybrid zone (Table 1). The inferred admixture (Q proportions) were more extreme for the alleles dataset, providing estimates closer to 1 or 0 at the opposite ends of the transect (Fig. 5). In terms of calculating admixture proportions from the mitochondrial data, the phylogeny and network were in 100% agreement (Fig. 6). When mitochondrial and nuclear clines are compared, the mitochondrial cline is shifted ∼7 kilometers to the south of the nDNA clines and is ∼13km narrower (Table 1; Fig. 5). When the nuclear data are constrained to the estimates of the mitochondrial cline center or width, the position of the center, but not the width, is inferred to be significantly different (Table 2).

Southern Hybrid Zone.—

Southern A.— As in the northern hybrid zone, admixture proportions inferred with the alleles dataset were more extreme than the unlinked SNPs dataset (Fig. 7a). The cline center inferred from the nDNA is ∼40km to the south of the northern-most sampling

locality, and ∼45km wide (Table 1). As in the northern hybrid zone, the admixture proportions calculated from the mtDNA data were identical between phylogeny and network approaches (Fig. 8a). The nDNA clines are in stark contrast to the mtDNA cline, whose center is ∼20km to the south and over twice as narrow as the nDNA clines at 21.37km. When the nDNA was constrained to fit the mtDNA cline center and width, the clines estimated from both data types were significantly different from each other in both of these characteristics (Table 2).

Southern B.— Cline center estimates were only 0.43km different between alleles and unlinked SNP datasets, however, the alleles cline width estimate was ∼10km narrower (Table 1). In comparison to the phylogenies inferred for the other two transects, the phylogeny of the southern B transect individuals did not contain two strongly supported clades (Fig. 8b). However, two distinct groups were inferred in the network that corresponded to a division created by the longest branch in the phylogeny. In contrast to the other two transects, the clines estimated in the Southern B transect were in the very southern portion of the transect (Fig. 7b). The mtDNA cline center is ∼4km to the south and much narrower (1.19km) when compared to the nDNA clines (Table 1; Fig. 7b). Constraining the nDNA cline center to the mtDNA estimate strangely led to an improvement in model score, however, the nDNA cline widths were significantly wider than the mtDNA width (Table 2).

Linkage Disequilibrium and Selection Estimates

Average estimates of linkage disequilibrium ($\overline{D}$) across the three transects ranged from 0.0025 – 0.0114, with the lowest estimate for the northern hybrid zone and highest for the southern B hybrid zone (Table 3). Dispersal estimates were ∼1km (over an entire lifetime) in the northern hybrid zone, and were larger in the two southern hybrid zones, which were

both approximately 2km. Selection values increased from north to south, with an estimate of 0.0067 for the northern hybrid zone, 0.0164 for southern A, and 0.0304 for southern B (Table 3).

Discussion

We studied three hybrid zones in the *Liolaemus fitzingerii* species group and showed that two species, *L. melanops* and *L. xanthoviridis* each hybridize with two other species. Our genetic cline analyses showed that these contact zones are fairly narrow, ∼40km according to the nuclear data, and that the mitochondrial clines are always displaced to the south and statistically different from the nuclear clines in either cline center or width. Dispersal estimates in the hybrid zones ranged from ∼1-2km, leading to estimates of selection that ranged from 0.007 – 0.03, with the strongest selection in the southern hybrid zones. Together, these results indicate that selection is operating to different degrees on the same species in each hybrid zone, on both mitochondrial and nuclear genomes, revealing distinct evolutionary outcomes in replicated hybrid zones.

Replicated Hybrid Zones

The most profitable hybrid zone systems for studying genetic or ecological interactions between species are those with naturally formed hybrid zone replicates (McKinnon and Rundle 2002). These systems offer the chance to measure the repeatability of evolutionary processes such as gene flow and selection. Replicate hybrid zones have mainly been studied in fish, which typically show a high amount of variability of introgression rates and genomic divergence between different hybrid zones. In *Xiphophorus* swordtail fish, Culumber et al. (2011) found that LD and Hardy-Weinberg equilibrium estimates varied substantially across seven transects. Nolte et al. (2009) also found little correlation

between in genomic differentiation between two hybrid zones of sculpin fish (*Cottus*). And similarly, hybridization rates were found to vary considerably across ten topminnow (*Fundulus*) replicate hybrid zones (Duvernell and Schaefer 2014). These differences identified across replicate hybrid zones are typically ascribed to distinct environments that characterize each hybrid zone (Aboim et al. 2010).

In this study, we have two instances of replicate hybrid zones: *Liolaemus melanops* hybridizes with *L. shehuen* in the northern transect as well as with *L. xanthoviridis* in the southern transect; in addition to hybridizing with *L. melanops*, *L. xanthoviridis* also hybridizes with *L. fitzingerii* in the south. In the northern hybrid zone, the interface of *L. melanops* and *L. shehuen* occurs on the eastern edge of the Somuncura Plateau, which is approximately 25 million years old (Kay et al. 2007) and reaches an elevation of ∼1600m. That this geologic feature is at the interface of two populations is perhaps not surprising, however, *L. shehuen* individuals are found both below (to the east) and on top of this plateau. The elevation imposed by this plateau does seem to form a western barrier for *L. melanops*, which is found in lower elevation Patagonian shrub-steppe habitats to the east and south of the plateau, where it comes into contact with *L. xanthoviridis*. The boundary between *L. melanops* and *L. xanthoviridis* corresponds with the Chubut River, which is typically >100m wide in this area. No obvious geographic or environmental barrier separates *L. xanthoviridis* from *L. fitzingerii*.

Liolaemus melanops hybridizes in both northern and southern A hybrid zones, where the nDNA cline widths are ∼32 and 45km, respectively (Table 1). Assuming equal dispersal capabilities of *L. melanops* throughout its range, this implies stronger selection in the northern transect, contrary to what we calculated (Table 3). In the northern hybrid zone, *L. melanops* (male maximum snout-vent length [SVL] = 83mm, female = 74) and *L. shehuen* (male max SVL = 90.6) are similar in size (Etheridge 2000; Abdala et al. 2012). The disparity in *L. melanops* and *L. xanthoviridis* body size is similar (male max SVL =

94mm, female max SVL = 84), the latter being ∼10mm larger. Therefore, differing selection based on size does not seem to be the reason for the different selection rates we inferred. An equally parsimonious explanation would be the dispersal capabilities of *L. melanops* individuals is greater in the southern hybrid zone with *L. xanthoviridis*. However, with a lack of mark-recapture studies or field observations will be necessary to evaluate this hypothesis.

In a similar replicated fashion, *Liolaemus xanthoviridis* hybridizes in two separate areas, to the north with *L. melanops* and to the south with *L. fitzingerii*. The nDNA cline width in the north with *L. melanops* is ∼45km, whereas it is ∼32km wide in the hybrid zone with *L. fitzingerii*. Assuming tension zones that are a balance of dispersal and selection, we calculated a higher selection coefficient for the southern hybrid zone between *L. xanthoviridis* and *L. fitzingerii*. The stronger selection seen in the southern B hybrid zone does not seem to be the result of higher phenotypic discordance, as these two taxa are similar in size, both being large-bodied (male max SVL = 94 vs. 102 for *L. xanthoviridis* and *L. fitzingerii*; Etheridge 2000). Previous analyses of both sequence capture nuclear data (580 loci) and genome-wide SNPs (897 loci) revealed that *L. xanthoviridis* and *L. fitzingerii* form a strongly supported sister-species pair, in fact one of the few highly supported interspecific relationships inferred in this group (Grummer et al. 2017b,a). The higher level of selection we calculated in this hybrid zone may reflect their close evolutionary relationship, where selection is strong against intermediate hybrids that break down this species barrier. This stronger selection seen between *L. xanthoviridis* and *L. fitzingerii* might also be due to exogenous (environmental) causes. *Liolaemus fitzingerii* is found in loosely formed sand dunes dominated by *Prosopis denudans*, whereas *L. xanthoviridis* occurs in Patagonian shrub-steppe habitat. Lastly, this higher inferred selection value might not be directly indicative of selection, rather of genetic diversity. Selection (s) is directly proportional to linkage disequilibrium (D), and D will be higher in

populations with lower genetic diversity. Grummer et al. (2017b) showed that *L. fitzingerii* has low genetic diversity due to a recent population bottleneck. Therefore, overall D would be expected to be higher in the southern B hybrid zone, thus elevating the estimated selection coefficient between *L. xanthoviridis* and *L. fitzingerii*.

Nuclear vs. Mitochondrial Clines

Geographic clines inferred from nuclear and mitochondrial DNA were significantly different from each other in cline center and/or width in all three hybrid zones. That we observed this pattern is not necessarily unexpected. MtDNA does not recombine during meiosis, and these two genomes have different modes of inheritance and are subject to different selection pressures (Ballard and Whitlock 2004). However, distinct biotic and evolutionary processes could also generate this pattern. Because mtDNA is maternally-inherited in vertebrates, sex-biased dispersal can cause this pattern (Funk and Omland 2003). In *Liolaemus* lizards, males leave their natal ground to establish home ranges, whereas females disperse shorter distances (Kacoliris et al. 2009). Following introgressive hybridization, an individual's nuclear DNA will be admixed but the mtDNA will be from the maternal species. Under sex-biased dispersal, a southerly shifted mtDNA cline indicates northward migration, where male dispersal is from the southern population into the northern population.

A second reason for the discordant mt- and nDNA clines is that these hybrid zones could be moving. Many empirical studies have documented moving hybrid zones over time (Buggs 2007). The causes of hybrid zone movement can be binned into two classes: endogenous or exogenous. Under endogenous selection, selection against hybrids is genetically countered by dispersal of parental forms into the hybrid zone (tension zone model; Barton and Hewitt 1985). Under exogenous selection, a change in the external environment causes selection along a gradient that leads to fitness differences (May et al. 1975). When an environmental gradient moves (e.g., as the result of a change in

environmental temperatures), geographic ranges and hybrid zones can shift with it. As geographic ranges shift, asymmetric introgression from the expanding species into the stationary one will cause neutral markers to trail behind non-neutral markers (McGuire et al. 2007). In particular, asymmetric introgression of the mitochondrial genome and its discordance with nuclear markers has been used to deduce a moving hybrid zone (Rohwer et al. 2001). Although hybrid zone movement over time can be inferred from discordant mt- and nDNA clines sampled from a single time-point, the most convincing cases of hybrid zone movement come from studies with replicated sampling efforts over time (e.g. Carling and Zuckerberg 2011; Taylor et al. 2014; Leaché et al. 2017). A lagging cline inferred from the putatively neutral mtDNA that is following the leading edge of an expanding population further suggests northward range expansion of *L. shehuen*, *L. xanthoviridis*, and *L. fitzingerii*.

However, assuming that mitochondrial DNA is neutral might not be warranted. Indirect selection through differential selection of the heterogametic sex (e.g., Haldane's Rule) or direct selection via cyto-nuclear incompatibilities would also impair the effective movement of mtDNA across the hybrid zone (Dasmahapatra et al. 2002). This leads to a third reason for mt-nDNA cline discordance, which is differential selection on the two genomes. If positive selection was in fact working on any site in the mitochondrial genome, that mitochondrial haplotype would sweep through the population (due to linkage) and the cline would not lag behind as expected for a neutral marker. Although we did not explicitly test for selection on our nuclear loci, it is unlikely to affect our results because loci under selection would likely be in the minority of our dataset. Nonetheless, we agree with Dasmahapatra et al. (2002) in that "asymmetry of introgression, or lack of introgression of molecular markers, is relatively unconvincing evidence either for or against hybrid zone movement."

We performed our Structure and cline analyses on two nuclear datasets, one where a

single variable site was used from a 39bp locus ("unlinked SNPs"), and a second dataset where the entire 39bp sequence was coded into alleles ("alleles"). The alleles dataset provided many more alleles per locus than the unlinked SNPs dataset, with 4.9 and 6.6 alleles per locus for the "alleles" dataset in the northern and southern transects, whereas the unlinked SNPs datasets contained two alleles per locus (all were biallelic). Although Structure plots between the two datasets were qualitatively similar (results not shown), admixture proportions (Q) were more "intermediate" for the unlinked SNPs dataset, meaning that the Q values weren't as extreme as in the alleles dataset. This can be seen in the cline estimates (Figs. 5,7), where the frequency of the northern genotype for the alleles dataset reached closer to 0.0 and 1.0. A similar pattern is seen in the cline width estimates (Table 1), where the widths estimated for two of the three transects from the alleles dataset were narrower by 5-10km. These narrower cline estimates, and more extreme Q estimates are almost certainly due to the increased information content associated with higher allelic richness in the alleles dataset. Whether the cline center and width estimated from the alleles or unlinked SNPs dataset are closer to the "true" cline would need to be explored through simulations and is beyond the scope of this study.

Dispersal, Population Equilibrium, and Assumptions

Throughout this study, we assumed a tension zone model for all three hybrid zones, where dispersal and selection are opposing forces that maintain the cline's width and position. In using this model to calculate dispersal (σ) and ultimately selection (s), we assumed random mating, selection is against intermediate genotypes (e.g., heterozygotes) and is weak ($\simeq$0.01), and no epistatic interactions occur between loci (Szymura and Barton 1986; Barton and Gale 1993). And finally, we assumed a recombination (r) value of 0.5, meaning all loci are completely unlinked. Lacking field observation data, testing some of these assumptions is difficult, such as random mating or selection against heterozygotes.

Similarly, with little known about the *Liolaemus* genome and very short fragments of sequenced genomic DNA (which are not unambiguously placed to a reference genome), testing for epistatic interactions and recombination rates between our loci would be difficult.

Given this set of assumptions, we were able to calculate dispersal and selection coefficients for individuals in these hybrid zones. Our lifetime dispersal estimates for all three hybrid zones ranged from roughly 1-2km (Table 3). Many mark-recapture studies have been performed on *Liolaemus* lizards, but these focused on estimating the home range size of adults (e.g. Frutos et al. 2007; Kacoliris et al. 2009). However, a study on *Liolaemus koslowskyi* by Frutos and Belver (2007) measured the shift in home range of the same individuals across breeding years and found that males dispersed further than females, on average ∼12m/year. These studies do not provide estimates of hatchling dispersal to their breeding grounds, which is a significant proportion of the total dispersal an individual performs in its lifetime. In another Iguanian lizard (*Sceloporus undulatus*), hatchling dispersal has been estimated at ∼50m (Massot et al. 2003).

In addition to these estimates of dispersal, Camargo et al. (2013) used a Bayesian phylogeographic approach to estimate historic dispersal rates of *Liolaemus darwinii* at 20m/year, which they conclude are likely a little high given the inferred population expansion occurring at that time. In light of these various dispersal estimates in the literature, our estimates seem quite high. To calculate dispersal, we estimated cline width (w) and D, alongside an assumed r. Given the relationship between these variables, the cline width would need to be reduced two orders of magnitude to put our estimates in the range of other *Liolaemus* estimates. Similarly, the recombination rate would need to decrease by 3-4 orders of magnitude, and the same holds true for D. Our estimates for each of these parameters are unlikely to be so far off, but incorrect estimations of each variable would compound the inaccuracy of our overall dispersal estimate, which is certainly

plausible.

Perhaps most realistically, assumptions about population equilibria might not be true for these populations. Previous work on the *Liolaemus fitzingerii* group showed that these populations have gone through a recent population bottleneck and seem to be currently expanding their population sizes (and likely ranges as well; Grummer et al. 2017a). Furthermore, if we assume that the mitochondrial genome is not subject to selection pressure and therefore behaves as a neutral marker in this group, the non-coincident n- and mtDNA clines could indicate a moving hybrid zone. Non-equilibrium populations would invalidate the theoretical assumptions of these models and cast doubt on our estimates of dispersal and selection.

Conclusions

In this study, we were able to compare independent replicates of hybridization that were formed in distinct regions of central Argentina. Our results revealed idiosyncratic outcomes of the evolutionary process, where selection is operating at different levels on the same species in replicate hybrid zones. This suggests that either the environment or genetic interactions that characterize each hybrid zone are distinct enough to create quantitatively different outcomes of the evolutionary process. The *Liolaemus fitzingerii* species group has thus provided another example of the unique outcomes of the evolutionary process when we are able to effectively "replay life's tape" (Gould 1989).

Acknowledgments

This work used the Vincent J. Coates Genomics Sequencing Laboratory at UC Berkeley, supported by NIH S10 OD018174 Instrumentation Grant. This research was funded in part by a National Science Foundation Doctoral Dissertation Improvement Grant (DEB-1500933) to JAG, and was facilitated though the use of advanced computational, storage, and networking infrastructure provided by the Hyak supercomputer system at the University of Washington.

*

References

Abdala, C. S., J. Díaz Gómez, and V. Juarez Heredia. 2012. From the far reaches of patagonia: new phylogenetic analyses and description of two new species of the *Liolaemus fitzingerii* clade (iguania: Liolaemidae). Zootaxa 3301:34–60.

Aboim, M., J. Mavárez, L. Bernatchez, and M. Coelho. 2010. Introgressive hybridization between two iberian endemic cyprinid fish: a comparison between two independent hybrid zones. Journal of Evolutionary Biology 23:817–828.

Avila, L., M. Morando, and J. Sites. 2006. Congeneric phylogeography: hypothesizing species limits and evolutionary processes in patagonian lizards of the liolaemus boulengeri group (squamata: Liolaemini). Biological Journal of the Linnean Society 89:241–275.

Avila, L. J., M. Morando, and J. W. Sites Jr. 2008. New species of the iguanian lizard genus liolaemus (squamata, iguania, liolaemini) from central patagonia, argentina. Journal of Herpetology 42:186–196.

Avila, L. J., C. H. F. Pérez, M. Morando, and J. Sites Jr. 2010. A new species of liolaemus (reptilia: Squamata) from southwestern rio negro province, northern patagonia, argentina. Zootaxa 2434:47–59.

Ballard, J. W. O. and M. C. Whitlock. 2004. The incomplete natural history of mitochondria. Molecular ecology 13:729–744.

Bandelt, H.-J., P. Forster, and A. Röhl. 1999. Median-joining networks for inferring intraspecific phylogenies. Molecular biology and evolution 16:37–48.

Barton, N. 1982. The structure of the hybrid zone in uroderma bilobatum (chiroptera: Phyllostomatidae). Evolution 36:863–866.

Barton, N. H. and K. S. Gale. 1993. Genetic analysis of hybrid zones. Hybrid zones and the evolutionary process Pages 13–45.

Barton, N. H. and G. M. Hewitt. 1985. Analysis of hybrid zones. Annual review of Ecology and Systematics 16:113–148.

Breitman, M. F., L. J. Avila, J. W. Sites, and M. Morando. 2011. Lizards from the end of the world: Phylogenetic relationships of the liolaemus lineomaculatus section (squamata: Iguania: Liolaemini). Molecular Phylogenetics and Evolution 59:364–376.

Buggs, R. 2007. Empirical study of hybrid zone movement. Heredity 99:301–312.

Camargo, A., M. Morando, L. J. Avila, and J. W. Sites. 2012. Species delimitation with abc and other coalescent-based methods: a test of accuracy with simulations and an empirical example with lizards of the liolaemus darwinii complex (squamata: Liolaemidae). Evolution 66:2834–2849.

Camargo, A., F. P. Werneck, M. Morando, J. W. Sites, and L. J. Avila. 2013. Quaternary range and demographic expansion of liolaemus darwinii (squamata: Liolaemidae) in the monte desert of central argentina using bayesian phylogeography and ecological niche modelling. Molecular ecology 22:4038–4054.

Carling, M. D. and B. Zuckerberg. 2011. Spatio-temporal changes in the genetic structure of the passerina bunting hybrid zone. Molecular Ecology 20:1166–1175.

Culumber, Z., H. Fisher, M. Tobler, M. Mateos, P. Barber, M. Sorenson, and G. Rosenthal. 2011. Replicated hybrid zones of xiphophorus swordtails along an elevational gradient. Molecular ecology 20:342–356.

Darriba, D., G. L. Taboada, R. Doallo, and D. Posada. 2012. jmodeltest 2: more models, new heuristics and parallel computing. Nature methods 9:772–772.

Darwin, C. 1862. Notes on the causes of cross and hybrid sterility. The Correspondence of Charles Darwin 10:700–711.

Dasmahapatra, K. K., M. J. Blum, A. Aiello, S. Hackwell, N. Davies, E. P. Bermingham, and J. Mallet. 2002. Inferences from a rapidly moving hybrid zone. Evolution 56:741–753.

Derryberry, E. P., G. E. Derryberry, J. M. Maley, and R. T. Brumfield. 2014. Hzar: hybrid zone analysis using an r software package. Molecular Ecology Resources 14:652–663.

Duvernell, D. D. and J. F. Schaefer. 2014. Variation in contact zone dynamics between two species of topminnows, fundulus notatus and f. olivaceus, across isolated drainage systems. Evolutionary Ecology 28:37–53.

Eaton, D. A. 2014. Pyrad: assembly of de novo radseq loci for phylogenetic analyses. Bioinformatics Page btu121.

Edgar, R. C. 2004. Muscle: multiple sequence alignment with high accuracy and high throughput. Nucleic acids research 32:1792–1797.

Etheridge, R. 2000. A review of lizards of the liolaemus wiegmannii group (squamata, iguania, tropiduridae), and a history of morphological change in the sand-dwelling species. Herpetological Monographs Pages 293–352.

Evanno, G., S. Regnaut, and J. Goudet. 2005. Detecting the number of clusters of individuals using the software structure: a simulation study. Molecular ecology 14:2611–2620.

Falush, D., M. Stephens, and J. K. Pritchard. 2007. Inference of population structure using multilocus genotype data: dominant markers and null alleles. Molecular ecology notes 7:574–578.

Frutos, N. and L. C. Belver. 2007. Dominio vital de liolaemus koslowskyi etheridge, 1993 (iguania: Liolaemini) en el noroeste de la provincia de la rioja, argentina. Cuadernos de Herpetología 21:83–92.

Frutos, N., L. A. Camporro, and L. J. Avila. 2007. Ámbito de hogar de liolaemus melanops burmeister, 1888 (squamata: Liolaemini) en el centro de chubut, argentina. Gayana (Concepción) 71:142–149.

Funk, D. J. and K. E. Omland. 2003. Species-level paraphyly and polyphyly: frequency, causes, and consequences, with insights from animal mitochondrial dna. Annual Review of Ecology, Evolution, and Systematics 34:397–423.

Gompert, Z., L. K. Lucas, J. A. Fordyce, M. L. Forister, and C. C. Nice. 2010. Secondary contact between lycaeides idas and l. melissa in the rocky mountains: extensive admixture and a patchy hybrid zone. Molecular ecology 19:3171–3192.

Gould, S. J. 1989. Wonderful Life: The Burgess Shale and the Nature of History. Norton, New York.

Grummer, J. A., L. J. Avila, M. M. Morando, J. W. Sites, and A. D. Leaché. 2017a. Lack of phylogenetic support matters: phylogenomic evidence for a recent and rapid radiation in lizards of the patagonian *Liolaemus fitzingerii* species group. In Preparation .

Grummer, J. A., M. M. Morando, L. J. Avila, and A. D. Leaché. 2017b. Rocks and ice: the effects of geographic features and pleistocene glaciations on the gondwanan *Liolaemus fitzingerii* species group. In Preparation .

Guindon, S. and O. Gascuel. 2003. A simple, fast, and accurate algorithm to estimate large phylogenies by maximum likelihood. Systematic biology 52:696–704.

Harrison, R. G. 1993. Hybrid zones and the evolutionary process. Oxford University Press on Demand.

Irwin, D. E., S. Bensch, and T. D. Price. 2001. Speciation in a ring. Nature 409:333–337.

Jakobsson, M. and N. A. Rosenberg. 2007. Clumpp: a cluster matching and permutation program for dealing with label switching and multimodality in analysis of population structure. Bioinformatics 23:1801–1806.

Kacoliris, F. P., J. D. Williams, C. R. De Arcaute, and C. Cassino. 2009. Home range size and overlap in liolaemus multimaculatus (squamata: Liolamidae) in pampean coastal dunes of argentina. South American Journal of Herpetology 4:229–234.

Kay, S. M., A. Ardolino, M. Gorring, and V. Ramos. 2007. The somuncura large igneous province in patagonia: interaction of a transient mantle thermal anomaly with a subducting slab. Journal of Petrology 48:43–77.

Larkin, M. A., G. Blackshields, N. Brown, R. Chenna, P. A. McGettigan, H. McWilliam, F. Valentin, I. M. Wallace, A. Wilm, R. Lopez, et al. 2007. Clustal w and clustal x version 2.0. bioinformatics 23:2947–2948.

Leaché, A. D. and C. J. Cole. 2007. Hybridization between multiple fence lizard lineages in an ecotone: locally discordant variation in mitochondrial dna, chromosomes, and morphology. Molecular Ecology 16:1035–1054.

Leaché, A. D., J. A. Grummer, R. B. Harris, and I. K. Breckheimer. 2017. Evidence for concerted movement of nuclear and mitochondrial clines in a lizard hybrid zone. Molecular Ecology 26:2306–2316.

MacManes, M. 2013. Available from: http://dx.doi.org/10.6084/m9.figshare.658946. Figshare 5.

Maddison, W. P. and D. Maddison. 2017. Mesquite: a modular system for evolutionary analysis. version 3.2. http://mesquiteproject.org.

Mallet, J. 2005. Hybridization as an invasion of the genome. Trends in ecology & evolution 20:229–237.

Mallet, J., N. Barton, G. Lamas, J. Santisteban, M. Muedas, and H. Eeley. 1990. Estimates of selection and gene flow from measures of cline width and linkage disequilibrium in heliconius hybrid zones. Genetics 124:921–936.

Massot, M., R. B. Huey, J. Tsuji, and F. H. van Berkum. 2003. Genetic, prenatal, and postnatal correlates of dispersal in hatchling fence lizards (sceloporus occidentalis). Behavioral Ecology 14:650–655.

May, R. M., J. A. Endler, and R. E. McMurtrie. 1975. Gene frequency clines in the presence of selection opposed by gene flow. The American Naturalist 109:659–676.

McGuire, J. A., C. W. Linkem, M. S. Koo, D. W. Hutchison, A. K. Lappin, D. I. Orange, J. Lemos-Espinal, B. R. Riddle, and J. R. Jaeger. 2007. Mitochondrial introgression and incomplete lineage sorting through space and time: phylogenetics of crotaphytid lizards. Evolution 61:2879–2897.

McKinnon, J. S. and H. D. Rundle. 2002. Speciation in nature: the threespine stickleback model systems. Trends in Ecology & Evolution 17:480–488.

Morando, M., L. J. Avila, J. Baker, J. W. Sites Jr, and M. Ashley. 2004. Phylogeny and phylogeography of the liolaemus darwinii complex (squamata: Liolaemidae): evidence for introgression and incomplete lineage sorting. Evolution 58:842–861.

Morando, M., L. J. Avila, and J. W. Sites. 2003. Sampling strategies for delimiting species:

genes, individuals, and populations in the liolaemus elongatus-kriegi complex (squamata: Liolaemidae) in andean–patagonian south america. Systematic Biology 52:159–185.

Moritz, C., C. J. Schneider, and D. B. Wake. 1992. Evolutionary relationships within the ensatina eschscholtzii complex confirm the ring species interpretation. Systematic biology 41:273–291.

Nolte, A., Z. Gompert, and C. Buerkle. 2009. Variable patterns of introgression in two sculpin hybrid zones suggest that genomic isolation differs among populations. Molecular Ecology 18:2615–2627.

Olave, M., L. E. Martinez, L. J. Avila, J. W. Sites, and M. Morando. 2011. Evidence of hybridization in the argentinean lizards liolaemus gracilis and liolaemus bibronii (iguania: Liolaemini): An integrative approach based on genes and morphology. Molecular Phylogenetics and Evolution 61:381–391.

Peterson, B. K., J. N. Weber, E. H. Kay, H. S. Fisher, and H. E. Hoekstra. 2012. Double digest radseq: an inexpensive method for de novo snp discovery and genotyping in model and non-model species. PloS one 7:e37135.

Pritchard, J. K., M. Stephens, and P. Donnelly. 2000. Inference of population structure using multilocus genotype data. Genetics 155:945–959.

Rieseberg, L. H., J. Whitton, and K. Gardner. 1999. Hybrid zones and the genetic architecture of a barrier to gene flow between two sunflower species. Genetics 152:713–727.

Rohwer, S., E. Bermingham, and C. Wood. 2001. Plumage and mitochondrial dna haplotype variation across a moving hybrid zone. Evolution 55:405–422.

Schulte, J. A. I., R. J. Macey, R. E. Espinoza, and A. Larson. 2000. Phylogenetic relationships in the iguanid lizard genus liolaemus: multiple origins of viviparous reproduction and evidence for recurring andean vicariance and dispersal. Biological Journal of the Linnean Society 69:75–102.

Servedio, M. R. and M. A. Noor. 2003. The role of reinforcement in speciation: theory and data. Annual Review of Ecology, Evolution, and Systematics 34:339–364.

Stamatakis, A. 2014. Raxml version 8: a tool for phylogenetic analysis and post-analysis of large phylogenies. Bioinformatics 30:1312–1313.

Szymura, J. M. and N. H. Barton. 1986. Genetic analysis of a hybrid zone between the fire-bellied toads, bombina bombina and b. variegata, near cracow in southern poland. Evolution Pages 1141–1159.

Taylor, S. A., T. A. White, W. M. Hochachka, V. Ferretti, R. L. Curry, and I. Lovette. 2014. Climate-mediated movement of an avian hybrid zone. Current Biology 24:671–676.

Data Accessibility:

- DNA Sequences: NCBI's Short Read Archive accession nos. xxxx-xxxx

- Sampling locality information is available in the Supplementary Table S1.

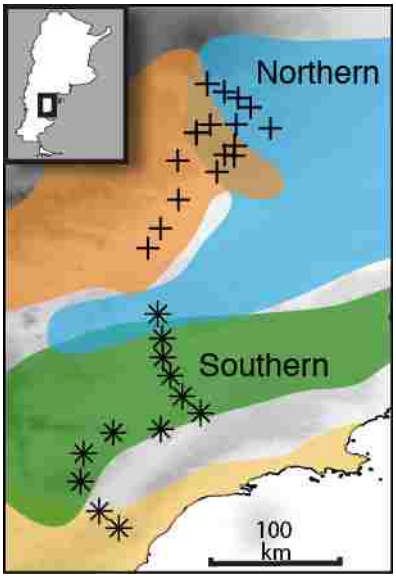

Figure 1: Map showing transect sampling localities for both northern and southern hybrid zone transects, with the inset highlighting the region of Argentina where this study took place. Colors on the map reflect population boundaries as determined by genome-wide SNP data in Grummer et al. (2017) that largely correlate to the species *Liolaemus melanops* (blue), *L. shehuen* (orange), *L. xanthoviridis* (green), and *L. fitzingerii* (yellow).

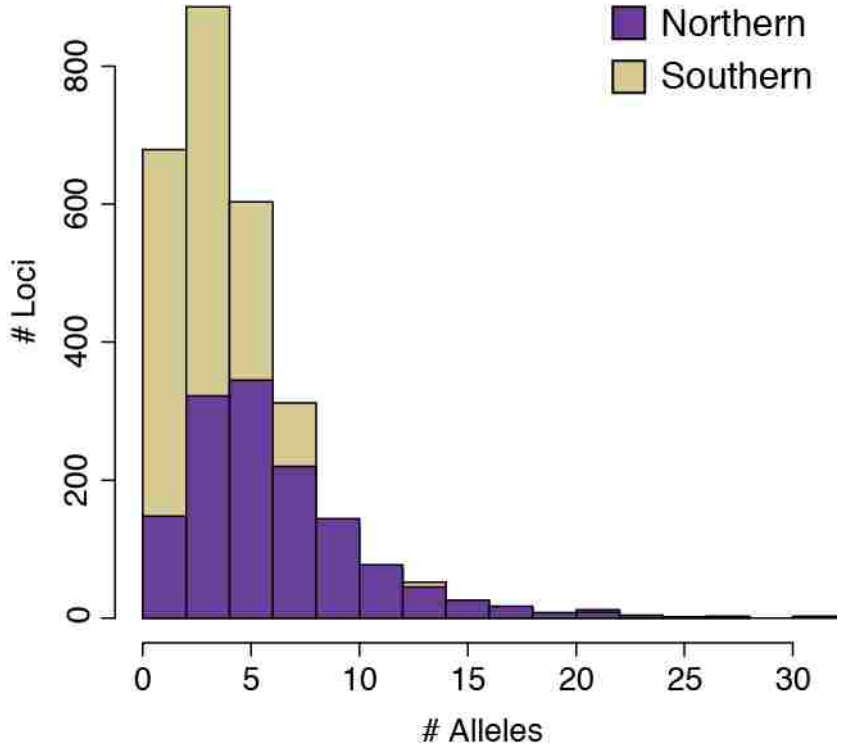

Figure 2: Plot showing the number of alleles per locus for both northern and southern transects when the sequence data were coded into alleles vs. unlinked SNPs.

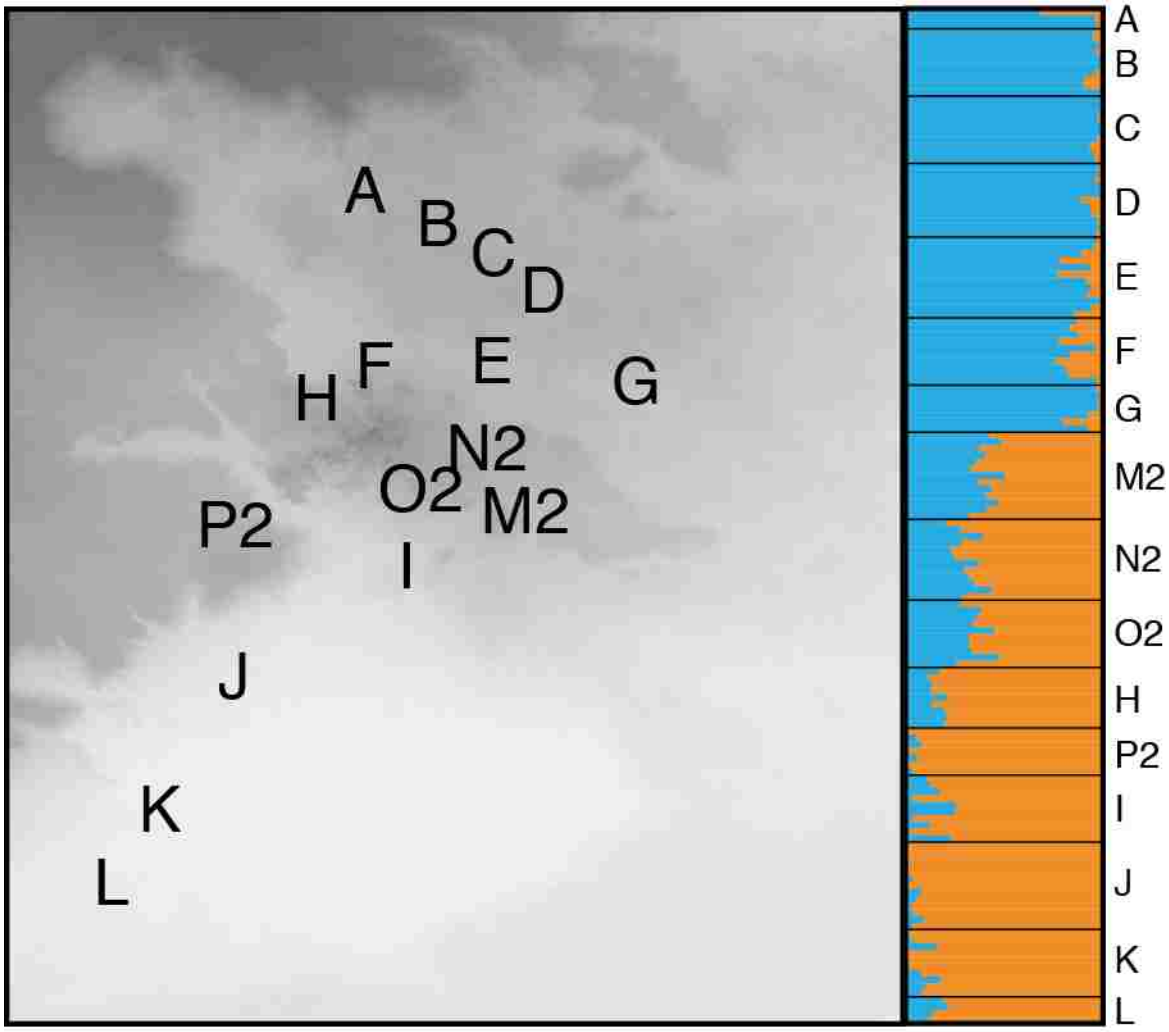

Figure 3: Map of the Structure results by sampling locality for the northern hybrid zone.

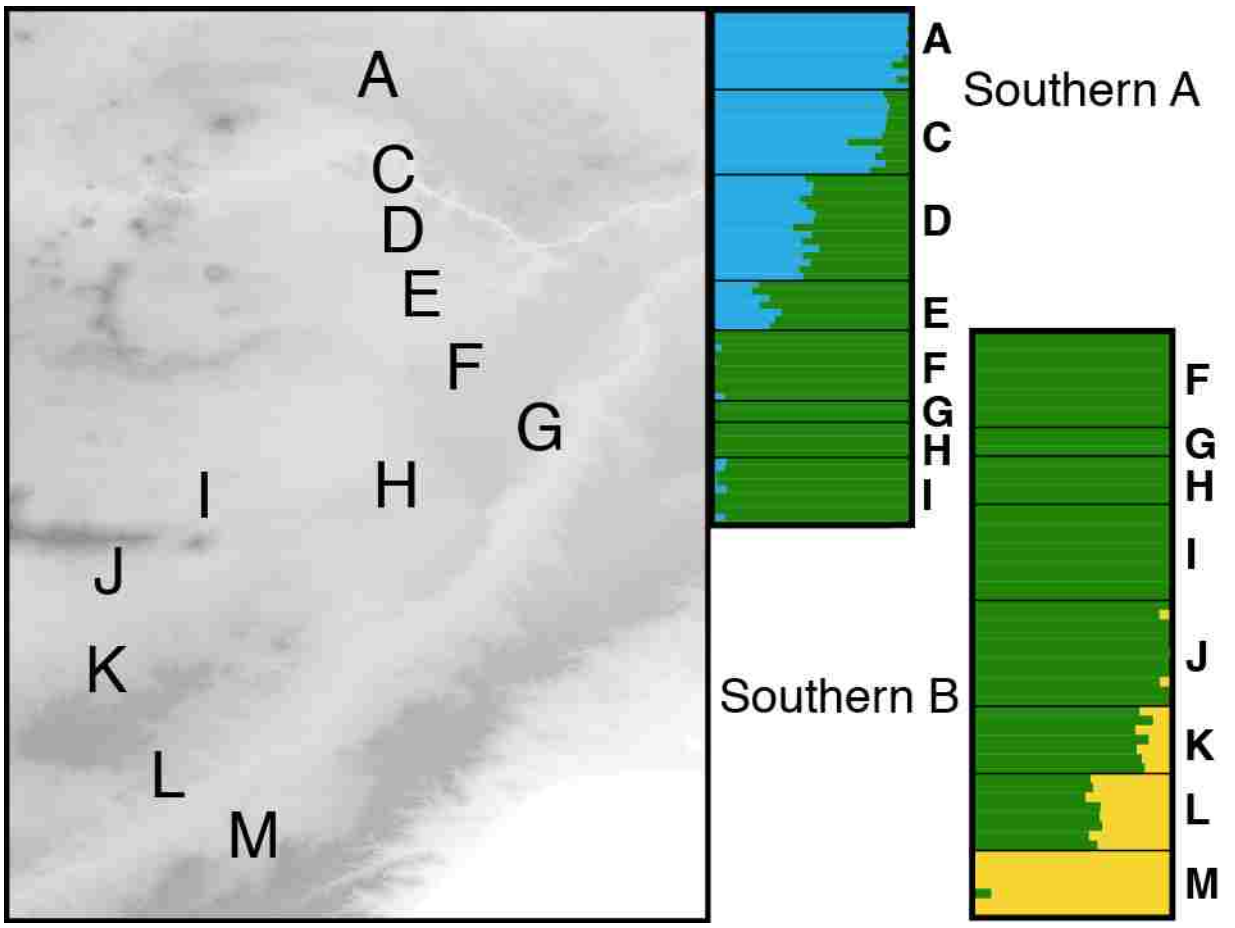

Figure 4: Structure results for the southern hybrid zone with the k=3 results revealing a central population that hybridizes with populations both to the north and south. The "Southern A" transect refers to the northern portion of the larger southern transect, whereas the "Southern B" transect refers to the southern portion.

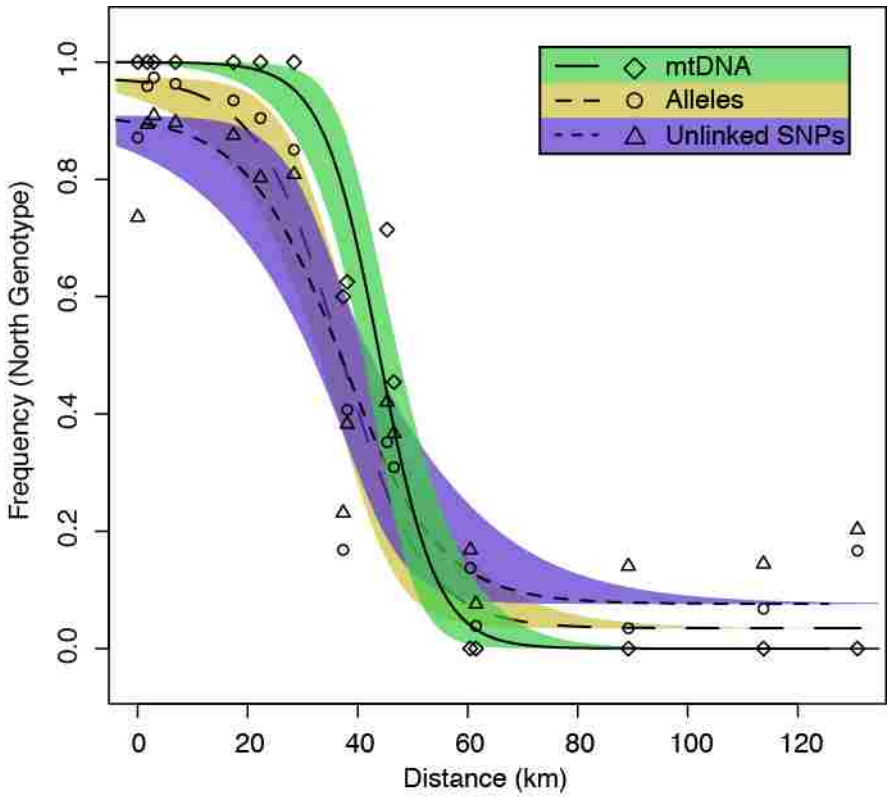

Figure 5: Hzar maximum likelihood cline estimates and 95% credible intervals for the northern hybrid zone between *L. melanops* and *L. shehuen* from nDNA and mtDNA datasets. The x-axis represents distances from the northern-most sampling locality.

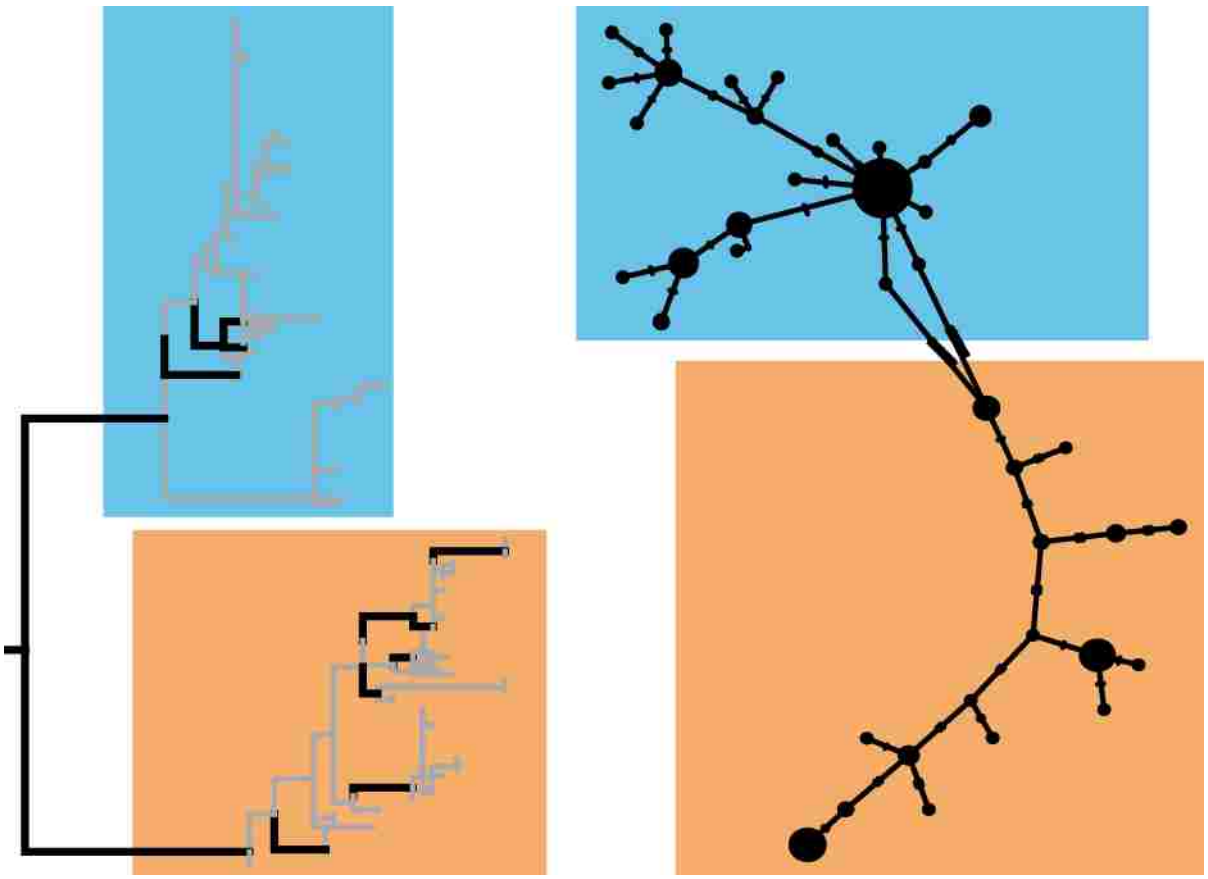

Figure 6: Maximum likelihood phylogeny and minimum-spanning network inferred for the northern hybrid zone, with the northern population in blue and southern in orange. In the phylogeny, the outgroup has been removed and branches receiving >70 bootstrap proportion are in black. In the network, unique haplotypes are depicted as circles, with the frequency of that haplotype represented by its size. Nucleotide substitutions are indicated by hash marks on the internal branches.

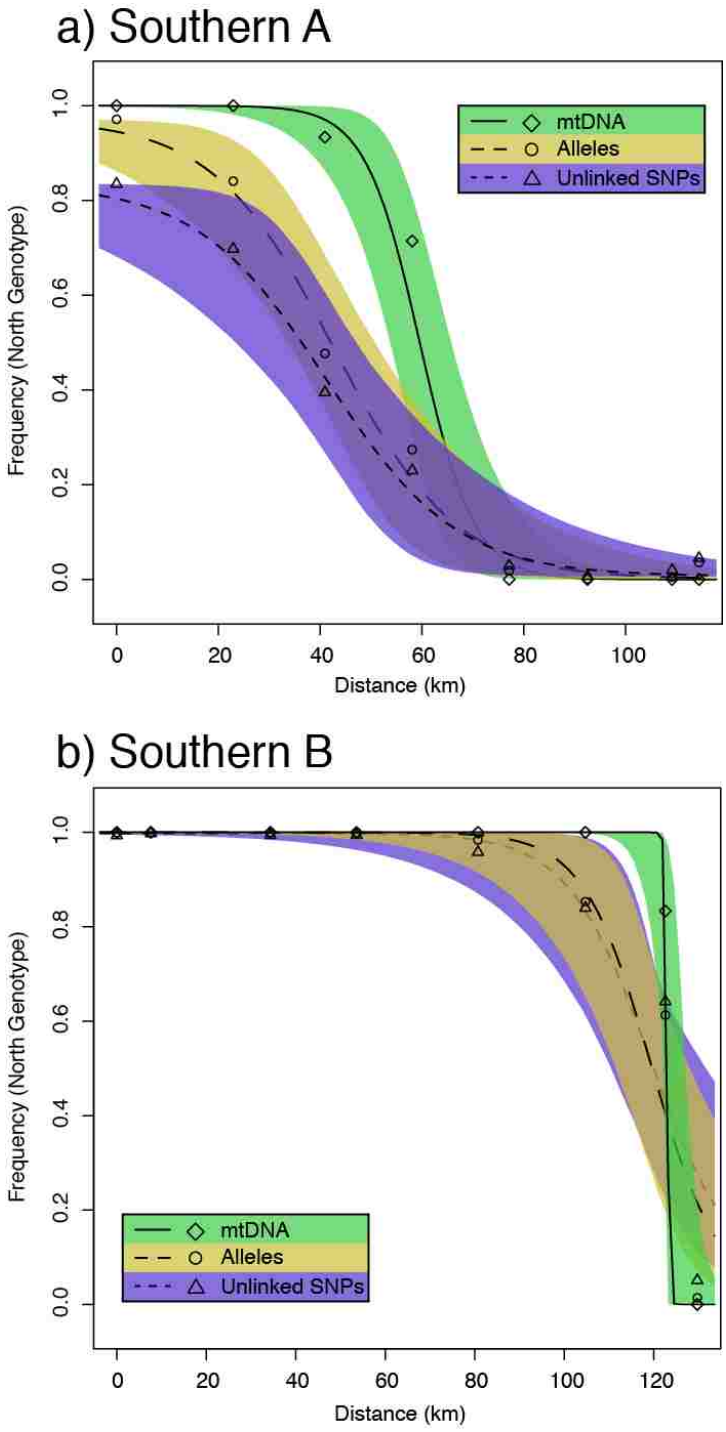

Figure 7: Hzar maximum likelihood cline estimates and 95% credible intervals for the two southern transects, "Southern A" and "Southern B", from nDNA and mtDNA datasets. The x-axis represents distances from the northern-most sampling locality.

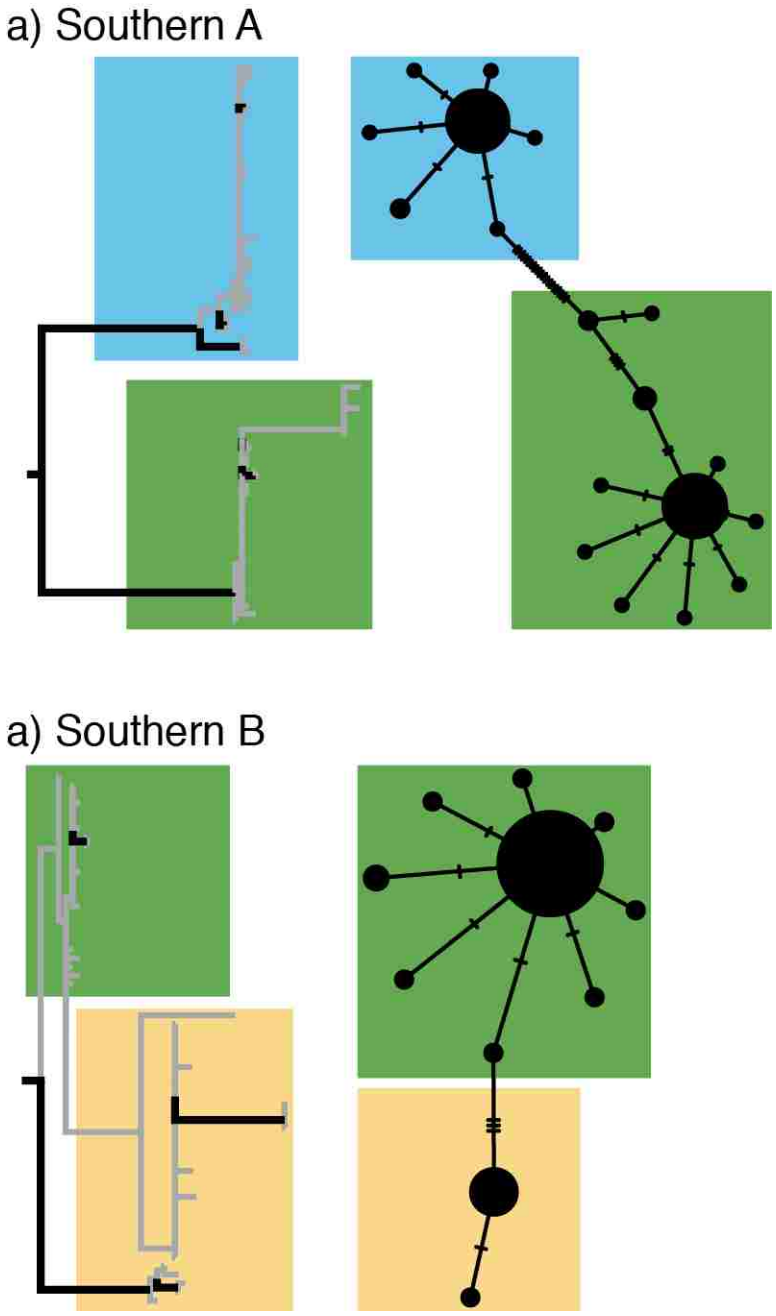

Figure 8: Maximum likelihood phylogenies and minimum-spanning networks inferred for the (a) Southern A and (b) Southern B transects. In the phylogenies, the outgroup has been removed and branches receiving >70 bootstrap proportion are in black. In the networks, unique haplotypes are depicted as circles, with the frequency of that haplotype represented by its size. Nucleotide substitutions are indicated by hash marks on the internal branches. Note that the north and south populations in the Southern B phylogeny do not form independent clades, but do form mutually exclusive networks.

Table 1: Cline analysis results from Hzar for northern and southern hybrid zones. The cline center results represent distance from the northern-most sampling locality, and all numbers represent kilometers.

Dataset	Northern		Southern A		Southern B	
	Center	Width	Center	Width	Center	Width
Alleles	36.82	30.13	42.77	47.61	119.43	27.42
Unlinked SNPs	37.21	35.27	38.22	43.18	119.00	37.14
mtDNA	43.96	20.64	59.57	21.37	123.08	1.19

Table 2: AIC scores for genetic clines from Hzar analyses. The nDNA value represents the AIC score when estimating the ML cline for the nDNA, whereas the mtDNA-fitted center and mtDNA-fitted width columns represent AIC scores when forcing the ML estimate of the mtDNA center or width on the nDNA ML cline estimates, respectively. Bold values indicate AIC scores >2 points different in comparison to the freely estimated nDNA clines.

	Northern			Southern A			Southern B		
	nDNA	mtDNA-Fitted Center	mtDNA-Fitted Width	nDNA	mtDNA-Fitted Center	mtDNA-Fitted Width	nDNA	mtDNA-Fitted Center	mtDNA-Fitted Width
Alleles	12.480	**18.932**	12.784	5.943	**13.663**	**10.257**	8.372	7.236	**296.191**
Unlinked SNPs	11.438	**14.003**	12.495	5.210	**10.696**	**7.525**	8.222	6.939	**11.890**

Table 3: Estimates of linkage disequilibrium (D), dispersal (σ) in kilometers, and selection (s) for the three hybrid zones.

	Northern	Southern A	Southern B
$\overline{D}$	0.0025	0.0061	0.0114
$\sigma_{alleles}$	0.874	2.155	1.690
σ_{uSNPs}	1.023	1.955	2.289
s	0.0067	0.0164	0.0304

Supplemental figures and tables for “Four species linked by three hybrid zones: two instances of repeated hybridization in one species group (genus *Liolaemus*)”

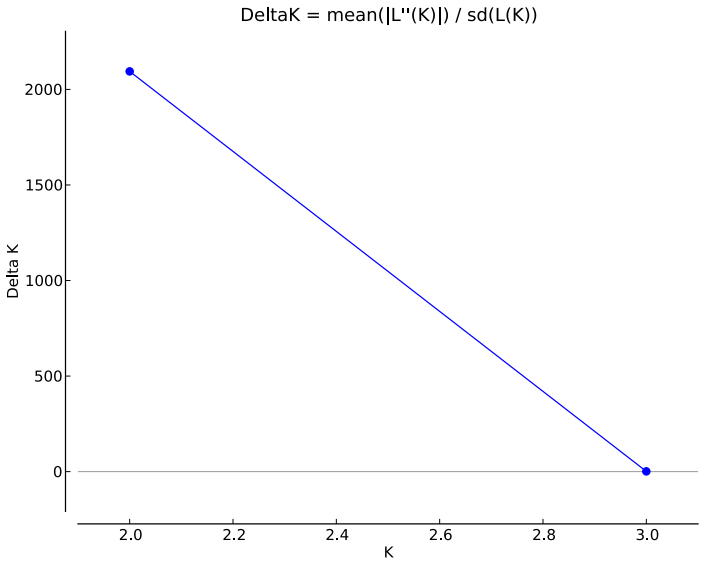

Supplemental Figure S1a. Results from the Evanno et al. (2005) method on the Structure analysis of the northern hybrid zone using the unlinked SNPs dataset.

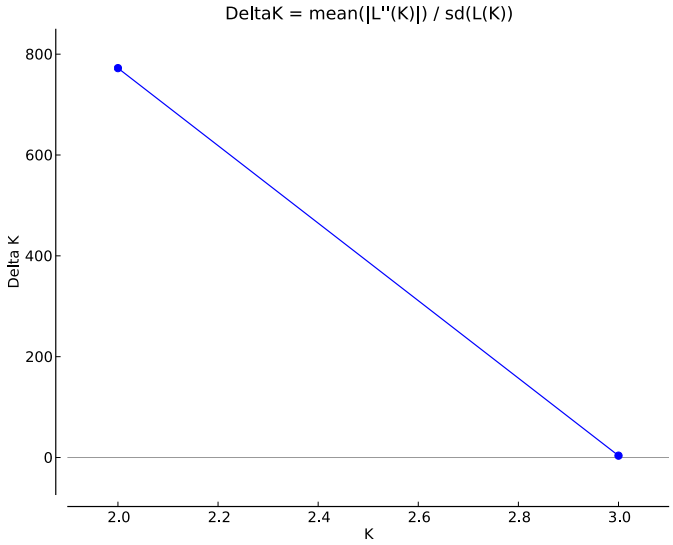

Supplemental Figure S1b. Results from the Evanno et al. (2005) method on the Structure analysis of the northern hybrid zone using the alleles dataset.

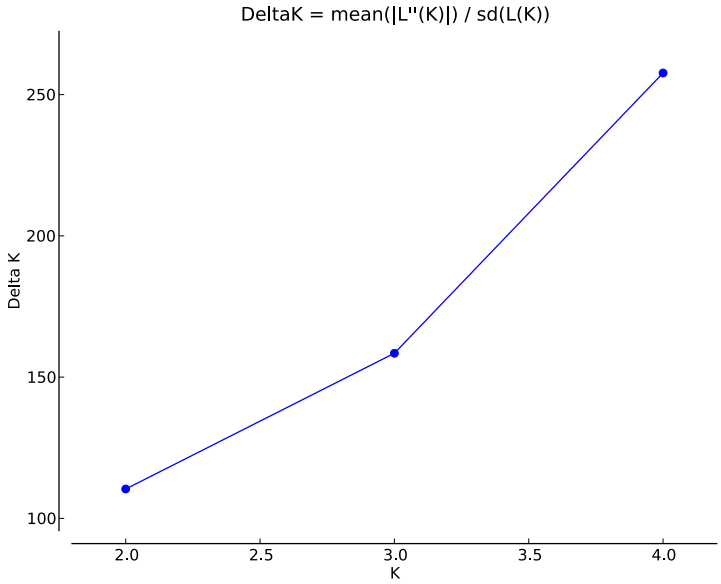

Supplemental Figure S2a. Results from the Evanno et al. (2005) method on the Structure analysis of the southern hybrid zone using the unlinked SNPs dataset.

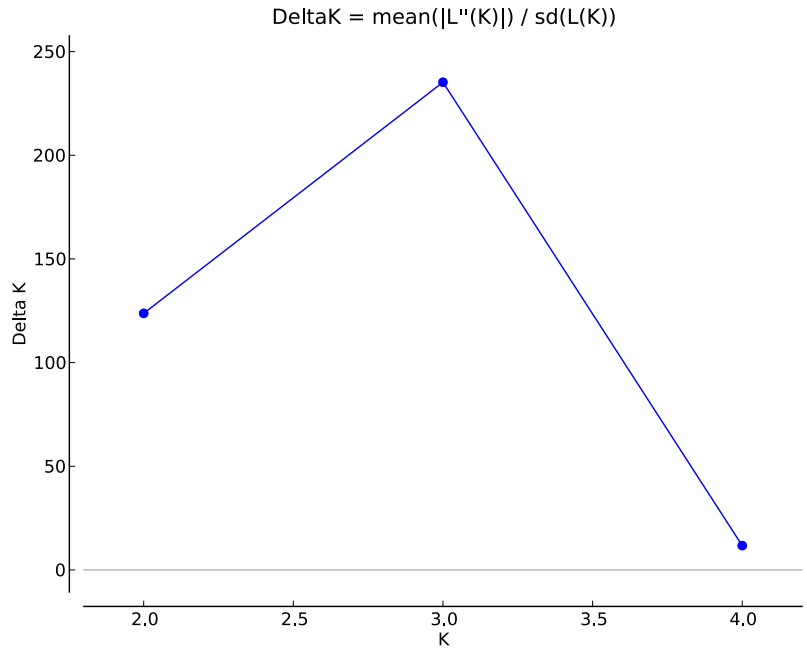

Supplemental Figure S2b. Results from the Evanno et al. (2005) method on the Structure analysis of the southern hybrid zone using the alleles dataset.

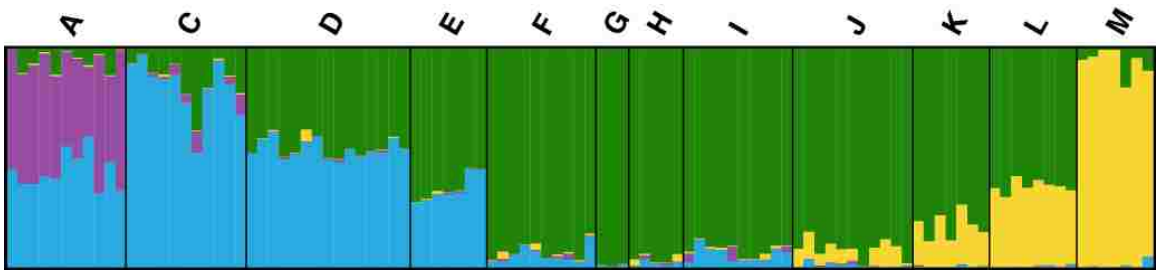

Supplemental Figure S3. Structure results from the southern hybrid zone with the unlinked SNPs dataset when $k = 4$. Transect localities are ordered north-south (A-M).

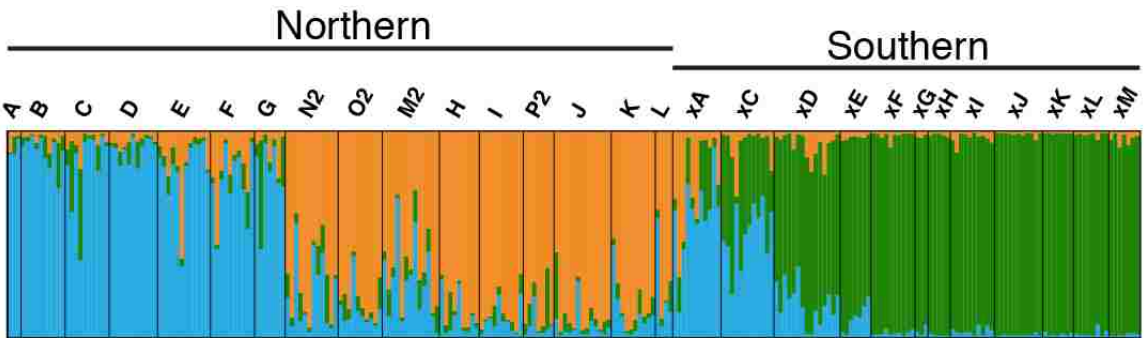

Supplemental Figure S4. Structure results from the unlinked SNP dataset when analyzing data from both northern and southern hybrid zones combined.

Supplemental Table S1. Sampling information for individuals yielding nuclear DNA in the northern hybrid zone.

Accession ID	Latitude	Longitude
LJAMM-CNP 16280	-42.07365599	-66.50916399
LJAMM-CNP 16281	-42.07365599	-66.50916399
LJAMM-CNP 16282	-42.07365599	-66.50916399
LJAMM-CNP 16283	-42.07365599	-66.50916399
LJAMM-CNP 16284	-42.07365599	-66.50916399
LJAMM-CNP 16285	-42.07365599	-66.50916399
LJAMM-CNP 16287	-42.07365599	-66.50916399
LJAMM-CNP 16288	-42.07365599	-66.50916399
LJAMM-CNP 16289	-42.07365599	-66.50916399
LJAMM-CNP 16290	-42.07365599	-66.50916399
LJAMM-CNP 16291	-42.07365599	-66.50916399
LJAMM-CNP 16294	-42.00812199	-66.59550397
LJAMM-CNP 16295	-42.00812199	-66.59550397
LJAMM-CNP 16296	-42.00812199	-66.59550397
LJAMM-CNP 16297	-42.00812199	-66.59550397
LJAMM-CNP 16298	-42.00812199	-66.59550397
LJAMM-CNP 16299	-42.00812199	-66.59550397
LJAMM-CNP 16300	-42.00812199	-66.59550397
LJAMM-CNP 16301	-42.00812199	-66.59550397
LJAMM-CNP 16302	-42.00812199	-66.59550397
LJAMM-CNP 16303	-42.00812199	-66.59550397
LJAMM-CNP 16304	-41.96589698	-66.69209702
LJAMM-CNP 16305	-41.96589698	-66.69209702
LJAMM-CNP 16308	-41.96589698	-66.69209702
LJAMM-CNP 16310	-41.96589698	-66.69209702
LJAMM-CNP 16311	-41.96589698	-66.69209702
LJAMM-CNP 16312	-41.96589698	-66.69209702
LJAMM-CNP 16313	-41.96589698	-66.69209702
LJAMM-CNP 16314	-41.96589698	-66.69209702
LJAMM-CNP 16315	-41.96589698	-66.69209702
LJAMM-CNP 16316	-41.96589698	-66.69209702
LJAMM-CNP 16317	-41.91090298	-66.81106598
LJAMM-CNP 16318	-41.91090298	-66.81106598
LJAMM-CNP 16319	-41.91090298	-66.81106598
LJAMM-CNP 16320	-42.22003503	-66.37060602
LJAMM-CNP 16321	-42.22003503	-66.37060602
LJAMM-CNP 16322	-42.22003503	-66.37060602
LJAMM-CNP 16323	-42.22003503	-66.37060602
LJAMM-CNP 16324	-42.22003503	-66.37060602
LJAMM-CNP 16325	-42.22003503	-66.37060602

LJAMM-CNP 16326	-42.22003503	-66.37060602
LJAMM-CNP 16327	-42.52366302	-66.74343299
LJAMM-CNP 16328	-42.52366302	-66.74343299
LJAMM-CNP 16329	-42.52366302	-66.74343299
LJAMM-CNP 16330	-42.52366302	-66.74343299
LJAMM-CNP 16331	-42.52366302	-66.74343299
LJAMM-CNP 16332	-42.52366302	-66.74343299
LJAMM-CNP 16333	-42.52366302	-66.74343299
LJAMM-CNP 16334	-42.52366302	-66.74343299
LJAMM-CNP 16335	-42.52366302	-66.74343299
LJAMM-CNP 16336	-42.52366302	-66.74343299
LJAMM-CNP 16337	-42.719475	-67.013744
LJAMM-CNP 16338	-42.719475	-67.013744
LJAMM-CNP 16339	-42.719475	-67.013744
LJAMM-CNP 16340	-42.719475	-67.013744
LJAMM-CNP 16341	-42.719475	-67.013744
LJAMM-CNP 16342	-42.719475	-67.013744
LJAMM-CNP 16343	-42.719475	-67.013744
LJAMM-CNP 16344	-42.719475	-67.013744
LJAMM-CNP 16345	-42.719475	-67.013744
LJAMM-CNP 16346	-42.719475	-67.013744
LJAMM-CNP 16347	-42.719475	-67.013744
LJAMM-CNP 16348	-42.719475	-67.013744
LJAMM-CNP 16349	-42.719475	-67.013744
LJAMM-CNP 16350	-42.19299199	-66.60935397
LJAMM-CNP 16351	-42.19299199	-66.60935397
LJAMM-CNP 16352	-42.19299199	-66.60935397
LJAMM-CNP 16353	-42.19299199	-66.60935397
LJAMM-CNP 16354	-42.19299199	-66.60935397
LJAMM-CNP 16355	-42.19299199	-66.60935397
LJAMM-CNP 16356	-42.19299199	-66.60935397
LJAMM-CNP 16357	-42.19299199	-66.60935397
LJAMM-CNP 16358	-42.19299199	-66.60935397
LJAMM-CNP 16360	-42.19299199	-66.60935397
LJAMM-CNP 16361	-42.19299199	-66.60935397
LJAMM-CNP 16362	-42.19299199	-66.60935397
LJAMM-CNP 16363	-42.19533004	-66.79049201
LJAMM-CNP 16364	-42.19533004	-66.79049201
LJAMM-CNP 16365	-42.19533004	-66.79049201
LJAMM-CNP 16366	-42.19533004	-66.79049201
LJAMM-CNP 16367	-42.19533004	-66.79049201
LJAMM-CNP 16368	-42.19533004	-66.79049201
LJAMM-CNP 16369	-42.19533004	-66.79049201

LJAMM-CNP 16370	-42.19533004	-66.79049201
LJAMM-CNP 16371	-42.19533004	-66.79049201
LJAMM-CNP 16373	-42.19533004	-66.79049201
LJAMM-CNP 16374	-42.25181803	-66.88787397
LJAMM-CNP 16375	-42.25181803	-66.88787397
LJAMM-CNP 16376	-42.25181803	-66.88787397
LJAMM-CNP 16377	-42.25181803	-66.88787397
LJAMM-CNP 16378	-42.25181803	-66.88787397
LJAMM-CNP 16379	-42.25181803	-66.88787397
LJAMM-CNP 16380	-42.25181803	-66.88787397
LJAMM-CNP 16381	-42.25181803	-66.88787397
LJAMM-CNP 16382	-42.25181803	-66.88787397
LJAMM-CNP 16385	-42.91986301	-67.14025601
LJAMM-CNP 16386	-42.91986301	-67.14025601
LJAMM-CNP 16387	-42.91986301	-67.14025601
LJAMM-CNP 16388	-42.91986301	-67.14025601
LJAMM-CNP 16389	-42.91986301	-67.14025601
LJAMM-CNP 16390	-42.91986301	-67.14025601
LJAMM-CNP 16392	-42.91986301	-67.14025601
LJAMM-CNP 16393	-42.91986301	-67.14025601
LJAMM-CNP 16394	-42.91986301	-67.14025601
LJAMM-CNP 16395	-42.91986301	-67.14025601
LJAMM-CNP 16396	-43.05974398	-67.22657503
LJAMM-CNP 16397	-43.05974398	-67.22657503
LJAMM-CNP 16398	-43.05974398	-67.22657503
LJAMM-CNP 16399	-43.05974398	-67.22657503
LJAMM-CNP 16646	-42.44653	-67.01861
LJAMM-CNP 16648	-42.44653	-67.01861
LJAMM-CNP 16649	-42.44653	-67.01861
LJAMM-CNP 16650	-42.44653	-67.01861
LJAMM-CNP 16651	-42.44653	-67.01861
LJAMM-CNP 16652	-42.44653	-67.01861
LJAMM-CNP 16653	-42.44653	-67.01861
LJAMM-CNP 16665	-42.66186	-66.28413
LJAMM-CNP 16666	-42.66186	-66.28413
LJAMM-CNP 16667	-42.66186	-66.28413
LJAMM-CNP 16668	-42.66186	-66.28413
LJAMM-CNP 16669	-42.66186	-66.28413
LJAMM-CNP 16670	-42.66186	-66.28413
LJAMM-CNP 16673	-42.40484	-66.68957
LJAMM-CNP 16674	-42.40484	-66.68957
LJAMM-CNP 16675	-42.40484	-66.68957
LJAMM-CNP 16676	-42.40484	-66.68957

LJAMM-CNP 16678	-42.41364	-66.62296
LJAMM-CNP 16679	-42.41364	-66.62296
LJAMM-CNP 16680	-42.41364	-66.62296
LJAMM-CNP 16681	-42.41364	-66.62296
LJAMM-CNP 16683	-42.3437	-66.62036
LJAMM-CNP 16684	-42.3437	-66.62036
LJAMM-CNP 16685	-42.3437	-66.62036
LJAMM-CNP 16686	-42.3437	-66.62036
LJAMM-CNP 16687	-42.3437	-66.62036
LJAMM-CNP 16806	-42.40484	-66.68957
LJAMM-CNP 16807	-42.40484	-66.68957
LJAMM-CNP 16808	-42.40484	-66.68957
LJAMM-CNP 16809	-42.40484	-66.68957
LJAMM-CNP 16810	-42.40484	-66.68957
LJAMM-CNP 16811	-42.40484	-66.68957
LJAMM-CNP 16812	-42.40484	-66.68957
LJAMM-CNP 16813	-42.40484	-66.68957
LJAMM-CNP 16814	-42.3437	-66.62036
LJAMM-CNP 16815	-42.3437	-66.62036
LJAMM-CNP 16816	-42.3437	-66.62036
LJAMM-CNP 16817	-42.3437	-66.62036
LJAMM-CNP 16818	-42.3437	-66.62036
LJAMM-CNP 16819	-42.3437	-66.62036
LJAMM-CNP 16820	-42.3437	-66.62036
LJAMM-CNP 16821	-42.3437	-66.62036
LJAMM-CNP 16822	-42.41364	-66.62296
LJAMM-CNP 16823	-42.41364	-66.62296
LJAMM-CNP 16824	-42.41364	-66.62296
LJAMM-CNP 16825	-42.41364	-66.62296
LJAMM-CNP 16826	-42.41364	-66.62296
LJAMM-CNP 16827	-42.41364	-66.62296

Supplemental Table S2. Sampling information for individuals yielding nuclear DNA in the southern hybrid zone.

Accession ID	Latitude	Longitude	Sex	Adult or Juvenile
LJAMM-CNP 16841	-43.561	-67.349	M	A
LJAMM-CNP 16842	-43.561	-67.349	M	J
LJAMM-CNP 16843	-43.561	-67.349	M	J
LJAMM-CNP 16845	-43.561	-67.349	F	J
LJAMM-CNP 16846	-43.561	-67.349	F	J
LJAMM-CNP 16847	-43.561	-67.349	M	A
LJAMM-CNP 16848	-43.561	-67.349	M	A
LJAMM-CNP 16849	-43.561	-67.349	M	A
LJAMM-CNP 16850	-43.561	-67.349	F	A
LJAMM-CNP 16851	-43.561	-67.349	F	J
LJAMM-CNP 16852	-43.561	-67.349	M	J
LJAMM-CNP 16854	-43.744	-67.303	F	J
LJAMM-CNP 16855	-43.769	-67.309	M	A
LJAMM-CNP 16856	-43.769	-67.309	M	A
LJAMM-CNP 16857	-43.769	-67.309	M	A
LJAMM-CNP 16858	-43.769	-67.309	M	A
LJAMM-CNP 16859	-43.769	-67.309	M	A
LJAMM-CNP 16860	-43.769	-67.309	M	J
LJAMM-CNP 16861	-43.769	-67.309	F	A
LJAMM-CNP 16862	-43.769	-67.309	F	A
LJAMM-CNP 16863	-43.769	-67.309	F	A
LJAMM-CNP 16864	-43.769	-67.309	F	A
LJAMM-CNP 16865	-43.769	-67.309	F	J
LJAMM-CNP 16866	-43.931	-67.305	M	A
LJAMM-CNP 16867	-43.931	-67.305	M	A
LJAMM-CNP 16868	-43.931	-67.305	M	A
LJAMM-CNP 16869	-43.931	-67.305	M	A
LJAMM-CNP 16870	-43.931	-67.305	M	J
LJAMM-CNP 16871	-43.931	-67.305	M	J
LJAMM-CNP 16872	-43.931	-67.305	M	J
LJAMM-CNP 16873	-43.931	-67.305	F	A
LJAMM-CNP 16874	-43.931	-67.305	F	A
LJAMM-CNP 16875	-43.931	-67.305	F	A
LJAMM-CNP 16876	-43.931	-67.305	F	A
LJAMM-CNP 16877	-43.931	-67.305	F	A
LJAMM-CNP 16878	-43.931	-67.305	F	A
LJAMM-CNP 16879	-43.931	-67.305	F	A
LJAMM-CNP 16880	-43.931	-67.305	F	A
LJAMM-CNP 16881	-44.088	-67.239	M	A

LJAMM-CNP 16882	-44.088	-67.239	M	J
LJAMM-CNP 16883	-44.088	-67.239	F	A
LJAMM-CNP 16884	-44.088	-67.239	F	A
LJAMM-CNP 16885	-44.088	-67.239	F	A
LJAMM-CNP 16886	-44.088	-67.239	F	J
LJAMM-CNP 16887	-44.088	-67.239	F	J
LJAMM-CNP 16889	-44.264	-67.140	M	A
LJAMM-CNP 16890	-44.264	-67.140	M	A
LJAMM-CNP 16891	-44.264	-67.140	M	A
LJAMM-CNP 16892	-44.264	-67.140	M	A
LJAMM-CNP 16893	-44.264	-67.140	M	A
LJAMM-CNP 16894	-44.264	-67.140	M	A
LJAMM-CNP 16896	-44.264	-67.140	F	A
LJAMM-CNP 16898	-44.264	-67.140	F	A
LJAMM-CNP 16899	-44.264	-67.140	F	A
LJAMM-CNP 16900	-44.264	-67.140	F	J
LJAMM-CNP 16903	-44.408	-66.982	F	A
LJAMM-CNP 16904	-44.408	-66.982	F	A
LJAMM-CNP 16908	-44.408	-66.982	M	J
LJAMM-CNP 16910	-45.390	-67.682	M	A
LJAMM-CNP 16914	-45.390	-67.682	M	J
LJAMM-CNP 16915	-45.390	-67.682	M	J
LJAMM-CNP 16916	-45.390	-67.682	F	A
LJAMM-CNP 16917	-45.390	-67.682	F	A
LJAMM-CNP 16918	-45.390	-67.682	F	A
LJAMM-CNP 16919	-45.390	-67.682	F	J
LJAMM-CNP 16920	-45.246	-67.849	M	A
LJAMM-CNP 16921	-45.246	-67.849	M	A
LJAMM-CNP 16922	-45.246	-67.849	M	A
LJAMM-CNP 16923	-45.246	-67.849	M	A
LJAMM-CNP 16924	-45.246	-67.849	M	A
LJAMM-CNP 16925	-45.246	-67.849	M	J
LJAMM-CNP 16926	-45.246	-67.849	M	J
LJAMM-CNP 16927	-45.246	-67.849	F	A
LJAMM-CNP 16947	-44.993	-68.009	M	A
LJAMM-CNP 16949	-44.993	-68.009	F	A
LJAMM-CNP 16950	-44.993	-68.009	F	A
LJAMM-CNP 16951	-44.993	-68.009	F	A
LJAMM-CNP 16952	-44.993	-68.009	F	A
LJAMM-CNP 16953	-44.993	-68.009	F	A
LJAMM-CNP 16954	-44.993	-68.009	F	J
LJAMM-CNP 16955	-44.752	-67.983	M	A
LJAMM-CNP 16956	-44.752	-67.983	M	A

LJAMM-CNP 16957	-44.752	-67.983	M	A
LJAMM-CNP 16958	-44.752	-67.983	M	A
LJAMM-CNP 16959	-44.752	-67.983	F	A
LJAMM-CNP 16960	-44.752	-67.983	F	A
LJAMM-CNP 16961	-44.752	-67.983	F	A
LJAMM-CNP 16962	-44.752	-67.983	F	A
LJAMM-CNP 16963	-44.993	-68.009	F	A
LJAMM-CNP 16964	-44.993	-68.009	F	A
LJAMM-CNP 16965	-44.993	-68.009	F	J
LJAMM-CNP 16966	-44.576	-67.728	M	A
LJAMM-CNP 16967	-44.576	-67.728	M	A
LJAMM-CNP 16968	-44.576	-67.728	M	A
LJAMM-CNP 16969	-44.576	-67.728	M	A
LJAMM-CNP 16971	-44.576	-67.728	F	A
LJAMM-CNP 16972	-44.576	-67.728	F	A
LJAMM-CNP 16973	-44.576	-67.728	F	A
LJAMM-CNP 16974	-44.576	-67.728	F	A
LJAMM-CNP 16975	-44.576	-67.728	F	A
LJAMM-CNP 16976	-44.576	-67.728	F	A
LJAMM-CNP 16977	-44.545	-67.322	M	A
LJAMM-CNP 16978	-44.545	-67.322	F	A
LJAMM-CNP 16979	-44.545	-67.322	F	A
LJAMM-CNP 16980	-44.545	-67.322	F	A
LJAMM-CNP 16981	-44.545	-67.322	F	A

Supplemental Table S3. Sampling information for individuals yielding mitochondrial DNA in the northern hybrid zone.

Accession ID	Latitude	Longitude
LJAMM-CNP 16280	-42.07365599	-66.50916399
LJAMM-CNP 16281	-42.07365599	-66.50916399
LJAMM-CNP 16282	-42.07365599	-66.50916399
LJAMM-CNP 16283	-42.07365599	-66.50916399
LJAMM-CNP 16284	-42.07365599	-66.50916399
LJAMM-CNP 16285	-42.07365599	-66.50916399
LJAMM-CNP 16286	-42.07365599	-66.50916399
LJAMM-CNP 16287	-42.07365599	-66.50916399
LJAMM-CNP 16288	-42.07365599	-66.50916399
LJAMM-CNP 16289	-42.07365599	-66.50916399
LJAMM-CNP 16290	-42.07365599	-66.50916399
LJAMM-CNP 16291	-42.07365599	-66.50916399
LJAMM-CNP 16294	-42.00812199	-66.59550397
LJAMM-CNP 16295	-42.00812199	-66.59550397
LJAMM-CNP 16296	-42.00812199	-66.59550397
LJAMM-CNP 16297	-42.00812199	-66.59550397
LJAMM-CNP 16298	-42.00812199	-66.59550397
LJAMM-CNP 16299	-42.00812199	-66.59550397
LJAMM-CNP 16300	-42.00812199	-66.59550397
LJAMM-CNP 16301	-42.00812199	-66.59550397
LJAMM-CNP 16302	-42.00812199	-66.59550397
LJAMM-CNP 16303	-42.00812199	-66.59550397
LJAMM-CNP 16304	-41.96589698	-66.69209702
LJAMM-CNP 16305	-41.96589698	-66.69209702
LJAMM-CNP 16307	-41.96589698	-66.69209702
LJAMM-CNP 16308	-41.96589698	-66.69209702
LJAMM-CNP 16310	-41.96589698	-66.69209702
LJAMM-CNP 16311	-41.96589698	-66.69209702
LJAMM-CNP 16312	-41.96589698	-66.69209702
LJAMM-CNP 16313	-41.96589698	-66.69209702
LJAMM-CNP 16314	-41.96589698	-66.69209702
LJAMM-CNP 16315	-41.96589698	-66.69209702
LJAMM-CNP 16317	-41.91090298	-66.81106598
LJAMM-CNP 16318	-41.91090298	-66.81106598
LJAMM-CNP 16320	-42.22003503	-66.37060602
LJAMM-CNP 16321	-42.22003503	-66.37060602
LJAMM-CNP 16322	-42.22003503	-66.37060602
LJAMM-CNP 16324	-42.22003503	-66.37060602
LJAMM-CNP 16327	-42.52366302	-66.74343299
LJAMM-CNP 16328	-42.52366302	-66.74343299

LJAMM-CNP 16329	-42.52366302	-66.74343299
LJAMM-CNP 16330	-42.52366302	-66.74343299
LJAMM-CNP 16331	-42.52366302	-66.74343299
LJAMM-CNP 16332	-42.52366302	-66.74343299
LJAMM-CNP 16333	-42.52366302	-66.74343299
LJAMM-CNP 16334	-42.52366302	-66.74343299
LJAMM-CNP 16335	-42.52366302	-66.74343299
LJAMM-CNP 16336	-42.52366302	-66.74343299
LJAMM-CNP 16337	-42.719475	-67.013744
LJAMM-CNP 16338	-42.719475	-67.013744
LJAMM-CNP 16339	-42.719475	-67.013744
LJAMM-CNP 16340	-42.719475	-67.013744
LJAMM-CNP 16341	-42.719475	-67.013744
LJAMM-CNP 16342	-42.719475	-67.013744
LJAMM-CNP 16343	-42.719475	-67.013744
LJAMM-CNP 16344	-42.719475	-67.013744
LJAMM-CNP 16345	-42.719475	-67.013744
LJAMM-CNP 16346	-42.719475	-67.013744
LJAMM-CNP 16347	-42.719475	-67.013744
LJAMM-CNP 16348	-42.719475	-67.013744
LJAMM-CNP 16349	-42.719475	-67.013744
LJAMM-CNP 16350	-42.19299199	-66.60935397
LJAMM-CNP 16351	-42.19299199	-66.60935397
LJAMM-CNP 16353	-42.19299199	-66.60935397
LJAMM-CNP 16354	-42.19299199	-66.60935397
LJAMM-CNP 16355	-42.19299199	-66.60935397
LJAMM-CNP 16356	-42.19299199	-66.60935397
LJAMM-CNP 16357	-42.19299199	-66.60935397
LJAMM-CNP 16358	-42.19299199	-66.60935397
LJAMM-CNP 16360	-42.19299199	-66.60935397
LJAMM-CNP 16361	-42.19299199	-66.60935397
LJAMM-CNP 16362	-42.19299199	-66.60935397
LJAMM-CNP 16363	-42.19533004	-66.79049201
LJAMM-CNP 16364	-42.19533004	-66.79049201
LJAMM-CNP 16365	-42.19533004	-66.79049201
LJAMM-CNP 16366	-42.19533004	-66.79049201
LJAMM-CNP 16367	-42.19533004	-66.79049201
LJAMM-CNP 16368	-42.19533004	-66.79049201
LJAMM-CNP 16369	-42.19533004	-66.79049201
LJAMM-CNP 16370	-42.19533004	-66.79049201
LJAMM-CNP 16371	-42.19533004	-66.79049201
LJAMM-CNP 16372	-42.19533004	-66.79049201
LJAMM-CNP 16373	-42.19533004	-66.79049201

LJAMM-CNP 16374	-42.25181803	-66.88787397
LJAMM-CNP 16375	-42.25181803	-66.88787397
LJAMM-CNP 16376	-42.25181803	-66.88787397
LJAMM-CNP 16377	-42.25181803	-66.88787397
LJAMM-CNP 16378	-42.25181803	-66.88787397
LJAMM-CNP 16379	-42.25181803	-66.88787397
LJAMM-CNP 16380	-42.25181803	-66.88787397
LJAMM-CNP 16381	-42.25181803	-66.88787397
LJAMM-CNP 16382	-42.25181803	-66.88787397
LJAMM-CNP 16384	-42.25181803	-66.88787397
LJAMM-CNP 16385	-42.91986301	-67.14025601
LJAMM-CNP 16386	-42.91986301	-67.14025601
LJAMM-CNP 16387	-42.91986301	-67.14025601
LJAMM-CNP 16388	-42.91986301	-67.14025601
LJAMM-CNP 16389	-42.91986301	-67.14025601
LJAMM-CNP 16390	-42.91986301	-67.14025601
LJAMM-CNP 16392	-42.91986301	-67.14025601
LJAMM-CNP 16393	-42.91986301	-67.14025601
LJAMM-CNP 16394	-42.91986301	-67.14025601
LJAMM-CNP 16395	-42.91986301	-67.14025601
LJAMM-CNP 16396	-43.05974398	-67.22657503
LJAMM-CNP 16397	-43.05974398	-67.22657503
LJAMM-CNP 16398	-43.05974398	-67.22657503
LJAMM-CNP 16399	-43.05974398	-67.22657503
LJAMM-CNP 16646	-42.44653	-67.01861
LJAMM-CNP 16647	-42.44653	-67.01861
LJAMM-CNP 16648	-42.44653	-67.01861
LJAMM-CNP 16649	-42.44653	-67.01861
LJAMM-CNP 16650	-42.44653	-67.01861
LJAMM-CNP 16651	-42.44653	-67.01861
LJAMM-CNP 16653	-42.44653	-67.01861
LJAMM-CNP 16665	-42.66186	-66.28413
LJAMM-CNP 16666	-42.66186	-66.28413
LJAMM-CNP 16667	-42.66186	-66.28413
LJAMM-CNP 16668	-42.66186	-66.28413
LJAMM-CNP 16669	-42.66186	-66.28413
LJAMM-CNP 16670	-42.66186	-66.28413
LJAMM-CNP 16673	-42.40484	-66.68957
LJAMM-CNP 16674	-42.40484	-66.68957
LJAMM-CNP 16675	-42.40484	-66.68957
LJAMM-CNP 16676	-42.40484	-66.68957
LJAMM-CNP 16678	-42.41364	-66.62296
LJAMM-CNP 16679	-42.41364	-66.62296

LJAMM-CNP 16680	-42.41364	-66.62296
LJAMM-CNP 16681	-42.41364	-66.62296
LJAMM-CNP 16683	-42.3437	-66.62036
LJAMM-CNP 16684	-42.3437	-66.62036
LJAMM-CNP 16685	-42.3437	-66.62036
LJAMM-CNP 16686	-42.3437	-66.62036
LJAMM-CNP 16687	-42.3437	-66.62036
LJAMM-CNP 16807	-42.40484	-66.68957
LJAMM-CNP 16808	-42.40484	-66.68957
LJAMM-CNP 16809	-42.40484	-66.68957
LJAMM-CNP 16810	-42.40484	-66.68957
LJAMM-CNP 16811	-42.40484	-66.68957
LJAMM-CNP 16812	-42.40484	-66.68957
LJAMM-CNP 16813	-42.40484	-66.68957
LJAMM-CNP 16814	-42.3437	-66.62036
LJAMM-CNP 16815	-42.3437	-66.62036
LJAMM-CNP 16821	-42.3437	-66.62036
LJAMM-CNP 16825	-42.41364	-66.62296
LJAMM-CNP 16826	-42.41364	-66.62296
LJAMM-CNP 16827	-42.41364	-66.62296

Supplemental Table S4. Sampling information for individuals yielding mitochondrial DNA in the southern hybrid zone.

Accession ID	Latitude	Longitude	Sex
LJAMM-CNP 16841	-43.56120	-67.34947	M
LJAMM-CNP 16842	-43.56120	-67.34947	M
LJAMM-CNP 16843	-43.56120	-67.34947	M
LJAMM-CNP 16844	-43.56120	-67.34947	F
LJAMM-CNP 16845	-43.56120	-67.34947	F
LJAMM-CNP 16846	-43.56120	-67.34947	F
LJAMM-CNP 16847	-43.56120	-67.34947	M
LJAMM-CNP 16849	-43.56120	-67.34947	M
LJAMM-CNP 16850	-43.56120	-67.34947	F
LJAMM-CNP 16851	-43.56120	-67.34947	F
LJAMM-CNP 16852	-43.56120	-67.34947	M
LJAMM-CNP 16853	-43.74428	-67.30293	F
LJAMM-CNP 16854	-43.74428	-67.30293	F
LJAMM-CNP 16855	-43.76920	-67.30861	M
LJAMM-CNP 16856	-43.76920	-67.30861	M
LJAMM-CNP 16857	-43.76920	-67.30861	M
LJAMM-CNP 16858	-43.76920	-67.30861	M
LJAMM-CNP 16859	-43.76920	-67.30861	M
LJAMM-CNP 16860	-43.76920	-67.30861	M
LJAMM-CNP 16861	-43.76920	-67.30861	F
LJAMM-CNP 16862	-43.76920	-67.30861	F
LJAMM-CNP 16863	-43.76920	-67.30861	F
LJAMM-CNP 16864	-43.76920	-67.30861	F
LJAMM-CNP 16865	-43.76920	-67.30861	F
LJAMM-CNP 16866	-43.93147	-67.30499	M
LJAMM-CNP 16867	-43.93147	-67.30499	M
LJAMM-CNP 16868	-43.93147	-67.30499	M
LJAMM-CNP 16869	-43.93147	-67.30499	M
LJAMM-CNP 16870	-43.93147	-67.30499	M
LJAMM-CNP 16871	-43.93147	-67.30499	M
LJAMM-CNP 16872	-43.93147	-67.30499	M
LJAMM-CNP 16873	-43.93147	-67.30499	F
LJAMM-CNP 16874	-43.93147	-67.30499	F
LJAMM-CNP 16875	-43.93147	-67.30499	F
LJAMM-CNP 16876	-43.93147	-67.30499	F
LJAMM-CNP 16877	-43.93147	-67.30499	F
LJAMM-CNP 16878	-43.93147	-67.30499	F
LJAMM-CNP 16879	-43.93147	-67.30499	F
LJAMM-CNP 16880	-43.93147	-67.30499	F
LJAMM-CNP 16881	-44.08842	-67.23920	M

LJAMM-CNP 16882	-44.08842	-67.23920	M
LJAMM-CNP 16883	-44.08842	-67.23920	F
LJAMM-CNP 16884	-44.08842	-67.23920	F
LJAMM-CNP 16885	-44.08842	-67.23920	F
LJAMM-CNP 16886	-44.08842	-67.23920	F
LJAMM-CNP 16887	-44.08842	-67.23920	F
LJAMM-CNP 16889	-44.26351	-67.14036	M
LJAMM-CNP 16890	-44.26351	-67.14036	M
LJAMM-CNP 16891	-44.26351	-67.14036	M
LJAMM-CNP 16892	-44.26351	-67.14036	M
LJAMM-CNP 16893	-44.26351	-67.14036	M
LJAMM-CNP 16894	-44.26351	-67.14036	M
LJAMM-CNP 16895	-44.26351	-67.14036	M
LJAMM-CNP 16896	-44.26351	-67.14036	F
LJAMM-CNP 16897	-44.26351	-67.14036	F
LJAMM-CNP 16898	-44.26351	-67.14036	F
LJAMM-CNP 16899	-44.26351	-67.14036	F
LJAMM-CNP 16900	-44.26351	-67.14036	F
LJAMM-CNP 16901	-44.26351	-67.14036	F
LJAMM-CNP 16904	-44.40788	-66.98195	F
LJAMM-CNP 16908	-44.40788	-66.98195	M
LJAMM-CNP 16909	-45.39003	-67.68237	M
LJAMM-CNP 16910	-45.39003	-67.68237	M
LJAMM-CNP 16914	-45.39003	-67.68237	M
LJAMM-CNP 16915	-45.39003	-67.68237	M
LJAMM-CNP 16916	-45.39003	-67.68237	F
LJAMM-CNP 16917	-45.39003	-67.68237	F
LJAMM-CNP 16918	-45.39003	-67.68237	F
LJAMM-CNP 16919	-45.39003	-67.68237	F
LJAMM-CNP 16920	-45.24637	-67.84865	M
LJAMM-CNP 16921	-45.24637	-67.84865	M
LJAMM-CNP 16922	-45.24637	-67.84865	M
LJAMM-CNP 16923	-45.24637	-67.84865	M
LJAMM-CNP 16924	-45.24637	-67.84865	M
LJAMM-CNP 16925	-45.24637	-67.84865	M
LJAMM-CNP 16947	-44.99274	-68.00871	M
LJAMM-CNP 16948	-44.99274	-68.00871	M
LJAMM-CNP 16949	-44.99274	-68.00871	F
LJAMM-CNP 16950	-44.99274	-68.00871	F
LJAMM-CNP 16951	-44.99274	-68.00871	F
LJAMM-CNP 16952	-44.99274	-68.00871	F
LJAMM-CNP 16953	-44.99274	-68.00871	F
LJAMM-CNP 16954	-44.99274	-68.00871	F

LJAMM-CNP 16955	-44.75241	-67.98312	M
LJAMM-CNP 16956	-44.75241	-67.98312	M
LJAMM-CNP 16957	-44.75241	-67.98312	M
LJAMM-CNP 16958	-44.75241	-67.98312	M
LJAMM-CNP 16959	-44.75241	-67.98312	F
LJAMM-CNP 16960	-44.75241	-67.98312	F
LJAMM-CNP 16961	-44.75241	-67.98312	F
LJAMM-CNP 16962	-44.75241	-67.98312	F
LJAMM-CNP 16963	-44.99274	-68.00871	F
LJAMM-CNP 16964	-44.99274	-68.00871	F
LJAMM-CNP 16965	-44.99274	-68.00871	F
LJAMM-CNP 16966	-44.57621	-67.72794	M
LJAMM-CNP 16967	-44.57621	-67.72794	M
LJAMM-CNP 16968	-44.57621	-67.72794	M
LJAMM-CNP 16969	-44.57621	-67.72794	M
LJAMM-CNP 16970	-44.57621	-67.72794	M
LJAMM-CNP 16971	-44.57621	-67.72794	F
LJAMM-CNP 16972	-44.57621	-67.72794	F
LJAMM-CNP 16973	-44.57621	-67.72794	F
LJAMM-CNP 16974	-44.57621	-67.72794	F
LJAMM-CNP 16975	-44.57621	-67.72794	F
LJAMM-CNP 16976	-44.57621	-67.72794	F
LJAMM-CNP 16977	-44.54505	-67.32176	M
LJAMM-CNP 16978	-44.54505	-67.32176	F
LJAMM-CNP 16979	-44.54505	-67.32176	F
LJAMM-CNP 16980	-44.54505	-67.32176	F
LJAMM-CNP 16981	-44.54505	-67.32176	F